AN ERROR-BASED VARIATIONAL APPROACH TO COMPUTATIONAL ELECTROMAGNETICS

A thesis submitted to the University of London
for the degree of Doctor of Philosophy

by

Ja'far Ali Haidar Al-Rikabi

1985

Electrical Engineering Department
Imperial College of Science and Technology
Exhibition Road, London SW7 2AZ

To Abbas

a lovely boy of six
who was fascinated by numbers
and believed firmly
though not unquestioningly
in a rational universe

" And when your sorrow is comforted
(time soothes all sorrows) you will
be content that you have known me. "

The Little Prince
Antoine de Saint-Exupéry

A B S T R A C T

A unifying framework is proposed for the formulation and solution of electromagnetic field problems, with emphasis on numerical implementation. It is based on a universally defined error that corresponds to the constitutive relationship between fields in electromagnetic media : the error is positive in general, and zero if, and only if, the fields satisfy the relationship exactly. Minimisation of the error provides a universal variational principle which generates complementary and dual solution formulations. The approach leads to a descriptive structural framework that divides fields, potentials, and governing equations between the two sides of the constitutive relationship.

For well-posed static problems, the constitutive error splits into complementary energy bounds. Complementary and dual formulations are derived for a range of problem specifications. Contributions are made to three areas of interest : inaccuracies in magnetostatic scalar potential formulations, limitations of mixed formulation, and solvability of vector potential formulations.

Error-based derivations are presented for standard finite difference, finite element, and boundary element equations. The constitutive error is shown to be a comprehensive measure of numerical errors in consistently specified formulations.

Two-dimensional finite element computation results are presented for linear and non-linear static problems, highlighting the comparative computational behaviour of complementary formulations. Error-guided mesh refinement is demonstrated. Estimates of non-linear lumped circuit parameters are shown to be non-bounding.

The approach is extended to the time-varying case. The constitutive error does not, in general, split into complementary functionals, but solution formulations can always be extracted. Complementary formulations are derived for the steady-state and transient eddy-current problems, as well as the high frequency problem.

A C K N O W L E D G E M E N T S

I am deeply grateful to my supervisor, Professor E. M. Freeman, for his guidance, encouragement, and support, both practical and moral.

I am also indebted to Dr. C. F. Bryant for help and advice, dispensed with patience and good humour, and for many an enlightening discussion.

I should like to thank Mr. C. W. Trowbridge, of the Rutherford-Appleton Laboratory, for his interest and encouragement.

Throughout the period of this research, financial support has been provided by an Iraqi Government scholarship, which is gratefully acknowledged. I should also like to thank the following persons for their various efforts which, together, allowed me to take up the grant : Mr. Hussayn Alrikabi, Dr. Riyadh Al-Muhaidi, Mr. Farouq Hussayn Salman, and Dr. Faiq Al-Azzawi.

Finally, I thank my wife Jihan for her support and patience, Abbas for the joy, and Ammar for the sunshine.

C O N T E N T S

N O T A T I O N

Symbols

Symbols will have the meanings listed below, unless defined differently in the text. Where more than one meaning are listed, the appropriate one may be inferred from the context. SI units are used throughout.

$\underline{A}$ vector potential: (1) abstract, (2) magnetic;
$\underline{B}$ flux density: (1) abstract, (2) magnetic;
$\underline{B}_r$ residual field: (1) abstract, (2) magnetic;
C capacitance;
$\underline{C}$ pre-defined component of flux density $\underline{B}$;
$\underline{D}$ electric flux density;
$\underline{E}$ electric field intensity;
$\underline{G}$ pre-defined component of field intensity $\underline{H}$;
$\underline{H}$ field intensity: (1) abstract, (2) magnetic;
$\underline{H}_c$ coercive force: (1) abstract, (2) magnetic;
I (1) identity operator, (2) electric current;
$\underline{J}$ (1) abstract vector source density, (2) electric current density;
$\underline{K}$ (1) abstract surface vector source density, (2) electric surface current density;
L (1) length of curve in space, (2) Lagrangian, (3) inductance;
M magnetomotive force;
Q electric charge;
R (1) three-dimensional region in space, (2) electric resistance, (3) magnetic reluctance;
S surface in space;
$\underline{T}$ electric current - describing vector potential;
V (1) abstract motive force, (2) voltage;
W (1) energy, (2) power .

$\underline{a}_i$ (1) unit vector in direction i, (2) $\underline{n} \times \underline{A}$;
b $\underline{n} \cdot \underline{B}$;
d $\underline{n} \cdot \underline{D}$;
$\underline{e}$ $\underline{n} \times \underline{E}$;
$\underline{h}$ $\underline{n} \times \underline{H}$;
j imaginary unit $\sqrt{-1}$;
ℓ curve in space;
$\underline{n}$ unit normal vector to a surface, outward if well-defined; otherwise see conventions below;
p time-differential operator $\partial/\partial t$;
p^{-1} time-integral operator $\int(\,)dt$, from t_o to t;
$\underline{r}$ position vector;
t time;
x Cartesian coordinate;
y Cartesian coordinate;
z Cartesian coordinate.

Γ functional in both system variables;
Z functional, eqns. 2.17;
Θ functional in one-system variables: (1) H-system, (2) E-system (static); (3) H-system (time-varying);
Λ global constitutive error;
Ξ functional in one-system variables: (1) B-system, (2) D-system, (3) J-system (static); (4) E-system (time-varying);
Φ flux: (1) abstract, (2) magnetic;
X functional, eqns. 2.17;
Ψ functional, eqns. 2.17;
Ω scalar potential: (1) abstract, (2) magnetic.

ε (1) electric permittivity, (2) general error;
ζ product, see eqn. 2.11;
λ constitutive error density;
μ (1) abstract constitutive operator, (2) magnetic permeability;
ν (1) abstract constitutive operator, (2) magnetic reluctivity;

ρ (1) abstract scalar source density, (2) electric charge density, (3) electric resistivity;

σ (1) abstract surface scalar source density, (2) surface charge density, (3) electric conductivity;

ϕ electric scalar potential;

χ see eqn. 2.8a;

ψ see eqn. 2.8b;

ω angular frequency.

Conventions

$\underline{U}$, U vector and its magnitude;

$\overline{U}$ specified value of U;

δU $= U_2 - U_1$; subscripts refer to two estimates of U;

ΔU $= U_2 - U_1$; subscripts refer to regions on two sides of a surface;

$\underline{n}\ \Delta U$ $= \underline{n}_1 (U_2 - U_1) = \underline{n}_2 (U_1 - U_2)$; subscripts refer to regions on two sides of a surface; $\underline{n}_i$ is the unit normal to the surface, outward from region i;

$p\,U$ $= \partial / \partial t\,(U)$;

$p^{-1}\,U$ $= \int_{t_o}^{t} U\,dt$;

$\mathrm{Re}\{U\}$ = real part of U;

$\mathrm{Im}\{U\}$ = imaginary part of U;

$\langle u , v \rangle$ $= u\,v$;

$\langle \underline{U} , \underline{V} \rangle$ $= \underline{U} \cdot \underline{V}$;

$\langle u , v \rangle_R = \int_R \langle u , v \rangle\, dR = \int_R u\,v\, dR$;

$\langle \underline{U} , \underline{V} \rangle_R = \int_R \langle \underline{U} , \underline{V} \rangle\, dR = \int_R \underline{U} \cdot \underline{V}\, dR$;

$[u , v]_S = \int_S \langle u , v \rangle\, dS = \int_S u\,v\, dS$;

$[\underline{U} , \underline{V}]_S = \int_S \langle \underline{U} , \underline{V} \rangle\, dS = \int_S \underline{U} \cdot \underline{V}\, dS$;

∇_s del-operator (nabla) defined on a surface, in terms of surface coordinates.

CHAPTER ONE

Introduction

1.1 Preview

This thesis is concerned with the formulation and solution of electromagnetic field problems. The emphasis is on numerical application, a topic marked by numerous developments since digital computers became widely available some twenty-five years ago.

The thesis identifies an error that corresponds to the constitutive relationship, and shows that many existing approaches are simply alternative ways of minimising it. The error-based approach thus provides a unifying framework that offers perspective and insight. The error itself can provide a common basis for comparison. The theory is particularly suited to numerical analysis, the error being identically zero in exact analysis.

This introductory chapter sets the background, and outlines the thesis. Sec. 1.2 describes the steps involved in computing the fields for a given problem. Sec. 1.3 is a brief survey of existing implementations of these steps. Sec. 1.4 reviews previous work on complementary variational principles, a major contribution to the establishment of a unifying framework. Finally, sec. 1.5 outlines the work presented in the thesis.

1.2 Problem specification and solution formulation

The process of solving an electromagnetic field problem is one of constraining the field variables to satisfy the given problem specifications. If the latter are well-posed,

the variables should acquire, everywhere in the region of the problem, the values corresponding to the unique field distributions.

A problem is uniquely specified by

(i) the constitutive relationship(s);
(ii) Maxwell's equations;
(iii) continuity conditions; and
(iv) boundary conditions.

The geometry and topology of the region are implicit in these position-dependent specifications.

As described, the process is analytic, and solution is possible for only a limited range of problem specifications. Numerical methods can handle a wider range by further constraining the field variables to mathematically tractable forms. In effect, the solution fields are numerically over-specified, and can only approximate the true fields.

The main steps of the solution process are outlined in the flow chart of fig. 1.1. It would be difficult to envisage a treatment that is not described by such a general procedure.

The equations formulated in step 2 may be partial differential equations, integral equations, or combinations. One might include variational energy principles, although these are often regarded as means of solving partial differential equations. Integral equations are also commonly presented as means of solving the corresponding partial differential equations. Such emphasis on the differential formulation is a carry-over from closed-form analysis; it does not necessarily provide the most suitable approach to numerical analysis.

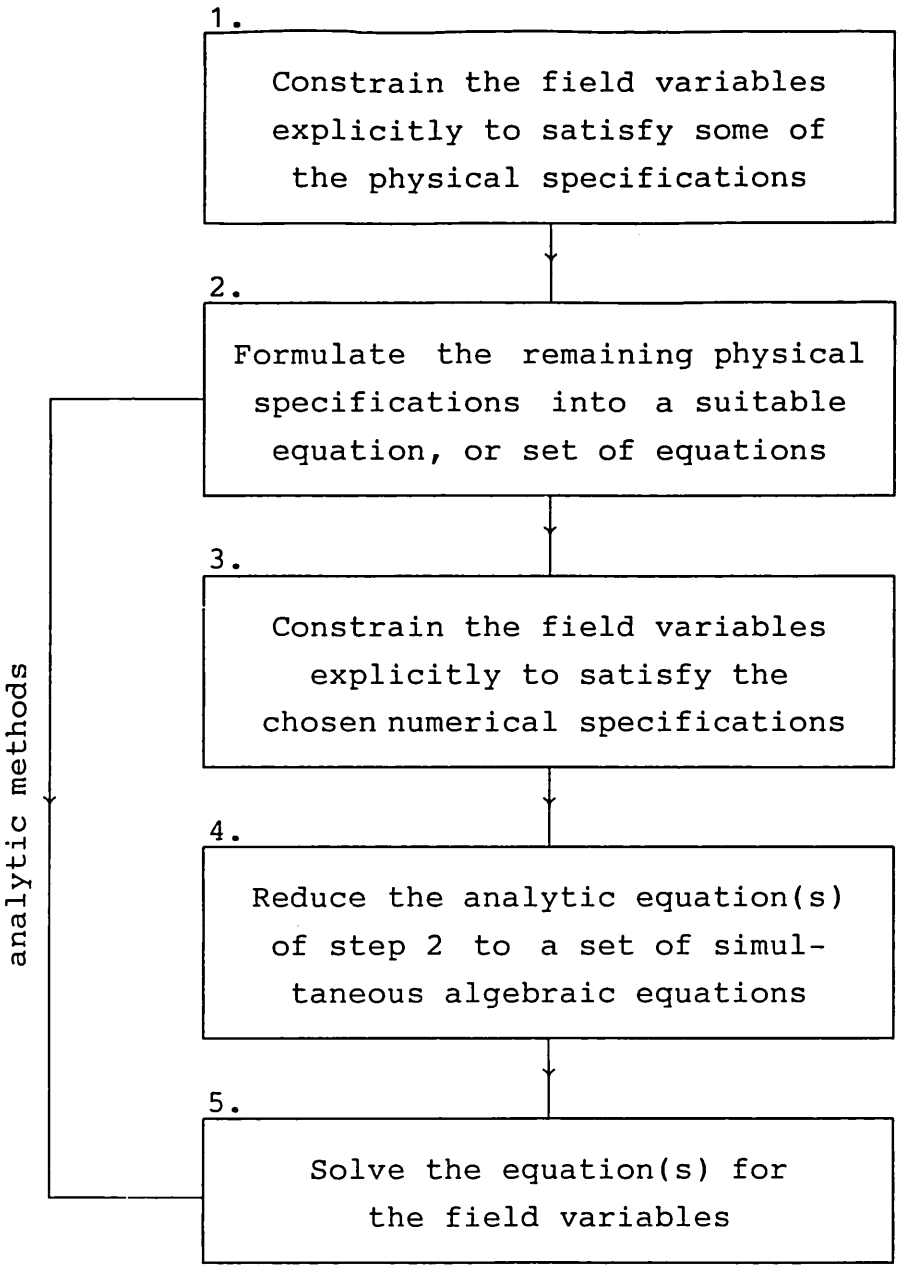

Fig. 1.1 General solution procedure.

1.3 Existing techniques

A cursory look through the literature reveals the variety of ways in which the general procedure of fig. 1.1 can be implemented. Choice is available, and has been exercised, at each step.

In general, the constitutive relationship is imposed explicitly in step 1. The main choice then is which of

Maxwell's equations to enforce explicitly, and which to base the solution formulation on. This may be viewed as a choice between potentials[1.1,2], or, more fundamentally, between complementary formulations[1.3,4]. Mixed formulations have been developed recently[1.5]. Variants include recasting Maxwell's field equations in network forms[1.6,7].

The solution formulation of step 2 may be differential[1.8,9], integral[1.10,11], or a combination of the two[1.12,13]. Alternatively, the variational principle, if one exists, may be regarded as the solution formulation[1.3,14].

Numerical methods, steps 3 and 4, are characterised mainly by the analytic formulation from which they originate, the process by which they are derived, and the numerical constraints they employ. Choice, once again, abounds. A short list of the more popular techniques would include the finite difference, finite element, and boundary integral methods[1.3,15]. The classification is not exhaustive, nor, indeed, rigid; Zienkiewicz[1.15], for example, extends the definition of the finite element method to encompass the other two.

The above brief survey can only hint at the extensive range of choice available. While abundance of choice is always desirable, it needs to be rationalised, preferably through some unifying theory or framework that allows systematic assessment of alternatives. In the absence of such a framework, the task of making a choice is more of an art than a science, possibly influenced by personal circumstance and bias. The magnitude of the difficulty of the task may be appreciated by noting the protracted, and apparently unresolved, debate on just one of its aspects, namely the relative merits of first-order finite difference and finite element implementations of two-dimensional magnetostatic vector potential formulations[1.16-20].

1.4 The energy approach

Energy is a physical quantity associated with the electromagnetic system in its entirety. It is stationary, possibly extremal, at the unique solution to the problem. The variational principle thus defined furnishes the solution formulation required in step 2 of the general procedure, fig. 1.1. The variation is constrained by one of Maxwell's equations, and enforces the other. Significantly, the energy approach shifts emphasis away from the governing partial differential equation.

Energy expressions are defined in pairs, giving rise to complementary variational principles[1.3,14,21,22]. Both principles are extremal under static conditions, one being a minimum, the other a maximum. The corresponding energy estimates thus constitute upper and lower bounds on the true system energy. Recognition of the interrelationship between complementary formulations is the essence of the contribution of the energy approach to a unifying framework. It leads to a concise mathematical structure that inter-links the various fields and potentials[1.4].

The main limitation of the approach has been its inability to generate well-defined functionals for certain problems, particularly under time-varying conditions. While it can often be extended to handle such cases[1.3,14], the process robs it of much of its attractive simplicity. The weighted residuals approach is generally considered more convenient because it provides a straightforward procedure for deriving workable solution formulations[1.15].

In the context of computational electromagnetics over the past fifteen years, the development of complementary energy principles has proceeded mainly by adapting parallel theory from other areas of mathematical physics.

Arthurs[1.21] used the theory of linear operators and functional analysis to generalise the principles of analytical mechanics into an abstract theory of complemen-

tary variational principles. He applied the theory to determine upper and lower bounds in a number of problems of mathematical physics, including electric capacitance and resistance.

Cambrell[1•22] used a similar approach to derive bounds on inductance and capacitance. He established a mathematical structure for the variables involved, and applied the complementary principles to numerical solution of electromagnetic field problems. He also considered the high frequency problem.

Fraser[1•14] and Penman and Fraser[1•23] used functional analysis to generalise the Hu-Washizu[1•24] functionals of elasticity into abstract expressions of complementary variational principles, and to describe the mathematical structure of the systems involved formally yet concisely. Applications of the general theory, which is restricted to static electromagnetics, emphasised numerical implementation by the finite element method[1•14,25]. Solution formulations were extended to the harmonic eddy-current problem[1•14], and the structural framework to the general time-varying case[1•4,14,23].

Each of the above derivations was shown to be equivalent to the hypercircle[1•26], an abstract treatment that is conducive to intuitive geometrical interpretation.

In contrast to the abstract formalism of the above treatments, Hammond and co-workers[1•3,27-29] emphasised the underlying physical processes. The theory of analytical mechanics was reinterpreted in electromagnetic terms to derive complementary formulations from the principle of virtual work. Physically based intuition was also used to devise simple ways of calculating highly accurate estimates of lumped circuit parameters; the finite element method was applied for the same purpose[1•30]. Hammond[1•3] and Hammond and Penman[1•31] treated time-varying problems by viewing complex conjugates of fields as belonging to an adjoint system having a negative time-sequence.

Thatcher[1•32] defined a positive error in terms of the difference between the complementary numerical estimates of the field distributions, and used it to assess mesh adequacy in an electrostatic finite element solution. Cendes et al.[1•33] used similar finite element errors, in conjunction with Delaunay triangulation, to develop a self-adaptive mesh refinement algorithm.

1.5 The proposed error-based approach

This thesis presents an alternative, error-based derivation of solution formulations. Chapter 2 gives a universal definition of the error in terms of the fields, and shows that it is non-negative, being zero if, and only if, the fields satisfy the constitutive relationship. In effect, error minimisation imposes the constitutive relationship on the fields. The universal variational principle thus defined furnishes the solution formulation required in step 2 of the general procedure of fig. 1.1. In contrast to existing approaches, the fields are constrained to satisfy both of Maxwell's equations explicitly during the variation. Details of this implementation of the general procedure are described in Chapter 3 for the static case. It is shown that, for a well-posed problem, the constitutive error separates into complementary functionals, or energies, thus providing an alternative derivation of complementary variational principles and energy bounds. Chapter 4 compares with existing derivations, and shows that the error is, in fact, the difference between established energy bounds. Extracting the bounds from the error, rather than the other way around, results in a degree of generalisation since the error has a standard, universal definition.

As a direct result of not enforcing the constitutive relationship explicitly, the approach leads to a structural framework that places each field on one side or the other of the relationship. It follows that the remaining physical specifications of sec. 1.2, namely Maxwell's equations,

continuity conditions, and boundary conditions, are similarly polarised. Potentials are viewed as solution tools that enforce Maxwell's equations on their corresponding fields.

Chapter 5 introduces numerical constraints, step 3 in fig. 1.1, and presents error-based derivations of standard finite difference, finite element, and boundary integral element equations, step 4. The constitutive error is a comprehensive measure of the numerical error, provided the trial fields satisfy the remaining physical specifications exactly.

Chapter 6 derives complementary formulations for a range of static problems. Linear two-dimensional finite element results are presented, highlighting the comparative computational behaviour of the complementary solutions. Error-guided mesh refinement is demonstrated; the constitutive error of the thesis is a generalisation of the error defined in references 1.32 and 1.33. Non-linear magnetostatic problems are solved in Chapter 7, where it is shown that energy bounds yield non-bounding estimates of non-linear lumped circuit parameters.

Chapters 8, 9, and 10 apply the proposed approach to three areas of some interest in computational electromagnetics : inaccuracies in magnetostatic scalar potential formulations, limitations of mixed formulation, and solvability of vector potential formulations. The approach is found to offer added perspective and insight, often suggesting improvements; it also provides a practical means for assessing alternatives.

Extension of the error-based approach to the time-varying case, detailed in Chapter 11, is straightforward because the error, unlike energy, has a standard, universal definition. It is shown that although the error is not guaranteed to separate as in the static case, complementary and dual solution formulations can always be extracted.

The presentation highlights the error-based numerical significance of various formulations, and compares them to existing treatments. Complementary formulations are derived for the eddy-current problem under steady and transient conditions, and for the high frequency problem.

Conclusions are summarised in Chapter 12, the principal conclusion being that minimisation of the constitutive error is, effectively, what many established formulations do, or attempt to do. This is the essence of the contribution of the proposed approach to a unifying framework, the error being universally defined and computable. The chapter goes on to suggest ways by which such an error-based framework can be put to good use in computational electromagnetics.

C H A P T E R T W O

The Constitutive Relationship

2.1 Preview

This chapter examines the constitutive relationship between fields in material media with the purpose of casting it in error form. Provided the relationship possesses two properties, given in sec. 2.2, such a formulation is possible, even for non-linear and anisotropic media. These properties are not unduly restrictive; most materials of practical interest can be accommodated. The error formulation is constructed in sec. 2.3 where its relevant properties are also investigated. A simple graphical interpretation of the error is presented in sec. 2.4.

2.2 Definitions

We shall be concerned with two vector fields, $\underline{H}$ and $\underline{B}$, in a region R whose relevant material properties can be represented, at any given point, by a constitutive relationship of the general form

$$\underline{B} = \mu(\underline{H})\underline{H} + \underline{B}_r \qquad (2.1a)$$

or

$$\underline{H} = \nu(\underline{B})\underline{B} + \underline{H}_c \qquad (2.1b)$$

where $\underline{B}_r$ and $\underline{H}_c$ are known constants. The constitutive operators $\mu(\underline{H})$ and $\nu(\underline{B})$ are, in the general case, non-linear and anisotropic tensors (or dyads).

This work is restricted to constitutive relationships that possess the following two properties :

1. If $\underline{H}_1$ and $\underline{B}_1$ are related to each other by eqns. 2.1, and so are $\underline{H}_2$ and $\underline{B}_2$, then

$$\langle \underline{H}_2-\underline{H}_1 \ , \ \underline{B}_2-\underline{B}_1 \rangle \geq 0 \qquad (2.2a)$$

with

$$\langle \underline{H}_2-\underline{H}_1 \ , \ \underline{B}_2-\underline{B}_1 \rangle = 0 \iff \underline{H}_2 = \underline{H}_1 \text{ and } \underline{B}_2 = \underline{B}_1 \qquad (2.2b)$$

2. The derivatives $\partial(\mu(\underline{H})\underline{H})/\partial\underline{H}$ and $\partial(\nu(\underline{B})\underline{B})/\partial\underline{B}$ are symmetric; i.e.

$$\partial(\mu(\underline{H})\underline{H})_i/\partial H_j = \partial(\mu(\underline{H})\underline{H})_j/\partial H_i \qquad (2.3a)$$

and

$$\partial(\nu(\underline{B})\underline{B})_i/\partial B_j = \partial(\nu(\underline{B})\underline{B})_j/\partial B_i \qquad (2.3b)$$

where the subscripts i and j refer to the space components of the respective vectors.

Formally, property 1 states that the constitutive operators are strictly monotone[2.1]. It excludes negative slopes, and implies single-valuedness, a one-to-one correspondence between $\underline{H}$ and $\underline{B}$. This, in turn, implies that $\mu(\underline{H})\underline{H}+\underline{B}_r$ and $\nu(\underline{B})\underline{B}+\underline{H}_c$ are continuous functions of $\underline{H}$ and $\underline{B}$ respectively, and that over no range of $\underline{H}$ (or $\underline{B}$) is $\mu(\underline{H})\underline{H}+\underline{B}_r$ (or $\nu(\underline{B})\underline{B}+\underline{H}_c$) constant.

Appendix A shows that one implication of property 2 is that $\mu(\underline{H})\underline{H}+\underline{B}_r$ and $\nu(\underline{B})B+\underline{H}_c$ are gradients of well-defined, computable scalars $\chi(\underline{H})$ and $\psi(\underline{B})$ w.r.t. the components of $\underline{H}$ and $\underline{B}$ respectively :

$$\mu(\underline{H})\underline{H} + \underline{B}_r = \sum_i \underline{a}_i \, \partial\chi(\underline{H})/\partial H_i = \text{grad}_H \, \chi \qquad (2.4a)$$

and

$$\nu(\underline{B})\underline{B} + \underline{H}_c = \sum_i \underline{a}_i \, \partial\psi(\underline{B})/\partial B_i = \text{grad}_B \, \psi \qquad (2.4b)$$

where i ranges over the three component directions, and $\underline{a}_i$ is a unit vector in the direction of the ith component; the subscripts H and B indicate that the partial derivatives, in the gradients, are w.r.t. the components of $\underline{H}$ and $\underline{B}$ respectively. Formally, eqns. 2.4 state that the constitutive operators are potential operators, with $\chi(\underline{H})$ and $\psi(\underline{B})$ as their potentials[2-1] . Appendix A further shows that

$$\chi(\underline{H}) = \chi(\underline{H}_o) + \int_{\underline{H}_o}^{\underline{H}} <\mu(\underline{h})\underline{h} + \underline{B}_r \ , \ d\underline{h}> \qquad (2.5a)$$

and

$$\psi(\underline{B}) = \psi(\underline{B}_o) + \int_{\underline{B}_o}^{\underline{B}} <\nu(\underline{b})\underline{b} + \underline{H}_c \ , \ d\underline{b}> \qquad (2.5b)$$

where $\underline{H}_o$ and $\underline{B}_o$ are arbitrary reference field values, and $\chi(\underline{H}_o)$ and $\psi(\underline{B}_o)$ are arbitrary constants. Moreover, Appendix B shows that, by virtue of prop. 1, these scalars, or potentials, are strictly convex[2-1]:

$$<\underline{H}_2 - \underline{H}_1 \ , \ \text{grad}_{H_2} \chi(\underline{H})> \geq \chi(\underline{H}_2) - \chi(\underline{H}_1) \qquad (2.6a)$$

and

$$<\underline{B}_2 - \underline{B}_1 \ , \ \text{grad}_{B_2} \psi(\underline{B})> \geq \psi(\underline{B}_2) - \psi(\underline{B}_1) \qquad (2.6b)$$

The practical implications of prop. 2 are somewhat abstract. A given constitutive relationship must be examined, using eqns. 2.3, to establish whether or not it possesses prop. 2. Materials of practical interest in numerical electromagnetism generally do. A linear material property tensor that is also symmetric possesses prop. 2. So does isotropic iron whose permeability is a function of field magnitude.

Eqns. 2.1 express the constitutive relationship in the most general form applicable to this work. In non-hysteretic materials they reduce to

$$\underline{B} = \mu(\underline{H})\underline{H} \quad \text{and} \quad \underline{H} = \nu(\underline{B})\underline{B} \qquad (2.7)$$

Moreover, in linear media, μ and ν are constant, although possibly anisotropic.

The constitutive relationship, described above in terms of abstract fields, applies to three distinct sets of fields in electromagnetism : magnetic fields in magnetically permeable regions, electrostatic fields in dielectrics, and current flow in conductors.

2.3 An error formulation

The general definitions of the scalars $\chi(\underline{H})$ and $\psi(\underline{B})$ are given in eqns. 2.5. Since the reference fields $\underline{H}_o$ and $\underline{B}_o$ are arbitrary, it is possible, without loss of generality, to set them both to zero, so that

$$\chi(\underline{H}) = \int_0^{\underline{H}} <\mu(\underline{h})\underline{h} + \underline{B}_r \ , \ d\underline{h}> + \chi(0) \qquad (2.8a)$$

and

$$\psi(\underline{B}) = \int_0^{\underline{B}} <\nu(\underline{b})\underline{b} + \underline{H}_c \ , \ d\underline{b}> + \psi(0) \qquad (2.8b)$$

$\chi(0)$ and $\psi(0)$ are arbitrary constants; we shall find it useful to define them as follows :

$$\chi(0) + \psi(0) = \int_{\underline{H}_c}^{0} <\mu(\underline{h})\underline{h}+\underline{B}_r, d\underline{h}> = \int_{\underline{B}_r}^{0} <\nu(\underline{b})\underline{b}+\underline{H}_c, d\underline{b}> \qquad (2.9)$$

The actual manner with which the constant sum is apportioned between $\chi(0)$ and $\psi(0)$ is immaterial.

Now for arbitrary field estimates $\underline{H}$ and $\underline{B}$ that are not necessarily related by eqns. 2.1, we can construct, and evaluate, the scalar

$$\lambda(\underline{H},\underline{B}) = \chi(\underline{H}) + \psi(\underline{B}) - \zeta(\underline{H},\underline{B}) \qquad (2.10)$$

where

$$\zeta(\underline{H},\underline{B}) = <\underline{H} \ , \ \underline{B}> \qquad (2.11)$$

Appendix C shows that, due to the convexity of $\chi(\underline{H})$ and $\psi(\underline{B})$, eqns. 2.6, the scalar $\lambda(\underline{H},\underline{B})$ has the following fundamental property :

$$\lambda(\underline{H},\underline{B}) \geq 0 \qquad (2.12a)$$

with

$$\lambda(\underline{H},\underline{B}) = 0 \iff \underline{B} = \mu(\underline{H})\underline{H} + \underline{B}_r \quad \text{and} \quad \underline{H} = \nu(\underline{B})\underline{B} + \underline{H}_c \qquad (2.12b)$$

i.e. strict inequality for $\underline{H}$ and $\underline{B}$ field values that do not satisfy the constitutive relationship, eqns. 2.1.

It is obvious from 2.12 that $\lambda(\underline{H},\underline{B})$ is an error form that corresponds to the constitutive relationship : it is zero for $\underline{H}$ and $\underline{B}$ field estimates that satisfy the constitutive relationship, and positive otherwise. λ is central to this work, and will be referred to as the constitutive error density. It is definable for constitutive relationships that possess prop. 2 of sec. 2.2, and its error significance, eqns. 2.12, arises from prop. 1.

It follows, from eqns. 2.12, that $\lambda(\underline{H},\underline{B})$ is minimum for field estimates that satisfy the constitutive relationship. From eqns. 2.8-11, the variation of λ is given by

$$\delta\lambda = \delta\chi + \delta\psi - \delta\zeta \qquad (2.13a)$$

$$= \langle \mu\underline{H} + \underline{B}_r - \underline{B} \, , \, \delta\underline{H} \rangle + \langle \nu\underline{B} + \underline{H}_c - \underline{H} \, , \, \delta\underline{B} \rangle \qquad (2.13b)$$

Clearly, if $\underline{H}$ and $\underline{B}$ are related by eqns. 2.1, then

$$\delta\lambda = 0 \qquad (2.14)$$

giving us the stationary point of λ, which is a strict minimum. It is noted in passing that the actual value of λ at its stationary minimum was made zero by a specific choice of the arbitrary constants $\chi(0)$ and $\psi(0)$ in eqn. 2.9.

It is instructive to note that for a linear, non-hysteretic constitutive relationship, the integrations of eqns. 2.8 are simple to perform; substituting the results

into eqn. 2.10, the expression for λ simplifies to

$$\lambda = \tfrac{1}{2}\langle \mu\underline{H} \, , \, \underline{H}\rangle + \tfrac{1}{2}\langle \nu\underline{B} \, , \, \underline{B}\rangle - \langle \underline{H} \, , \, \underline{B}\rangle \qquad (2.15a)$$

$$= \tfrac{1}{2}\langle \mu\underline{H} - \underline{B} \, , \, \underline{H}\rangle + \tfrac{1}{2}\langle \nu\underline{B} - \underline{H} \, , \, \underline{B}\rangle \qquad (2.15b)$$

and the error significance of λ is obvious in this case.

Now consider a region in space, R, where arbitrary estimates are made for the field distributions $\underline{H}(\underline{r})$ and $\underline{B}(\underline{r})$. Clearly, $\lambda(\underline{H},\underline{B})$ is a point-defined error. Its volume integral over R is the total constitutive error Λ attributed to R for the given estimates of the field distributions :

$$\Lambda = \int_R \lambda \, dR = X + \Psi - Z \qquad (2.16)$$

where

$$X = \int_R \chi \, dR \, , \quad \Psi = \int_R \psi \, dR \, , \quad \text{and} \quad Z = \int_R \zeta \, dR = \langle \underline{H} \, , \, \underline{B}\rangle_R \qquad (2.17)$$

The volume integral of a non-negative scalar cannot be negative, and can be zero only if the scalar is zero everywhere (with the possible exception of singularity points, if any). Thus, from eqns. 2.12 and 2.16, we have

$$\Lambda \geq 0 \qquad (2.18a)$$

with

$$\Lambda = 0 \iff \underline{B}=\mu(\underline{H})\underline{H}+\underline{B}_r \text{ and } \underline{H}=\nu(\underline{B})\underline{B}+\underline{H}_c \text{ everywhere in R .} \qquad (2.18b)$$

Strictly, the forward implication does not apply at points where λ is singular.

From eqns. 2.13 and 2.16, the variation of the global constitutive error Λ is given by

$$\delta\Lambda = \delta X + \delta\Psi - \delta Z \qquad (2.19a)$$

$$= \langle \mu\underline{H} + \underline{B}_r - \underline{B} \, , \, \delta\underline{H}\rangle_R + \langle \nu\underline{B} + \underline{H}_c - \underline{H} \, , \, \delta\underline{B}\rangle_R \qquad (2.19b)$$

Clearly, if the estimated distributions $\underline{H}(\underline{r})$ and $\underline{B}(\underline{r})$ satisfy the constitutive relationship everywhere in R, then

$$\delta\Lambda = 0 \qquad (2.20)$$

giving us the stationary point of Λ, which is a strict minimum corresponding to eqn. 2.18b.

2.4 A graphical interpretation

This section presents a graphical interpretation of the constitutive error density λ for the simple case of an isotropic medium in which the constitutive relationship is a function of the field magnitudes. Such a relationship possesses prop. 2 of sec. 2.2. It is illustrated by the B-H curve of fig. 2.1. In accordance with prop. 1, the curve is continuous and has a strictly positive slope.

Independently made estimates of $\underline{H}$ and $\underline{B}$ define a point (H,B) that may fall above, below, or on the B-H curve. $\chi(\underline{H})$ and $\psi(\underline{B})$ are, respectively, the shaded areas below and above the curve, so that $\chi+\psi$ is the total shaded area in either figure. It is noted in passing that in magnetic

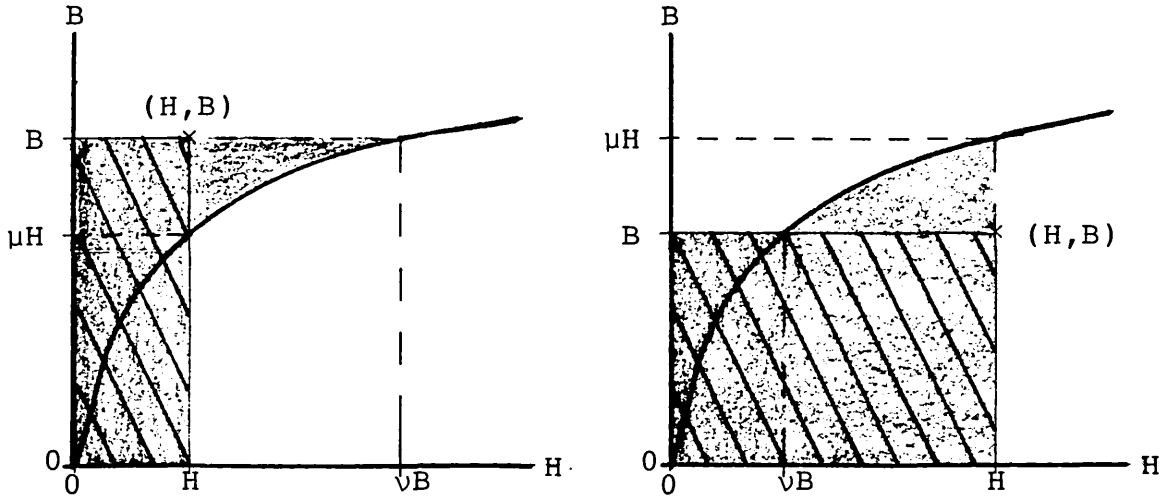

(a) (H,B) above curve. (b) (H,B) below curve.

Fig. 2.1 Illustrating the constitutive relationship and error density for different field estimates.

applications, χ corresponds to the energy, while ψ corresponds to the co-energy.

The hatched rectangle represents the product of magnitudes H B. From either figure

$$\chi + \psi \geqq H B \geqq H B \cos \alpha \qquad (2.21a)$$

where α is the space angle between $\underline{H}$ and $\underline{B}$. But

$$\zeta = H B \cos \alpha$$

by definition, eqn. 2.11. Thus

$$\chi + \psi \geqq \zeta \qquad (2.21b)$$

Subtracting ζ from both sides, and noting eqn. 2.10

$$\lambda = \chi + \psi - \zeta \geqq 0$$

as in ineq. 2.12a. For λ to be zero, both inequalities in 2.21a must be reduced to equalities: $\underline{H}$ and $\underline{B}$ must be parallel so that $\alpha = 0$, and the point (H,B) must lie on the B-H curve. Thus λ is a comprehensive measure of the error in the constitutive relationship, accounting for both magnitude and direction. In either figure, the shaded but unhatched triangular area corresponds to $(\chi + \psi - HB)$; it is therefore generally smaller than λ, becoming equal to it at $\cos \alpha = 1$, i.e. $\alpha = 0$.

C H A P T E R T H R E E

Specification and Solution of Static Electromagnetic Problems

3.1 Preview

The purpose of this chapter is to present a compact theory of static electromagnetic problems, based on the error formulation of Chapter 2, and particularly suited to numerical solution.

Under static conditions, Maxwell's equations reduce to three sets of independent equations relating to magnetostatics, electrostatics, and steady current flow. Recognising a unifying pattern, a general model is defined in sec. 3.3. The model can, of course, represent other physical problems that adhere to the same pattern.

Sec. 3.4 presents a thorough study of physical uniqueness of model fields through an extended development of the Helmholtz theorem. The study also covers the implementation and interpretation of physical uniqueness in terms of potentials, as well as the uniqueness requirements of the potentials themselves for problem solvability.

Sec. 3.5 applies the conditions of physical uniqueness to the constitutive error formulation devised in Chapter 2, resulting in a general, yet concise, theory for the solution of the model problem. By way of demonstration, sec. 3.6 applies the proposed approach to a particular class of problem where the specifications, being relatively simple, are of some general interest.

3.2 Maxwell's equations

Maxwell's equations in differential form are

$$\text{curl } \underline{H} = \underline{J} + \frac{\partial}{\partial t} \underline{D} \tag{3.1a}$$

$$\text{div } \underline{D} = \rho \tag{3.1b}$$

$$\text{curl } \underline{E} = \frac{\partial}{\partial t} \underline{B} \tag{3.1c}$$

$$\text{div } \underline{B} = 0 \tag{3.1d}$$

Under static conditions, where all fields are constant in time, eqns. 3.1 reduce to three independent pairs of equations corresponding to the three material properties of interest in electromagnetics.

(i) In magnetically permeable regions, the relevant variables are the magnetic field intensity $\underline{H}$ and the magnetic flux density $\underline{B}$, related by the constitutive relationship

$$\underline{B} = \mu \underline{H} + \underline{B}_r \quad \text{or} \quad \underline{H} = \nu \underline{B} + \underline{H}_c \tag{3.2}$$

where μ is the magnetic permeability, ν is the reluctivity, $\underline{B}_r$ is the residual flux density, and $\underline{H}_c$ is the coercive force. Under static conditions, eqns. 3.1a and 3.1d yield

$$\text{curl } \underline{H} = \underline{J} \tag{3.3}$$

and

$$\text{div } \underline{B} = 0 \tag{3.4}$$

where $\underline{J}$ is the current density. A familiar treatment of eqn. 3.3 shows that, across any surface, the discontinuity in the tangential component of $\underline{H}$ is given by

$$\underline{n} \times \Delta \underline{H} = \underline{K} \tag{3.5}$$

where $\underline{K}$ is the sheet current flowing over that surface. The corresponding treatment of eqn. 3.4 shows that the normal component of $\underline{B}$ is continuous, so that

$$\underline{n} \cdot \Delta \underline{B} = 0 \tag{3.6}$$

across any surface.

(ii) In dielectrics, the relevant variables are the electric field intensity $\underline{E}$ and the electric flux density $\underline{D}$, related by the constitutive relationship

$$\underline{D} = \varepsilon \underline{E} \quad \text{or} \quad \underline{E} = \varepsilon^{-1} \underline{D} \tag{3.7}$$

where ε is the permittivity. Under static conditions, eqns. 3.1c and 3.1b yield

$$\text{curl } \underline{E} = 0 \tag{3.8}$$

and

$$\text{div } \underline{D} = \rho \tag{3.9}$$

where ρ is the charge density. Across any surface, the tangential component of $\underline{E}$ is continuous

$$\underline{n} \times \Delta \underline{E} = 0 \tag{3.10}$$

while the discontinuity in the normal component of $\underline{D}$ is given by

$$\underline{n} \cdot \Delta \underline{D} = \sigma \tag{3.11}$$

where σ is the sheet charge density on that surface.

(iii) In electrical conductors, the relevant variables are the electric field intensity $\underline{E}$ and the electric current density $\underline{J}$, related by the constitutive relationship

$$\underline{J} = \sigma \underline{E} \quad \text{or} \quad \underline{E} = \rho \underline{J} \tag{3.12}$$

where σ is the electric conductivity and ρ is the resistivity. Under static conditions, eqns. 3.1c and 3.1a yield

$$\text{curl } \underline{E} = 0 \tag{3.13}$$

and

$$\text{div } \underline{J} = 0 \tag{3.14}$$

The tangential component of $\underline{E}$ and the normal component of $\underline{J}$ are continuous across all surfaces, so that

$$\underline{n} \times \Delta \underline{E} = 0 \tag{3.15}$$

and

$$\underline{n} \cdot \Delta \underline{J} = 0 \tag{3.16}$$

3.3 A model

The static field equations of sec. 3.2 clearly adhere to a pattern. For each type of material, there is a pair of fields that are related by a constitutive relationship; one is an intensity field whose curl and tangential discontinuities (vector sources) are specified, while the other is a flux density whose divergence and normal discontinuities (scalar sources) are specified.

In Chapter 2 we considered the constitutive relationship between two abstract fields $\underline{H}$ and $\underline{B}$:

$$\underline{B} = \mu(\underline{H})\underline{H} + \underline{B}_r \quad \text{or} \quad \underline{H} = \nu(\underline{B})\underline{B} + \underline{H}_c \tag{3.17}$$

We now make these fields less abstract by requiring them to be piecewise differentiable, and to satisfy the canonical equations

$$\text{curl } \underline{H} = \underline{J} \tag{3.18}$$

and

$$\text{div } \underline{B} = \rho \tag{3.19}$$

as well as the continuity equations

$$\underline{n} \times \Delta\underline{H} = \underline{K} \tag{3.20}$$

and

$$\underline{n} \cdot \Delta\underline{B} = \sigma \tag{3.21}$$

Clearly, the abstract fields $\underline{H}$ and $\underline{B}$ now conform to the pattern described earlier. They are a generalisation of the physical pairs of fields identified in sec. 3.2. The abstract pair, as defined by eqns. 3.18-21, can therefore be used to model the physical pairs. Table 3.1 shows the correspondence between physical and model systems, and fig. 3.1 shows the structure of the model.

It will be helpful to think of the model as being composed of two complementary systems : the H-system comprising the left half of fig. 3.1, and the B-system comprising the right half. Eqns. 3.18 and 3.20, the

	Model systems	Magneto-statics	Electro-statics	Steady current flow
H-system	$\underline{H}$	$\underline{H}$	$\underline{E}$	$\underline{E}$
	μ	μ	ε	σ
	$\underline{B}_r$	$\underline{B}_r$	0	0
	$\underline{J}$	$\underline{J}$	0	0
	$\underline{K}$	$\underline{K}$	0	0
B-system	$\underline{B}$	$\underline{B}$	$\underline{D}$	$\underline{J}$
	ν	ν	ε^{-1}	ρ
	$\underline{H}_c$	$\underline{H}_c$	0	0
	ρ	0	ρ	0
	σ	0	σ	0

Table 3.1 Correspondence between physical and model systems.

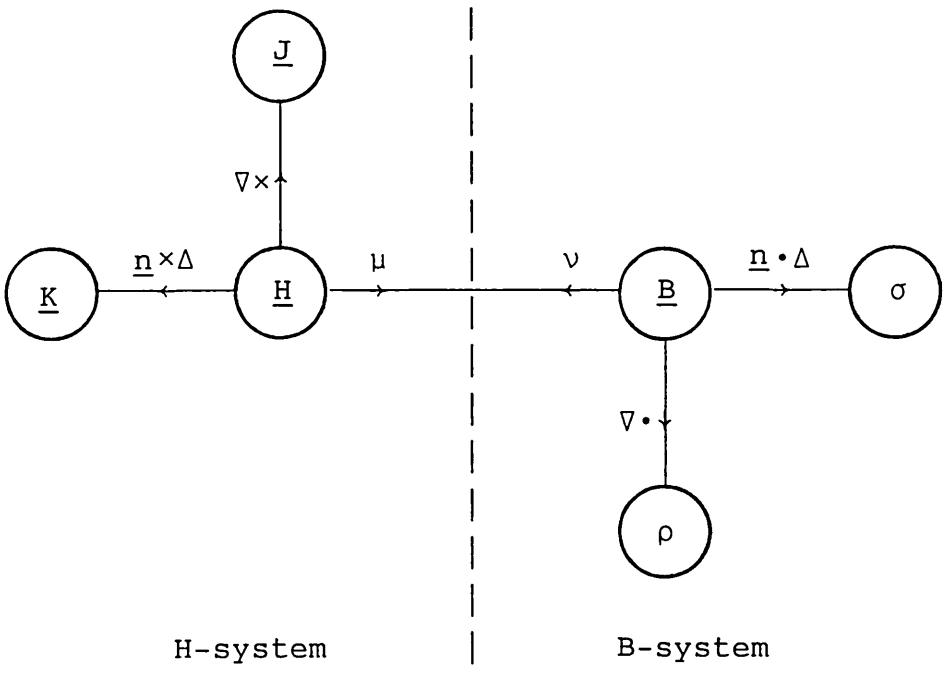

Fig. 3.1 Model structure.

variable $\underline{H}$, and the vector sources $\underline{J}$ and $\underline{K}$ belong to the H-system; eqns. 3.19 and 3.21, the variable $\underline{B}$, and the scalar sources ρ and σ belong to the B-system. Clearly, the only link between the two systems is the constitutive relationship, eqns. 3.17.

3.4 Problem specification

For our purposes, a problem involves a region in space, R, where the model fields of sec. 3.3, $\underline{H}$ and $\underline{B}$, coexist. Solving the problem is the process of determining the field distributions.

We define R to be a simply-connected region in three-dimensional space, bounded by surface S. In general, S is composed of N simply-connected sub-sections, so that

$$S = S_1 \cup S_2 \ldots \cup S_N \tag{3.22a}$$

with

$$S_i \cap S_j = 0 \quad \text{for} \quad i \neq j \tag{3.22b}$$

Within R there are M surfaces across which the tangential component $\underline{H}$ and/or the normal component of $\underline{B}$ are/is discontinuous, i.e. where $\underline{K}$ and/or σ are/is non-zero. Denote the union of these discontinuities by S^{Δ} :

$$S^{\Delta} = S_1^{\Delta} \cup S_2^{\Delta} \ldots \cup S_M^{\Delta} \tag{3.23}$$

Multiply-connected regions are converted into simply-connected ones by the introduction of cuts as in fig. 3.2; they can thus be accommodated into the above definition of R by including the two facets of every such cut with the N sub-sections of S as shown in the figure.

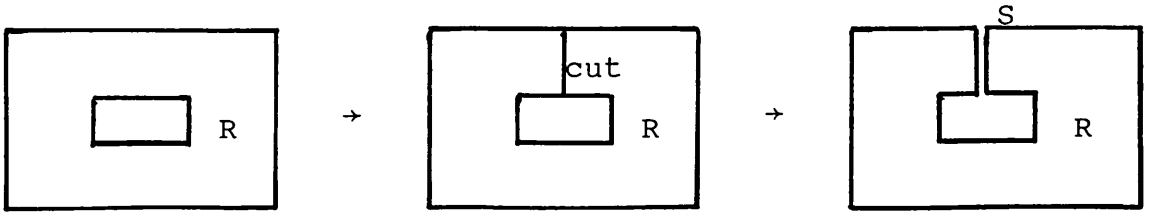

Fig. 3.2 Converting a multiply-connected region into a simply-connected one.

3.4.1 Uniqueness of fields

To be able to solve a given problem, it must be well-posed, i.e. there must exist unique field distributions for the given problem specifications. The purpose of this section is to determine what constitutes adequate specification for the uniqueness of the model fields $\underline{H}(\underline{r})$ and $\underline{B}(\underline{r})$.

With the problem region R, bounding surface S, and discontinuities S^{Δ} as defined above, we start from the following premises :

1. The constitutive relationship :
   Everywhere in R, $\underline{H}$ and $\underline{B}$ are related by a known constitutive relationship, eqns. 3.17, which possesses property 1 of sec. 2.2.

2. Canonical equations :
   Everywhere in R, $\underline{H}$ and $\underline{B}$ are piecewise differentiable, with the curl of $\underline{H}$ and the divergence of $\underline{B}$ specified by eqns. 3.18 and 3.19 respectively; the source densities $\underline{J}(\underline{r})$ and $\rho(\underline{r})$ are known and finite.

3. Continuity conditions :
   Across any surface within R, the discontinuities in the tangential component of $\underline{H}$ and the normal component of $\underline{B}$ are specified, respectively, by eqns. 3.20 and 3.21, with the source densities $\underline{K}(\underline{r})$ and $\sigma(\underline{r})$ known and finite.

The above three specifications constitute a concise description of the model we have developed so far. To investigate the uniqueness of the fields thus specified, we postulate two pairs of distributions, $\underline{H}_1(\underline{r})$, $\underline{B}_1(\underline{r})$ and $\underline{H}_2(\underline{r})$, $\underline{B}_2(\underline{r})$, with each pair satisfying all three specifications; the fields are unique if the two pairs coincide. Next define

$$\delta\underline{H}(\underline{r}) = \underline{H}_2(\underline{r}) - \underline{H}_1(\underline{r}) \qquad (3.24a)$$

$$\delta\underline{B}(r) = \underline{B}_2(\underline{r}) - \underline{B}_1(\underline{r}) \qquad (3.24b)$$

and

$$W = \langle \delta H \ , \ \delta B \rangle_R \tag{3.25}$$

As each pair satisfies specification 1 above, we can substitute eqns. 3.24 and 3.25 into eqns. 2.2 to get

$$W \geq 0 \tag{3.26a}$$

with

$$W = 0 \quad \Leftrightarrow \quad \delta \underline{H} = 0 \quad \text{and} \quad \delta \underline{B} = 0 \tag{3.26b}$$

Clearly, uniqueness is ensured by any set of specifications that forces the equality in 3.26. Appendix D imposes specifications 2 and 3 on $\delta \underline{H}$ and $\delta \underline{B}$ reducing W to

$$W = \sum_{n=1}^{N} w_n \tag{3.27a}$$

where the summation is over all sub-sections of the boundary S, the contribution of each sub-section being

$$w_n = [\delta \int_{\underline{r}_n}^{\underline{r}} \underline{H} \cdot d\underline{\ell} \ , \ \delta(\underline{n} \cdot \underline{B})]_{S_n} + (\delta \int_{\underline{r}_o}^{\underline{r}_n} \underline{H} \cdot d\underline{\ell})(\delta \int_{S_n} \underline{B} \cdot d\underline{S}) \tag{3.27b}$$

$\underline{r}_o$ defines an arbitrary global reference point in R;
$\underline{r}_n$ defines an arbitrary local reference point on S_n.

As W is not universally zero in eqn. 3.27, it is evident that specs. 1, 2, and 3 do not, in themselves, suffice for uniqueness. A further specification is needed :

4. Boundary conditions :
   Over the entire boundary S, the fields $\underline{H}$ and $\underline{B}$ are so constrained that

$$W = \sum_{n=1}^{N} w_n = 0 \tag{3.28}$$

   where w_n is as defined in eqn. 3.27b, and the summation is over all sub-sections of S.

The apparent indefiniteness of spec. 4 reflects the large, indeed infinite, variety of boundary specifications that are consistent with a unique solution. In the next section we examine some of the more common cases.

3.4.2 Boundary specifications

To investigate ways by which spec. 4 of sec. 3.4.1 can be satisfied, we shall find it useful to make a few definitions. First let

$$\underline{h} = \underline{n} \times \underline{H} \tag{3.29}$$

and

$$b = \underline{n} \cdot \underline{B} \tag{3.30}$$

at any point on the bounding surface S. Also let

$$V_n = \int_{\underline{r}_o}^{\underline{r}_n} \underline{H} \cdot d\underline{\ell} \tag{3.31}$$

and

$$\Phi_n = \int_{S_n} \underline{B} \cdot d\underline{S} \tag{3.32}$$

where the subscript n refers to a particular sub-section, S_n, of the bounding surface S, eqns. 3.22. V_n may be regarded as an abstract motive force at $\underline{r}_n$ relative to $\underline{r}_o$; Φ_n may be regarded as an abstract flux through S_n.

Substituting eqns. 3.31 and 3.32 into 3.27, we can write

$$W = W' + W'' \tag{3.33a}$$

and

$$w_n = w_n' + w_n'' \tag{3.33b}$$

where

$$W' = \sum_{n=1}^{N} w_n' \tag{3.34a}$$

with

$$w_n' = [\delta \int_{\underline{r}_n}^{\underline{r}} \underline{H} \cdot d\underline{\ell} \ , \ \delta(\underline{n} \cdot \underline{B})]_{S_n} \tag{3.34b}$$

and

$$W'' = \sum_{n=1}^{N} w_n'' \tag{3.35a}$$

with

$$w_n'' = \delta V_n \ \delta \Phi_n \tag{3.35b}$$

Satisfaction of spec. 4 requires W to vanish. The above definitions allow us to examine the contributions, to W, from the individual sub-sections of S.

Consider first w_n', eqn. 3.34b. Clearly, it vanishes if either $\delta\underline{h}$ or δb is zero, i.e. either $\underline{h}$ or b is known on S_n. This leads us to define S_h as the union of boundary sub-sections over which $\underline{h}$ is pre-specified, and S_b as the union of boundary sub-sections over which b is pre-specified; thus

$$\text{on } S_h \subset S : \underline{h} \text{ is specified} \Rightarrow \delta\underline{h} = 0 \qquad (3.36)$$

and

$$\text{on } S_b \subset S : b \text{ is specified} \Rightarrow \delta b = 0 \qquad (3.37)$$

$\underline{h}$ and b are defined in eqns. 3.29 and 3.30 respectively.

w_n' also vanishes if S_n is an open boundary section where H and B approach zero at least as fast as the inverse of r^2. Denoting the union of open-boundary sub-sections by S_∞, we must have

$$\text{on } S_\infty \subset S : r^2H \text{ and } r^2B \text{ are bounded} \qquad (3.38)$$

If the conditions on two, or possibly more, boundary sections are suitably related to each other, their w_n' contributions to W can cancel out. This happens with certain recurrence relationships. It also happens on the two facets of a cut since their outward normals are in opposite directions.

Consider next w_n''. From eqn. 3.35b, it is clear that w_n'' vanishes if either δV_n or $\delta\Phi_n$ is zero, i.e. if either V_n or Φ_n is known on S_n. According to the definition of S_b in 3.37 and of Φ_n in eqn. 3.32, Φ_n is pre-specified on all S_b sub-sections so that their w_n'' contributions automatically vanish. The same cannot be said for S_h and S_∞; on such boundary sections, w_n'' must be accounted for explicitly.

If the motive forces V_n and fluxes Φ_n on two or more boundary sections are suitably related, their w_n'' contribu-

tions to W can cancel out. Of particular interest is the situation arising on the two facets of a cut. Obviously, their outgoing fluxes are equal in magnitude and opposite in sign; thus

$$\Phi_{n2} = -\Phi_{n1} = \Phi_n$$

where the subscripts refer to the two facets; substituting into 3.35b and adding the contributions of the two facets :

$$w''_n = w''_{n1} + w''_{n2} = \delta\Phi_n(\delta V_{n2} - \delta V_{n1})$$

Substituting for V_{n1} and V_{n2} from eqn. 3.31 :

$$w''_n = \delta\Phi_n\left(\delta\int_{\underline{r}_o}^{\underline{r}_2}\underline{H}\cdot d\underline{\ell} - \delta\int_{\underline{r}_o}^{\underline{r}_1}\underline{H}\cdot d\underline{\ell}\right) = \delta\Phi_n\left(\delta\int_{\underline{r}_1}^{\underline{r}_2}\underline{H}\cdot d\underline{\ell}\right)$$

where $\underline{r}_1$ and $\underline{r}_2$ are reference points on the two facets; choosing these to coincide in space, and substituting for Φ_n from eqn. 3.32, we get

$$w''_n = \left(\delta\int_{S_n}\underline{B}\cdot d\underline{S}\right)\left(\delta\oint_{\ell''_n}\underline{H}\cdot d\underline{\ell}\right) \qquad (3.39)$$

where ℓ''_n is a path in R that pierces the cut. It is thus evident that w''_n vanishes if we specify either the flux through the cut, or the motive force around a closed path that pierces the cut once.

It is instructive to note that w''_n is implicitly accounted for in problems with certain simple boundary specifications. For example, consider the case where S is composed of only two simply-connected sub-sections, S_h and S_b, which conform to the definitions 3.36 and 3.37; on S_b, w''_b vanishes as explained earlier; it also vanishes on S_h by, effectively, allowing the global reference point $\underline{r}_o$ to coincide with the reference point on S_h so that V_h becomes zero. This implicit treatment is not possible when S includes two or more unconnected S_h and/or S_∞ sub-sections. The motive forces between these sections, or the fluxes through them, must be pre-specified if W" is to vanish. The situation is, in fact, a generalisation of resistive circuit analysis, with V_n and Φ_n corresponding, respectively,

to terminal voltages and currents, with one terminal acting as a reference for voltages.

3.4.3 Potentials

Having determined the specifications necessary to ensure well-posedness, we now address the question of how to impose these specifications on the model fields. We shall deal with spec. 1, covering the constitutive relationship, in sec. 3.5, and consider only specs. 2, 3, and 4 in this section.

A common method for imposing the canonical equations of spec. 2 on the fields involves the definition of potentials. Let

$$\underline{H} = \underline{G} - \text{grad } \Omega \tag{3.40a}$$

where Ω is a scalar potential, and $\underline{G}$ is any pre-defined field that satisfies

$$\text{curl } \underline{G} = \underline{J} \tag{3.40b}$$

everywhere in R. Substituting for $\underline{H}$ from eqns. 3.40 into 3.18, the latter is satisfied. Also let

$$\underline{B} = \underline{C} + \text{curl } \underline{A} \tag{3.41a}$$

where $\underline{A}$ is a vector potential, and $\underline{C}$ is any pre-defined field that satisfies

$$\text{div } \underline{C} = \rho \tag{3.41b}$$

everywhere in R. Substituting for $\underline{B}$ from eqns. 3.41 into 3.19, the latter is satisfied.

With spec. 2 accounted for, the potentials must be so constrained as to effectively impose specs. 3 and 4 on their respective fields. We derive the necessary constraints below.

Consider, first, the continuity conditions of spec.3. Substituting for $\underline{H}$ from eqn. 3.40a into 3.20, and

rearranging, we get

$$\underline{n} \times \text{grad } \Delta\Omega = \underline{n} \times \Delta\underline{G} - \underline{K} \qquad (3.42)$$

over any surface within R. Similarly, substituting for $\underline{B}$ from eqn. 3.41a into 3.21, and rearranging, we get

$$\underline{n} \cdot \text{curl } \Delta\underline{A} = \sigma - \underline{n} \cdot \Delta\underline{C} \qquad (3.43)$$

over any surface within R.

Thus far, the potentials have been considered in differential form only. While on the subject of continuity, we need to examine the corresponding integral forms as they may necessitate the definition of artificial discontinuities in the potentials.

Integrating eqn. 3.18 over any surface S_i in R, and applying Stokes' theorem, we get

$$\oint_{\ell_i} \underline{H} \cdot d\underline{\ell} = \int_{S_i} \underline{J} \cdot d\underline{S} + \int_{\ell_i^\Delta} \underline{K} \times \underline{n} \cdot d\underline{\ell} \qquad (3.44)$$

where ℓ_i is the contour of S_i, and ℓ_i^Δ refers to any discontinuities in $\underline{n} \times \underline{H}$ along S_i. Substituting for $\underline{H}$ from eqn. 3.40a and rearranging, we get

$$\sum_{\ell_i} \Delta\Omega = \oint_{\ell_i} \underline{G} \cdot d\underline{\ell} - \int_{S_i} \underline{J} \cdot d\underline{S} - \int_{\ell_i^\Delta} \underline{K} \times \underline{n} \cdot d\ell \qquad (3.45)$$

where the summation covers the discontinuities in Ω encountered by the path ℓ_i.

Integrating, next, eqn. 3.19 over any sub-region R_i within R, and applying the divergence theorem, we get

$$\oint_{S_i} \underline{B} \cdot d\underline{S} = \int_{R_i} \rho \, dR + \int_{S_i^\Delta} \sigma \, dS \qquad (3.46)$$

where S_i is the surface that encloses R_i, and S_i^Δ refers to any discontinuities in $\underline{n} \cdot \underline{B}$ within R_i. Substituting for $\underline{B}$ from eqn. 3.41a, applying Stokes' theorem, and rearranging, we get

$$\sum_{S_i} \int_{\ell_\Delta} \Delta\underline{A}\cdot d\underline{\ell} = \int_{R_i} \rho \, dR + \int_{S_i^\Delta} \sigma \, dS - \oint_{S_i} \underline{C}\cdot d\underline{S} \qquad (3.47)$$

where ℓ_Δ refers to a slit, piercing S_i, along which $\underline{n}\times\underline{A}$ is discontinuous; the summation covers all such slits.

The right hand sides of eqns. 3.45 and 3.47 are prespecified, and they are not necessarily zero, thus possibly requiring the introduction of artificial discontinuities in the respective potentials to balance the equations on their left hand sides. Such cuts are in addition to any that may be required to convert a multiply-connected region into a simply-connected one, as explained earlier with reference to fig. 3.2.

Consider, next, the boundary conditions of spec. 4. This is best done using the definitions of sec. 3.4.2.

Substituting eqn. 3.40a into 3.29, and applying the result to 3.36, we get

$$\text{on } S_h : \quad \underline{n} \times \text{grad } \Omega = \underline{n} \times \underline{G} - \underline{h} \qquad (3.48)$$

Substituting eqn. 3.41a into 3.30, and applying the result to 3.37, we get

$$\text{on } S_b : \quad \underline{n} \cdot \text{curl } \underline{A} = b - \underline{n} \cdot \underline{C} \qquad (3.49)$$

Substituting eqn. 3.40a into 3.38, we get

$$\text{on } S_\infty : \quad r^2|\underline{G} - \text{grad } \Omega| \quad \text{bounded} \qquad (3.50a)$$

which simplifies to

$$\text{on } S_\infty : \quad r\,\Omega \quad \text{bounded} \qquad (3.50b)$$

if $\underline{G}$ is zero in the open boundary region. Substituting eqn. 3.41a into 3.38, we get

$$\text{on } S_\infty : \quad r^2|\underline{C} + \text{curl } \underline{A}| \quad \text{bounded} \qquad (3.51a)$$

which simplifies to

$$\text{on } S_\infty : \quad r^2 A \quad \text{bounded} \tag{3.51b}$$

if $\underline{C}$ is zero in the open boundary region.

Substituting eqn. 3.40a into 3.31, performing the integration in Ω, and rearranging, we get

$$\Omega(\underline{r}_n) - \Omega(\underline{r}_o) = \sum \Delta\Omega + \int_{\underline{r}_o}^{\underline{r}_n} \underline{G} \cdot d\underline{\ell} - V_n \tag{3.52}$$

where the summation covers all discontinuities in Ω encountered by the path from $\underline{r}_o$ to $\underline{r}_n$. Substituting eqn. 3.41a into 3.32, applying Stokes' theorem, and rearranging, we get

$$\oint_{\ell_n} \underline{A} \cdot d\underline{\ell} = \Phi_n - \int_{S_n} \underline{C} \cdot d\underline{S} \tag{3.53}$$

where ℓ_n is the contour of S_n, including any slits of the form of ℓ_Δ, described in conjunction with eqn. 3.47, that may pierce S_n.

This completes the interpretation of specs. 2, 3, and 4 in terms of potentials. The equations of this section are to be viewed as constraints on the potentials; the right hand sides are, in general, pre-specified. Forcing these constraints on the potentials effectively imposes the respective specifications on the corresponding fields.

3.4.4 Uniqueness of potentials - solvability

If the problem is to be posed, and eventually solved, in terms of potentials, they must, naturally, be uniquely specified. Imposing the specifications of sec. 3.4.1 on the potentials, as was done in sec. 3.4.3, ensures the uniqueness of the resulting $\underline{H}$ and $\underline{B}$ fields, but not that of the potentials themselves. The potential specifications must therefore be completed by introducing additional constraints on them. A degree of flexibility is available in the choice of such constraints, the main criterion being consistency with the original, physical, specifications which may not be violated, whether explicitly or implicitly.

As potentials are, in essence, solution tools, the additional specifications can be regarded as requirements of solvability. In contrast, $\underline{H}$ and $\underline{B}$ model the physical fields, sec. 3.2, and the specifications on them are requirements of physical uniqueness.

3.4.4.1 The H-system scalar potential

Integrating eqn. 4.30a from a global reference point $\underline{r}_o$ to a general point $\underline{r}$ in R, we have

$$\int_{\underline{r}_o}^{\underline{r}} \underline{H} \cdot d\underline{\ell} = \int_{\underline{r}_o}^{\underline{r}} \underline{G} \cdot d\underline{\ell} - \int_{\underline{r}_o}^{\underline{r}} \text{grad}\,\Omega \cdot d\underline{\ell} \qquad (3.54a)$$

Performing the integration in Ω, and rearranging :

$$\Omega(\underline{r}) = \Omega(\underline{r}_o) + \sum \Delta\Omega \Big|_{\underline{r}_o}^{\underline{r}} + \int_{\underline{r}_o}^{\underline{r}} \underline{G}\cdot d\underline{\ell} - \int_{\underline{r}_o}^{\underline{r}} \underline{H}\cdot d\underline{\ell} \qquad (3.54b)$$

where the summation covers discontinuities in Ω encountered by the selected path from $\underline{r}_o$ to $\underline{r}$. The uniqueness of Ω is contingent upon the uniqueness of the right hand side, and we now examine the individual terms. The line integral in $\underline{G}$ is known since $\underline{G}$ is pre-defined everywhere. The line integral in $\underline{H}$ is unique if the requirements of physical uniqueness are observed.

A discontinuity in Ω across a cut necessitated by eqn. 3.45 is known. A discontinuity in Ω arising from $\underline{n} \times \Delta\underline{H}$ and/or $\underline{n} \times \Delta\underline{G}$ is given by integrating eqn. 3.42 along a curve lying in S_n, the surface of discontinuity :

$$\Delta\Omega(\underline{r}) = \Delta\Omega(\underline{r}_n) + \sum \Delta'\Omega \Big|_{\underline{r}_n}^{\underline{r}} + \int_{\underline{r}_n}^{\underline{r}} \Delta\underline{G}\cdot d\underline{\ell} - \int_{\underline{r}_n} \underline{K}\times\underline{n}\cdot d\underline{\ell} \qquad (3.55)$$

$\underline{r}_n$ is a reference point on S_n : if S_n divides R into two sub-regions, $\Delta\Omega(\underline{r}_n)$ can be chosen arbitrarily; if S_n has a floating edge, $\underline{r}_n$ is placed at the edge where $\Delta\Omega(\underline{r}_n)$ is zero. The line integrals are known. The summation

accounts for other surfaces of discontinuity intersecting S_n : the contributions of cuts are known; the contributions of surfaces of discontinuity in $\underline{n} \times \underline{H}$ and/or $\underline{n} \times \underline{G}$, similar to S_n, can be determined sequentially. In effect, $\Delta\Omega$ is known, or pre-specified, however it may arise.

The right hand side of eqn. 3.54b is thus unique to within a single additive constant, $\Omega(\underline{r}_o)$, which must be specified, arbitrarily, to force a unique $\Omega(\underline{r})$.

3.4.4.2 The B-system vector potential

The four specifications of sec. 3.4.1 can be viewed as a general theorem of vector uniqueness. It is therefore possible to investigate the uniqueness of the vector potential $\underline{A}$ by inserting it into a two system model of its own, and applying the theorem.

We begin by introducing a complementary vector $\underline{F}$, and relating it to $\underline{A}$ by the constitutive relationship

$$\underline{F} = \alpha\, \underline{A} \tag{3.56}$$

Spec. 1 of sec. 3.4.1 requires that the constitutive operator α should possess property 1 of sec. 2.2. α is often made the unit operator, but other definitions are sometimes preferable[3.1].

The first canonical equation is obtained by rearranging eqn. 3.41a :

$$\text{curl } \underline{A} = \underline{B} - \underline{C} \tag{3.57}$$

The second canonical equation must therefore be

$$\text{div } \underline{F} = \rho' \tag{3.58}$$

where ρ' is an arbitrary scalar distribution, often chosen as zero. Eqns. 3.57 and 3.58 correspond to eqns. 3.18 and 3.19 of the model of sec. 3.3; $\underline{A}$ and $\underline{F}$ correspond to the abstract $\underline{H}$ and $\underline{B}$ fields respectively.

Eqn. 3.57 satisfies spec. 2 of sec. 3.4.1 since $\underline{C}$ is pre-defined, and $\underline{B}$ is implicitly specified in a well-posed problem. However, nothing in the physical specifications of the problem can force eqn. 3.58 which is often referred to as the gauging of the vector potential.

The continuity conditions corresponding to eqns. 3.20 and 3.21 can be written

$$\underline{n} \times \Delta\underline{A} = \underline{K}' \tag{3.59}$$

and

$$\underline{n} \cdot \Delta\underline{F} = \sigma' \tag{3.60}$$

Spec. 3 requires that $\underline{K}'$ and σ' be specified over all surfaces within R. The physical specifications provide a constraint on $\underline{K}'$: applying a vector identity to the LHS of eqn. 3.43, and substituting from 3.59 into the result, we find

$$\mathrm{div}_s\, \underline{K}' = \underline{n} \cdot \Delta\underline{C} - \sigma \tag{3.61}$$

The boundary conditions are best considered through the definitions of sec. 3.4.2. The A-F equations corresponding to 3.29-32 are

$$\underline{a} = \underline{n} \times \underline{A} \tag{3.62}$$

$$f = \underline{n} \cdot \underline{F} \tag{3.63}$$

$$V_n' = \int_{\underline{r}_o}^{\underline{r}_n} \underline{A} \cdot d\underline{\ell} \tag{3.64}$$

$$\Phi_n' = \int_{S_n} \underline{F} \cdot d\underline{S} \tag{3.65}$$

Using eqns. 3.62 and 3.63, the boundary specifications 3.36 and 3.37 can be expressed in the form

$$\text{on } S_a \subset S : \ \underline{a} \text{ is specified} \tag{3.66}$$

and

$$\text{on } S_f \subset S : \ f \text{ is specified} \tag{3.67}$$

The original, physically specified S_b provides a constraint on $\underline{a}$ wherever it coincides with S_a : applying a vector identity to 3.49, and substituting from 3.62 into the result, we find

$$\mathrm{div}_S\, \underline{a} = \underline{n} \cdot \underline{C} - b \qquad (3.68)$$

In open boundary regions we must have

$$\text{on } S_\infty \subset S : \quad r^2 A \text{ and } r^2 F \quad \text{bounded} \qquad (3.69)$$

according to 3.38. The specification in 3.69 is stricter than 3.51, which represents the physical requirement.

The motive force V_n' and the flux Φ_n' must comply with the corresponding requirements discussed in sec. 3.4.2. V_n' is partially constrained by eqn. 3.53.

The physical specifications on the vector potential $\underline{A}$, derived in sec. 3.4.3, fully enforce eqn. 3.57, partially constrain eqns. 3.59, 3.64, and 3.66, and leave entirely free the specifications of eqns. 3.58, 3.60, 3.65, 3.67, and 3.68. Yet all these specifications must be enforced to ensure a unique $\underline{A}$. It is therefore necessary to complete the specification of $\underline{A}$ by defining, and imposing, the indicated additional constraints without, of course, violating the original physical constraints, explicitly or implicitly.

3.4.5 Model structure

The structure of the model shown in fig. 3.1 accounts for specs. 1, 2, and 3 of sec. 3.4.1. Fig. 3.3 extends it to account for spec. 4 by including those boundary conditions of sec. 3.4.2 that can be accommodated on such a diagram. It also shows the potentials for completeness.

The constitutive relationship is the only link between the H- and B-systems in the structure of fig. 3.3. But the structure shown does not exhaust the possibilities of allowable boundary specifications; it excludes conditions

related to recurrence boundaries, cuts, and abstract motive forces and fluxes. In principle, allowable specifications that link $\underline{H}$ and $\underline{B}$ on parts of the boundary can arise. In most applications, however, boundary conditions are specified independently for the H- and B-systems.

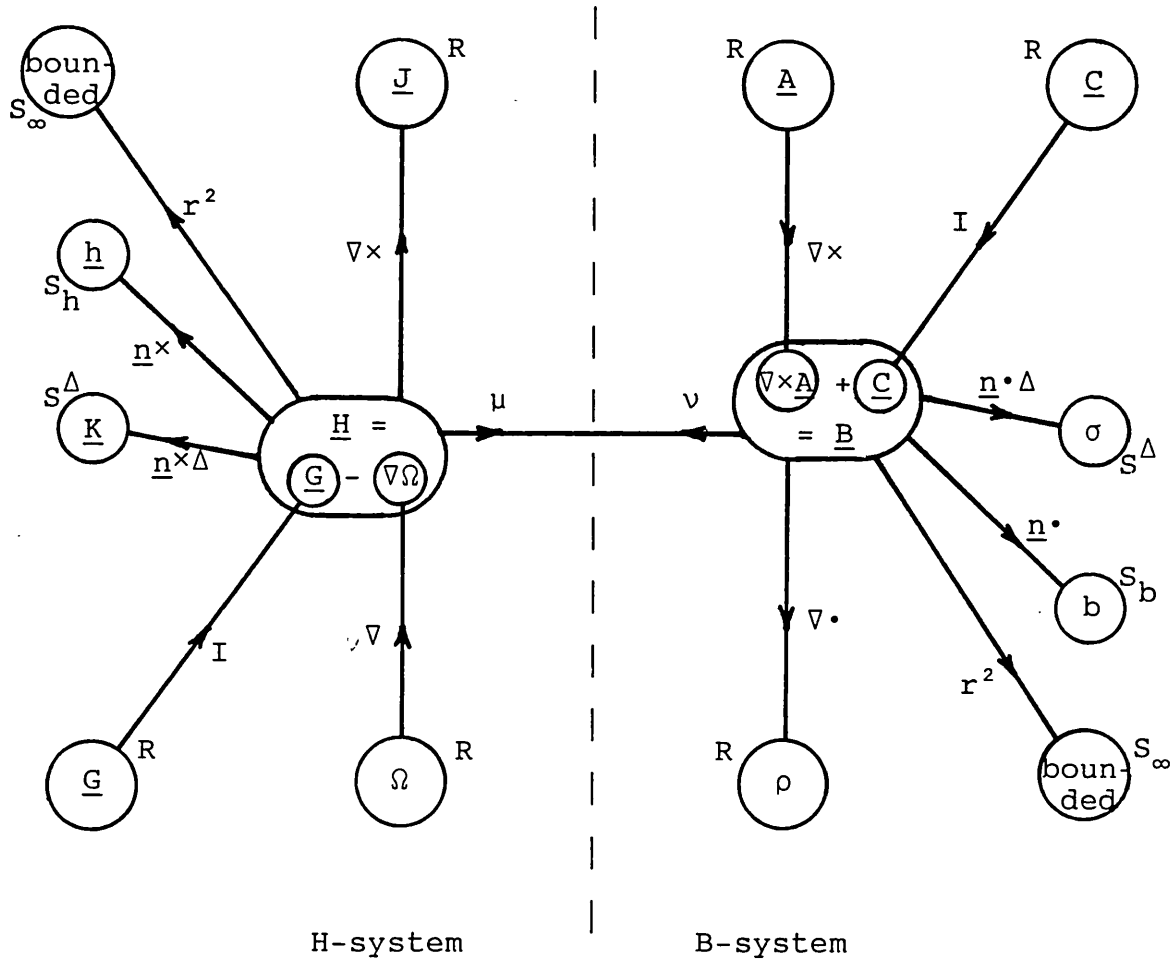

Fig. 3.3 Model structure.

3.5 Solution

The process of solving a physical problem is one of imposing the given specifications on the fields to force them to acquire, everywhere in R, the values unique to those specifications. A variety of approaches, differing in philosophy and/or technique, can be used to implement the process. In this section, we present a compact approach that is particularly suited to numerical analysis.

It is proposed that a well-posed problem can be solved by minimising the constitutive error, with the fields constrained to satisfy specifications 2, 3, and 4 of sec 3.4.1.

The validity of the proposition is established simply by recalling inequality 2.18, which was

$$\Lambda \geq 0 \tag{3.70a}$$

with

$$\Lambda = 0 \iff \underline{B} = \mu\underline{H}+\underline{B}_r \text{ and } \underline{H} = \nu\underline{B}+\underline{H}_c \text{ everywhere in R.} \tag{3.70b}$$

Clearly, then, spec. 1 is satisfied when Λ is minimum, thus completing the requirements of uniqueness given in sec. 3.4.1. Having defined Λ as a positive error, it is logical to expect it to be zero at the correct solution.

The global constitutive error is defined in eqn. 2.16 as

$$\Lambda(\underline{H},\underline{B}) = X(\underline{H}) + \Psi(\underline{B}) - Z(\underline{H},\underline{B}) \tag{3.71}$$

where it is evident that $X(\underline{H})$ is strictly an H-system functional, and $\Psi(\underline{B})$ is strictly a B-system functional. Only $Z(\underline{H},\underline{B})$ spans both systems.

Let us now investigate the effect, on the constitutive error, of constraining $\underline{H}(\underline{r})$ and $\underline{B}(\underline{r})$ as proposed, i.e. the behaviour of Λ for the model problem defined in this chapter. We first note that the means by which the fields are constrained is inessential to the proposition and its validity; any means can be used, provided it ensures strict satisfaction of specs. 2, 3, and 4. The potentials of sec. 3.4.3 are the tools that we shall use for the purpose. In particular, we introduce the scalar potential Ω by substituting eqn. 3.40a for $\underline{H}$ in $Z(\underline{H},\underline{B})$. Imposing, moreover, specs. 2 and 3 on the fields in Z, we get, after some algebra given in Appendix E :

$$\Lambda(\Omega,\underline{H},\underline{B}) = \Theta_0(\Omega,\underline{H}) + \Xi_0(\underline{B}) - \Gamma_0(\underline{H},\underline{B}) \tag{3.72}$$

with

$$\Theta_o(\Omega,\underline{H}) = X(\underline{H}) - \langle\Omega,\rho\rangle_R - \sum_{m=1}^{M} [\Omega_1,\sigma]_{S_m^\Delta} + \Omega(\underline{r}_o)\left(\int_R \rho dR + \sum_{m=1}^{M}\int_{S_m^\Delta}\sigma dS\right)$$

$$\Xi_o(\underline{B}) = \Psi(\underline{B}) - \langle\underline{G},\underline{B}\rangle_R - \sum_{m=1}^{M} [\Delta\Omega,\underline{n}\cdot\underline{B}_2]_{S_m^\Delta} + \left[\sum\Delta\Omega\Big|_{\underline{r}_o}^{\underline{r}} + \int_{\underline{r}_o}^{\underline{r}}\underline{G}\cdot d\underline{\ell},\underline{n}\cdot\underline{B}\right]_S$$

and

$$\Gamma_o(\Omega,\underline{H},\underline{B}) = \left[\int_{\underline{r}_o}^{\underline{r}}\underline{H}\cdot d\underline{\ell}\ ,\ \underline{n}\cdot\underline{B}\right]_S$$

where $\underline{r}_o$ is, as before, an arbitrary global reference point; $\sum\Delta\Omega$ covers all discontinuities in Ω encountered by the selected path from $\underline{r}_o$ to $\underline{r}$; the subscripts 1 and 2 refer to the two sides of S_m^Δ. Θ_o is a functional in the H-system variables Ω and $\underline{H}$ since ρ and σ are known according to specs. 2 and 3 respectively. Ξ_o is a functional in the B-system variable $\underline{B}$ since $\underline{G}$ is pre-defined according to eqn. 3.40b, and $\Delta\Omega$ is known according to eqn. 3.55.

The development from eqn. 3.71 to 3.72 is simply this : the imposition of specs. 2 and 3 on the fields has caused $Z(\underline{H},\underline{B})$ to decompose partially into functionals of H-system variables, and functionals of B-system variables; the former are included with Θ_o, and the latter are included with Ξ_o. The residue is Γ_o, and it clearly relates to the conditions on the boundary S. But the boundary conditions of spec. 4 have not been imposed yet. We shall now show that if the constraints on the fields are completed by imposing spec. 4, as required by our proposition, the decomposition of Γ_o, and hence that of Z, will be complete, allowing us to write

$$\Gamma_o(\Omega,\underline{H},\underline{B}) = \Gamma_H(\Omega,\underline{H}) + \Gamma_B(\underline{B}) \qquad (3.73)$$

With an eye on W in eqns. 3.27, 3.28, and 3.33, we proceed by expressing Γ_o in the form

$$\Gamma_o = \sum_{n=1}^{N}\gamma_n = \sum_{n=1}^{N}\{\gamma_n' + \gamma_n''\} \qquad (3.74a)$$

where the summation is over all sub-sections of the

boundary S, the contribution of each sub-section S_n being

$$\gamma_n = [\int_{\underline{r}_n}^{\underline{r}} \underline{H}\cdot d\underline{\ell} \ , \ \underline{n}\cdot\underline{B}]_{S_n} + (\int_{\underline{r}_o}^{\underline{r}_n} \underline{H}\cdot d\underline{\ell})(\int_{S_n} \underline{B}\cdot d\underline{S}) \qquad (3.74b)$$

Also

$$\gamma_n' = [\int_{\underline{r}_n}^{\underline{r}} \underline{H}\cdot d\underline{\ell} \ , \ \underline{n}\cdot\underline{B}]_{S_n} \qquad (3.74c)$$

and

$$\gamma_n'' = V_n \Phi_n \qquad (3.74d)$$

$\underline{r}_n$ is, as before, an arbitrary local reference point on S_n; the abstract motive force V_n and flux Φ_n are defined in eqns. 3.31 and 3.32 repectively.

According to spec. 4, unique boundary specifications are those which cause W to vanish, eqn. 3.28. In sec. 3.4.2 we examined boundary conditions which caused w_n, the contribution of S_n to W, to vanish. Noting the kinship between Γ_o and W, we shall show that the same conditions cause the corresponding γ_n to either vanish, or become a functional of only one system rather than both, as anticipated by eqn. 3.73.

From its definition in eqn. 3.34b, w_n' vanishes if either the H-factor or the B-factor of the product is zero. This implies that either the H-factor or the B-factor is specified in the corresponding γ_n' product, eqn. 3.74c. In the former case, the term goes into Γ_B, and in the latter it goes into Γ_H. Similarly for w_n'' and γ_n'', eqns. 3.35b and 3.74d.

w_n' also vanishes on open boundaries, S_∞ in 3.38. Under these conditions, the corresponding γ_n' also vanishes, and hence drops out entirely from Γ_o.

The w_n' and/or w_n'' contributions of two or more boundary sections can cancel out if suitably related to each other, as with recurrence relationships, or cuts. The corresponding γ_n' and/or γ_n'' contributions to Γ_o also cancel out under the same conditions.

Thus eqn. 3.73 is established, at least for the boundary specifications of interest. Later examples in this work will demonstrate various applications of the above reasoning. For now, we substitute eqn. 3.73 back into 3.72 to get

$$\Lambda(\Omega,\underline{H},\underline{B}) = \left(\Theta_o(\Omega,\underline{H}) - \Gamma_H(\Omega,\underline{H})\right) + \left(\Xi_o(\underline{B}) - \Gamma_B(\underline{B})\right)$$

$$= \Theta(\Omega,\underline{H}) + \Xi(\underline{B}) \qquad (3.75)$$

Thus, for a well-posed problem, the global constitutive error Λ can be expressed as the sum of two functionals : Θ in H-system variables, and Ξ in B-system variables. These functionals correspond to energies in magnetostatics and electrostatics, and to power in conduction problems. According to ineq. 3.70, they are related by

$$\Theta + \Xi = 0 \qquad (3.76)$$

at the exact solution. Moreover, since Λ is minimum, and hence stationary, at the solution, it constitutes a valid variational principle so that we can solve

$$0 = \delta\Lambda \qquad (3.77a)$$

$$= \delta\Theta + \delta\Xi \qquad (3.77b)$$

to obtain the required fields.

According to the proposition, the minimisation of Λ in eqn. 3.77 is to be carried out with the fields $\underline{H}$ and $\underline{B}$ constrained to satisfy specs. 2, 3, and 4. If the constraints leave $\underline{H}$ and $\underline{B}$ unrelated, which is often the case as discussed in sec. 3.4.5, Θ and Ξ are themselves stationary at the correct $\underline{H}$ and $\underline{B}$ distributions. This conclusion, derived in Appendix F, leads to

$$\delta\Theta = 0 \qquad (3.78)$$

at the correct $\underline{H}$ solution, and

$$\delta\Xi = 0 \qquad (3.79)$$

at the correct $\underline{B}$ solution. Solving eqns. 3.78 and 3.79 is

equivalent to solving 3.77; the solutions are independent of each other. In an exact solution, the resultant fields are related by the constitutive relationship, which is imposed by eqn. 3.77.

We close this section with a summary of its thesis : (i) The model problem can be solved by minimising the global constitutive error, eqn. 3.77a, with the fields constrained to satisfy the canonical equations, 3.18 and 3.19, the continuity conditions, 3.20 and 3.21, and the boundary conditions, 3.28. (ii) In a well-posed problem, the constitutive error separates into an H-system functional and a B-system functional, eqn. 3.75. (iii) If the boundary conditions do not introduce links between the H- and B-systems, the two functionals are themselves stationary at the correct distributions of their respective fields, which can thus be solved for independently of each other, eqns. 3.78 and 3.79.

3.6 An application

The principles of the previous sections will now be illustrated for a particular problem. So as not to mask fundamental issues by too much detail, the problem specifications are deliberately made simple; the proposition of sec. 3.5 allows a considerably wider range.

3.6.1 The problem

The complete statement of the problem is as follows :

Given a simply connected region R throughout which the fields $\underline{H}$ and $\underline{B}$ are required to satisfy the constitutive relationship

$$\underline{B} = \mu(\underline{H})\underline{H} + \underline{B}_r \qquad (3.80a)$$

and

$$\underline{H} = \nu(\underline{B})\underline{B} + \underline{H}_c \qquad (3.80b)$$

as in eqns. 3.17. The constitutive relationship in 3.80 possesses properties 1 and 2 of sec. 2.2.

The fields $\underline{H}$ and $\underline{B}$ are also required to satisfy the canonical equations

$$\text{curl } \underline{H} = \underline{J} \tag{3.81a}$$

and

$$\text{div } \underline{B} = \rho \tag{3.81b}$$

as in eqns. 3.18 and 3.19. $\underline{J}$ and ρ are known and finite everywhere in R.

The components $\underline{n} \times \underline{H}$ and $\underline{n} \cdot \underline{B}$ are required to be continuous across all surfaces within R, so that

$$\underline{n} \times \Delta\underline{H} = 0 \tag{3.82a}$$

and

$$\underline{n} \cdot \Delta\underline{B} = 0 \tag{3.82b}$$

Eqns. 3.82 are a special case of eqns. 3.20 and 3.21 for which $\underline{K} = 0$ and $\sigma = 0$.

R is bounded by a closed surface S which is composed of two simply-connected sections S_h and S_b such that

$$S = S_h \cup S_b \ , \quad S_h \cap S_b = 0 \tag{3.83a}$$

as a special case of 3.22. Moreover

$$\text{on } S_h : \underline{n} \times \underline{H} = \underline{h} \tag{3.83b}$$

and

$$\text{on } S_b : \underline{n} \cdot \underline{B} = b \tag{3.83c}$$

as in 3.36 and 3.37; $\underline{h}$ is known and finite on S_h, and b is known and finite on S_b.

This completes the statement of the problem, and we now examine it for physical uniqueness. Specifications 1, 2, and 3 of sec. 3.4.1 are satisfied by eqns. 3.80, 3.81, and 3.82 respectively. Spec. 4 requires that

$$W = w_h' + w_b' + w_h'' + w_b'' = 0 \tag{3.84}$$

as in 3.33-35 and 3.28. w_h' and w_b' are both given by

eqn. 3.34b, and they vanish by 3.83b and 3.83c, respectively. Φ_b, defined in eqn. 3.32, is known according to 3.83c, so that w''_b also vanishes, eqn. 3.35b. V_h is defined in eqn. 3.31; it can be made zero by allowing the global reference point $\underline{r}_o$ to coincide with the local reference on S_h; w''_h, given in eqn. 3.35b, accordingly vanishes. But this treatment of w''_h is not essential; a more fundamental alternative involves integrating eqn. 3.81b over R, applying the divergence theorem, and noting 3.82b and 3.83a, to get

$$\int_{S_h} \underline{B}\cdot d\underline{S} + \int_{S_b} \underline{B}\cdot d\underline{S} = \int_R \rho \, dR \qquad (3.85)$$

The volume integral over R and the surface integral over S_b are known from eqns. 3.81b and 3.83c respectively. Thus the integral over S_h, which is Φ_h by eqn. 3.32, is implicitly pre-specified; $\delta\Phi_h$ is thus zero, causing w''_h to vanish, eqn. 3.35b. It is thus evident that each of the four contributions to W in 3.84 is zero, so that W itself vanishes, and the requirements of spec. 4 are satisfied. All four specifications of sec. 3.4.1 are thus accounted for, and we can conclude that the given problem does have a unique solution.

Since the problem is well-posed, the constitutive error of eqn. 3.71 is guaranteed to separate into H- and B-system functionals as in eqn. 3.75 :

$$\Lambda = X(\underline{H}) + \Psi(\underline{B}) - Z(\underline{H},\underline{B}) \qquad (3.86a)$$

$$= \Theta(\Omega,\underline{H}) + \Xi(\underline{A},\underline{B}) \qquad (3.86b)$$

The $\underline{H}$ and $\underline{B}$ distributions can be obtained by minimising the error as in eqn. 3.77

$$0 = \delta\Lambda = \delta\Theta + \delta\Xi \qquad (3.87)$$

with the fields constrained to satisfy eqns. 3.81-83, for which purpose we shall use potentials in sections 3.6.2 and 3.6.3. Before doing that, we observe that the boundary conditions in 3.83 are specified independently for the H- and B-systems, which means that the separated functionals are entirely independent of each other. They are, therefore,

individually stationary in 3.87, allowing us to solve

$$\delta\Theta = 0 \tag{3.88a}$$

and

$$\delta\Xi = 0 \tag{3.88b}$$

independently of each other to obtain the $\underline{H}(\underline{r})$ and $\underline{B}(\underline{r})$ distributions respectively.

3.6.2 H-system potential

The field $\underline{H}$ can be constrained to satisfy the H-system canonical equation 3.81a by defining a scalar potential, Ω, as follows :

$$\underline{H} = \underline{G} - \text{grad } \Omega \tag{3.89}$$

as in eqn. 3.40a. $\underline{G}$ is any pre-specified field that satisfies

$$\text{curl } \underline{G} = \underline{J} \tag{3.90a}$$

as in eqn. 3.40b. The particular $\underline{G}$ distribution we choose here has a continuous tangential component, so that

$$\underline{n} \times \Delta\underline{G} = 0 \tag{3.90b}$$

across any surface within R. Substituting eqns. 3.82a and 3.90b into 3.42, we find that $\Delta\Omega$ is constant over any surface of discontinuity in R. We can, moreover, make Ω continuous by suitable choice of $\underline{G}$ in eqn. 3.45 so that

$$\Delta\Omega = 0 \tag{3.91}$$

across any surface in R.

To enforce the boundary condition of 3.83b, Ω must satisfy 3.48; using 3.54, and noting 3.91, we can write

$$\Omega(\underline{r}) = \Omega(\underline{r}_h) + \int_{\underline{r}_h}^{\underline{r}} \underline{G}\cdot d\underline{\ell} - \int_{\underline{r}_h}^{\underline{r}} \underline{H}\cdot d\underline{\ell} \tag{3.92a}$$

where $\underline{r}$ is any point on S_h, $\underline{r}_h$ is the local reference point on S_h, and

$$\Omega(\underline{r}_h) = \Omega(\underline{r}_o) + \int_{\underline{r}_o}^{\underline{r}_h} \underline{G}\cdot d\underline{\ell} - V_h \tag{3.92b}$$

The pre-defined $\underline{G}$ distribution and 3.83b specify $\Omega(\underline{r})$ in 3.92a to within a single unknown, $\Omega(\underline{r}_h)$.

Having expressed the H-system physical specifications in terms of the scalar potential Ω, we can proceed with the decomposition of the constitutive error Λ. Substituting eqn. 3.89 for $\underline{H}$ in $Z(\underline{H},\underline{B})$, eqn. 2.11, we get

$$Z = \langle \underline{G} \ , \ \underline{B} \rangle_R - \langle \text{grad } \Omega \ , \ \underline{B} \rangle_R$$

Applying a vector identity to the second term :

$$Z = \langle \underline{G} \ , \ \underline{B} \rangle_R + \langle \Omega \ , \ \text{div } \underline{B} \rangle_R - \int_R \text{div}(\Omega \underline{B}) \ dR$$

Applying the divergence theorem, and noting 3.81b, 3.82b, and 3.91 :

$$Z = \langle \underline{G} \ , \ \underline{B} \rangle_R + \langle \Omega \ , \ \rho \rangle_R - [\Omega \ , \ \underline{n} \cdot \underline{B}]_S$$

Substituting back into 3.86a, we can write

$$\Lambda = \Theta'_o(\Omega,\underline{H}) + \Xi'_o(\underline{B}) - \Gamma'_o(\Omega,\underline{B}) \qquad (3.93)$$

with

$$\Theta'_o(\Omega,\underline{H}) = X(\underline{H}) - \langle \Omega \ , \ \rho \rangle_R$$

$$\Xi'_o(\underline{B}) = \Psi(\underline{B}) - \langle \underline{G} \ , \ \underline{B} \rangle_R$$

and

$$\Gamma'_o(\Omega,\underline{B}) = - [\Omega \ , \ \underline{n} \cdot \underline{B}]_S$$

Eqn. 3.93 expresses the partial decomposition of Λ that results from imposing the canonical equations, 3.81, and the continuity conditions, 3.82; i.e. specs. 2 and 3 of sec. 3.4.1. Γ'_o, which relates to boundary conditions, is a functional of both H- and B-systems. It decomposes by substituting for S from 3.83a, and for $\Omega|_{S_h}$ from 3.92a, and using 3.32 to write

$$\Gamma'_o = - \Omega(\underline{r}_h)\Phi_h + [\int_{\underline{r}_h}^{\underline{r}} (\underline{H}-\underline{G}) \cdot d\underline{\ell} \ , \ \underline{n} \cdot \underline{B}]_{S_h} - [\Omega \ , \ b]_{S_b}$$

In the first term on the RHS, Φ_h is known from eqn. 3.85; in the second term, the line integral is known from 3.83b and the pre-definition of $\underline{G}$; in the third term, b is known from 3.83c. Thus the decomposition of Γ'_o is complete, and back substitution into 3.93 yields

$$\Lambda = \Theta'(\Omega,\underline{H}) + \Xi'(\underline{B}) \qquad (3.94)$$

with

$$\Theta'(\Omega,\underline{H}) = X(\underline{H}) - \langle\Omega \ , \ \rho\rangle_R + [\Omega \ , \ b]_{S_b} + \Omega(\underline{r}_h)\Phi_h$$

and

$$\Xi'(\underline{B}) = \Psi(\underline{B}) - \langle\underline{G} \ , \ \underline{B}\rangle_R - [\int_{\underline{r}_h}^{\underline{r}} (\underline{H}-\underline{G})\cdot d\underline{\ell} \ , \ \underline{n}\cdot\underline{B}]_{S_h}$$

Eqn. 3.94 expresses the final decomposition of Λ that results from constraining the fields to satisfy all the physical specifications of the problem, including boundary conditions, 3.83.

At this stage, we need to complete the requirements of solvability. To perform the H-system solution in Ω, it is necessary to specify its value at some point in R, sec. 3.4.4.1. An obvious choice is $\underline{r}_h$. Pre-specification of $\Omega(\underline{r}_h)$ causes the last term in Θ', namely $\Omega(\underline{r}_h)\Phi_h$, to drop out from the extremisation process, 3.88a. In particular, we can choose

$$\Omega(\underline{r}_h) = 0 \qquad (3.95)$$

to drop the term from Θ' itself, leaving

$$\Theta'(\Omega,\underline{H}) = X(\underline{H}) - \langle\Omega \ , \ \rho\rangle_R + [\Omega \ , \ b]_{S_b} \qquad (3.96)$$

Eqn. 3.96 expresses the H-system functional for a particular implementation of the requirements of solvability on the scalar potential Ω. The B-system functional, Ξ', remains unchanged.

The H- and B-system functionals of this section were derived using a scalar potential, Ω, to constrain $\underline{H}$. Although the derivation requires $\underline{B}$ also to be constrained, the means by which this is achieved has been left unspecified.

3.6.3 B-system potential

The field $\underline{B}$ can be constrained to satisfy the B-system canonical equation, 3.81b, by defining a vector potential,

$\underline{A}$, as follows :

$$\underline{B} = \underline{C} + \text{curl } \underline{A} \tag{3.97}$$

as in eqn. 3.41a. $\underline{C}$ is any pre-specified field that satisfies

$$\text{div } \underline{C} = \rho \tag{3.98a}$$

as in eqn. 3.41b. The particular $\underline{C}$ distribution we choose here has a continuous normal component, so that

$$\underline{n} \cdot \Delta\underline{C} = 0 \tag{3.98b}$$

across any surface within R. Substituting eqns. 3.82b and 3.98b into 3.61, and comparing with 3.59, we find that $\text{div}_s(\underline{n}\times\Delta\underline{A})$ is zero over any surface of discontinuity within R. We can, moreover, make $\underline{n} \times \underline{A}$ continuous by suitable choice of $\underline{C}$ in 3.47, so that

$$\underline{n} \times \Delta\underline{A} = 0 \tag{3.99}$$

across any surface within R.

To enforce the boundary condition of 3.83c, $\underline{A}$ must satisfy eqn. 3.49 on S_b or, equivalently, $\underline{a}=\underline{n}\times\underline{A}$ must satisfy eqn. 3.68. If we let $\underline{a}_b$ represent any continuous tangential vector on S_b, pre-defined to satisfy

$$\text{div}_s \underline{a}_b = \underline{n}\cdot\underline{C} - b \tag{3.100a}$$

then eqn. 3.83c can be enforced by letting

$$\underline{a} = \underline{a}_b + \underline{n} \times \text{grad}_s \beta \tag{3.100b}$$

where β is a continuous scalar distribution on S_b. In this way, the freedom available in the specification of $\underline{a}$ has been assigned to β.

Integrating eqn. 3.97 on S_b, applying Stokes' theorem, and noting 3.99, we get

$$\int_{S_b} \underline{B}\cdot d\underline{S} = \oint_{\ell_b} \underline{A}\cdot d\underline{\ell} + \int_{S_b} \underline{C}\cdot d\underline{S}$$

where ℓ_b is the contour of S_b. Repeating the procedure on S_h, we get

$$\int_{S_h} \underline{B}\cdot dS = \oint_{\ell_h} \underline{A}\cdot d\underline{\ell} + \int_{S_h} \underline{C}\cdot d\underline{S}$$

where ℓ_h is the contour of S_h, which, according to 3.83a, is ℓ_b traversed in reverse. Thus the contour integrals are equal in magnitude and opposite in sign. Eliminating them between the two equations, and rearranging, we can write

$$\int_{S_h} \underline{B}\cdot d\underline{S} + \int_{S_b} \underline{B}\cdot d\underline{S} = \int_{S_h} \underline{C}\cdot d\underline{S} + \int_{S_b} \underline{C}\cdot d\underline{S} = \oint_{S} \underline{C}\cdot d\underline{S}$$

Applying the divergence theorem to the RHS, and noting eqns. 3.98, we get eqn. 3.85 again. This short exercise is intended to show that the imposition of the boundary conditions of S_b on $\underline{A}$ is sufficient, in this case, to implicitly force the correct flux through S_h. For more complex boundary specifications and different definitions of the pre-specified field $\underline{C}$, we may need to impose additional explicit constraints on $\underline{a}$.

Having expressed the B-system physical specifications in terms of the vector potential $\underline{A}$, we can proceed with the decomposition of the constitutive error Λ. Substituting eqn. 3.97 for $\underline{B}$ in $Z(\underline{H},\underline{B})$, eqn. 2.11, we get

$$Z = \langle \underline{H} \, , \, \underline{C} \rangle_R + \langle \underline{H} \, , \, \text{curl } \underline{A} \rangle_R$$

Applying a vector identity to the second term :

$$Z = \langle \underline{H} \, , \, \underline{C} \rangle_R + \langle \text{curl } \underline{H} \, , \, \underline{A} \rangle_R - \int_R \text{div}(\underline{H}\times\underline{A}) \, dR$$

Applying the divergence theorem, and noting 3.81a, 3.82a, and 3.99 :

$$Z = \langle \underline{H} \, , \, \underline{C} \rangle_R + \langle \underline{J} \, , \, \underline{A} \rangle_R - [\underline{n}\times\underline{H} \, , \, \underline{A}]_S$$

Substituting back into 3.86a, we can write

$$\Lambda = \Theta''_o(\underline{H}) + \Xi''_o(\underline{A},\underline{B}) - \Gamma''_o(\underline{H},\underline{A},\underline{B}) \qquad (3.101)$$

with

$$\Theta''_o(\underline{H}) = X(\underline{H}) - \langle \underline{H} \, , \, \underline{C} \rangle_R$$

$$\Xi''_o(\underline{A},\underline{B}) = \Psi(\underline{B}) - \langle \underline{J} \, , \, \underline{A} \rangle_R$$

and

$$\Gamma''_o(\underline{H},\underline{A}) = - [\underline{n}\times\underline{H} \, , \, \underline{A}]_S$$

Eqn. 3.101 expresses the partial decomposition of Λ that results from imposing the canonical equations, 3.81, and the continuity conditions, 3.82; i.e. specs. 2 and 3 of

sec. 3.4.1. Γ''_o, which relates to boundary conditions, is a functional of both H- and B-systems. Its decomposition proceeds by substituting for S from 3.83a, and for $\underline{a}=\underline{n}\times\underline{A}|_{S_b}$ from 3.100b

$$\Gamma''_o = - [\underline{h} , \underline{A}]_{S_h} + [\underline{H} , \underline{a}_b]_{S_b} + [\underline{H} , \underline{n} \times \text{grad } \beta]_{S_b}$$

Applying a vector identity and Stokes' theorem to the last term, and substituting from 3.81a into the result, we get

$$\Gamma''_o = - [\underline{h},\underline{A}]_{S_h} + [\underline{H},\underline{a}_b]_{S_b} - [\underline{n}\cdot\underline{J},\beta]_{S_b} - \oint_{\ell_h} \beta\underline{H}\cdot d\underline{\ell}$$

where, in the last term, we have made use of the fact that ℓ_b is ℓ_h traversed in reverse. In the first term on the RHS, $\underline{h}$ is known from 3.83b; in the second term, $\underline{a}_b$ is pre-defined; in the third term, $\underline{J}$ is known; in the fourth term, the tangential component of $\underline{H}$ is known, from 3.83b, over S_h and hence over ℓ_h. Thus the decomposition of Γ''_o is complete, and back substitution into 3.101 yields

$$\Lambda = \Theta''(\underline{H}) + \Xi''(\underline{A},\underline{B},\beta) \qquad (3.102)$$

with

$$\Theta''(\underline{H}) = X(\underline{H}) - \langle\underline{H} , \underline{C}\rangle_R - [\underline{H} , \underline{a}_b]_{S_b}$$

and

$$\Xi''(\underline{A},\underline{B},\beta) = \Psi(\underline{B}) - \langle\underline{J} , \underline{A}\rangle_R + [\underline{h} , \underline{A}]_{S_h} + [\underline{n}\cdot\underline{J} , \beta]_{S_b} + \oint_{\ell_h} \beta\underline{H} \cdot d\underline{\ell}$$

Eqn. 3.102 represents the final decomposition of Λ that results from constraining the fields to satisfy all the physical specifications of the problem, including boundary conditions, 3.83.

At this stage we need to complete the requirements of solvability. Sec. 3.4.4.2 presents these in terms of a two-system model. We shall define the simplest such model by making the constitutive operator of eqn. 3.56 the identity operator so that $\underline{F} = \underline{A}$; we also set ρ' in 3.58 and σ' in 3.60 to zero, and divide the boundary S into at most two simply-connected sub-sections, S_a and S_f. $\underline{K}'$ of 3.59 is already zero by 3.99. In such a model, $\underline{A}$ is unique if we impose on it the following additional constraints :

$$\text{in } R: \quad \text{div } \underline{A} = 0 \tag{3.103}$$

$$\text{on } S_a: \quad \underline{a} = \underline{a}' \tag{3.104a}$$

and

$$\text{on } S_f: \quad \underline{n} \cdot \underline{A} = f \tag{3.104b}$$

where $\underline{a}'$ and f are to be pre-specified. The gauge on $\underline{A}$, eqn. 3.103, does not affect the decomposition of Λ since div $\underline{A}$ does not appear anywhere in Λ; means of imposing it are discussed in Chapter 10. The auxiliary boundary conditions, eqns. 3.104, can be introduced by choosing

$$S_f = S \quad \text{and} \quad S_a = 0 \tag{3.105}$$

to specify the normal component of $\underline{A}$, via 3.104b, over the entire boundary. The tangential component is constrained by 3.100 on S_b, but nowhere is it completely pre-specified. β must be assigned some value at an arbitrary point on S_b, and the decomposition of Λ in 3.102 remains unaltered. Alternatively, we can choose

$$S_f = S_h \quad \text{and} \quad S_a = S_b \tag{3.106a}$$

with

$$\text{on } S_a: \quad \underline{a} = \underline{a}_b \tag{3.106b}$$

to specify the normal component on S_h and the tangential component on S_b. Comparison of 3.106b with 3.100b shows that β is constant on S_b. As β must be specified at some point, it is completely pre-specified on S_b. In this case, the last two terms in Ξ'' do not participate in the extremisation process, 3.88b. In particular, we can choose

$$\beta = 0 \tag{3.106c}$$

to drop the terms from Ξ'' itself, leaving

$$\Xi''(\underline{A},\underline{B}) = \Psi(\underline{B}) - \langle \underline{J} , \underline{A} \rangle_R + [\underline{h} , \underline{A}]_{S_h} \tag{3.107}$$

Eqn. 3.107 expresses the B-system functional for a particular implementation of the requirements of solvability on the vector potential $\underline{A}$. The H-system functional, Θ'', remains unchanged.

The H- and B-ystem functionals of this section were derived using a vector potential, $\underline{A}$, to constrain $\underline{B}$.

Although the derivation requires $\underline{H}$ also to be constrained, the means by which this is achieved has been left unspecified.

3.7 Conclusions

Main features of the proposed approach are :

(i) the various aspects of the problem are divided, along clear-cut lines, between complementary H- and B-systems;

(ii) minimisation of the constitutive error provides a universal variational principle;

(iii) solution formulation is closely linked to the requirements of physical uniqueness.

The constitutive error splits into H- and B-system functionals, or energies, whose independent extremisations provide the complementary solution formulations; complementarity of the functionals is further discussed in Chapter 4.

The procedure for extracting complementary functionals from the constitutive error is detailed, in sec. 3.6, for a particular set of problem specifications. Other specifications, especially boundary conditions, are considered in Chapter 6.

The proposed approach appears to lend itself to a systematic categorisation of the various aspects of computational electromagnetics : H- and B-systems; fields and potentials; physical uniqueness and solvability; etc. In particular, the physical significance of the fields is emphasised : the constitutive error, as well as the physical specifications, are given in terms of fields; potentials are viewed as solution tools. The presentation of the approach proceeds from Maxwell's equations, via uniqueness requirements, to solution formulation, with no explicit reference, at any stage, to the associated partial differential equations.

CHAPTER FOUR

Complementary Variational Principles

4.1 Introduction

A functional is said to provide a variational principle for a given problem if it is known to be stationary at the correct solution to the problem. Two such functionals may be found that represent the same physical quantity. If, at their stationary points, one is a maximum and the other a minimum, the two variational principles are said to be complementary; the respective functionals define lower and upper bounds on the quantity they represent. Sec. 4.2 presents complementary variational principles in static electromagnetics in terms of the approach proposed in Chapter 3.

A number of approaches [4.1—6], all essentially equivalent, have already been used to derive complementary variational principles in electromagnetism. They have generally followed the treatments used in other disciplines, notably mechanics, elasticity, and structures. Two representative derivations are outlined in sections 4.4 and 4.5. An overview of the subject is presented in sec. 4.6; it includes a comparative review of the various derivations.

4.2 The constitutive error approach

The constitutive error provides a universal variational principle for the model problem in $\underline{H}$ and $\underline{B}$. This follows directly from its fundamental property, ineq. 3.70, and is expressed in eqn. 3.77a, which was

$$\delta\Lambda(\underline{H},\underline{B}) = 0 \qquad (4.1)$$

at the correct $\underline{H}$ and $\underline{B}$ distributions, provided the fields are constrained to satisfy specifications 2,3, and 4 of sec. 3.4.1 during the variation. Recalling that these constraints cause Λ to separate into H- and B-system functionals

$$\Lambda = \Theta(H) + \Xi(B) \tag{4.2}$$

we can rewrite 4.1

$$\delta\Theta(H) + \delta\Xi(B) = 0 \tag{4.3}$$

If, moreover, the specifications for the two systems are independent of each other, the functionals are individually stationary at the solution, so that

$$\delta\Theta(H) = 0 \tag{4.4}$$

and

$$\delta\Xi(B) = 0 \tag{4.5}$$

as in eqns. 3.78 and 3.79. In the above equations, H and B, between brackets, refer, respectively, to the H-system variables, $\underline{H}$ and Ω, and the B-system variables, $\underline{B}$ and $\underline{A}$. The functionals $\Theta(H)$ and $\Xi(B)$ provide the complementary variational principles although, strictly, they are not themselves the complementary functionals : recalling that the constitutive error is zero at the correct solution, eqn. 4.2 yields

$$0 = \Theta(H_o) + \Xi(B_o) \tag{4.6}$$

where $\underline{H}_o$ and $\underline{B}_o$ denote the correct distributions; either functional, and the negative of the other, represent the same quantity, and hence are complementary.

We elaborate by considering the upper and lower bounds. Let $\underline{H}$ and $\underline{B}$ denote distributions that are constrained as required by the proposition of sec. 3.5; i.e. they satisfy the (Maxwell) canonical equations of spec. 2, the continuity conditions of spec. 3, and the boundary conditions of spec. 4. They do not necessarily satisfy the constitutive relationship of spec. 1. Substituting from eqn. 4.2 for Λ in ineq. 3.70, we get

$$\Theta(H) + \Xi(B) \geq 0 \qquad (4.7a)$$

with

$$\Theta(H) + \Xi(B) = 0 \iff \underline{H} = \underline{H}_o \text{ and } \underline{B} = \underline{B}_o \qquad (4.7b)$$

where the implication in 4.7b holds for a well-posed problem having a unique solution, namely $\underline{H}_o$ and $\underline{B}_o$. A special case of 4.7a is given by

$$\Theta(H) + \Xi(B_o) \geq 0$$

which, in conjunction with eqn. 4.6, yields

$$\Theta(H) \geq \Theta(H_o) = - \Xi(B_o) \qquad (4.8)$$

Similarly

$$\Xi(B) \geq \Xi(B_o) = - \Theta(H_o) \qquad (4.9)$$

If, moreover, the specifications for the H- and B-systems are independent of each other, 4.8 and 4.9 can be combined to give

$$\Theta(H) \geq \Theta(H_o) = - \Xi(B_o) \geq - \Xi(B) \qquad (4.10a)$$

or, equally well,

$$\Xi(B) \geq \Xi(B_o) = - \Theta(H_o) \geq - \Theta(H) \qquad (4.10b)$$

The upper and lower bounds on the decomposed functionals Θ and Ξ are thus established. Any trial pair of distributions $\underline{H}$ and $\underline{B}$ that satisfies specifications 2, 3, and 4 will bracket the exact functionals as in 4.10.

If the problem specifications do relate the H- and B-systems, inequalities 4.8-10 still hold, but with the added qualification that the common variable, γ in Appendix F, is assigned its exact solution value in $\Theta(H)$ and $\Xi(B)$.

Clearly, insofar as the abstract model and, indeed, the solution are concerned, it is immaterial whether we consider the complementary functionals to be Θ and $-\Xi$, or $-\Theta$ and Ξ. In electromagnetic applications, however, the functionals are associated with a physically meaningful energy, or power, which dictates the choice; inequalities

4.10 provide the upper and lower bounds on the energy, or power, for either combination of functionals.

Equations 4.4 and 4.5, and inequalities 4.10, establish the complementary variational principles for our model, and hence for the static electromagnetic systems it represents. The principles are definable where the problem specifications allow the constitutive error Λ to separate into independent H-system and B-system functionals, $\Theta(H)$ and $\Xi(B)$. According to sec. 3.5, such separation is guaranteed if

(i) the problem is physically well-posed according to the requirements of sec. 3.4.1;

(ii) the constitutive relationship possesses properties 1 and 2 of sec. 2.2; and

(iii) the boundary specifications for $\underline{H}$ and $\underline{B}$ are independent of each other.

Regarding the composition of the functionals $\Theta(H)$ and $\Xi(B)$, it is obvious, from eqn. 3.71, that $X(\underline{H})$ appears in $\Theta(H)$, and $\Psi(\underline{B})$ appears in $\Xi(B)$. The remaining terms depend on the manner with which $Z(\underline{H},\underline{B})$ splits between the H- and B-systems; which, in turn, depends on the potential used to effect the decomposition (Ω as in sec. 3.6.2, or $\underline{A}$ as in sec. 3.6.3), and on the particular boundary specifications of the given problem. For either potential, the decomposition of Z, and hence that of Λ, is universal insofar as it accounts for Maxwell's equations and continuity conditions. As for boundary conditions, the wide range of acceptable specifications, sec. 3.4.2, renders universal expressions impracticable.

4.3 Alternative derivations

In the published literature, two distinct methods have been used to derive the complementary functionals for static electromagnetic systems. The first[4.1-4] is based on Hamilton's principle of analytical mechanics, with Legendre transformations leading, effectively, to Toupin's principle[4.5]. The second[4.5,6] is based on a generalised energy principle constructed by direct integration, originally developed in the theory of elasticity[4.7].

Both methods address a static problem similar to that of sec. 3.3. All fields and potentials are taken to be continuous throughout the region R. The boundary S is composed of two non-intersecting sections S_h and S_b, so that

$$S = S_h \cup S_b \quad \text{with} \quad S_h \cap S_b = 0 \qquad (4.12)$$

Using the H-system potential Ω, and the B-system field $\underline{B}$, the problem is described by the following, primal, set of canonical equations :

$$\text{grad } \Omega = \underline{G} - \underline{H} \qquad (4.13) \qquad \Omega = \Omega_h \text{ on } S_h \qquad (4.14)$$

$$\mu\underline{H} = \underline{B} \qquad (4.15)$$

$$\text{div } \underline{B} = \rho \qquad (4.16) \qquad \underline{n}\cdot\underline{B} = b \text{ on } S_b \qquad (4.17)$$

with Ω_h, ρ, b, and $\underline{J}$ known; $\underline{G}$ is any field pre-defined to satisfy

$$\text{curl } \underline{G} = \underline{J} \qquad (4.18)$$

Alternatively, using the H-system field $\underline{H}$, and the B-system potential $\underline{A}$, the problem is described by the following, dual, set of canonical equations :

$$\text{curl } \underline{H} = \underline{J} \qquad (4.19) \qquad \underline{n}\times\underline{H} = \underline{h} \text{ on } S_h \qquad (4.20)$$

$$\nu\underline{B} = \underline{H} \qquad (4.21)$$

$$\text{curl } \underline{A} = \underline{B} - \underline{C} \qquad (4.22) \qquad \underline{n}\times\underline{A} = \underline{a}_b \text{ on } S_b \qquad (4.23)$$

with $\underline{J}$, $\underline{h}$, $\underline{a}_b$, and ρ known; $\underline{C}$ is any field pre-defined to satisfy

$$\text{div } \underline{C} = \rho \tag{4.24}$$

The terms 'primal' and 'dual' above follow Fraser's[4,5,6] usage for electrostatics; they are the reverse of his usage for magnetostatics.

4.4 Analytical mechanics

4.4.1 Primal formulations

If Ω, $\underline{H}$, and $\underline{B}$ are constrained to satisfy eqns. 4.13, 4.14, and 4.15, then the correct solution to the primal set must satisfy

$$0 = \langle \text{div } \underline{B} - \rho \ , \ \delta\Omega \rangle_R - [\underline{n}\cdot\underline{B} - b \ , \ \delta\Omega]_{S_b}$$

for arbitrary infinitesimal variations $\delta\Omega$. Applying a vector identity and the divergence theorem :

$$0 = - \langle \underline{B} \ , \ \delta(\text{grad } \Omega) \rangle_R - \langle \rho \ , \ \delta\Omega \rangle_R + [\underline{n}\cdot\underline{B} \ , \ \delta\Omega]_S + [b \ , \ \delta\Omega]_{S_b} - [\underline{n}\cdot\underline{B} \ , \ \delta\Omega]_{S_b}$$

Substituting for $\underline{B}$ from 4.15, for grad Ω from 4.13, for S from 4.12, and for $\Omega|_{S_h}$ from 4.14 :

$$0 = \langle \mu\underline{H} \ , \ \delta\underline{H} \rangle_R - \langle \rho \ , \ \delta\Omega \rangle_R + [b \ , \ \delta\Omega]_{S_b}$$

This is equivalent to

$$0 = \delta\Theta'(\Omega, \underline{H}) \tag{4.25}$$

where

$$\Theta'(\Omega, \underline{H}) = X(\underline{H}) - \langle \rho \ , \ \Omega \rangle_R + [b \ , \ \Omega]_{S_b} \tag{4.26}$$

Θ' is the standard primal functional corresponding to Hamilton's variational principle in 4.25. The standard primal Lagrangian is defined by

$$L_{sp}(\Omega,\underline{H}) = \chi(\underline{H}) - \langle \rho \ , \ \Omega \rangle \tag{4.27}$$

so that

$$\Theta'(\Omega,\underline{H}) = \int_R L_{sp} \, dR + [b \ , \ \Omega]_{S_b} \tag{4.28}$$

Alternatively, if $\underline{H}$ and $\underline{B}$ are constrained to satisfy eqns. 4.15, 4.16, and 4.17, then the correct solution to the primal set must satisfy

$$0 = \langle \text{grad } \Omega - \underline{G} + \underline{H} \ , \ \delta\underline{B} \rangle_R - [\Omega - \Omega_h \ , \ \underline{n}\cdot\delta\underline{B}]_{S_h}$$

for arbitrary infinitesimal variations $\delta\underline{B}$. Applying a vector identity and the divergence theorem :

$$0 = \langle \underline{H} \ , \ \delta\underline{B} \rangle_R - \langle \underline{G} \ , \ \delta\underline{B} \rangle_R - \langle \Omega, \delta(\text{div } \underline{B}) \rangle_R + [\Omega \ , \delta(\underline{n}\cdot\underline{B})]_S + [\Omega_h, \delta(\underline{n}\cdot\underline{B})]_{S_h} - [\Omega \ , \delta(\underline{n}\cdot\underline{B})]_{S_h}$$

Substituting for $\underline{H}$ from 4.15, for div $\underline{B}$ from 4.16, for S from 4.12, and for $\underline{n}\cdot\underline{B}|_{S_b}$ from 4.17 :

$$0 = \langle \nu\underline{B} \ , \ \delta\underline{B} \rangle_R - \langle \underline{G} \ , \ \delta\underline{B} \rangle_R + [\Omega_h \ , \ \delta(\underline{n}\cdot\underline{B})]_{S_h}$$

This is equivalent to

$$0 = \delta\Xi'(\underline{B}) \tag{4.29}$$

where

$$\Xi'(\underline{B}) = \Psi(\underline{B}) - \langle \underline{G} \ , \ \underline{B} \rangle_R + [\Omega_h \ , \ \underline{n}\cdot\underline{B}]_{S_h} \tag{4.30}$$

Ξ' is the complementary primal functional corresponding to Toupin's variational principle in 4.29. The complementary primal Lagrangian is defined by

$$L_{cp}(\underline{B}) = - \psi(\underline{B}) + \langle \underline{G} \ , \ \underline{B} \rangle \tag{4.31}$$

so that

$$\Xi'(\underline{B}) = - \int_R L_{cp} \, dR + [\Omega_h \ , \ \underline{n}\cdot\underline{B}]_{S_h} \tag{4.32}$$

4.4.2 Dual formulations

If $\underline{A}$, $\underline{B}$, and $\underline{H}$ are constrained to satisfy eqns. 4.21, 4.22, and 4.23, then the correct solution to the dual set must satisfy

$$0 = \langle \text{curl } \underline{H} - \underline{J} \, , \, \delta\underline{A} \rangle_R - [\underline{n}\times\underline{H} - \underline{h} \, , \, \delta\underline{A}]_{S_h}$$

for arbitrary infinitesimal variations $\delta\underline{A}$. Applying a vector identity and the divergence theorem :

$$0 = \langle \underline{H} \, , \, \delta(\text{curl } \underline{A}) \rangle_R - \langle \underline{J} \, , \, \delta\underline{A} \rangle_R + [\underline{n}\times\underline{H} \, , \, \delta\underline{A}]_S + [\underline{h} \, , \, \delta\underline{A}]_{S_h} - [\underline{n}\times\underline{H} \, , \, \delta\underline{A}]_{S_h}$$

Substituting for $\underline{H}$ from 4.21, for curl $\underline{A}$ from 4.22, for S from 4.12, and for $\underline{n}\times\underline{A}|_{S_b}$ from 4.23 :

$$0 = \langle \nu\underline{B} \, , \, \delta\underline{B} \rangle_R - \langle \underline{J} \, , \, \delta\underline{A} \rangle_R + [\underline{h} \, , \, \delta\underline{A}]_{S_h}$$

This is equivalent to

$$0 = \delta\Xi''(\underline{A},\underline{B}) \tag{4.33}$$

where

$$\Xi''(\underline{A},\underline{B}) = \Psi(\underline{B}) - \langle \underline{J} \, , \, \underline{A} \rangle_R + [\underline{h} \, , \, \underline{A}]_{S_h} \tag{4.34}$$

Ξ'' is the standard dual functional corresponding to Hamilton's variational principle in 4.33. The standard dual Lagrangian is defined by

$$L_{sd}(\underline{A},\underline{B}) = \psi(\underline{B}) - \langle \underline{J} \, , \, \underline{A} \rangle \tag{4.35}$$

so that

$$\Xi''(\underline{A},\underline{B}) = \int_R L_{sd} \, dR + [\underline{h} \, , \, \underline{A}]_{S_h} \tag{4.36}$$

Alternatively, if $\underline{B}$ and $\underline{H}$ are constrained to satisfy eqns. 4.19, 4.20, and 4.21, then the correct solution to the dual set must satisfy

$$0 = \langle \text{curl } \underline{A} + \underline{C} - \underline{B} \, , \, \delta\underline{H} \rangle_R - [\underline{n}\times\underline{A} - \underline{\alpha}_b \, , \, \delta\underline{H}]_{S_b}$$

for arbitrary infinitesimal variations $\delta\underline{H}$. Applying a vector identity and the divergence theorem :

$$0 = - \langle \underline{B} , \delta\underline{H} \rangle_R + \langle \underline{C} , \delta\underline{H} \rangle_R + \langle \underline{A} , \delta(\text{curl } \underline{H}) \rangle_R + [\underline{n}\times\underline{A} , \delta\underline{H}]_S + [\underline{a}_b , \delta\underline{H}]_{S_b} - [\underline{n}\times\underline{A} , \delta\underline{H}]_{S_b}$$

Substituting for $\underline{B}$ from 4.21, for curl $\underline{H}$ from 4.19, for S from 4.12, and for $\underline{n}\times\underline{H}|_{S_h}$ from 4.20 :

$$0 = - \langle \mu\underline{H} , \delta\underline{H} \rangle_R + \langle \underline{C} , \delta\underline{H} \rangle_R + [\underline{a}_b , \delta\underline{H}]_{S_b}$$

This is equivalent to

$$0 = \delta\Theta''(\underline{H}) \tag{4.37}$$

where

$$\Theta''(\underline{H}) = X(\underline{H}) - \langle \underline{C} , \underline{H} \rangle_R - [\underline{a}_b , \underline{H}]_{S_b} \tag{4.38}$$

Θ'' is the complementary dual functional corresponding to Toupin's variational principle in 4.37. The complementary dual Lagrangian is defined by

$$L_{cd}(\underline{H}) = - \chi(\underline{H}) + \langle \underline{C} , \underline{H} \rangle \tag{4.39}$$

so that

$$\Theta''(\underline{H}) = - \int_R L_{cd} \, dR - [\underline{a}_b , \underline{H}]_{S_b} \tag{4.40}$$

4.5 Direct integration

4.5.1 Primal formulations

Direct integration of the primal set of canonical equations, 4.13-17, yields the Hu-Washizu functional[4.5, 7]

$$\begin{aligned}\Pi_p(\Omega,\underline{H},\underline{B}) = {} & -\tfrac{1}{2}\langle \nabla\Omega, \underline{B} \rangle_R - \tfrac{1}{2}\langle \underline{H}, \underline{B} \rangle_R + \langle \underline{G}, \underline{B} \rangle_R + \tfrac{1}{2}[\Omega, \underline{n}\cdot\underline{B}]_{S_h} - [\Omega_h, \underline{n}\cdot\underline{B}]_{S_h} \\ & + \tfrac{1}{2}\langle \mu\underline{H} - \underline{B}, \underline{H} \rangle_R \\ & + \tfrac{1}{2}\langle \nabla\cdot\underline{B}, \Omega \rangle_R - \langle \rho, \Omega \rangle_R - \tfrac{1}{2}[\underline{n}\cdot\underline{B}, \Omega]_{S_b} + [b, \Omega]_{S_b}\end{aligned} \tag{4.41}$$

Π_p is stationary at the correct solution to the primal set:

$$\delta\Pi_p = 0 \tag{4.42}$$

If Ω, $\underline{H}$, and $\underline{B}$ are constrained to satisfy eqns. 4.13, 4.14, and 4.15, Π_p reduces to

$$\Pi_p = \Theta' = \tfrac{1}{2}\langle\nabla\cdot\underline{B},\Omega\rangle_R - \langle\rho,\Omega\rangle_R + [b,\Omega]_{S_b} + \tfrac{1}{2}\langle\underline{G},\underline{B}\rangle_R - \tfrac{1}{2}[\Omega,\underline{n}\cdot\underline{B}]_S$$

Applying a vector identity and the divergence theorem, and substituting from eqns. 4.13 and 4.15 into the result :

$$\Theta'(\Omega,\underline{H}) = \tfrac{1}{2}\langle\mu\underline{H}\ ,\ \underline{H}\rangle_R - \langle\rho\ ,\ \Omega\rangle_R + [b\ ,\ \Omega]_{S_b} \qquad (4.43)$$

Θ' is the standard primal functional. The variational principle is given by eqn. 4.42, which now becomes

$$\delta\Theta'(\Omega,\underline{H}) = 0 \qquad (4.44)$$

Alternatively, if $\underline{H}$ and $\underline{B}$ are constrained to satisfy eqns. 4.15, 4.16, and 4.17, Π_p reduces to

$$\Pi_p = -\Xi' = -\tfrac{1}{2}\langle\nabla\cdot\underline{B},\Omega\rangle_R + \tfrac{1}{2}[\Omega,\underline{n}\cdot\underline{B}]_S$$
$$- \tfrac{1}{2}\langle\nabla\,\Omega\ ,\underline{B}\rangle_R - \tfrac{1}{2}\langle\nu\underline{B},\underline{B}\rangle_R + \langle\underline{G},\underline{B}\rangle_R - [\Omega_h,\underline{n}\cdot\underline{B}]_{S_h}$$

Applying a vector identity and the divergence theorem :

$$\Xi'(\underline{B}) = \tfrac{1}{2}\langle\nu\underline{B}\ ,\ \underline{B}\rangle_R - \langle\underline{G}\ ,\ \underline{B}\rangle_R + [\Omega_h\ ,\ \underline{n}\cdot\underline{B}]_{S_h} \qquad (4.45)$$

Ξ' is the complementary primal functional. The variational principle is given by eqn. 4.42, which now becomes

$$\delta\Xi'(\underline{B}) = 0 \qquad (4.46)$$

4.5.2 Dual formulations

Direct integration of the dual set of canonical equations, 4.19-23, yields the Hu-Washizu functional[4.5, 7]

$$\begin{aligned}\Pi_d(\underline{A},\underline{B},\underline{H}) = {} & \tfrac{1}{2}\langle\nabla\times\underline{H},\underline{A}\rangle_R - \langle\underline{J},\underline{A}\rangle_R - \tfrac{1}{2}[\underline{n}\times\underline{H},\underline{A}]_{S_h} + [\underline{h},\underline{A}]_{S_h} \\ & + \tfrac{1}{2}\langle\nu\underline{B}-\underline{H},\underline{B}\rangle_R \\ & + \tfrac{1}{2}\langle\nabla\times\underline{A},\underline{H}\rangle_R - \tfrac{1}{2}\langle\underline{B},\underline{H}\rangle_R + \langle\underline{C},\underline{H}\rangle_R - \tfrac{1}{2}[\underline{n}\times\underline{A},\underline{H}]_{S_b} + [\underline{a}_b,\underline{H}]_{S_b}\end{aligned} \qquad (4.47)$$

Π_d is stationary at the correct solution to the dual set :

$$\delta\Pi_d = 0 \qquad (4.48)$$

If $\underline{A}$, $\underline{B}$, and $\underline{H}$ are constrained to satisfy eqns. 4.21, 4.22, and 4.23, Π_d reduces to

$$\Pi_d = \Xi'' = \tfrac{1}{2}\langle\nabla\times\underline{H},\underline{A}\rangle_R - \langle\underline{J},\underline{A}\rangle_R + [\underline{h},\underline{A}]_{S_h} + \tfrac{1}{2}\langle\underline{C},\underline{H}\rangle_R - \tfrac{1}{2}[\underline{n}\times\underline{H},\underline{A}]_S$$

Applying a vector identity and the divergence theorem, and substituting from eqns. 4.21 and 4.22 into the result :

$$\Xi''(\underline{A},\underline{B}) = \tfrac{1}{2}\langle\nu\underline{B}\ ,\ \underline{B}\rangle_R - \langle\underline{J}\ ,\ \underline{A}\rangle_R + [\underline{h}\ ,\ \underline{A}]_{S_h} \qquad (4.49)$$

Ξ'' is the standard dual functional. The variational principle is given by eqn. 4.48, which now becomes

$$\delta\Xi''(\underline{A},\underline{B}) = 0 \qquad (4.50)$$

Alternatively, if $\underline{B}$ and $\underline{H}$ are constrained to satisfy eqns. 4.19, 4.20, and 4.21, Π_d reduces to

$$\Pi_d = -\Theta'' = -\tfrac{1}{2}\langle\nabla\times\underline{H},\underline{A}\rangle_R + \tfrac{1}{2}[\underline{n}\times\underline{H},\underline{A}]_S$$
$$+ \tfrac{1}{2}\langle\nabla\times\underline{A},\underline{H}\rangle_R - \tfrac{1}{2}\langle\underline{H},\mu\underline{H}\rangle_R + \langle\underline{C},\underline{H}\rangle_R + [\underline{a}_b,\underline{H}]_{S_b}$$

Applying a vector identity and the divergence theorem :

$$\Theta''(\underline{H}) = \tfrac{1}{2}\langle\mu\underline{H}\ ,\ \underline{H}\rangle_R - \langle\underline{C}\ ,\ \underline{H}\rangle_R - [\underline{a}_b\ ,\ \underline{H}]_{S_b} \qquad (4.51)$$

Θ'' is the complementary dual functional. The variational principle is given by eqn. 4.48, which now becomes

$$\delta\Theta''(\underline{H}) = 0 \qquad (4.52)$$

4.6 Overview

The derivation of complementary variational principles in sec. 4.4 follows Hammond's approach[4.4]. He develops the theory in mechanics, and transports it into electromagnetism, always emphasising physical implications and highlighting analogies. He allows non-linear constitutive relationships for a restricted class of non-linearities[4.8]; the restrictions are consistent with those of sec. 2.2. It is to be noted that Hammond uses the term 'dual' in the sense that 'complementary' is used in this thesis.

The derivation in sec. 4.5 is the electromagnetic interpretation of Fraser's approach[4,5]. He uses abstract operators and functional analysis to develop a formal theory that encompasses a number of engineering field problems. He also constructs formal Tonti diagrams to describe the primal and dual system structures and the inter-relationships between them; the structures shown in figures 3.1 and 3.3 are, in fact, informal versions of these. Fraser does not allude to the restrictions on the constitutive relationship in sec. 2.2; he does, however, require the constitutive operator to be self-adjoint.

We shall compare the functionals derived by the various approaches for a particular application of the problem described in sec. 4.3 : we require each of S_h and S_b to be simply-connected, and thus obtain the problem described in sec. 3.6. The error-based derivations of section 3.6 are then directly comparable with the derivations of sections 4.4 and 4.5. We note that the primal statement of the problem employs the H-system scalar potential Ω as in sec. 3.6.2, while the dual statement employs the B-system vector potential $\underline{A}$ as in sec. 3.6.3. The comparison reveals complete agreement between the respective functionals of sections 3.6 and 4.4. However, agreement with the functionals of sec. 4.5 are restricted to the linear case where $X(\underline{H})$ and $\Psi(\underline{B})$ simplify to

$$X(\underline{H}) = \tfrac{1}{2}\langle \mu\underline{H} \ , \ \underline{H}\rangle_R \quad \text{and} \quad \Psi(\underline{B}) = \tfrac{1}{2}\langle \nu\underline{B} \ , \ \underline{B}\rangle_R \qquad (4.53)$$

This indicates that the Hu-Washizu functionals in eqns. 4.41 and 4.47 are defined for linear constitutive relationships. The integration can, in fact, be extended to allow non-linearities that subscribe to property 2 of sec. 2.2; agreement with the other approaches would then be complete.

Having established equivalence for the simple problem of sec. 3.6, let us now examine the general problem of sec. 4.3. Both primal and dual statements of the problem satisfy the uniqueness requirements of sec. 3.4.1, but neither statement exhausts their possibilities : the field

discontinuities of spec. 3 are excluded, and boundary conditions are restricted to a particular sub-set of those allowed by spec. 4 (see sec. 3.4.2). Moreover, both statements are given directly in terms of potentials, which further restricts the physical specifications and geometry of the problem, especially since potential discontinuities are excluded. A careful reading of sections 3.4.3 and 3.4.4, which show how the physical specifications on the fields partially constrain the potentials, reveals that the reverse process of specifying the potentials, as in sec. 4.3, imposes a number of implicit restrictions on the physical specifications. We illustrate by showing that the primal and dual statements of sec. 4.3 are not, in general, equivalent. This follows immediately from noting that while eqn. 4.14 can imply eqn. 4.20, the reverse is not true, i.e. eqn. 4.20 does not imply 4.14. Similarly for eqns. 4.17 and 4.23. It is evident from eqns. 3.52 and 3.53 that the primal and dual statements specify, respectively, the motive force at, and the flux through, every simply-connected sub-section of S_h. These specifications are not generally equivalent, and hence describe physically different problems. The distinction becomes trivial in special cases, such as the problem of sec. 3.6 (see eqn. 3.85 and related text).

We can therefore conclude that the problem statements of sec. 4.3 describe a particular class of specification of the static electromagnetic problem of sec. 3.4.1, and not the general problem itself. It follows that the expressions for the complementary functionals derived in sections 4.4 and 4.5 are not universally applicable : they are restricted to that particular class.

The constitutive error approach extends the theory of complementary variational principles to the general static electromagnetic problem of sec. 3.4.1, establishing, in the process, its limitations; sec. 4.2. Moreover, it starts from a physical specification of the problem in terms of fields, and views potentials as tools of implementation; sections 3.4.3 and 3.4.4.

While it does not attempt to derive universal expressions for the complementary functionals, the proposed approach does establish a universal expression for the constitutive error, together with the conditions that allow it to split into complementary functionals. The solution process is viewed as one of minimising the constitutive error, with both fields constrained to satisfy their respective system specifications; the minimisation effectively imposes the constitutive relationship, thus completing the requirements of uniqueness.

In contrast, the derivations of sections 4.4 and 4.5 restrict the range of problem specifications, and derive the expressions for the corresponding complementary functionals directly. The solution for either field is viewed as a process of extremising the corresponding functional, with the field constrained to satisfy its own system canonical equations as well as the constitutive relationship; the extremisation effectively imposes the canonical equations of the complementary system, thus completing the requirements of uniqueness.

In exact analysis that enforces the constitutive relationship, for example sections 4.4 and 4.5, the constitutive error is identically zero, and hence invisible to the analysis. But according to eqn. 4.2, the error is the difference between the complementary functionals

$$\Lambda = \Theta - (-\Xi) = \Xi - (-\Theta) \qquad (4.54)$$

In retrospect, it is possible to state that irrespective of the approach actually used to derive the complementary functionals, the difference between them is, in effect, the constitutive error as defined in Chapter two.

For completeness, Appendix G determines the relationship between the constitutive error Λ and the Lagrangians of analytical mechanics, sec. 4.4, and between Λ and the Hu-Washizu functionals of elasticity, sec. 4.5.

C H A P T E R F I V E

Numerical Solution

5.1 Introduction

The practical solution of a given physical problem generally involves two distinct sets of assumptions : the first set approximates the actual problem by a simplified model, and the second set restricts the solution fields to mathematically manageable forms. Analytic solutions attempt simple models, and do without restrictions. Numerical solutions can treat highly accurate models by introducing a variety of restrictions. The constitutive error approach is especially suited to numerical solution because it acknowledges, at the outset, numerical errors; the solution is then viewed as a process of minimising a global estimate of error.

The numerical restrictions on the solution fields are not part of the essential physical specifications of the problem. They are, therefore, an over-specification. Section 5.2 examines them, together with other inessential constraints, from the viewpoint of the constitutive error approach.

Sec. 5.3 presents three established, and widely used, numerical techniques as alternative implementations of the variational error-based approach. The presentation attempts to highlight common characteristics, as well as distinguishing features.

5.2 Over-specification

The solution of a physical problem is the process of imposing the unique problem specifications on the fields. In the error-based approach, the fields are constrained to satisfy Maxwell's equations, continuity conditions, and boundary conditions; minimising the constitutive error then imposes the constitutive relationship.

It is always possible to impose additional constraints on the fields during minimisation; such constraints effectively over-specify the fields, the essential, physical, constraints being sufficient to determine the unique solution. The following sub-sections examine, and attempt to classify, over-specifications that are commonly used, often implicitly, in numerical analysis.

5.2.1 Numerical over-specification

Analytic solutions that do not restrict the space variation of the trial fields are mathematically intractable for problems whose physical specifications, geometries in particular, are not essentially simple. The alternative is to restrict the field and potential distributions to forms that can be handled with relative ease, and acknowledge the resulting error. This is the essence of numerical techniques, as well as methods involving truncated series.

The error arises from the fact that the true field distributions are not, in general, describable by the chosen trial functions. The minimisation process cannot be guaranteed to yield zero constitutive error as in eqn. 2.12b (or 3.70b). However, according to ineq. 2.12a (or 3.70a), the error is universally positive, i.e. for any estimate of the solution fields. As the solution is actually an error minimising process, its outcome is the particular distribution, in the chosen restricted class, having the minimum constitutive error.

5.2.2 Redundant over-specification

Explicit imposition of the constitutive relationship on the fields, in all or part of the problem region, prior to the minimisation of the error, constitutes a redundant over-specification. The redundancy arises from the fact that the minimisation seeks to impose the same relationship on the fields. If the fields are constrained in this way everywhere, minimisation becomes meaningless because the error is zero to begin with.

In closed-form analysis, this type of over-specification can be introduced at any stage, in the knowledge that the solution fields satisfy the constitutive relationship exactly; this results in alternative, but entirely equivalent, formulations. In numerical analysis, on the other hand, redundant over-specification has a distinct, possibly adverse, effect on accuracy. We illustrate by means of boundary conditions, natural and forced.

In sec. 3.4.2, eqns. 3.36 and 3.37, we defined boundary sub-sections S_h and S_b thus

$$\underline{n} \times \underline{H} = \underline{h} \quad \text{on } S_h \quad \text{and} \quad \underline{n} \cdot \underline{B} = b \quad \text{on } S_b \qquad (5.1)$$

where $\underline{h}$ and b are given in the physical specifications of the problem. Exact minimisation of the constitutive error yields field distributions that satisfy, among other things,

$$\underline{n} \times \nu\underline{B} = \underline{h} \quad \text{on } S_h \quad \text{and} \quad \underline{n} \cdot \mu\underline{H} = b \quad \text{on } S_b \qquad (5.2)$$

The fields resulting from a numerical solution, on the other hand, satisfy 5.2 only approximately, so that

$$\underline{n} \times \nu\underline{B} \simeq \underline{h} \quad \text{on } S_h \quad \text{and} \quad \underline{n} \cdot \mu\underline{H} \simeq b \quad \text{on } S_b \qquad (5.3)$$

Eqns. 5.1 describe forced boundary conditions on $\underline{H}|_{S_h}$ and $\underline{B}|_{S_b}$; eqns. 5.2 and 5.3 describe natural boundary conditions on $\underline{B}|_{S_h}$ and $\underline{H}|_{S_b}$. Forcing 5.2 a priori amounts to a redundant over-specification as described above. Clearly, it does not alter the results, but only anticipates them, in an exact solution. It does, however, alter the outcome

of a numerical solution which, otherwise, would produce 5.3. But the unconstrained solution also produces the minimum global constitutive error for the chosen numerical over-specifications, sec. 5.2.1; constraining the fields as in eqns. 5.2 will certainly increase the global error. We can thus conclude that forcing natural boundary conditions a priori in a numerical solution trades global accuracy, in terms of the constitutive error, for local accuracy on boundary sections S_h and S_b. This conclusion can be generalised to all forms of redundant over-specification.

5.2.3 Inconsistent specification

In general, any additional constraints and specifications that are introduced must be consistent with the essential physical specifications; otherwise, the problem actually solved will be different from the one originally posed, and the solution will diverge from the correct, unique one. The distinction between consistent over-specifications (eg. numerical) and inconsistent specifications of any form is of particular significance to the present error-based approach : all effects of the former are accounted for in the constitutive error, while the latter are entirely invisible to it. We illustrate by an extreme, if trivial, example. Inspection of eqns. 2.8-11 immediately reveals that the constitutive error is identically zero if the medium is non-hysteretic, and the $\underline{H}$ and $\underline{B}$ field distributions are identically zero everywhere. The fact that the error is zero means that the fields satisfy the constitutive relationship which, in fact, they do. But such null distributions violate the essential specifications of any non-trivial problem; they are therefore inconsistently specified, and the constitutive error cannot provide an estimate of the inaccuracy involved.

Inconsistent specifications do arise in practice. In all the various forms they can take, they are, in general, justified by the need to simplify the solution process. In fact, the simplified approximate model mentioned in sec. 5.1

involves inconsistent specification because it is different from the actual physical problem. The inaccuracy incurred by the approximation is not included in the constitutive error. The latter provides a comprehensive measure of inaccuracies resulting from consistent over-specifications only; alternatively, it can be viewed as a measure of the error in the approximate model, rather than the original physical problem.

5.3 Numerical techniques

Numerical solution methods represent the trial fields as prescribed space functions of a finite number of unknown parameters u_i, i=1,..,n. Substituting such numerically over-specified fields into the constitutive error $\lambda(\underline{H},\underline{B})$, we can write

$$\lambda = \lambda(u_1, u_2, \ldots, u_n) \tag{5.4}$$

According to sec. 3.5, the correct solution minimises the global constitutive error, so that

$$0 = \delta\Lambda \tag{5.5}$$

Recalling eqn. 2.16, we can substitute from 5.4 into 5.5 :

$$0 = \sum_i \frac{\partial\Lambda}{\partial u_i}\ \delta u_i \tag{5.6}$$

If a particular u_i is unconstrained, its variation δu_i is free, and we must have

$$0 = \frac{\partial\Lambda}{\partial u_i} \tag{5.7}$$

Clearly, there are as many equations of the form of 5.7 as there are free variables. Solving these simultaneously determines the unknown parameters u_i, and solves eqns. 5.6 and 5.5. The numerical procedure thus replaces the original infinite degrees of freedom by a finite number of unknown parameters[5.1]. The universal variational principle of eqn. 5.5 can then be used to determine the values of the parameters for which the constitutive error is minimum.

The decomposition of Λ into H- and B-system functionals, Θ and Ξ in sections 3.5 and 4.2, allows us to write

$$\Lambda = \Theta(\Omega_1,\Omega_2,\ldots,\Omega_N) + \Xi(\underline{A}_1,\underline{A}_2,\ldots,\underline{A}_M) \qquad (5.8)$$

where Ω_i and $\underline{A}_i$ are the unknown parameters of the H- and B-systems, respectively; in this work, they are the potentials at preselected points, or nodes, in space. The split functionals are extremised as in eqns. 3.78 and 3.79 :

$$0 = \delta\Theta = \sum_i \frac{\partial\Theta}{\partial\Omega_i}\,\delta\Omega_i \qquad (5.9)$$

and

$$0 = \delta\Xi = \sum_j \sum_q \frac{\partial\Xi}{\partial A_{jq}}\,\delta A_{jq} \qquad (5.10)$$

where the subscript q refers to a particular space component of $\underline{A}_j$. Thus, for nodal potentials having free variations, we must have

$$0 = \frac{\partial\Theta}{\partial\Omega_i} \qquad (5.11)$$

and

$$0 = \frac{\partial\Xi}{\partial A_{jq}} \qquad (5.12)$$

As before, there are as many equations as there are free variables. 5.11 and 5.12 define two sets of simultaneous equations, one for each system. The two sets can be solved independently of each other to determine the H-system parameters, Ω_i, and the B-system parameters, A_{jq}.

It is usual, although not strictly necessary, to associate the unknown parameters, and the corresponding prescribed space functions, with some form of discretisation of the region of the problem R. In the following sub-sections we shall consider three common forms of discretisation. In all three cases, R is divided into a number, say m, of non-overlapping sub-regions

$$R = R_1 \cup R_2 \cup \ldots \cup R_m \quad \text{with} \quad R_i \cap R_j = 0 \text{ for } i \neq j \qquad (5.13)$$

which allows global integrations to be obtained as sums of sub-region contributions.

5.3.1 The finite difference method

The finite difference method superimposes a grid over the region of the problem. The unknown parameters are the potentials at grid intersections, or nodes. We shall illustrate the derivations for a two-dimensional region using a rectangular grid; extension to three dimensions and/or other types of grid is straightforward, if cumbersome.

Fig. 5.1 shows the grid in the region surrounding node 0. We stipulate that boundaries, cuts, discontinuities, and material interfaces coincide with grid lines, so that, within each mesh, potentials and fields are continuous, and source densities and material properties are uniform.

Along grid lines, the potentials are taken to vary linearly between their nodal values. Thus, along the x-directed segment 0-1

$$\Omega = \Omega_o + \frac{x - x_o}{h_1}(\Omega_1 - \Omega_o) \quad \Rightarrow \quad \frac{\partial \Omega}{\partial x} = \frac{1}{h_1}(\Omega_1 - \Omega_o) \qquad (5.14a)$$

and

$$A = A_o + \frac{x - x_o}{h_1}(A_1 - A_o) \quad \Rightarrow \quad \frac{\partial A}{\partial x} = \frac{1}{h_1}(A_1 - A_o) \qquad (5.14b)$$

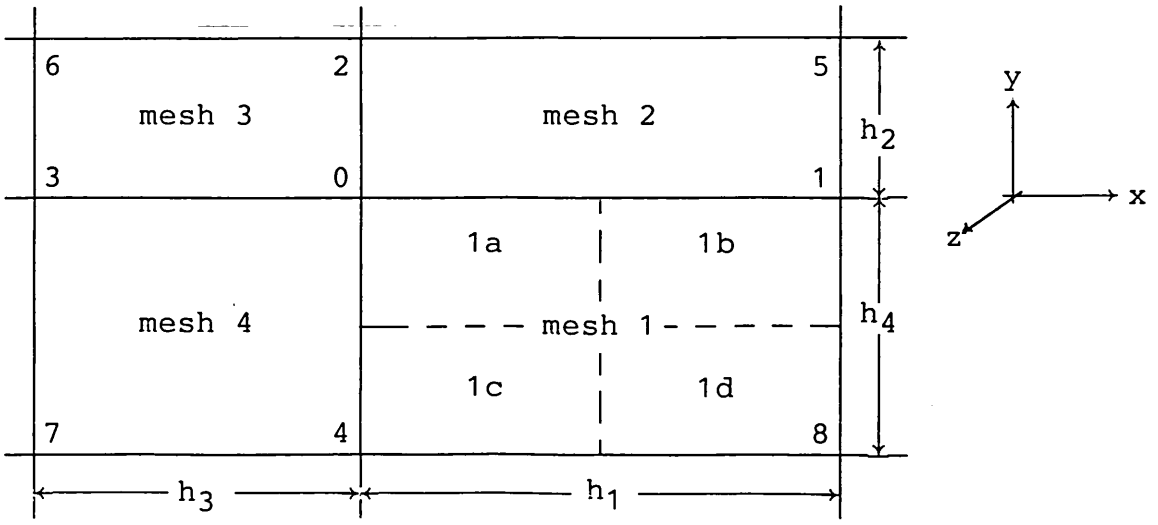

Fig. 5.1 Finite difference grid module.

Similarly, along the y-directed segment 4-0

$$\Omega = \Omega_o - \frac{y - y_o}{h_4}(\Omega_4 - \Omega_o) \quad \Rightarrow \quad \frac{\partial \Omega}{\partial y} = \frac{1}{h_4}(\Omega_o - \Omega_4) \qquad (5.14c)$$

and

$$A = A_o - \frac{y - y_o}{h_4}(A_4 - A_o) \quad \Rightarrow \quad \frac{\partial A}{\partial y} = \frac{1}{h_4}(A_o - A_4) \qquad (5.14d)$$

It is noted that $\underline{A} = A\underline{a}_z$, the analysis being two-dimensional.

No specific definition is given to the space variation of the potentials within the meshes. However, the space derivatives along each grid line are attributed also to the two adjoining half-mesh strips.

The fields $\underline{H}$ and $\underline{B}$, and hence the pre-specified fields $\underline{G}$ and $\underline{C}$, have only x- and y-components in two-dimensional analysis. We shall take $\underline{G}$ and $\underline{C}$ to vary linearly within meshes; thus, for mesh 1 of fig. 5.1, we define

$$\underline{G} = \left(G_{o1} - \frac{y-y_o}{h_4}(G_{48}-G_{o1})\right)\underline{a}_x + \left(G_{4o} + \frac{x-x_o}{h_1}(G_{81}-G_{4o})\right)\underline{a}_y$$

and (5.15)

$$\underline{C} = \left(C_{4o} + \frac{x-x_o}{h_1}(C_{81}-C_{4o})\right)\underline{a}_x + \left(C_{o1} - \frac{y-y_o}{h_4}(C_{48}-C_{o1})\right)\underline{a}_y$$

$\underline{G}_{ij}$ and $\underline{C}_{ij}$ are pre-defined constant vectors associated with grid segment ij; they are, respectively, parallel and normal to the segment ij, always in the sense of the positive x- and y-axis directions. Recalling eqns. 3.40b and 3.41b, these vectors must satisfy, in mesh 1,

$$\underline{J}_1 = \nabla \times \underline{G} = \left((G_{81} - G_{4o})/h_1 + (G_{48} - G_{o1})/h_4\right)\underline{a}_z$$

and (5.16)

$$\rho_1 = \nabla \cdot \underline{C} = (C_{81} - C_{4o})/h_1 - (C_{48} - C_{o1})/h_4$$

or, equivalently,

$$I_1 = h_1 h_4 J_1 = \oint_1 \underline{G} \cdot d\underline{\ell} = h_1 G_{48} + h_4 G_{81} - h_1 G_{o1} - h_4 G_{4o}$$

and (5.17)

$$Q_1 = h_1 h_4 \rho_1 = \oint_1 \underline{C} \cdot d\underline{S} = h_4 C_{81} + h_1 C_{o1} - h_4 C_{4o} - h_1 C_{48}$$

$\underline{J}_1$ and ρ_1 are, respectively, the vector and scalar source

densities in mesh 1. With reference to the surface integral in 5.17, it is noted that unit length has been assumed in the z direction.

Having defined the potential derivatives and pre-specified fields within the individual meshes, we can obtain the fields from eqns. 3.40a and 3.41a, which are

$$\underline{H} = \underline{G} - \text{grad } \Omega \tag{5.18a}$$

and

$$\underline{B} = \underline{C} + \text{curl } \underline{A} \tag{5.18b}$$

The resulting components of $\underline{H}$ and $\underline{B}$ are listed in table 5.1 for the four quadrants of mesh 1, shown in fig. 5.1.

	Mesh quadrants			
	1a	1b	1c	1d
H_x	$G_x-(\Omega_1-\Omega_o)/h_1$	$G_x-(\Omega_1-\Omega_o)/h_1$	$G_x-(\Omega_8-\Omega_4)/h_1$	$G_x-(\Omega_8-\Omega_4)/h_1$
H_y	$G_y-(\Omega_o-\Omega_4)/h_4$	$G_y-(\Omega_1-\Omega_8)/h_4$	$G_y-(\Omega_o-\Omega_4)/h_4$	$G_y-(\Omega_1-\Omega_8)/h_4$
B_x	$C_x+(A_o-A_4)/h_4$	$C_x+(A_1-A_8)/h_4$	$C_x+(A_o-A_4)/h_4$	$C_x+(A_1-A_8)/h_4$
B_y	$C_y-(A_1-A_o)/h_1$	$C_y-(A_1-A_o)/h_1$	$C_y-(A_8-A_4)/h_1$	$C_y-(A_8-A_4)/h_1$

Table 5.1 Field components in mesh 1, fig. 5.1; G_x, G_y, C_x, and C_y as defined in eqns. 5.15.

The constitutive error in mesh 1, Λ_1, can now be defined by substituting the fields of table 5.1 into eqn. 2.16

$$\Lambda_1 = \int_{\text{mesh 1}} (\chi(\underline{H}) + \psi(\underline{B}) - \zeta(\underline{H},\underline{B}))\, dR \tag{5.19}$$

In a similar fashion, the fields and constitutive errors can be defined in all meshes of the discretisation. The meshes correspond to the sub-regions of eqn. 5.13, and the global constitutive error Λ can be obtained as the sum of the individual mesh errors

$$\Lambda = \sum \Lambda_k \tag{5.20}$$

According to eqn. 5.7, if Ω_o is unconstrained, we must have

$$0 = \frac{\partial \Lambda}{\partial \Omega_o} = \sum \frac{\partial \Lambda_k}{\partial \Omega_o} \qquad (5.21a)$$

and if A_o is unconstrained

$$0 = \frac{\partial \Lambda}{\partial A_o} = \sum \frac{\partial \Lambda_k}{\partial A_o} \qquad (5.21b)$$

Eqns. 5.21 provide the rule for constructing the solution equations : the derivatives are determined for each mesh, and summed for all meshes to yield the solution equations corresponding to node 0. However, it is only in the four meshes immediately adjoining node 0 that the fields are functions of the potentials at 0, making the derivatives of 5.21 identically zero for other meshes. Therefore, only the contributions of meshes 1, 2, 3, and 4 of fig. 5.1 need be considered for the solution equations corresponding to node 0. As a sample, let us determine the contribution from mesh 1. Assuming isotropic and non-hysteretic material properties, and noting eqn. 5.19, we can write

$$\frac{\partial \Lambda_1}{\partial \Omega_o} = \langle \mu \underline{H} \ , \ \frac{\partial \underline{H}}{\partial \Omega_o} \rangle_1 - \langle \underline{B} \ , \ \frac{\partial \underline{H}}{\partial \Omega_o} \rangle_1 \qquad (5.22a)$$

and

$$\frac{\partial \Lambda_1}{\partial A_o} = \langle \nu \underline{B} \ , \ \frac{\partial \underline{B}}{\partial A_o} \rangle_1 - \langle \underline{H} \ , \ \frac{\partial \underline{B}}{\partial A_o} \rangle_1 \qquad (5.22b)$$

Substituting for the fields from table 5.1, and performing the algebra, we eventually find

$$\begin{aligned} \frac{\partial \Lambda_1}{\partial \Omega_o} = \ & \frac{\mu_1}{2h_1h_4}\left[(h_1^2+h_4^2)\Omega_o - h_4^2\Omega_1 - h_1^2\Omega_4\right] - \frac{1}{2}\left[A_1 - A_4\right] \\ & + \frac{\mu_1}{8}\left[h_4(3G_{o1} + G_{48}) - h_1(3G_{4o} + G_{81})\right] \\ & + \frac{1}{4}\left[h_1(C_{o1} + C_{48}) - h_4(C_{4o} + C_{81})\right] \end{aligned} \qquad (5.23a)$$

and

$$\begin{aligned} \frac{\partial \Lambda_1}{\partial A_o} = \ & \frac{\nu_1}{2h_1h_4}\left[(h_1^2+h_4^2)A_o - h_4^2A_1 - h_1^2A_4\right] - \frac{1}{2}\left[\Omega_4 - \Omega_1\right] \\ & + \frac{\nu_1}{8}\left[h_1(3C_{40} + C_{81}) + h_4(3C_{o1} + C_{48})\right] \\ & - \frac{1}{4}\left[h_1(G_{o1} + G_{48}) + h_4(G_{4o} + G_{81})\right] \end{aligned} \qquad (5.23b)$$

Similar expressions can be derived for the contributions of the remaining meshes in fig. 5.1. Adding the contributions in accordance with eqns. 5.21, simplifying, and substituting from eqn. 5.17 (and its counterparts for other meshes) into the result, we finally get the finite difference equations :

$$
\begin{aligned}
0 = \; & \tfrac{1}{2}(\mu_1\beta_{41} + \mu_2\beta_{12} + \mu_3\beta_{23} + \mu_4\beta_{34})\Omega_o \\
& - \tfrac{1}{2}(\mu_1\alpha_{41} + \mu_2\alpha_{21})\Omega_1 - \tfrac{1}{2}(\mu_2\alpha_{12} + \mu_3\alpha_{32})\Omega_2 \\
& - \tfrac{1}{2}(\mu_3\alpha_{23} + \mu_4\alpha_{43})\Omega_3 - \tfrac{1}{2}(\mu_4\alpha_{34} + \mu_1\alpha_{14})\Omega_4 \\
& - \tfrac{1}{4}(Q_1 + Q_2 + Q_3 + Q_4) \\
& - \tfrac{1}{8}(\mu_1 h_1(3G_{4o}+G_{81}) - \mu_1 h_4(3G_{o1}+G_{48}) - \mu_2 h_2(3G_{o1}+G_{25}) \\
& \quad - \mu_2 h_1(3G_{o2}+G_{15}) - \mu_3 h_3(3G_{o2}+G_{36}) + \mu_3 h_2(3G_{3o}+G_{62}) \\
& \quad + \mu_4 h_4(3G_{3o}+G_{74}) + \mu_4 h_3(3G_{4o}+G_{73}))
\end{aligned}
\qquad (5.24a)
$$

and

$$
\begin{aligned}
0 = \; & \tfrac{1}{2}(\nu_1\beta_{41} + \nu_2\beta_{12} + \nu_3\beta_{23} + \nu_4\beta_{34})A_o \\
& - \tfrac{1}{2}(\nu_1\alpha_{41} + \nu_2\alpha_{21})A_1 - \tfrac{1}{2}(\nu_2\alpha_{12} + \nu_3\alpha_{32})A_2 \\
& - \tfrac{1}{2}(\nu_3\alpha_{23} + \nu_4\alpha_{43})A_3 - \tfrac{1}{2}(\nu_4\alpha_{34} + \nu_1\alpha_{14})A_4 \\
& - \tfrac{1}{4}(I_1 + I_2 + I_3 + I_4) \\
& - \tfrac{1}{8}(-\nu_1 h_1(3C_{4o}+C_{81}) - \nu_1 h_4(3C_{o1}+C_{48}) - \nu_2 h_2(3C_{o1}+C_{25}) \\
& \quad + \nu_2 h_1(3C_{o2}+C_{15}) + \nu_3 h_3(3C_{o2}+C_{36}) + \nu_3 h_2(3C_{3o}+C_{62}) \\
& \quad + \nu_4 h_4(3C_{3o}+C_{74}) - \nu_4 h_3(3C_{4o}+C_{73}))
\end{aligned}
\qquad (5.24b)
$$

where

$$\alpha_{ij} = h_i/h_j \quad \text{and} \quad \beta_{ij} = \alpha_{ij} + \alpha_{ji}$$

Eqns. 5.24 are the standard five-point finite difference equations[5.2, 3], with pre-specified fields included. Similar equations can be written for all nodes to set up the solution matrices. Boundary conditions and discontinuities are forced explicitly on their own system variables, and naturally, via $\zeta(\underline{H},\underline{B})$ in eqn. 5.19, on the complementary system solution.

A characteristic feature of the finite difference method is the absence of a specific definition for the space variation of the potentials within the volume of the mesh.

One consequence is that the derivation resorted to the error equation 5.7, rather than the split functional equations 5.11 and 5.12; the latter would involve the volume integrals $\langle \Omega , \rho \rangle_1$ and $\langle \underline{J} , \underline{A} \rangle_1$, eg. eqns. 3.96 and 3.107. (It is noted that the decomposition is complete in eqns. 5.24; the complementary potentials, A_i in 5.23a and Ω_i in 5.23b, cancel out upon adding the contributions of the four meshes.) A more serious consequence is the rather arbitrary definition of fields within meshes, table 5.1 : while the continuity of $\underline{n} \times \underline{H}$ and $\underline{n} \cdot \underline{B}$ is forced across grid lines, unspecified discontinuities arise on the interfaces between mesh quadrants, shown dotted in fig. 5.1. Such discontinuities amount to sheet sources, eqns. 3.20 and 3.21, and violate spec. 3 of sec. 3.4.1, which requires sheet sources to be pre-specified. However, it can be easily verified that the vertical and horizontal sources cancel out within the individual meshes, and are thus invisible to the global formulation. The sheet sources can be eliminated entirely by allowing the potential derivatives to vary linearly, across the mesh, between their values at opposing edges; this would introduce the corner potentials at nodes 5, 6, 7, and 8 into the equations for node 0, resulting in nine-point finite difference equations.

5.3.2 The finite element method

The finite element process involves (i) replacement of the infinite degrees of freedom by a finite number of parameters, eqns. 5.4-12, and (ii) division of the problem region into sub-regions, eqn. 5.13, called finite elements[5.1, 4]. We shall find it advantageous to begin by considering item (i) alone at first.

The numerical over-specification is effected by restricting the potential trial distributions to product sums of the form

$$\Omega(\underline{r}) = \sum_{i=1}^{N} \Omega_i \alpha_i(\underline{r}) \qquad (5.25a)$$

and

$$\underline{A}(\underline{r}) = \sum_{j=1}^{M} \sum_{q} \underline{a}_q A_{jq} \beta_j(\underline{r}) \qquad (5.25b)$$

where N nodes have been defined for the H-system, and M nodes for the B-system; Ω_i and $\underline{A}_j$ are the nodal potentials; α_i and β_j are the corresponding prescribed space functions; q indicates the components of $\underline{A}_j$, and $\underline{a}_q$ is a unit vector. As defined, α and β are dimensionless, with $\alpha_i(\underline{r}_i)=\beta_j(\underline{r}_j)=1$; in conjunction with their corresponding nodal potentials in eqns. 5.25, they must ensure that $\Omega(\underline{r})$ and $\underline{A}(\underline{r})$ satisfy the physical specifications of the problem. This implies, among other things, that α and β are piecewise differentiable in R, so that substitution from eqns. 5.25 into eqns. 3.40a and 3.41a yields

$$\underline{H}(\underline{r}) = \underline{G}(\underline{r}) - \sum_{i} \Omega_i \nabla\alpha_i(\underline{r}) \qquad (5.26a)$$

and

$$\underline{B}(\underline{r}) = \underline{C}(\underline{r}) - \sum_{j} \sum_{q} A_{jq} \underline{a}_q \times \nabla\beta_j(\underline{r}) \qquad (5.26b)$$

for the numerically over-specified fields.

We shall now use the constrained potentials and fields to formulate the complementary solutions for the problem of sec. 3.6. H- and B-system functionals are given in eqns. 3.96 and 3.107 :

$$\Theta'(\Omega,\underline{H}) = X(\underline{H}) - \langle\Omega \ , \ \rho\rangle_R + [\Omega \ , \ b]_{S_b} \qquad (5.27a)$$

and

$$\Xi''(\underline{A},\underline{B}) = \Psi(\underline{B}) - \langle\underline{J} \ , \ \underline{A}\rangle_R + [\underline{h} \ , \ \underline{A}]_{S_h} \qquad (5.27b)$$

In general, the functionals Θ' and Ξ'' are not strictly complementary : they do not necessarily satisfy eqns. 4.2 and 4.6 because they represent dual formulations. The strict complements of Θ' and Ξ'' are Ξ' and Θ'', given, respectively, in eqns. 3.94 and 3.102. However, if the problem is well-posed, and the same solvability specifications are imposed on the corresponding potentials in primal (Ω-based) and dual ($\underline{A}$-based) formulations, we must have

$$\delta\Theta' = \delta\Theta'' \quad \text{and} \quad \delta\Xi' = \delta\Xi'' \qquad (5.28)$$

so that

$$\delta\Theta' + \delta\Xi' = \delta\Theta'' + \delta\Xi'' = \delta\Theta' + \delta\Xi'' \qquad (5.29)$$

Eqns. 5.28 and 5.29 arise from the uniqueness of solutions; they imply that any differences between dual functionals, Θ' and Θ'', or Ξ' and Ξ'', are pre-specified and therefore have zero variations. The validity of 5.28 and 5.29 can be demonstrated by substitution of the expressions for the various functionals. In any case, the constitutive error is computable for any pair of estimates, $\underline{H}(\underline{r})$ and $\underline{B}(\underline{r})$, irrespective of the manner by which they are obtained, eqn. 3.71. Moreover, the variational principles of eqns. 5.9 and 5.10 remain valid; to apply them, we need the variations of Θ' and Ξ'' in eqns. 5.27 :

$$\delta\Theta' = \langle\mu(\underline{H})\underline{H} + \underline{B}_r \, , \, \delta\underline{H}\rangle_R - \langle\rho \, , \, \delta\Omega\rangle_R + [b \, , \, \delta\Omega]_{S_b} \qquad (5.30a)$$

and

$$\delta\Xi'' = \langle\nu(\underline{B})\underline{B} + \underline{H}_c \, , \, \delta\underline{B}\rangle_R - \langle\underline{J} \, , \, \delta\underline{A}\rangle_R + [\underline{h} \, , \, \delta\underline{A}]_{S_h} \qquad (5.30b)$$

The variations of fields and potentials are obtainable from eqns. 5.25 and 5.26 where, with the exception of the nodal potentials, all terms are pre-specified and hence have zero variations. Substituting, moreover, for the fields from 5.26, and taking the spatially invariant nodal potentials out from the volume and surface integrals, we find

$$\delta\Theta' = \sum_i \delta\Omega_i \{ \sum_j S^H_{ij}\Omega_j - T^H_i\} \qquad (5.31a)$$

where

$$S^H_{ij} = \langle\mu(\underline{H}) \, \nabla\alpha_j \, , \, \nabla\alpha_i\rangle_R$$

$$T^H_i = \langle\mu(\underline{H})\underline{G} + \underline{B}_r \, , \, \nabla\alpha_i\rangle_R + \langle\rho \, , \, \alpha_i\rangle_R - [b \, , \, \alpha_i]_{S_b}$$

and

$$\delta\Xi'' = \sum_i \sum_q \delta A_{iq} \{ \sum_j \sum_p S^B_{iqjp} A_{jp} - T^B_{iq}\} \qquad (5.31b)$$

where

$$S^B_{iqjp} = \langle\nu(\underline{B})(\underline{a}_p \times \nabla\beta_j) \, , \, \underline{a}_q \times \nabla\beta_i\rangle_R$$

$$T^B_{iq} = \langle\nu(\underline{B})\underline{C}+\underline{H}_c \, , \, \underline{a}_q \times \nabla\beta_i\rangle_R + \langle\underline{J} \, , \, \underline{a}_q\beta_i\rangle_R - [\underline{h} \, , \, \underline{a}_q\beta_i]_{S_h}$$

Recalling eqns. 5.9-12, the solution equation for each unconstrained potential Ω_i is

$$\frac{\partial \Theta'}{\partial \Omega_i} = \sum_j S^H_{ij} \Omega_j - T^H_i = 0 \qquad (5.32a)$$

and for each unconstrained potential components A_{iq} it is

$$\frac{\partial \Xi''}{\partial A_{iq}} = \sum_j \sum_p S^B_{i_q j_p} A_{jp} - T^B_{iq} = 0 \qquad (5.32b)$$

The forms of eqns. 5.32 are general for the trial functions of eqns. 5.25; the definitions of their terms in 5.31 apply to the particular problem where the functionals are as given in 5.27. The definitions for problems with different specifications can be obtained by the same procedure, once the H- and B-system functionals have been extracted from the universal constitutive error. In general, the decomposition introduces complementary boundary and continuity conditions naturally.

The finite element method is a computationally convenient implementation of the above procedure. The overall region R is divided into sub-regions, called elements, as in 5.13; moreover, the space functions $\alpha_i(\underline{r})$ and $\beta_i(\underline{r})$ in eqns. 5.25, now called element shape functions, are defined in a piecewise manner over the individual elements. Thus

$$\alpha_i(\underline{r}) = \alpha^e_i(\underline{r}) \quad \text{for} \quad \underline{r} \subset \underline{r}_e \qquad (5.33a)$$

and

$$\beta_j(\underline{r}) = \beta^e_j(\underline{r}) \quad \text{for} \quad \underline{r} \subset \underline{r}_e \qquad (5.33b)$$

where $\underline{r}_e$ refers to points lying in element e. In particular, the method stipulates that

$$0 = \alpha^e_k(\underline{r}) = \beta^e_k(\underline{r}) \quad \text{for} \quad \underline{r}_k \not\subset \underline{r}_e \qquad (5.34)$$

so that the trial potential distribution within a given element is independent of nodal potentials that do not themselves lie in the element. Thus, within each element, the summations in eqns. 5.25 need not cover all nodes in R, N and M, but only those lying in that element.

The discretisation of R into finite elements means that the volume and surface integrals in 5.31 can be obtained by summing element contributions; moreover, according to eqns. 5.33 and 5.34, the contributions are zero for elements that do not include node i of eqns. 5.31. This further implies that the coefficient S_{ij} is zero if nodes i and j share no elements.

The shape functions must allow the trial potential and field distributions, eqns. 3.25 and 3.26, to satisfy, as far as possible, the required problem specifications. It is generally possible to impose boundary and continuity conditions on $\underline{n} \times \underline{H}$ and $\underline{n} \cdot \underline{B}$ exactly, provided the trial potential distributions on planar element facets are independent of nodal potentials not lying on that facet[5.4]; the established families of shape functions can cater for most practical requirements[5.4, 5].

5.3.3 The boundary integral method

Similar to the finite element method, the boundary integral method is an implementation of the general procedure that led to eqns. 5.11 and 5.12. The method is characterised by its treatment of linear sourceless sub-regions which avoids discretisation of their interiors.

Let R_k denote a linear sub-region of R that is free of internal volume and sheet source densities. It follows that the fields are continuous within R_k, eqns. 3.20 and 3.21, and that we can set the pre-specified fields $\underline{G}$ and $\underline{C}$ to zero, eqns. 3.40b and 3.41b; Maxwell's eqns. 3.18 and 3.19 take the forms

$$\nabla \times \underline{H} = 0 \quad \Rightarrow \quad \underline{H} = -\nabla \Omega \tag{5.35a}$$

and

$$\nabla \cdot \underline{B} = 0 \quad \Rightarrow \quad \underline{B} = \nabla \times \underline{A} \tag{5.35b}$$

For any twice differentiable scalar $w_H(\underline{r})$ and vector $\underline{w}_B(\underline{r})$, vector identities and the divergence theorem yield Green's theorem

$$\langle \Omega, \nabla\cdot\mu\nabla w_H\rangle_{R_k} - \langle w_H, \nabla\cdot\mu\nabla\Omega\rangle_{R_k} = [\Omega, \underline{n}\cdot\mu\nabla w_H]_{S_k} - [w_H, \xi(\underline{r}_s)]_{S_k}$$

and (5.36)

$$\langle \underline{A}, \nabla\times\nu\nabla\times\underline{w}_B\rangle_{R_k} - \langle \underline{w}_B, \nabla\times\nu\nabla\times\underline{A}\rangle_{R_k} = [\underline{A}, \underline{n}\times\nu\nabla\times\underline{w}_B]_{S_k} + [\underline{w}_B, \underline{F}(\underline{r}_s)]_{S_k}$$

where $\underline{r}_s$ refers to points on S_k, the surface enclosing R_k, and

$$\xi(\underline{r}_s) = \underline{n}\cdot\mu\nabla\Omega \ , \qquad \underline{F}(\underline{r}_s) = \underline{n}\times\nu\nabla\times\underline{A} \tag{5.37}$$

The method over-specifies the fields in R_k to the extent that each satisfies the complementary system Maxwell equation; thus, noting eqns. 5.35,

$$0 = \nabla\times\nu\underline{B} = \nabla\times\nu\nabla\times\underline{A} \tag{5.38a}$$

and

$$0 = \nabla\cdot\mu\underline{H} = -\nabla\cdot\mu\nabla\Omega \tag{5.38b}$$

The over-specification is imposed by substituting 5.38 into 5.36 to drop the corresponding terms. Moreover, w_H and $\underline{w}_B$ are substituted for by suitable singularity functions for which we can write

$$\Omega(\underline{r}') = \eta_H(\underline{r}')\langle\Omega(\underline{r}) \ , \ \nabla_r\cdot\mu\nabla_r w_H(\underline{r},\underline{r}')\rangle_{R_k} \tag{5.39a}$$

and

$$A_q(\underline{r}') = \eta_B^q(\underline{r}')\langle\underline{A}(\underline{r}) \ , \ \nabla_r\times\nu\nabla_r\times\underline{w}_B^q(\underline{r},\underline{r}')\rangle_{R_k} \tag{5.39b}$$

where $\underline{r}'$ refers to any point in R_k, A_q is a particular space component of $\underline{A}$, and η_H and η_B^q are known functions associated with w_H and $\underline{w}_B^q$ respectively. Substituting from 5.38 and 5.39 into 5.36, we get

$$\Omega(\underline{r}') = \eta_H(\underline{r}')\left([\Omega(\underline{r}), \underline{n}\cdot\mu\nabla_r w_H(\underline{r},\underline{r}')]_{S_k} - [w_H(\underline{r},\underline{r}'), \xi(\underline{r})]_{S_k}\right)$$

and (5.40)

$$A_q(\underline{r}') = \eta_B^q(\underline{r}')\left([\underline{A}(\underline{r}).\underline{n}\times\nu\nabla_r\times\underline{w}_B^q(\underline{r},\underline{r}')]_{S_k} + [\underline{w}_B^q(\underline{r},\underline{r}'), \underline{F}(\underline{r})]_{S_k}\right)$$

The numerical over-specification in R_k is restricted to the surface S_k where a number of nodes are defined and trial functions of the form of 5.25 are used for all four surface variables :

$$\Omega(\underline{r}_s) = \sum_i \Omega_i\alpha_i'(\underline{r}_s) \ , \qquad \xi(\underline{r}_s) = \sum_i \xi_i\alpha_i''(\underline{r}_s) \tag{5.41a}$$

and

$$\underline{A}(\underline{r}_s) = \sum_j \underline{A}_j\beta_j'(\underline{r}_s) \ , \qquad \underline{F}(\underline{r}_s) = \sum_j \underline{F}_j\beta_j''(\underline{r}_s) \tag{5.41b}$$

where Ω_i, ξ_i, $\underline{A}_j$, and $\underline{F}_j$ are the values of the variables at node i; α'_i, α''_i, β'_j, and β''_j are the corresponding prescribed space functions; as before, $\underline{r}_S$ refers to points on S_k. Substituting the trial functions of eqns. 5.41 into 5.40, and rearranging, we get

$$\sum_i \{\Omega_i \alpha'_i(\underline{r}'_S) - \eta_H(\underline{r}'_S)[\Omega_i \alpha'_i(\underline{r}_S) \, , \, \underline{n}\cdot\mu\nabla_r w_H(\underline{r}_S,\underline{r}'_S)]_{S_k}\}$$
$$= - \sum_j \eta_H(\underline{r}'_S)[\xi_j \alpha''_j(\underline{r}_S) \, , \, w_H(\underline{r}_S,\underline{r}'_S)]_{S_k} \tag{5.42}$$

and

$$\sum_i \{A_{iq}\beta'_i(\underline{r}'_S) - \eta^q_B(\underline{r}'_S)[\underline{A}_i \beta'_i(\underline{r}_S) \, , \, \underline{n}\times\nu\nabla_r\times\underline{w}^q_B(\underline{r}_S,\underline{r}'_S)]_{S_k}\}$$
$$= \sum_j \eta^q_B(\underline{r}'_S)[\underline{F}_j \beta''_j(\underline{r}_S) \, , \, \underline{w}^q_B(\underline{r}_S,\underline{r}'_S)]_{S_k}$$

Applying eqns. 5.42 at a sufficient number of test points $\underline{r}'_S$ on S_k, the following matrix relationships can be constructed to link the nodal variables

$$[M']\{\Omega\} = [M'']\{\xi\} \tag{5.43a}$$

and

$$[N']\{A\} = [N'']\{F\} \tag{5.43b}$$

where $\{\Omega\}$, $\{\xi\}$, $\{A\}$, and $\{F\}$ are column vectors listing, respectively, the nodal parameters Ω_i, ξ_i, A_{iq}, and F_{iq}; [M'], [M''], [N'], and [N''] are coefficient matrices whose elements are computed using eqns. 5.42; singularities arise where the integration point $\underline{r}_S$ coincides with the test point $\underline{r}'_S$, but these are treatable[5.4]. By choosing as many test points as there are nodes, the coefficient matrices can be made square, providing an invertible relationship between the nodal potentials and the nodal values of their surface derivatives. It is important to note, however, that these relationships incorporate an inherent inconsistency resulting from treating the nodal derivatives ξ and $\underline{F}$ as being independent of their respective potentials, Ω and $\underline{A}$, in the definition of the trial functions, eqns. 5.41[5.4]: with the variables in 5.40 represented by the trial functions of 5.41, the left hand sides cannot, in general, model the exact outcome of the computations on the right hand sides continuously over S_k. However, equality can be forced at a finite number of test points to produce 5.43.

Now the contribution of sub-region R_k to the global constitutive error is given by

$$\Lambda_k = X_k(\underline{H}) + \Psi_k(\underline{B}) - Z_k(\underline{H},\underline{B}) \qquad (5.44)$$

Substituting from eqns. 5.35 for the fields in Z_k, eqn. 2.11, we get

$$Z_k = - \langle \nabla\Omega , \underline{B} \rangle_{R_k} = \langle \underline{H} , \nabla\times\underline{A} \rangle_{R_k} \qquad (5.45)$$

Applying vector identities, recalling the absence of volume and sheet source densities, and using the divergence theorem, we get

$$Z_k = - [\Omega , \underline{n}\cdot\underline{B}]_{S_k} = - [\underline{n}\times\underline{H} , \underline{A}]_{S_k} \qquad (5.46)$$

In either form, the decomposition produces surface terms only; these are matched with similar terms contributed by adjacent sub-regions sharing S_k, or with specified boundary conditions if S_k is part of S. The absence of volume terms in 5.46 is a direct consequence of the sourcelessness of R_k.

Consider, next, X_k and Ψ_k. Substituting for the fields from eqns. 5.35 into the linear forms of eqn. 4.53 :

$$X_k = \tfrac{1}{2}\langle \mu\underline{H} , \underline{H} \rangle_{R_k} = \tfrac{1}{2}\langle \mu\nabla\Omega , \nabla\Omega \rangle_{R_k} \qquad (5.47a)$$

and

$$\Psi_k = \tfrac{1}{2}\langle \nu\underline{B} , \underline{B} \rangle_{R_k} = \tfrac{1}{2}\langle \nu\nabla\times\underline{A} , \nabla\times\underline{A} \rangle_{R_k} \qquad (5.47b)$$

Applying vector identities and the divergence theorem, and substituting from eqns. 5.37 and 5.38 into the result :

$$X_k = \tfrac{1}{2}[\xi , \Omega]_{S_k} \quad \text{and} \quad \Psi_k = - \tfrac{1}{2}[\underline{F} , \underline{A}]_{S_k} \qquad (5.48)$$

As only surface terms remain, we can substitute for all variables their numerically constrained forms in 5.41 :

$$X_k = \tfrac{1}{2} \sum_i \sum_j [\Omega_i \alpha'_i(\underline{r}_s) , \xi_j \alpha''_j(\underline{r}_s)]_{S_k} \qquad (5.49a)$$

and

$$\Psi_k = - \tfrac{1}{2} \sum_i \sum_j [\underline{A}_i \beta'_i(\underline{r}_s) , \underline{F}_j \beta''_j(\underline{r}_s)]_{S_k} \qquad (5.49b)$$

Using the column vectors defined with relation to eqns. 5.43, we can rewrite eqns. 5.49 in the form

$$X_k = \tfrac{1}{2}\{\Omega\}^T[D_H]\{\xi\} \tag{5.50a}$$

and

$$\Psi_k = \tfrac{1}{2}\{A\}^T[D_B]\{F\} \tag{5.50b}$$

where the superscript T indicates transposition. Using eqns. 5.43 to eliminate $\{\xi\}$ and $\{F\}$, we finally get

$$X_k = \tfrac{1}{2}\{\Omega\}^T[D_H][M'']^{-1}[M']\{\Omega\} \tag{5.51a}$$

and

$$\Psi_k = \tfrac{1}{2}\{A\}^T[D_B][N'']^{-1}[N']\{A\} \tag{5.51b}$$

X_k and Ψ_k, expressed here in terms of nodal potentials on S_k, go into the global system functionals Θ and Ξ, respectively; the solution equations are then obtained using eqns. 5.11 and 5.12. The interior of R_k is not discretised because the entire contribution of R_k to Λ is in terms of the variables on S_k, eqns. 5.46 and 5.51. Exact boundary and continuity conditions can be imposed by matching the trial functions on S_k, eqns. 5.41, to the boundary conditions and/or the discretisation used in the regions surrounding R_k.

5.4 Conclusions

The error-based variational procedure of sec. 5.3 applies to a number of established numerical methods. The various methods, characterised essentially by the numerical over-specifications they impose, result in solution equations which can be put in a general, matrix, form

$$0 = [S^H]\{\Omega\} - \{T^H\} \tag{5.52a}$$

and

$$0 = [S^B]\{A\} - \{T^B\} \tag{5.52b}$$

$\{\Omega\}$ and $\{A\}$ are column vectors listing the nodal potentials. $[S^H]$ and $[S^B]$ are square coefficient matrices; they evolve from $X(\underline{H})$ and $\Psi(\underline{B})$, respectively, and thus have standard forms in the various numerical methods. $\{T^H\}$ and $\{T^B\}$ are forcing vectors; their composition depends on the specifications of the particular problem being considered; see,

for example, eqns. 5.31. The two vectors reflect the decomposition of $Z(\underline{H},\underline{B})$ between the H- and B-systems, and thus are the mechanism by which the sources, continuity conditions, and boundary conditions of one system are imposed on the solution of the complementary system; sec. 5.2.2 argues for the natural imposition of continuity and boundary conditions in this way, as opposed to explicit imposition at the outset. $\{T^H\}$ and $\{T^B\}$ also force own system sources in terms of the pre-specified fields $\underline{G}$ and $\underline{C}$.

Solution of eqns. 5.52 yields the values of the nodal potentials, $\{\Omega\}$ and $\{A\}$, which correspond to the minimum constitutive error for the numerical over-specifications used. Once the potentials have been determined, the corresponding field distributions can be estimated, and the constitutive error computed, locally as the error density λ, and globally as the total error Λ. In fact, the error is computable for any pair of estimated field distributions, $\underline{H}(\underline{r})$ and $\underline{B}(\underline{r})$, irrespective of the means used to make the estimates. There is no fundamental requirement that the solution methods used for the two systems should correspond to each other in any way; for example, the space functions and node numbers in eqns. 5.25 are not necessarily the same for the H- and B-systems.

The constitutive error, which is zero in an exact solution, is attributable to the totality of over-specifications in a numerical solution. It is, moreover, a comprehensive measure of numerical error if the specifications are entirely consistent, sec. 5.2.3; accordingly, it can be used to assess the accuracy of the over-specifications, locally and globally[5,6,7]. The boundary integral method, sec. 5.3.3, provides an example of inconsistent specification where additional errors arise that are not accounted for by the constitutive error.

Solving either of the two complementary systems alone can be viewed as the minimisation of that system's contribution to the constitutive error; however, the solution does

not produce an estimate of the contribution. As defined in this work, the constitutive error resides in both systems together, being the sum of their individual errors relative to the true solution; both systems must therefore be solved if the error is to be determined. Chapters 6 and 7 give the errors resulting from complementary finite element solutions of a number of static problems.

The error cannot be used directly to assess either of the complementary solutions on its own, or to evaluate their comparative merits. Indirect schemes can, however, be devised. For example, the error may be viewed as an approximate, pessimistic estimate of either system error relative to the true solution. Alternatively, one solution may be retained as reference, with the error computed for different implementations of the complementary solution; the corresponding changes in the error then reflect the effects of the various implementations. This latter scheme is used in Chapter 8 to compare alternative definitions of the pre-specified fields in the H-solution : the same B-solution is used with different definitions.

C H A P T E R S I X

Linear Applications

6.1 Introduction

This chapter presents complementary solutions to a number of static, linear, two-dimensional problems; numerical results are obtained by the finite element method. The selection of problems and the presentation of results are intended to highlight the insight provided by the constitutive error approach. Particular aspects are emphasised, including : generation of complementary functionals, especially with regard to boundary specifications; comparative behaviour of complementary solutions; distribution of discretisation errors; bounds on circuit parameters; etc.

6.2 Two-dimensional simplification

According to section 3.4, the solution to a well-posed problem imposes the following relationships on the fields $\underline{H}$ and $\underline{B}$:

$$\underline{B} = \mu(\underline{H})\underline{H} + \underline{B}_r \quad ; \quad \underline{H} = \nu(\underline{B})\underline{B} + \underline{H}_c \qquad (6.1)$$

$$\underline{J} = \text{curl } \underline{H} \quad ; \quad \rho = \text{div } \underline{B} \qquad (6.2)$$

$$\underline{K} = \underline{n} \times \Delta\underline{H} \text{ on } S_\Delta \quad ; \quad \sigma = \underline{n} \cdot \Delta\underline{B} \text{ on } S_\Delta \qquad (6.3)$$

$$\underline{h} = \underline{n} \times \underline{H} \text{ on } S_h \quad ; \quad b = \underline{n} \cdot \underline{B} \text{ on } S_b \qquad (6.4)$$

with, possibly, other boundary conditions, sec. 3.4.2. The constitutive error approach imposes eqns. 6.2-4 explicitly, and eqn. 6.1 weakly by minimising the error

$$\Lambda(\underline{H},\underline{B}) = X(\underline{H}) + \Psi(\underline{B}) - Z(\underline{H},\underline{B}) \qquad (6.5)$$

Two-dimensional analysis is possible if sources, fields, geometry, and material properties are invariant in a particular direction, say the z-axis. The following equations then describe a consistent set of restrictions :

$$\underline{H} = H_x\underline{a}_x + H_y\underline{a}_y \quad ; \quad \underline{B} = B_x\underline{a}_x + B_y\underline{a}_y \tag{6.6}$$

and

$$\underline{J} = J_z\underline{a}_z \quad ; \quad \underline{K} = K_z\underline{a}_z \quad ; \quad \underline{h} = h_z\underline{a}_z \tag{6.7}$$

Surfaces of discontinuity, S_Δ, are parallel to the z-axis, so that

$$\text{on } S_\Delta : \quad \underline{n} = n_x\underline{a}_x + n_y\underline{a}_y \tag{6.8}$$

The bounding surface, S, is composed of two main sections :

$$S = S_s \cup S_o \tag{6.9a}$$

where

$$\text{on } S_s : \quad \underline{n} = n_x\underline{a}_x + n_y\underline{a}_y \tag{6.9b}$$

and

$$\text{on } S_o : \quad \underline{n} = \pm\,\underline{a}_z \quad \text{with} \quad \underline{n} \cdot \underline{B} = 0 \tag{6.9c}$$

In effect, the region R is a right cylinder; its length in the z-direction is taken to be unity.

The above restrictions are sufficient, but not strictly necessary, to extract a two-dimensional solution from the general, three-dimensional constitutive error Λ. They allow the potentials to be defined as follows :

$$\underline{H} = \underline{G}(x,y) - \text{grad } \Omega(x,y) \tag{6.10a}$$

with

$$\underline{G} = G_x\underline{a}_x + G_y\underline{a}_y \quad ; \quad \text{curl } \underline{G} = \underline{J} \tag{6.10b}$$

and

$$\underline{B} = \underline{C}(x,y) + \text{curl } \underline{A}(x,y) \quad ; \quad \underline{A} = A\,\underline{a}_z \tag{6.11a}$$

with

$$\underline{C} = C_x\underline{a}_x + C_y\underline{a}_y \quad ; \quad \text{div } \underline{C} = \rho \tag{6.11b}$$

The above definition of the vector potential $\underline{A}$ satisfies the following solvability requirements from sec. 3.4.4.2 :

$$\text{div } \underline{A} = 0 \quad ; \quad \underline{n} \cdot \Delta\underline{A} = 0 \quad \text{on } S_\Delta \tag{6.12a}$$

and

$$\underline{n} \cdot \underline{A} = 0 \quad \text{on } S_s \quad ; \quad \underline{n} \times \underline{A} = 0 \quad \text{on } S_o \tag{6.12b}$$

The remaining requirement on $\underline{n} \times \Delta\underline{A}|_{S_\Delta}$ is problem-dependent. On S_b sections of S_s, $\underline{n} \times \underline{A}$ may be specified, which results in a consistent over-specification of $\underline{A}$ since $\underline{n} \cdot \underline{A}$ is also specified on S_s, eqns. 6.12b.

6.3 Linear problems

In linear media, the constitutive relationship simplifies to

$$\underline{B} = \mu \underline{H} \quad \text{or} \quad \underline{H} = \nu \underline{B} \tag{6.13a}$$

with

$$\nu = \mu^{-1} \quad \text{or} \quad \mu = \nu^{-1} \tag{6.13b}$$

The constitutive operators can vary with position, but are independent of the fields. They are, moreover, symmetric according to property 2 of sec. 2.2. In the examples, we shall consider isotropic media only.

Substituting from eqns. 6.13 into 2.8, $\chi(\underline{H})$ and $\psi(\underline{B})$ simplify to

$$\chi(\underline{H}) = \tfrac{1}{2}\langle \mu\underline{H} , \underline{H}\rangle \quad \text{and} \quad \psi(\underline{B}) = \tfrac{1}{2}\langle \nu\underline{B} , \underline{B}\rangle \tag{6.14}$$

The exact solution fields, $\underline{H}_o$ and $\underline{B}_o$, satisfy the constitutive relationship 6.13a, so that substitution into 6.14 yields

$$\chi(\underline{H}_o) = \tfrac{1}{2}\langle \underline{B}_o, \underline{H}_o\rangle \quad \text{and} \quad \psi(\underline{B}_o) = \tfrac{1}{2}\langle \underline{H}_o, \underline{B}_o\rangle \tag{6.15}$$

Recalling the definition of $\zeta(\underline{H},\underline{B})$ in eqn. 2.11, we find

$$\chi(\underline{H}_o) = \psi(\underline{B}_o) = \tfrac{1}{2}\zeta(\underline{H}_o, \underline{B}_o) = w \tag{6.16a}$$

Integrating over the region R, we obtain the globals

$$X(\underline{H}_o) = \Psi(\underline{B}_o) = \tfrac{1}{2}Z(\underline{H}_o, \underline{B}_o) = W \tag{6.16b}$$

W denotes the exact energy, or co-energy, in magnetostatic and electrostatic applications, and half the exact power dissipation in current flow applications; w is the corresponding density distribution.

6.4 Implementation

The examples are solved by the finite element method, a general description of which is given in sec. 5.3.2. The discretisation employs first-order triangular elements, with the potentials at the vertices as the unknowns; these elements are well-documented in the literature[6.1,2], and will not be elaborated here. We only note that the shape functions yield constant potential derivatives, and hence fields, within the individual elements, and continuous $\underline{n} \times \underline{H}$ and $\underline{n} \cdot \underline{B}$ across element interfaces.

Software was developed on an LSI 11/23 with facilities for interactive colour graphics. The package is structured in distinct stages, fig. 6.1, and uses files to store and communicate data[6.3,4]. Mesh geometry is defined manually using MAGMESH, the interactive mesh-generating program in MAGNET-11[6.5,6]. The problem specifier assigns material properties, source distributions, boundary conditions, and potential discontinuities. The solution matrices are formed in the matrix assembler, and inverted in the solver, independently for the two complementary solutions. The solver employs the incomplete Choleski-conjugate gradient method with Manteuffel shifts[6.7,8]; the program was made available by the electromagnetics group at the Rutherford Appleton Laboratory. An auxiliary loop updates permeabilities and re-forms matrices in non-linear applications. The geometry and solution files are finally fed into a special-purpose postprocessor that computes a range of relevant results, and produces colour graphic displays by means of QUARTO subroutines[6.9].

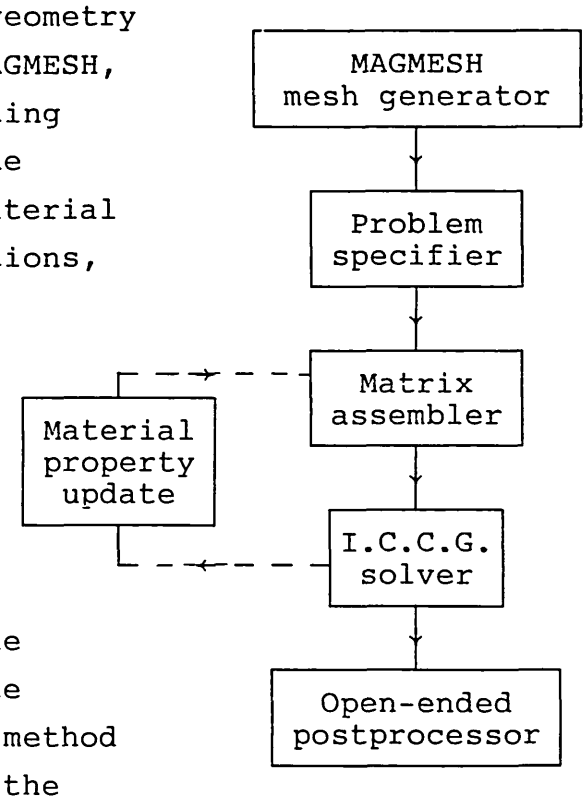

Fig. 6.1 Program structure.

6.5 Magnetostatic examples

In magnetostatics, the equations for fields and potentials are :

$$\underline{J} = \text{curl } \underline{H} \quad ; \quad 0 = \text{div } \underline{B} \tag{6.17}$$

$$\underline{k} = \underline{n} \times \Delta\underline{H} \text{ on } S_k ; \quad 0 = \underline{n} \cdot \Delta\underline{B} \tag{6.18}$$

$$\underline{H} = \underline{G} - \nabla\Omega \quad ; \quad \underline{B} = \nabla \times \underline{A} \tag{6.19}$$

$$0 = \underline{n} \times \Delta\underline{A} \tag{6.20}$$

Using the B-system vector potential $\underline{A}$, $Z(\underline{H},\underline{B})$ splits as follows :

$$\begin{aligned} Z(\underline{H},\underline{B}) &= \langle \underline{H} , \underline{B} \rangle_R = \langle \underline{H} , \nabla\times\underline{A} \rangle_R = \langle \nabla\times\underline{H} , \underline{A} \rangle_R - \int_R \nabla\cdot(\underline{H}\times\underline{A})\, dR \\ &= \langle \underline{J} , \underline{A} \rangle_R + [\underline{n} \times \underline{H} , \underline{A}]_{S_k} - [\underline{n}\times\underline{H} , \underline{A}]_{S_s} + [\underline{H} , \underline{n}\times\underline{A}]_{S_o} \\ &= \langle \underline{J} , \underline{A} \rangle_R + [\underline{K} , \underline{A}]_{S_k} - [\underline{n} \times \underline{H} , \underline{A}]_{S_s} \end{aligned}$$

At this stage, we can rewrite eqn. 6.5 in the form

$$\Lambda = \Theta_o(H) + \Xi_o(B) - \Gamma_o(H,A) \tag{6.21}$$

where

$$\Theta_o(H) = X(\underline{H})$$

$$\Xi_o(B) = \Psi(B) - \langle \underline{J} , \underline{A} \rangle_R - [\underline{K} , \underline{A}]_{S_k}$$

$$\Gamma_o(H,A) = - [\underline{n} \times \underline{H} , \underline{A}]_{S_s} = [\underline{H} , \underline{n} \times \underline{A}]_{S_s}$$

Alternative definitions of the H-system pre-specified field $\underline{G}$ are analysed at length in Chapter 8; the following definition is shown to be consistent with linear shape functions for Ω

$$\underline{G}(\underline{r}) = \tfrac{1}{2}\, \underline{J} \times (\underline{r} - \underline{r}_o) \quad \Rightarrow \quad \text{curl } \underline{G} = \underline{J} \tag{6.22}$$

and will be used here. $\underline{r}_o$ is an arbitrary reference point that can be chosen independently for each conductor. $\underline{J}$ is constant in conductors, and zero in iron and air. Thus $\underline{G}$ is zero outside conductors; the resulting discontinuity in $\underline{n} \times \underline{G}$ at conductor surfaces is absorbed by a jump in Ω, computed using eqn. 3.55[6,10]. A cut is defined for each totally enclosed conductor, eqn. 3.45, with $\Delta\Omega$ equal to the conductor current.

6.5.1 C-magnet

Fig. 6.2 shows a C-magnet similar to that of reference 6.11. From symmetry

$$\text{on } S_h : \quad \underline{n} \times \underline{H} = 0 \quad \Rightarrow \quad \Omega = \overline{\Omega}_h \quad (= 0) \tag{6.23a}$$

Moreover, the semi-closed nature of the magnetic circuit allows us to approximate

$$\text{on } S_b : \quad \underline{n} \cdot \underline{B} = 0 \quad \Rightarrow \quad \underline{A} = \overline{\underline{A}}_b \quad (= 0) \tag{6.23b}$$

Substituting these boundary conditions into Γ_o in eqn. 6.21, we find

$$\Gamma_o = - [\underline{n} \times \underline{H} , \underline{A}]_{S_h} + [\underline{H} , \underline{n} \times \underline{A}]_{S_b} = 0$$

so that

$$\Lambda = \Theta(H) + \Xi(B) \tag{6.24a}$$

with

$$\Theta(H) = X(\underline{H}) \quad \text{and} \quad \Xi(B) = \Psi(\underline{B}) - \langle \underline{J} , \underline{A} \rangle_R \tag{6.24b}$$

From ineq. 4.10a and eqn. 6.16, we have

$$\Theta(H) \geq W \geq - \Xi(B) \tag{6.25}$$

where W is the exact energy in the half-section under consideration. The average of numerically computed energy bounds

$$\ddot{W} = \tfrac{1}{2}\left(\Theta(H) + (-\Xi(B))\right) \tag{6.26}$$

is generally a better estimate of W than either. On the electric circuit side, W is given by

$$W = \tfrac{1}{2} L I^2 \tag{6.27}$$

where L and I are the inductance and current of the upper coil.

Numerical results are based on a coil mmf of 7700 Ampere-turns, which corresponds to a current density of 1 A/mm^2. The relative permeability of the iron core is taken to be 500.

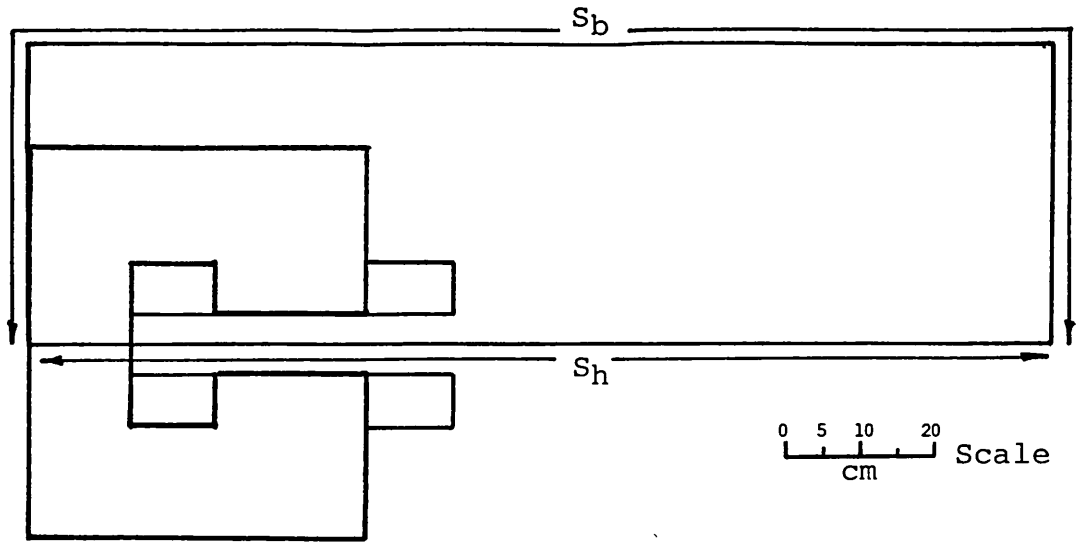

Fig. 6.2 C-magnet outline.

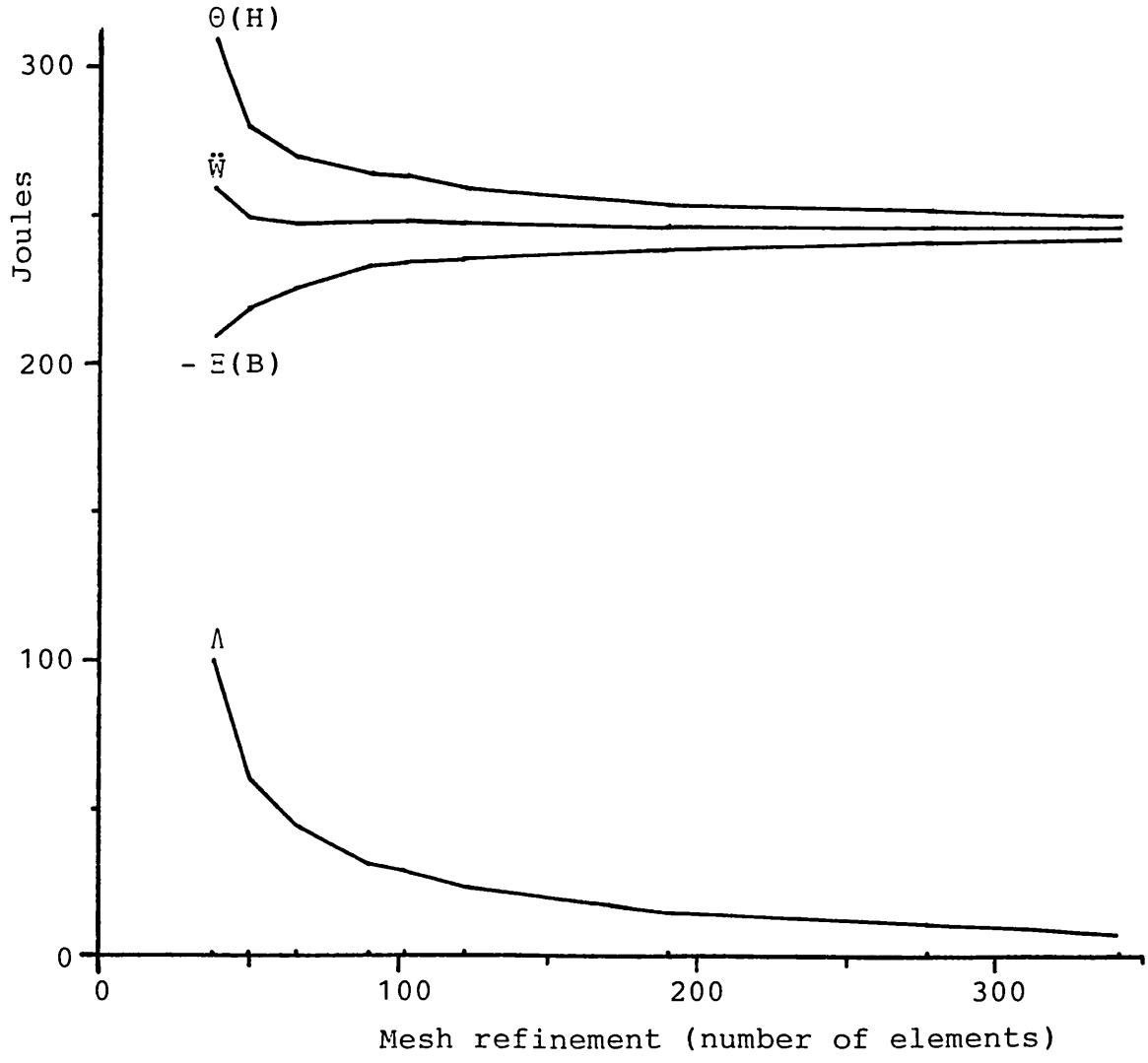

Fig. 6.3 C-magnet convergence curves.

Complementary solutions were performed on nine successively refined meshes, starting with 38 elements and 27 nodes, and ending with 341 elements and 189 nodes. Refinement was guided by the distribution of the constitutive error density λ : regions of high error concentrations were broken down into finer elements. The resulting convergence curves are shown in fig. 6.3. The finest mesh placed the exact energy W at 246.4 J ± 1.6%; the corresponding global constitutive error is 7.82 J, and the coil inductance is 8.31 N^2 μH, N being the number of turns.

The average of the energy bounds, $\ddot{W}$, exhibits a general downward trend, with occasional slight oscillation. The bounds are therefore not strictly symmetric about the exact energy, the B-solution (lower bound) being marginally more accurate than the H-solution (upper bound) in this problem. However, by the third mesh refinement (66 elements, 41 nodes), $\ddot{W}$ was already within 1% of the final value it attained. The constitutive error, Λ, improved from 41% to 3.2% with mesh refinement. Beyond the initial coarse meshes, roughly half the error may be associated with each of the complementary energy estimates. It follows that averaging complementary solutions at 66 elements and 41 nodes yields a more accurate estimate of W, and hence L, than either solution alone does at 341 elements and 189 nodes.

The above findings regarding global quantities corroborate those reported by Penman and Fraser[6•12] and by Hammond and Tsiboukis[6•13]. We now proceed to examine space distributions.

Complementary estimates of energy distributions are shown in fig. 6.4, where colour coding provides an indication of actual values*. Linear shape functions for the

---

* In general, density increases as colours shift from bright to dark. More specifically, each colour indicates a density value greater than the figure beneath it, and less than the figure above it, in the colour-code key of the margin. At the bottom of the scale, white is implicitly greater than zero since all energy densities are positive. There is no upper limit at the top of the scale, so that black provides a 'greater than' indication only.

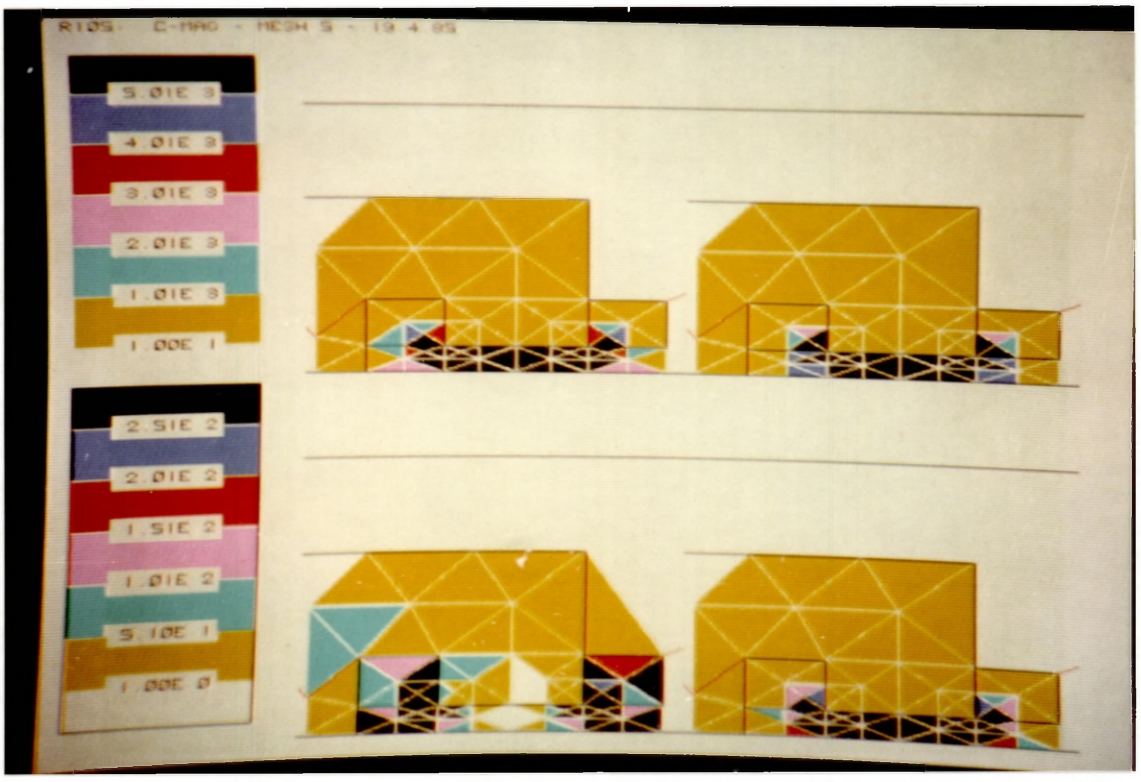

Fig. 6.4 C-magnet energy and error density distributions in 102-element mesh. Clockwise from top left : $\chi(\underline{H})$, $\psi(\underline{B})$, $\frac{1}{2}\zeta(\underline{H},\underline{B})$, and $\lambda(\underline{H},\underline{B})$. Upper scale corresponds to energies, lower scale to error.

potentials result in constant fields, and hence constant energy densities, within each current-free element. In a conductor element, however, $\chi(\underline{H})$ and $\zeta(\underline{H},\underline{B})$ are position-dependent due to the space variation of $\underline{G}$, and hence $\underline{H}$; in this case, colour coding is determined by average densities.

Fig. 6.4 shows substantially similar distributions for the three energy estimates, $\chi(\underline{H})$, $\psi(\underline{B})$, and $\frac{1}{2}\zeta(\underline{H},\underline{B})$. Energy density is greatest in the air-gap, which accounts for some 70% of the total energy. In fact, for all meshes attempted, $X(\underline{H})$ and $\Psi(\underline{B})$ in the air-gap fell within 69.59-70.56 % of the final value of $\ddot{W}$; neither exhibited a discernible pattern with mesh refinement.

Fig. 6.4 also includes the constitutive error density distribution. It is noted that the colour scale for λ indicates smaller density values than the energy scale. In this way, the λ-distribution highlights the discrepancies between the complementary solutions. Clearly, errors tend to concentrate around corners; λ thus quantises this well-known feature of numerical analysis. Despite the large energy stored in the air-gap, errors are seen to be small due to field uniformity.

The influence of the mesh on the numerical results is highlighted by the wide variation of error concentration over the region of the problem. It is recalled from sec. 5.2.3 that the constitutive error is a comprehensive measure of the numerical inaccuracy. It is therefore natural to base mesh refinement on λ. Fig. 6.5 shows λ-distributions at three other stages of the refinement process. Error concentrations are seen to recede in the general direction of their sources, namely corners. The process may be terminated when the global error becomes sufficiently small, with acceptable levels of local error in regions of interest. The constitutive error thus provides a useful indication of solution accuracy locally and globally.

Strictly, the constitutive error density λ only indicates how closely the complementary field estimates, $\underline{H}$ and

Fig. 6.5 C-magnet constitutive error density distributions at three stages of mesh refinement. Clockwise from top left : 50-, 90-, and 277-element meshes.

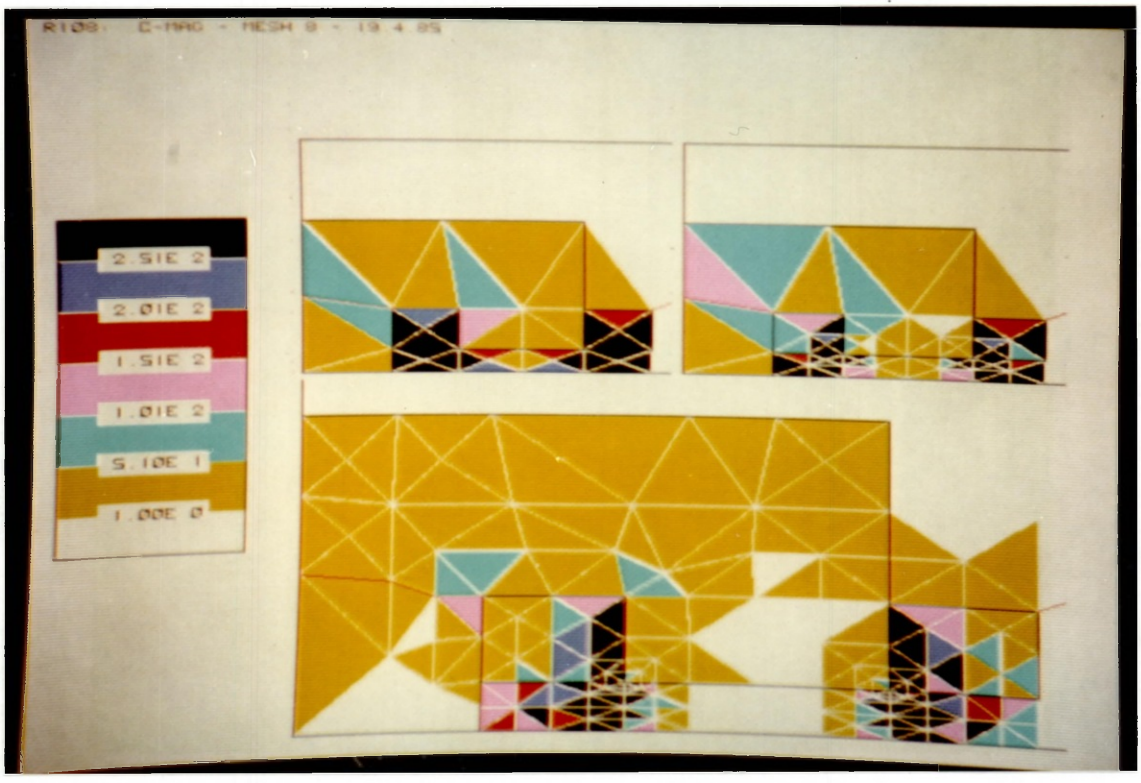

$\underline{B}$, satisfy the constitutive relationship. A vanishingly small λ, at a given point, does not guarantee that the two fields are approaching the true values at that point; the true solution requires λ to vanish everywhere simultaneously, eqn. 2.12b. It is therefore important to keep track of the global error Λ during the refinement process. Moreover, the actual value of Λ has significance only in relation to the energy level; to give a practical indication of overall accuracy, Λ must be normalised, preferably with respect to $\ddot{W}$.

Thatcher[6•14] and Cendes et al.[6•15] base mesh refinement on errors of the form

$$\varepsilon' = \langle \mu\underline{H} - \underline{B} \, , \, \mu\underline{H} - \underline{B} \rangle \qquad (6.28a)$$

and

$$\varepsilon'' = \langle \nu\underline{B} - \underline{H} \, , \, \nu\underline{B} - \underline{H} \rangle \qquad (6.28b)$$

For linear material properties, these can be related to the constitutive error density λ. Recalling eqn. 2.15b, we have

$$\lambda = \tfrac{1}{2}\langle \mu\underline{H} - \underline{B} \, , \, \underline{H} \rangle + \tfrac{1}{2}\langle \nu\underline{B} - \underline{H} \, , \, \underline{B} \rangle$$

As the constitutive operators are symmetric by property 2 of sec. 2.2, we can modify the second product, and collect terms, as follows

$$\lambda = \tfrac{1}{2}\langle \mu\underline{H} - \underline{B} \, , \, \underline{H} \rangle + \tfrac{1}{2}\langle \underline{B} - \mu\underline{H} \, , \, \nu\underline{B} \rangle$$

$$= \tfrac{1}{2}\langle \mu\underline{H} - \underline{B} \, , \, \underline{H} - \nu\underline{B} \rangle \qquad (6.29)$$

The similarity with ε' and ε'' is now evident. In particular, for isotropic media we have

$$\varepsilon' = 2\,\mu\,\lambda \qquad \text{and} \qquad \varepsilon'' = 2\,\nu\,\lambda \qquad (6.30)$$

While the error forms ε' and ε'' are entirely valid, λ is more symmetric, and has the advantage of a clear link, via Λ, to the bounding physical energies.

As demonstrated in sec. 2.4, the constitutive error accounts for discrepancies in both magnitude and space orientation of the complementary field estimates $\underline{H}$ and $\underline{B}$. Fig. 6.6 attempts to show these two aspects separately.

The B-H plots highlight discrepancies between complementary field magnitudes, H and B. Each plotted point corresponds to one of the elements in the mesh detail shown; the horizontal coordinate is the value of H, in the element, as obtained from the H-solution; the vertical coordinate is the value of B from the B-solution. The constitutive relationship is represented by the straight line, on which all points should fall in an analytic solution. As the mesh is refined, the number of points increases simply because the number of elements increases. Clearly, complementary estimates of the fields can differ considerably. There is, however, a definite migration towards the line as the mesh

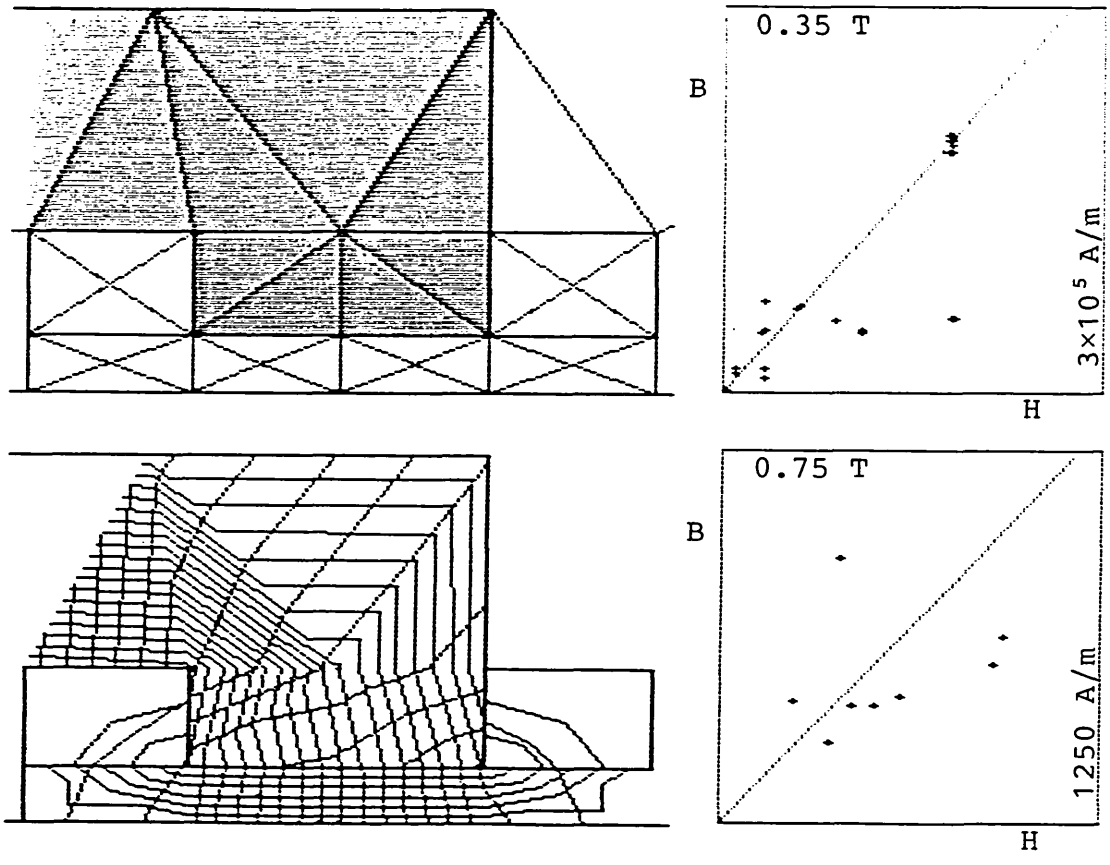

(a) 50-element, 33-node mesh; $\Lambda/\ddot{W} = 24.5\%$.

Fig. 6.6 C-magnet sub-region at three stages of mesh refinement. Clockwise from top left : finite element mesh; B-H plot in air; B-H plot in iron; and equipotential contours. NB Steps between scalar potential (Ω) contours in iron are 80 times smaller than in air.

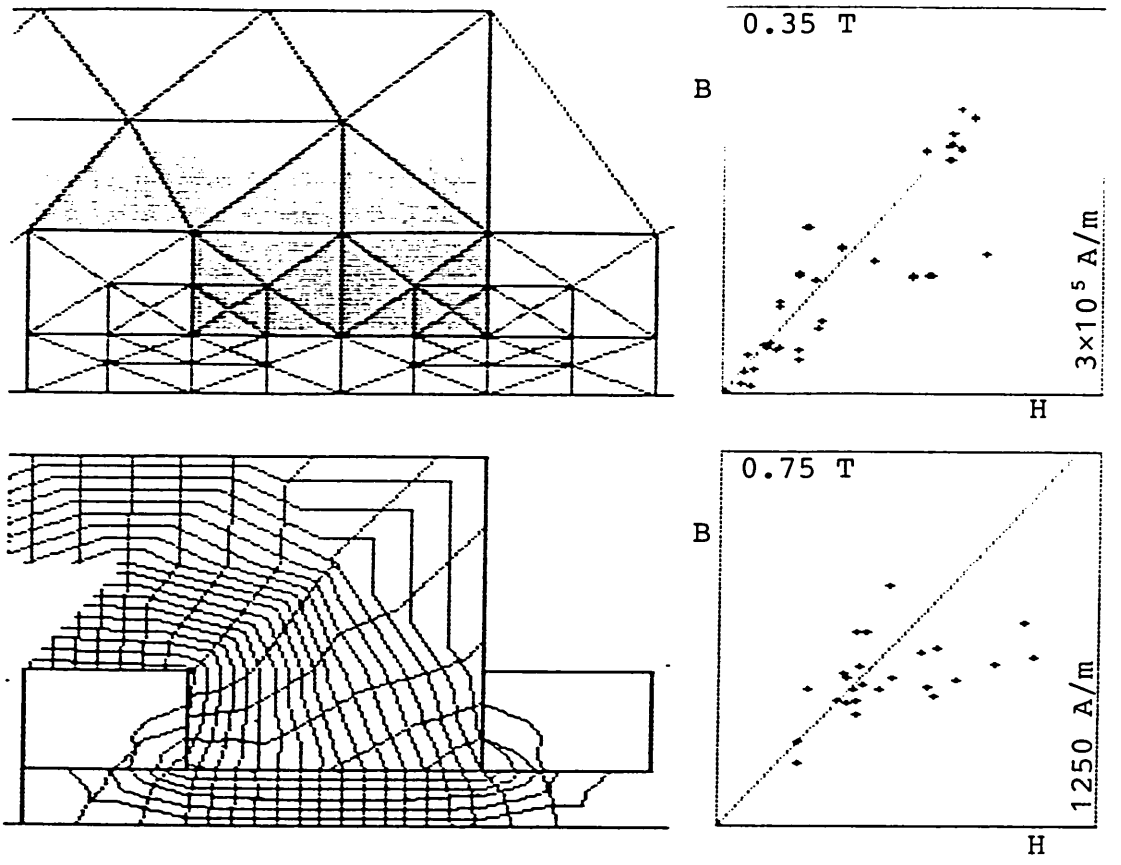

(b) 102-element, 62-node mesh; $\Lambda/\ddot{W} = 11.9\%$.

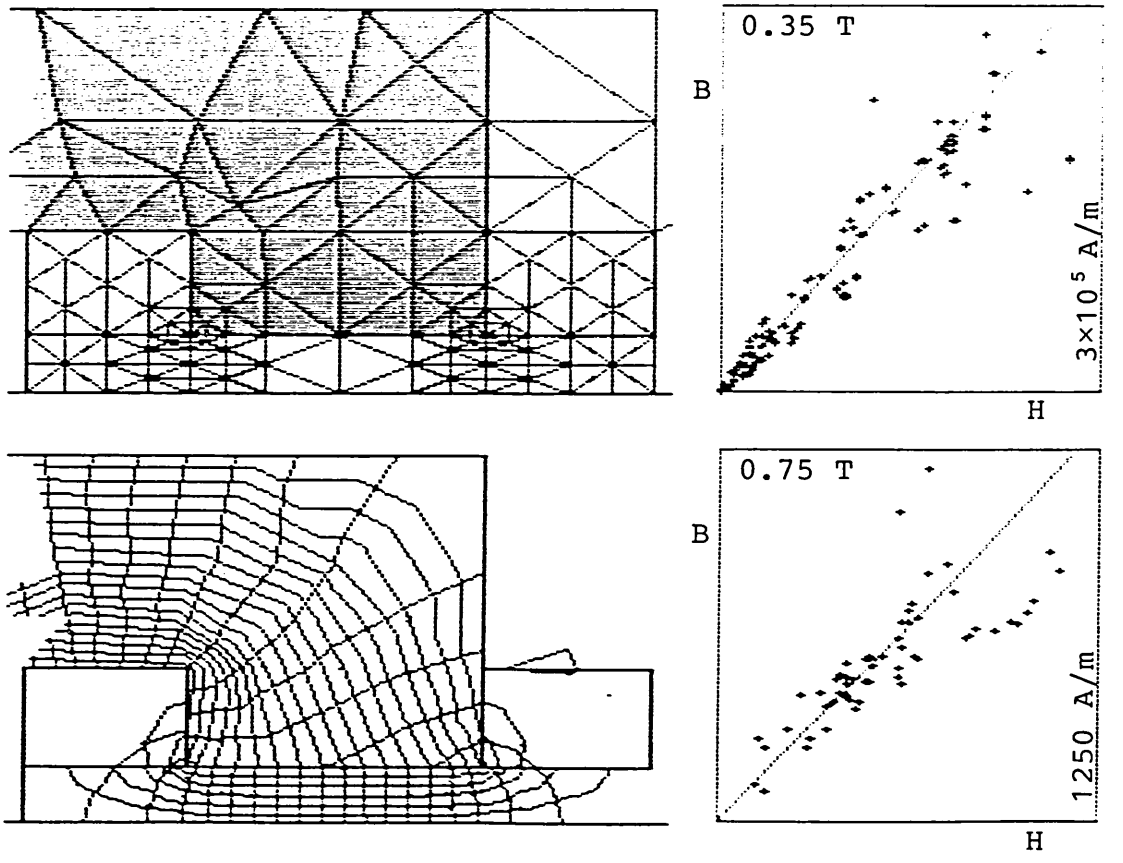

(c) 277-element, 156-node mesh; $\Lambda/\ddot{W} = 4.4\%$.

Fig. 6.6 (continued).

is refined. Moreover, finer meshes provide field estimates closer to corners, where fields tend to be high; plotted points thus appear to climb up the line. One conclusion is that the average of complementary field estimates is not, in general, more accurate than the fields, as has been suggested[6•12] : averages from coarser meshes do not approach these higher fields.

Discrepancies between space orientations of complementary field estimates are highlighted by superposition of their equipotential contours. Outside conductors, the Ω- and A-contours should be perpendicular to each other, which is seen to be largely true inside the air-gap, less so at the edges. Clearly, the two sets of contours approach orthogonality as the mesh is refined; note, in particular, the upper right corner of the iron core. The B-system A-contours represent flux lines, while the H-system Ω-contours represent the drop in magnetomotive force around the magnetic circuit. Most of the available mmf is consumed in driving flux across the air-gap. The drop in the iron core is negligibly small. It is therefore necessary to use smaller Ω steps in the iron to display the contours; the iron/air step ratio in fig. 6.6 is 1/80. Inside conductors, $\nabla\Omega$ is augmented by $\underline{G}$ to yield $\underline{H}$, eqn. 6.19; thus, no physically meaningful significance can be associated with Ω-contours there. Note, also, the discontinuity in Ω at copper/air interfaces, eqn. 3.55; the discontinuity also arises at copper/iron interfaces, but is masked in fig. 6.6 by the different potential steps used in the two regions.

The various points discussed above are further illustrated by the examples of the following sections.

6.5.2 D.C. machine

Fig. 6.7 shows a half-pole section of a 4-pole d.c. machine having a square frame. The closed magnetic circuit allows us to approximate

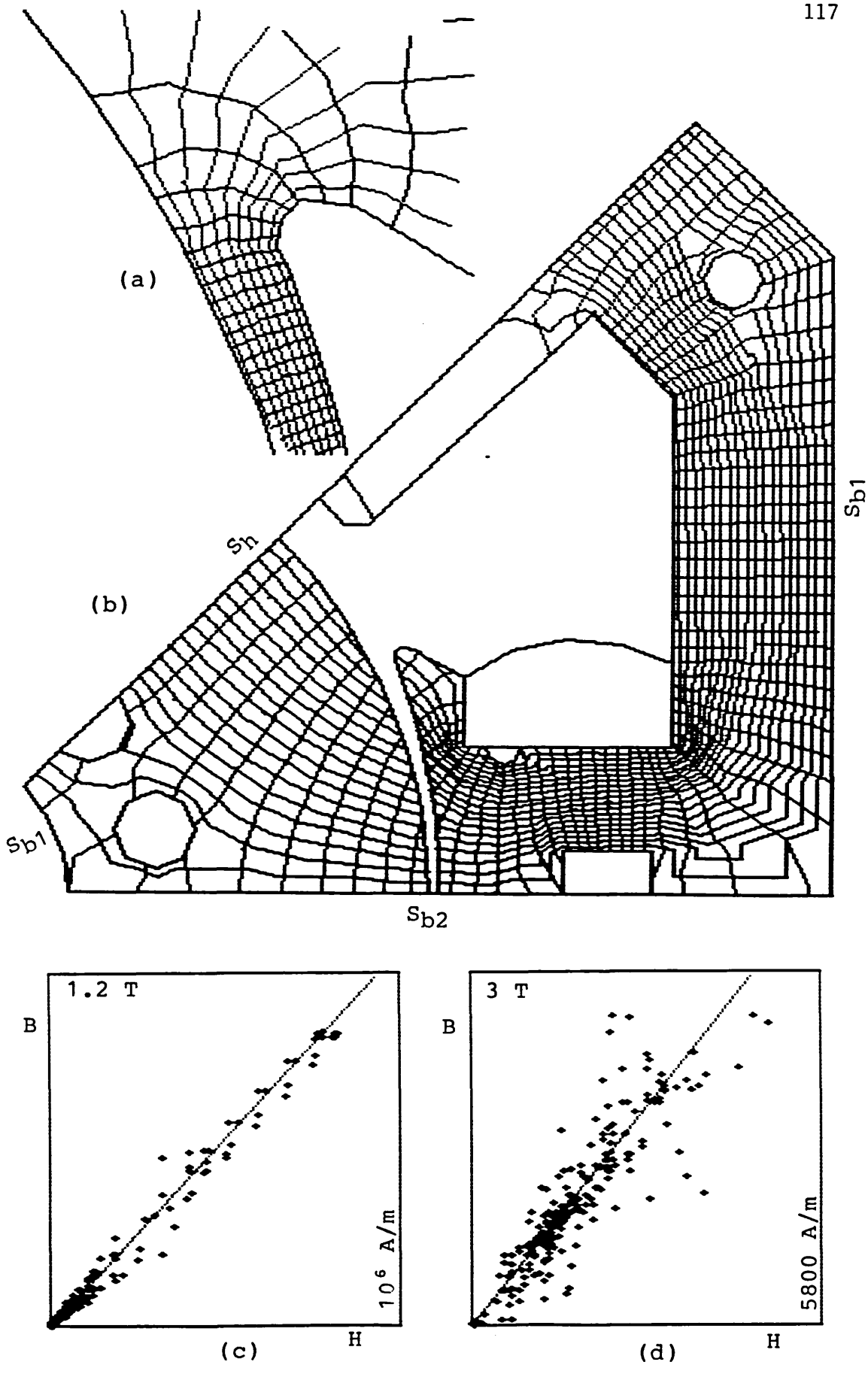

Fig. 6.7 D.C. machine : (a) equipotentials in air near pole tip; (b) equipotentials in iron; Ω steps 20 times smaller than in air; scale 1:1 ; (c) B-H plot in air; (d) B-H plot in iron.

$$\text{on } S_{b1} : \underline{n} \cdot \underline{B} = 0$$

Symmetry at no-load yields

$$\text{on } S_{b2} : \underline{n} \cdot \underline{B} = 0$$

and

$$\text{on } S_{h} : \underline{n} \times \underline{H} = 0$$

Summarising, we may write

$$\text{on } S_{h} : \underline{n} \times \underline{H} = 0 \quad \Rightarrow \quad \Omega = \overline{\Omega}_{h} \ (= 0) \qquad (6.31a)$$

and

$$\text{on } S_{b} : \underline{n} \cdot \underline{B} = 0 \quad \Rightarrow \quad \underline{A} = \overline{\underline{A}}_{b} \ (= 0) \qquad (6.31b)$$

Eqns. 6.31 are identical to eqns. 6.23 for the C-magnet, so that Γ_o vanishes as before to yield eqns. 6.24 and 6.25 again. The problem was solved for an iron relative permeability of 500, and a field excitation of 2000 Ampere-turns. A 457-element, 251-node mesh was used, resulting in a constitutive error of 1.247 Joules, with the exact energy estimated at 38.11 Joules ± 1.65%. Fig. 6.7 shows equipotential contours and B-H plots separately for iron and air. Locations of the apparently large discrepancies between complementary field magnitudes in iron may be deduced from the constitutive error density distribution of fig. 6.8. Once again, errors are seen to concentrate around corners. The air elements inside the gap and in the vicinity of the pole tip, inset to fig. 6.8, account for approximately 35% of the global error; the black elements alone account for 27.6%.

On load, symmetry that led to eqns. 6.31 can no longer be assumed. A full pole pitch must therefore be analysed, fig. 6.9. On the external periphery of the yoke, we assume, as before,

$$\text{on } S_{12} : \underline{n} \cdot \underline{B} = 0 \quad \Rightarrow \quad A = A_{b} = \text{constant} \qquad (6.32)$$

Periodicity conditions on S_{01} and S_{02} yield, for corresponding points,

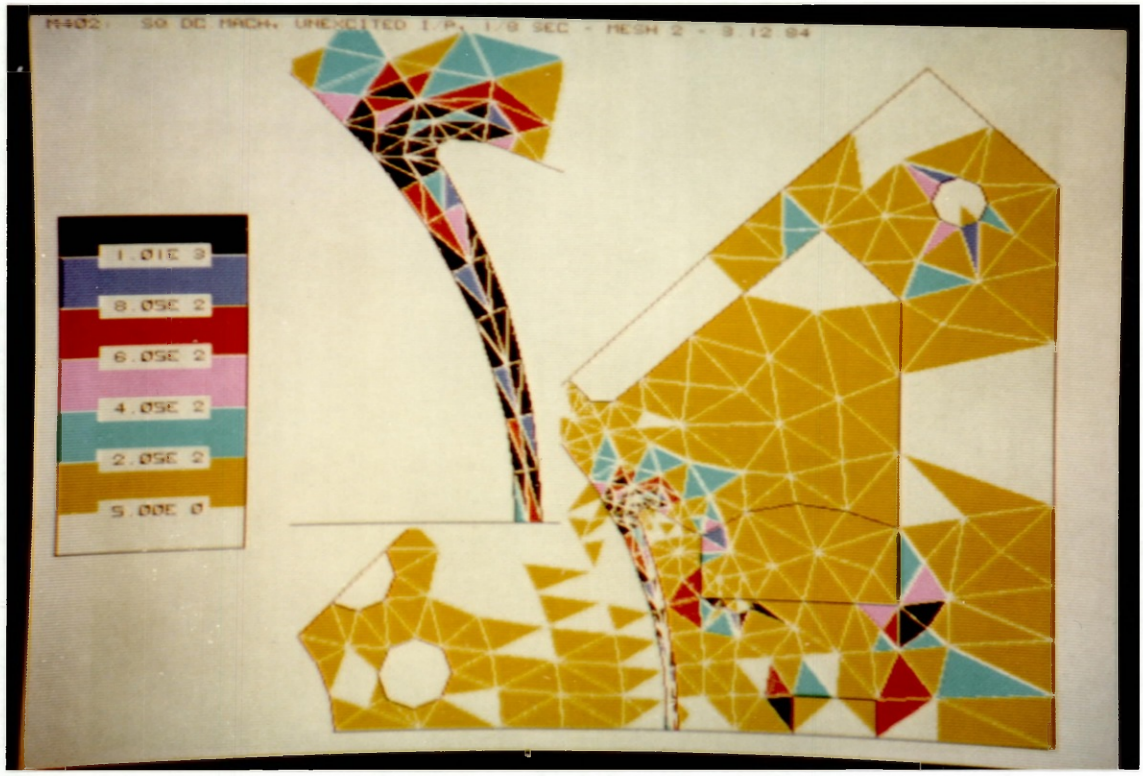

Fig. 6.8 D.C. machine constitutive error density distribution. Inset shows enlarged air elements inside gap and near pole tip, with iron elements masked.

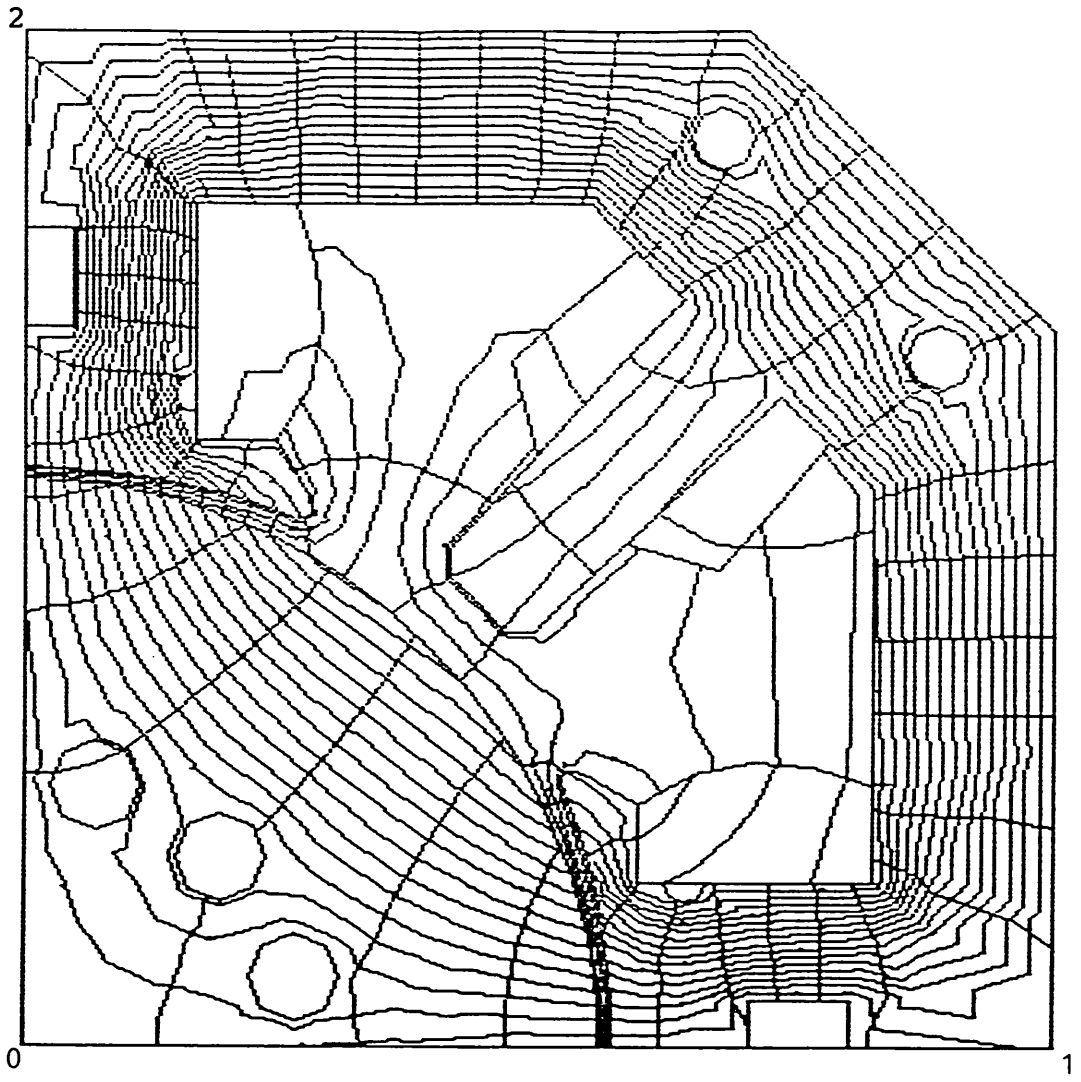

Fig. 6.9 Equipotential contours in d.c. machine with periodic boundary conditions. Scalar potential steps in iron 20 times smaller than in air.

$$\underline{n} \times \underline{H}|_{S_{01}} = \underline{n} \times \underline{H}|_{S_{02}} \quad \Rightarrow \quad \Omega|_{S_{01}} - \Omega_0 = \Omega_0 - \Omega|_{S_{02}}$$

and

$$\underline{n} \cdot \underline{B}|_{S_{01}} = \underline{n} \cdot \underline{B}|_{S_{02}} \quad \Rightarrow \quad A|_{S_{01}} - A_0 = A_0 - A|_{S_{02}}$$

(6.33)

where Ω_0 and A_0 are the potential values at point 0. At corner points 1 and 2, we must have

$$A_b - A_0 = A_0 - A_b \quad \Rightarrow \quad A_b = A_0$$

so that

$$0 = \Phi_{01} = \Phi_{02}$$

where Φ, the flux through the indicated section, is defined in eqn. 3.32. Choosing, arbitrarily,

$$\Omega_0 = 0 \qquad \text{and} \qquad A_b = A_0 = 0$$

the boundary conditions simplify to

$$\text{on } S_{12} : \ \underline{n} \cdot \underline{B} = 0 \quad \Rightarrow \quad A = A_b = 0 \tag{6.34a}$$

and

$$\Omega|_{S_{01}} = -\Omega|_{S_{02}} \qquad \text{and} \qquad A|_{S_{01}} = -A|_{S_{02}} \tag{6.34b}$$

The null values of Ω_0 and A_0 are implicit in 6.34b. Substituting into eqn. 6.21

$$\Gamma_o = -[\underline{n} \times \underline{H}, \underline{A}]_{S_{01}} - [\underline{n} \times \underline{H}, \underline{A}]_{S_{02}} + [\underline{H}, \underline{n} \times \underline{A}]_{S_{12}}$$

$$= 0$$

Γ_o thus vanishes to yield eqns. 6.24 and 6.25 again. Complementary equipotential contours illustrating such periodic boundary conditions are shown in fig. 6.9. The solution was based on an interpole excitation of 1500 Ampere-turns. Limitations of the computer program prevented inclusion of armature currents for a true on-load solution.

6.5.3 Lamination

Fig. 6.10 shows an iron lamination permeated by magnetic flux. Because of symmetry, it is sufficient to consider the indicated trapezoidal region, with

$$\text{on } S_{h1} : \ \underline{n} \times \underline{H} = 0 \quad \Rightarrow \quad \Omega = 0 \tag{6.35a}$$

and

$$\text{on } S_{h2} : \ \underline{n} \times \underline{H} = 0 \quad \Rightarrow \quad \Omega = M \tag{6.35b}$$

The zero potential in 6.35a is chosen arbitrarily; M is the magnetomotive force

$$M = -\int_{\underline{r}_1}^{\underline{r}_2} \underline{H} \cdot d\underline{\ell} = \Omega|_{S_{h2}} \tag{6.35c}$$

$\underline{r}_1$ is any point on S_{h1}, and $\underline{r}_2$ is any point on S_{h2}.

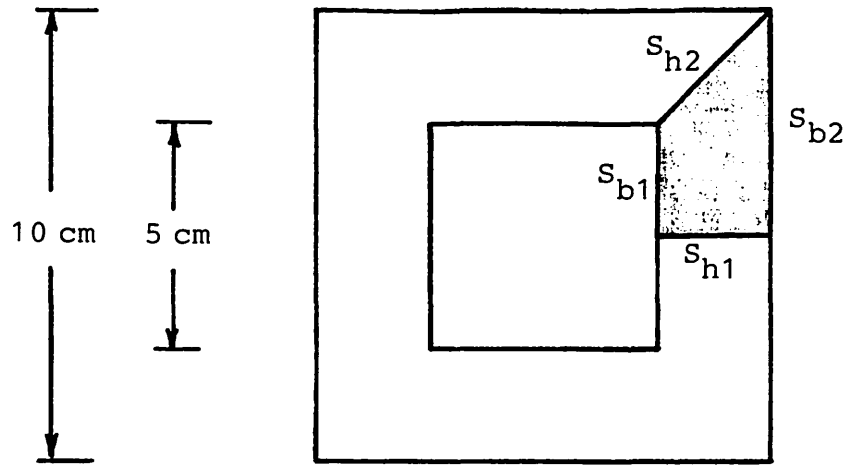

Fig. 6.10 Square iron lamination.

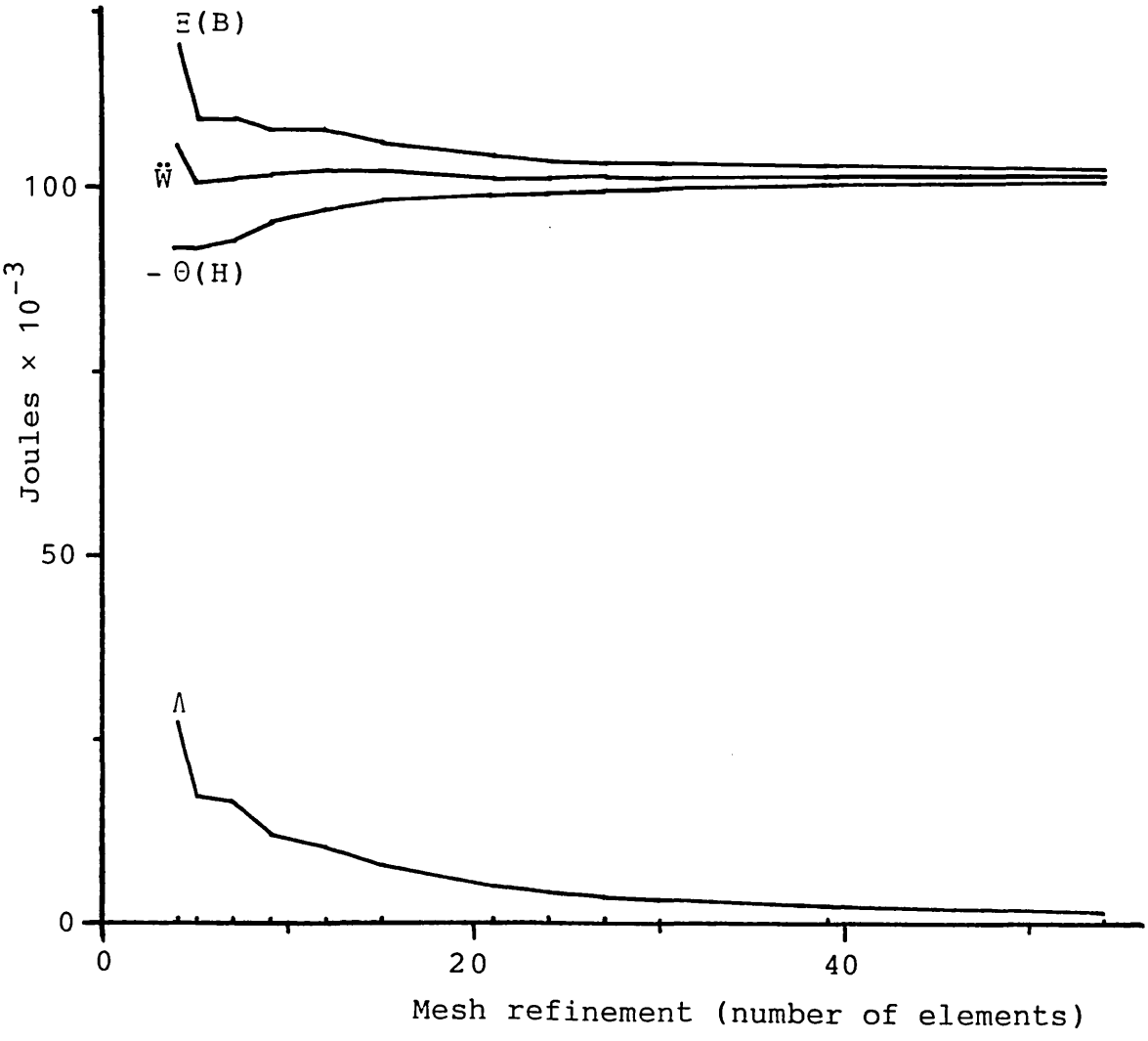

Fig. 6.11 Lamination convergence curves (specified flux).

Assuming the flux to be confined to the high permeability iron, we have

$$\text{on } S_{b1} : \quad \underline{n} \cdot \underline{B} = 0 \qquad \Rightarrow \qquad A = 0 \tag{6.36a}$$

and

$$\text{on } S_{b2} : \quad \underline{n} \cdot \underline{B} = 0 \qquad \Rightarrow \qquad A = \Phi \tag{6.36b}$$

The zero potential in 6.36a is chosen arbitrarily; Φ is the magnetic flux

$$\Phi = \int_{S_{h1}} \underline{B} \cdot d\underline{S} = A|_{S_{b2}} \tag{6.36c}$$

We now substitute the boundary conditions of eqns. 6.35 and 6.36 into Γ_o in eqn. 6.21 :

$$\begin{aligned} \Gamma_o &= - [\underline{n} \times \underline{H} , \underline{A}]_{S_s} = - [\underline{n} \times \underline{H} , \underline{A}]_{S_{b2}} = -\int_{S_{b2}} \underline{H} \cdot \underline{A} \times d\underline{S} \\ &= - \int_{S_{b2}} \underline{H} \cdot (A \, \underline{a}_z) \times (\underline{a}_\ell \times \underline{a}_z) \, d\ell \, dz \\ &= - A|_{S_{b2}} \int_{\underline{r}_1}^{\underline{r}_2} \underline{H} \cdot d\underline{\ell} \\ &= M \Phi \end{aligned} \tag{6.37}$$

Clearly, Γ_o does not vanish in this case. But M and Φ correspond to the abstract motive force and flux of eqns. 3.21 and 3.22 of sec. 3.4.2, where it was shown that physical uniqueness would require one of them to be specified. Two physically distinct possibilities arise as we substitute Γ_o back into eqn. 6.21 :

(i) Specified mmf $(M = \overline{M})$:

$$\Theta_M(H) = X(\underline{H}) , \qquad \Xi_M(B) = \Psi(\underline{B}) - \overline{M} \Phi \tag{6.38}$$

The term $\overline{M} \Phi$ forces the specified mmf on the B-solution which then estimates the flux accordingly.

(ii) Specified flux $(\Phi = \overline{\Phi})$:

$$\Theta_\phi(H) = X(\underline{H}) - M \overline{\Phi} , \qquad \Xi_\phi(B) = \Psi(\underline{B}) \tag{6.39}$$

The term $M\bar{\Phi}$ now forces the specified flux on the H-solution, which then estimates the mmf accordingly.

The above demonstrates how the constitutive error Λ splits to yield complementary functionals for both types of specification. This type of boundary specification also demonstrates the inequivalence of the primal and dual statements of sec. 4.3 on alternative derivations of complementary variational principles. The primal statement corresponds to an assigned mmf specification, while the dual statement corresponds to an assigned flux specification. Fraser[6.16] attempts to solve the assigned flux problem, and is led to conclude that the H-solution requires the exact energy to be known in advance; he employs a highly refined B-solution for the purpose. The present derivation shows that this is not necessary. This type of specification is more common in electrostatic and current flow problems, and will come up again in later sections. Hammond[6.13,17-19] uses the same geometry of the present lamination problem to pose an electrostatic one, using S_{b1} and S_{b2} to denote capacitor plates.

The energy bounds are obtained by applying ineq. 4.10 and eqn. 6.16 to eqns. 6.38 and 6.39 :

$$\Theta_M(H) \geq W_M \geq -\Xi_M(B) \tag{6.40a}$$

and

$$\Xi_\Phi(B) \geq W_\Phi \geq -\Theta_\Phi(H) \tag{6.40b}$$

where W_M and W_Φ are the exact magnetic energies in the trapezoidal section for the specified mmf and specified flux problems respectively. They are related to the magnetic reluctance R by

$$W_M = \tfrac{1}{2}\bar{M}^2 / R_M \quad \text{and} \quad W_\Phi = \tfrac{1}{2}\bar{\Phi}^2 R_\Phi \tag{6.41}$$

Substituting into ineqs. 6.40, and rearranging, we get

$$2\Theta_M(H) / \bar{M}^2 \geq \frac{1}{R_M} \geq -2\Xi_M(B) / \bar{M}^2 \tag{6.42a}$$

and

$$2\Xi_\Phi(B) / \bar{\Phi}^2 \geq R_\Phi \geq -2\Theta_\Phi(H) / \bar{\Phi}^2 \tag{6.42b}$$

In both cases, $\Theta(H)$ and hence the H-solution are associated with the lower bound on reluctance; $\Xi(B)$ and the B-solution are associated with the upper bound. This is in basic agreement with Hammond's description of the physical processes underlying his treatment in terms of slices and tubes[6,18,19], which he attributes to Maxwell.

The lamination problem was solved for a specified flux of 10 mWb and an iron relative permeability of 500. Complementary solutions were performed for a number of successively refined meshes, starting with 4 elements and 6 nodes. Fig. 6.11 shows convergence curves up to 54 elements and 38 nodes, at which stage the energy in the trapezoid is estimated at 101.9 mJ ± 0.88%, the constitutive error being 1.83 mJ. The corresponding reluctance is 2038 Amp-turn/Wb. Solutions were actually performed for further error-guided refinements; at 213 elements and 128 nodes the energy was 101.9 mJ ± 0.25%, the error being 0.49 mJ. This is slightly more accurate than a regular mesh of 768 elements and 425 nodes.

The convergence curves of fig. 6.11 exhibit some sharp changes initially. This may be attributed to the fact that at the extremely coarse meshes in question, the actual location of an added node can have significant influence on computed results.

Figures 6.12-14 show energy distributions, error distributions, equipotential contours, and B-H plots at certain stages of the refinement process. These conform to the findings discussed in sec. 6.5.1. Note in particular the concentration of energy and error at the inside corner of the lamination, where the highest fields arise.

The dual problem of specified mmf was solved using the same meshes. As expected, the only differences were in scaling due to the use of different forcing values. While the actual energies differ, reluctance estimates, and, indeed, all normalised distributions etc. are identical.

Fig. 6.12 Lamination energy density distributions in 39-element mesh. From left : $\chi(\underline{H})$, $\psi(\underline{B})$, and $\frac{1}{2}\zeta(\underline{H},\underline{B})$.

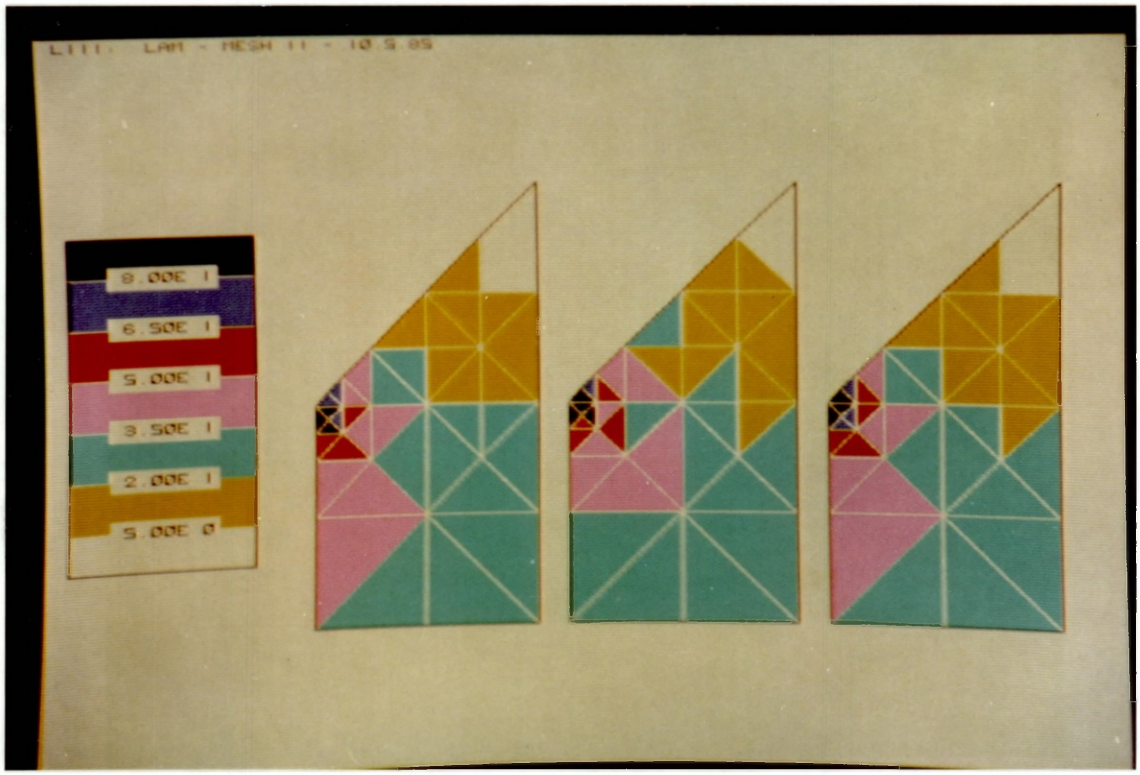

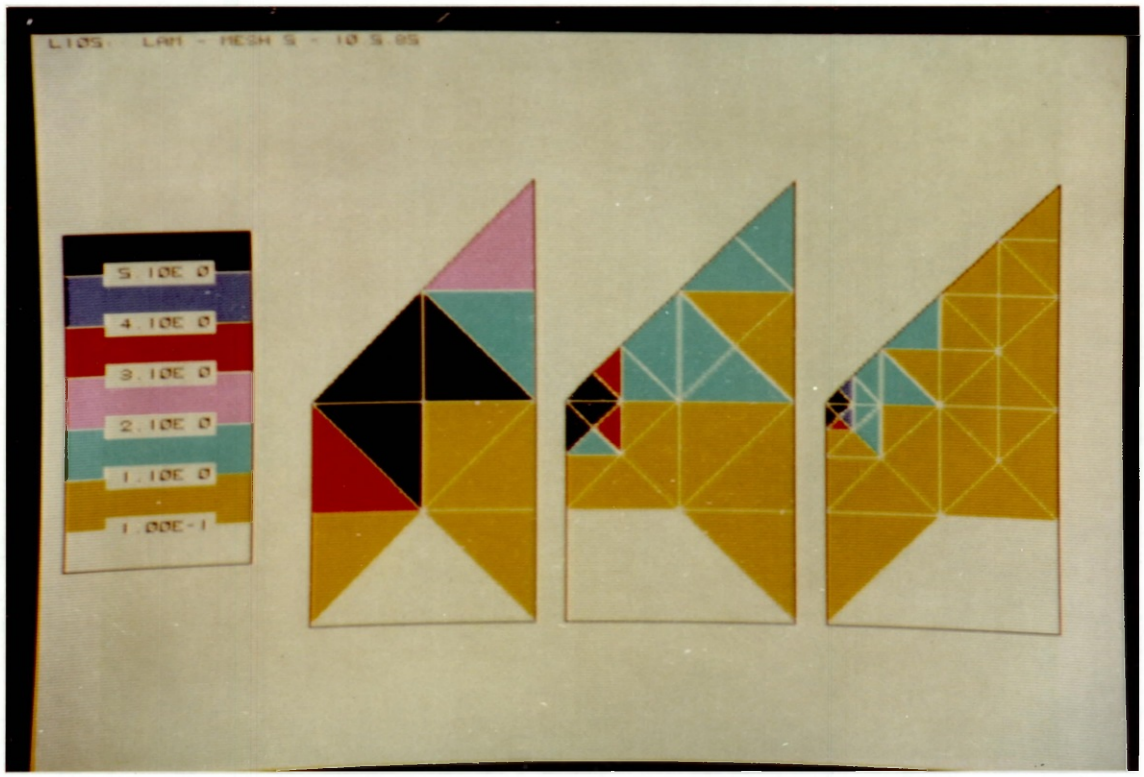

Fig. 6.13 Lamination constitutive error density distributions at three stages of mesh refinement : 12, 24, and 39 elements.

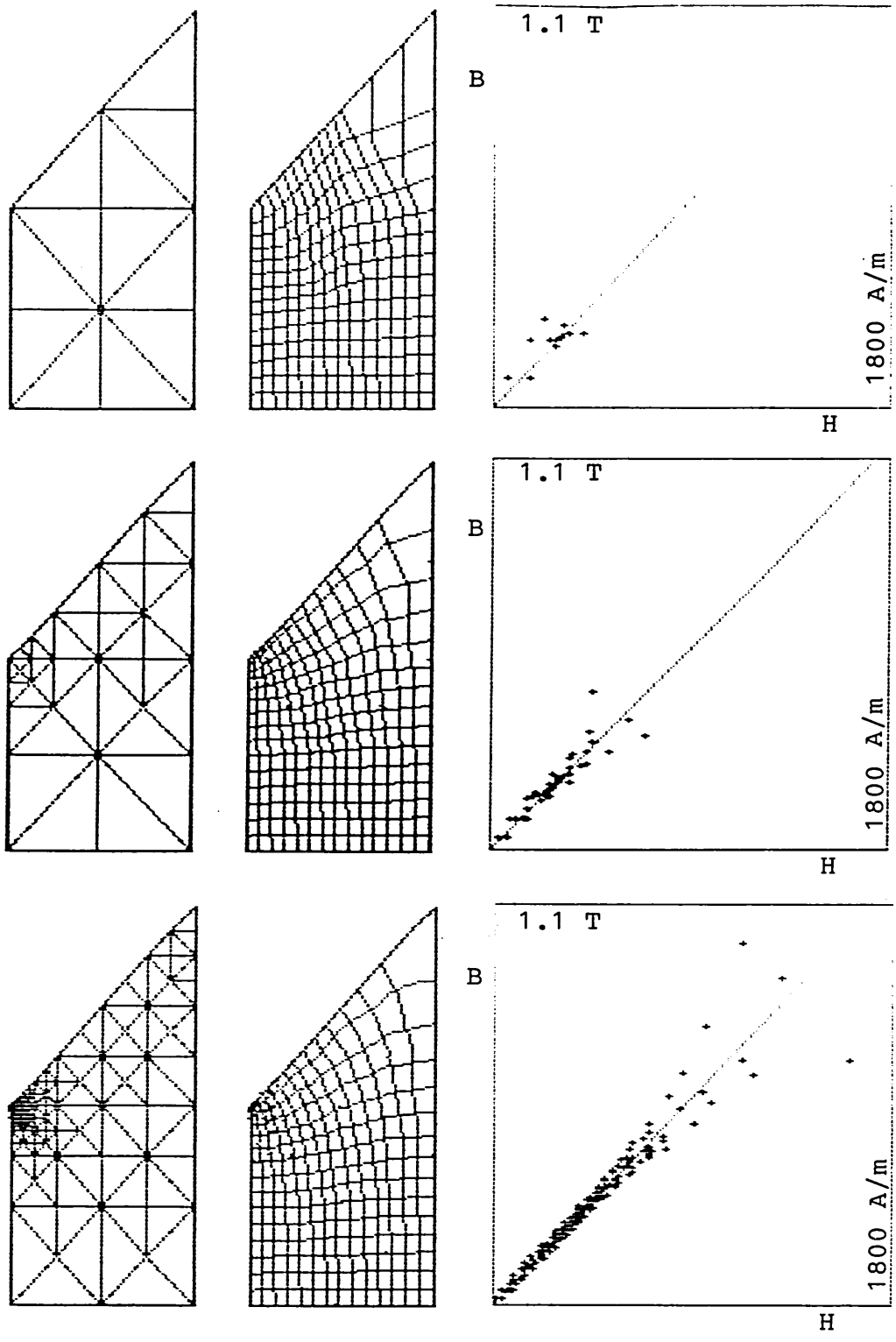

Fig. 6.14 Lamination finite element mesh, equipotential contours, and B-H plot at three stages of mesh refinement; specified flux.

(a) 12 elements and 12 nodes; $\Lambda/\ddot{W} = 10.5\%$;
(b) 39 elements and 29 nodes; $\Lambda/\ddot{W} = 2.5\%$;
(c) 163 elements and 101 nodes; $\Lambda/\ddot{W} = 0.8\%$.

The reluctance may be expressed by

$$R = M / \Phi \qquad (6.43)$$

Given $\bar{\Phi} = 10$ mWb, the H-solution in eqn. 6.39 acts on the lower bound of R to yield M = 20.13 Ampere-turns for a mesh of 39 elements. Forcing this $\bar{M}$ on the B-solution of the dual problem, eqn. 6.38, results in $\Phi = 9.758$ mWb since it acts on the upper bound of R.

6.5.4 Slot conductor

Fig. 6.15 shows a T-shaped conductor embedded in a slot. Because of high iron permeability, we may assume

$$\text{on } S_{h1} : \quad \underline{n} \times \underline{H} = 0$$

Symmetry allows the analysis to be confined to the half-slot indicated on the figure, with

$$\text{on } S_{h2} : \quad \underline{n} \times \underline{H} = 0$$

Combining these two conditions, we may write

$$\text{on } S_h : \quad \underline{n} \times \underline{H} = 0 \quad \Rightarrow \quad \Omega = \bar{\Omega}(\underline{r}_o) + \int_{\underline{r}_o}^{\underline{r}} \underline{G} \cdot d\underline{\ell} \qquad (6.44)$$

where

$$S_h = S_{h1} \cup S_{h2}$$

$\underline{r}_o$ is an arbitrary reference point on S_h; $\bar{\Omega}(\underline{r}_o)$ is set to zero arbitrarily. The top surface of the conductor is exposed to air in the slot neck where we assume

$$\text{on } S_b : \quad \underline{n} \cdot \underline{B} = 0 \quad \Rightarrow \quad \underline{A} = \bar{\underline{A}}_b \quad (= 0) \qquad (6.45)$$

The boundary conditions of eqns. 6.44 and 6.45 cause Γ_o to vanish as in the case of the C-magnet, sec. 6.5.1, so that eqns. 6.24-27 apply once again. L in eqn. 6.27 now represents the d.c. inductance of the half-slot.

This problem has been examined by Hammond[6.13,17,18] and by Fraser[6.16] for the following dimensions

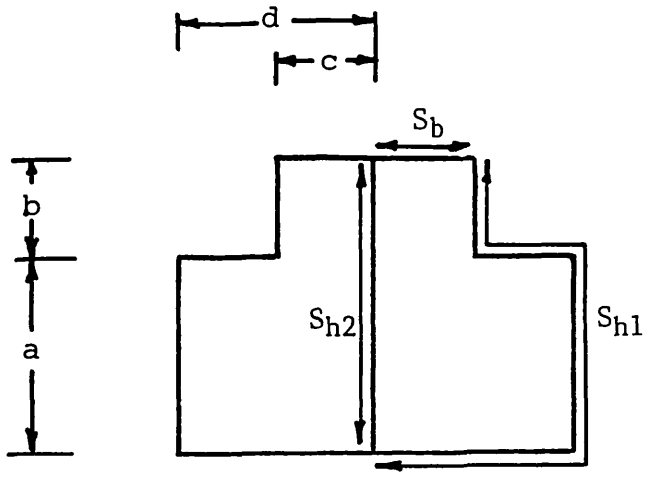

Fig. 6.15 T-conductor in iron.

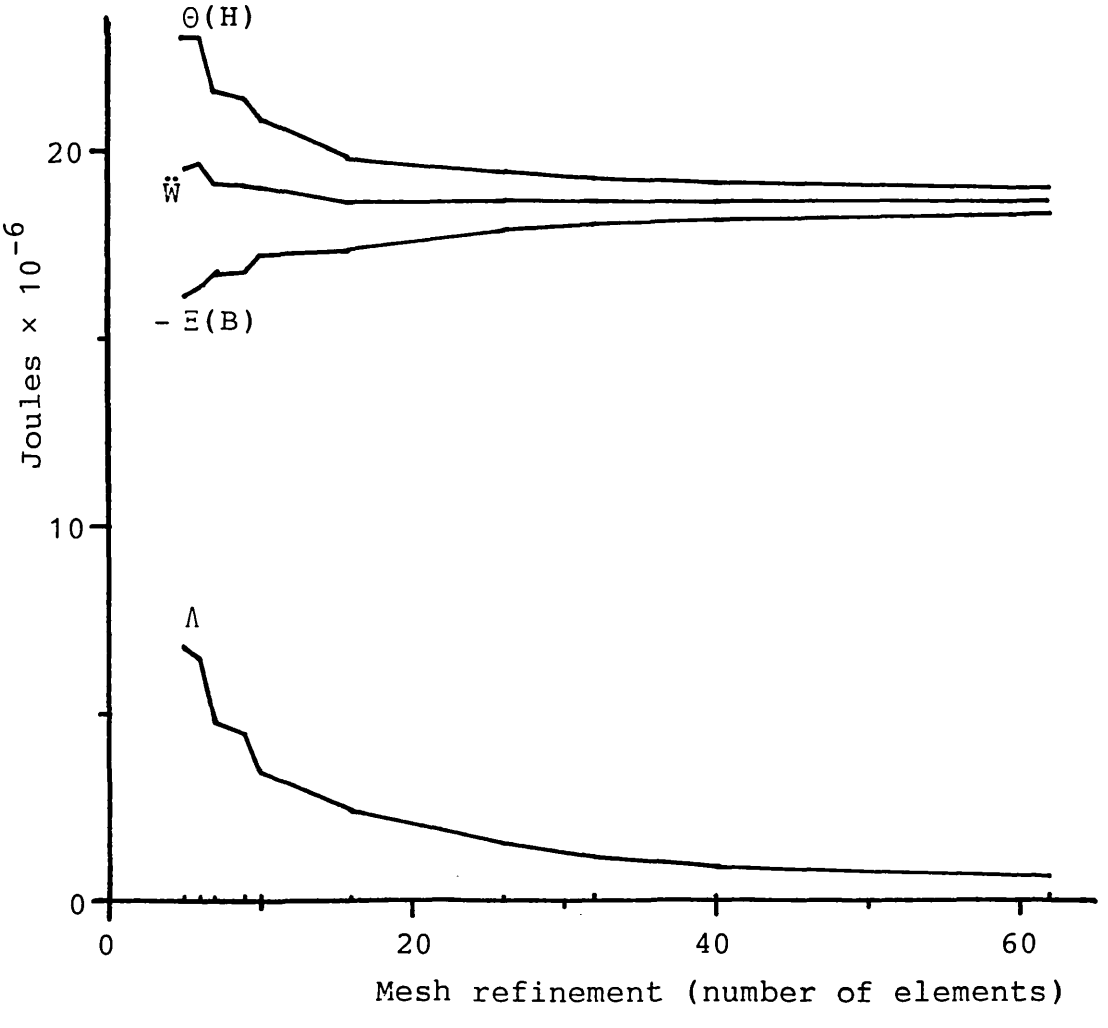

Fig. 6.16 Slot conductor convergence curves.

$$a = d = 2 \text{ cm}, \qquad b = c = 1 \text{ cm} \tag{6.46}$$

and a current density of 1 A/cm^2, so that the half-slot current is 5 A.

Using the above dimensions and current, complementary solutions were performed for a number of successively refined meshes, starting with 5 elements and 7 nodes. Fig. 6.16 shows convergence curves up to 62 elements and 42 nodes, at which stage the half-slot energy is estimated at 18.63 micro-Joules ± 1.83%, the constitutive error being 0.68 μJ. The corresponding inductance is 1.49 μH. Solutions were actually performed for further error-guided mesh refinements; at 158 elements and 97 nodes, the energy was 18.64 μJ ± 0.7%, the error being 0.263 μJ. This is slightly more accurate than a regular mesh of 500 elements and 276 nodes.

Fig. 6.17 shows energy and error distributions. Energy is seen to concentrate in the neck, while errors, as usual, are highest at the re-entrant corner. In the 40-element mesh, black triangles account for 33.6% of the global error. Fig. 6.18 shows equipotential contours and B-H plots. It is recalled that Ω-contours have no physically meaningful significance since $\nabla\Omega$ is augmented by $\underline{G}$ to yield $\underline{H}$ in the conductor, eqn. 6.19. Figures 6.17 and 6.18 illustrate, once again, various points discussed in sec. 6.5.1.

Fraser[6.16] attempted complementary solutions of the slot problem with part of the surrounding iron ($\mu_r = 2000$) included in the region of analysis. The H-solution was found to be unsatisfactory, resulting in too much energy in the iron part; the error, which was emphasised by juxta-position of upper and lower bounds, is attributable to the use of a Biot-Savart defined $\underline{G}$ in both copper and iron; see Chapter 8. The present treatment, which confines $\underline{G}$ to the conducting sub-region, gave satisfactory bounds : for a mesh of 640 elements and 357 nodes, the over-all energy was estimated at 18.59 μJ ± 1.56%, the constitutive error being 0.58 μJ. The conducting sub-region had 80 of the

Fig. 6.17 Slot conductor density distributions. Top : energies in 40-element mesh, $\chi(\underline{H})$, $\psi(\underline{B})$, and $\frac{1}{2}\zeta(\underline{H},\underline{B})$ (from left). Bottom : constitutive error in 10-, 16-, and 40-element meshes.

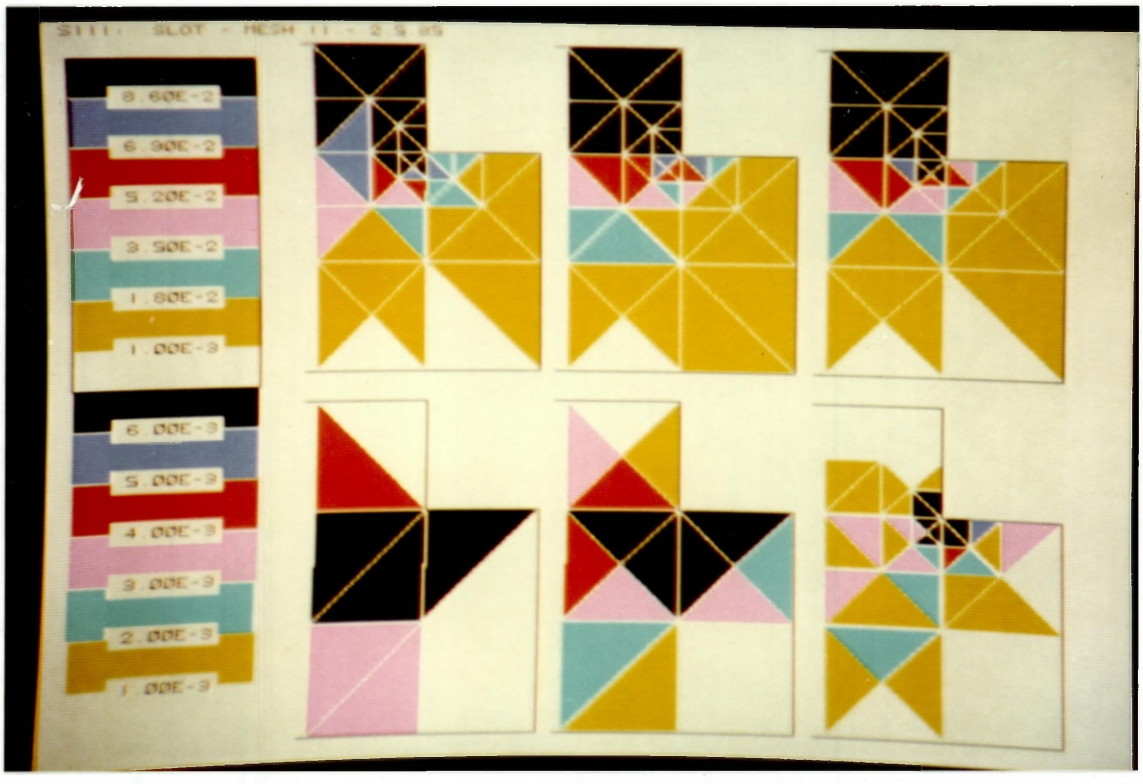

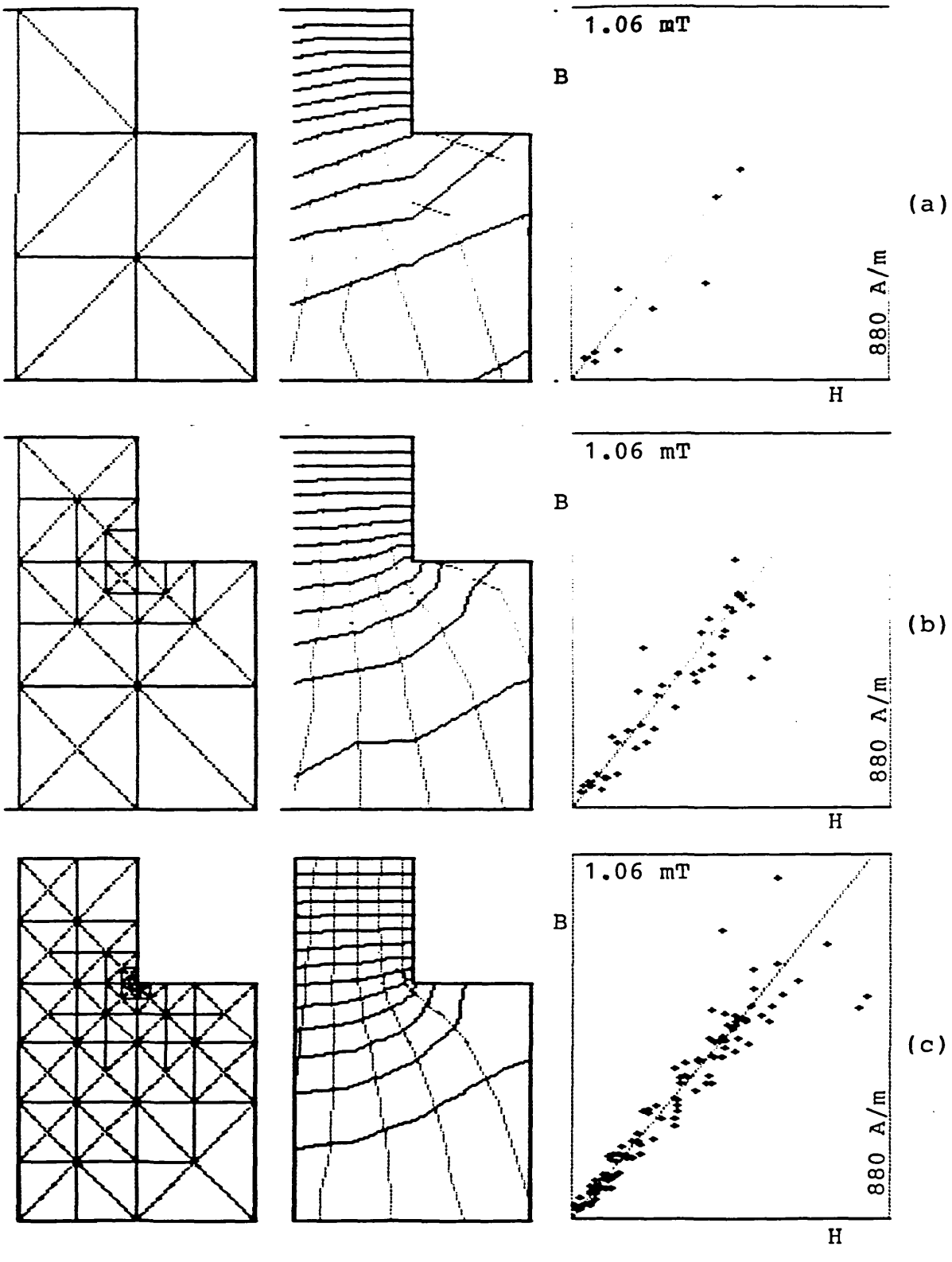

Fig. 6.18 Slot conductor finite element mesh, equipotential contours, and B-H plot at three stages of mesh refinement :

(a) 10 elements and 11 nodes; $\Lambda/\ddot{W} = 18.7\%$;
(b) 40 elements and 29 nodes; $\Lambda/\ddot{W} = 5.2\%$;
(c) 106 elements and 66 nodes; $\Lambda/\ddot{W} = 2.0\%$.

elements, 18.55 μJ of the energy, and 0.57 μJ of the error; the figures are very close, although not identical, to those quoted earlier for the conductor-only solution. Bounds, it is noted, are defined for the over-all energy only. Fig. 6.19 shows equi-potential contours and boundary specifications for the problem including iron. Of course, the examples of sections 6.5.1 and 6.5.2 provide even more general illustrations of the applicability of complementary principles to multi-material regions.

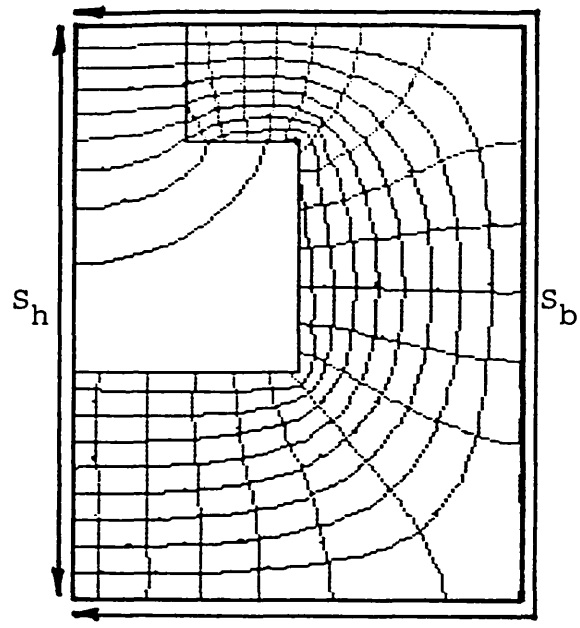

Fig. 6.19 Slot conductor in iron : boundary specification and potential contours. Ω-contours not shown in conducting sub-region.

One reason why the slot problem has figured so much in the literature on complementary energy bounds[6·13/16-18] is the availability of an analytic solution[6·20]; it yields

$$L' = 0.57\,\mu_o \qquad (6.47)$$

for the d.c. inductance of the over-all T-shaped conductor having the dimensions given in 6.46[6·13/17/18]. The most accurate solution attempted here (348 elements, 199 nodes) estimated the half-slot energy at 18.64 μJ ± 0.43%; the corresponding half-slot inductance is 1.4912 μH. Noting that the two half-slot conductors are in parallel, the present estimate of the T-conductor inductance may be written

$$L'' = 0.5933\,\mu_o \pm 0.43\% \qquad (6.48)$$

Clearly, the present formulation does not converge to the analytic one of eqn. 6.47. It is instructive to examine the cause of the apparent anomaly, which is the boundary specification on S_b, fig. 6.15 and eqn. 6.45. The analytic

solution is based on the somewhat different boundary condition

$$\text{on } S_b \quad : \quad \underline{n} \times \underline{H} = \underline{h} = (I / c)\, \underline{a}_z \tag{6.49}$$

where I is the half-slot current, and c is the half-width of the slot mouth, fig. 6.15. With $\underline{h}$ assumed constant, its value in 6.49 is obtainable from Ampere's circuital law, with $\underline{n} \times \underline{H}|_{S_h} = 0$ as in 6.44.

Now both boundary specifications, 6.45 and 6.49, are adequate descriptions of actual physical conditions on an S_b lying well inside a long and narrow slot neck; a crucial parameter is the ratio

$$\alpha = b / 2c \tag{6.50}$$

which must be large. Reference 6.20 lists inductance values for four sets of slot dimensions; the smallest α attempted corresponds to the following set (in cm)

$$a = 1.5,\ b = 1.3,\ c = 0.2,\ d = 0.75 \quad \Rightarrow \quad \alpha = 3.25 \tag{6.51}$$

The resulting d.c. inductance, using 6.49, is

$$L' = 3.097\, \mu_o \tag{6.52}$$

Complementary numerical solutions of this slot, at 575 elements and 316 nodes, and using the boundary specification of 6.45, yielded

$$L'' = 3.098\, \mu_o \pm 0.21\% \tag{6.53}$$

Clearly, the two boundary conditions are practically equivalent for the slot dimensions in 6.51. Evidently, equivalence is not retained for the dimensions in 6.46, where

$$\alpha = 0.5 \tag{6.54}$$

giving rise to the discrepancy between L' and L" in eqns. 6.47 and 6.48.

By way of experiment, the slot dimensions of 6.46 were solved once more, this time with a 6 cm column of air introduced between the conductor top surface and S_b, fig.

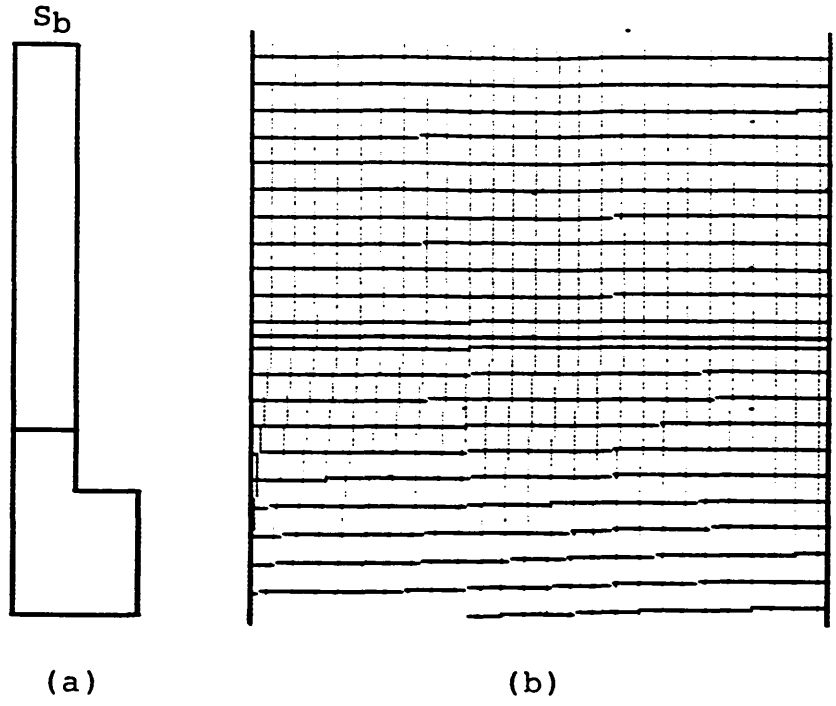

Fig. 6.20 Slot conductor problem including long, current-free neck.
(a) Region of analysis.
(b) Equipotential contours in the vicinity of the conductor top surface.

6.20a. In this way, S_b is pushed well into the neck, with $\alpha = 3.5$. For a mesh of 704 elements and 398 nodes, the over-all half-energy, in conductor and neck, was estimated at 112.86 μJ ± 0.186%, the error being 0.3624 μJ. The conducting sub-region accounted for 18.64 μJ of the energy, and 0.3623 μJ of the error. The corresponding full-slot inductance is 0.5932 μH, which is much closer to L" in 6.48 than to L' in 6.47. This suggests that the boundary specification of 6.45 is to be preferred over that of 6.49 when α is small. The divergence of both specifications from actual conditions at the conductor top surface is just discernible in fig. 6.20b : the one-pixel kink in the horizontal A-contours indicates that $\underline{n} \cdot \underline{B}$ is not quite zero as in eqn. 6.45, while the slight compaction of the vertical Ω-contours from left to right indicates that $\underline{h}$ is not quite constant as in eqn. 6.49.

6.6 Electrostatic examples

In electrostatics, the equations for fields and potentials are :

$$0 = \text{curl } \underline{E} \quad ; \quad \rho = \text{div } \underline{D} \tag{6.55}$$

$$0 = \underline{n} \times \Delta\underline{E} \quad ; \quad \sigma = \underline{n} \cdot \Delta\underline{D} \text{ on } S_\sigma \tag{6.56}$$

$$\underline{E} = -\nabla\phi \quad ; \quad \underline{D} = \underline{C}^e + \nabla \times \underline{A}^e \tag{6.57}$$

$$0 = \Delta\phi \tag{6.58}$$

ϕ is the familiar electric scalar potential; $\underline{A}^e$ is an electric flux-describing vector potential; $\underline{C}^e$ is the D-system pre-specified field that accounts for charge distributions :

$$\text{div } \underline{C}^e = \rho \tag{6.59}$$

Eqns. 6.55-59 describe the electrostatic interpretation of the abstract model of sections 3.3 and 3.4.5; the potentials ϕ and $\underline{A}^e$ correspond to the abstract potentials Ω and $\underline{A}$ of sections 3.4.3 and 3.4.4. The electrostatic constitutive error may be written

$$\Lambda(\underline{E},\underline{D}) = X(\underline{E}) + \Psi(\underline{D}) - Z(\underline{E},\underline{D}) \tag{6.60}$$

Minimisation of $\Lambda(\underline{E},\underline{D})$ enforces the constitutive relationship on the fields $\underline{E}$ and $\underline{D}$.

Using the E-system scalar potential ϕ, $Z(\underline{E},\underline{D})$ splits as follows

$$\begin{aligned} Z(\underline{E},\underline{D}) &= \langle \underline{E} , \underline{D} \rangle_R = -\langle \nabla\phi , \underline{D} \rangle_R = \langle \phi , \nabla\cdot\underline{D} \rangle_R - \int_R \nabla\cdot(\phi\underline{D})\, dR \\ &= \langle \phi , \rho \rangle_R + [\phi , \underline{n}\cdot\Delta\underline{D}]_{S_\sigma} - [\phi , \underline{n}\cdot\underline{D}]_{S_s} - [\phi , n\cdot\underline{D}]_{S_o} \\ &= \langle \phi , \rho \rangle_R + [\phi , \sigma]_{S_\sigma} - [\phi , \underline{n}\cdot\underline{D}]_{S_s} \end{aligned}$$

At this stage, we can rewrite eqn. 6.60 in the form

$$\Lambda = \Theta_o(E) + \Xi_o(D) - \Gamma_o(E,D) \tag{6.61}$$

where

$$\Theta_o(E) = X(\underline{E}) - \langle \phi , \rho \rangle_R - [\phi , \sigma]_{S_\sigma}$$

$$\Xi_o(D) = \Psi(\underline{D})$$

$$\Gamma_o(E,D) = - [\phi , \underline{n} \cdot \underline{D}]_{S_s}$$

Clearly, further decomposition depends on the boundary conditions of the given problem.

To satisfy eqn. 6.59, the definition of $\underline{C}^e$ may be based on Coulomb's law

$$\underline{C}^e(\underline{r}) = \int_R \frac{(\underline{r} - \underline{r}') \rho(\underline{r}')}{4 \pi |\underline{r} - \underline{r}'|^3} \, dR(\underline{r}') \qquad (6.62a)$$

A numerically simpler definition is available for uniform charge distributions

$$\underline{C}^e(\underline{r}) = \tfrac{1}{3} (\underline{r} - \underline{r}_o) \rho(\underline{r}) \qquad (6.62b)$$

where r_o is an arbitrary reference point. Comparison between the two definitions is similar to that between $\underline{H}_s$ and $\underline{T}$ in Chapter 8 on the magnetic pre-specified field. Eqn. 6.62b sets $\underline{C}^e$ to zero in charge-free regions, resulting in a discontinuity on the interface between charged and uncharged regions. The discontinuity is absorbed by a jump in $\underline{A}^e$, eqn. 3.43. A cut is defined for each totally enclosed charge distribution, eqn. 3.47.

6.6.1 Remote parallel conductors

The textbook problem of parallel cylinders, fig. 6.21, will be used to illustrate some points of interest. Because of symmetry, only the indicated quadrant need be analysed :

$$\text{on } S_{e1} : \quad \underline{n} \times \underline{E} = 0 \quad \Rightarrow \quad \phi = 0 \qquad (6.63a)$$

where the constant potential is set to zero arbitrarily. The tangential component of the electric field at the conductor surface vanishes under static conditions :

$$\text{on } S_{e2} : \quad \underline{n} \times \underline{E} = 0 \quad \Rightarrow \quad \phi = V \qquad (6.63b)$$

V is the voltage

$$V = -\int_{\underline{r}_1}^{\underline{r}_2} \underline{E} \cdot d\underline{\ell}$$

$$= \phi|_{S_{e2}} \qquad (6.63c)$$

$\underline{r}_1$ is any point on S_{e1}, and $\underline{r}_2$ is any point on S_{e2}. The voltage between conductors is 2V.

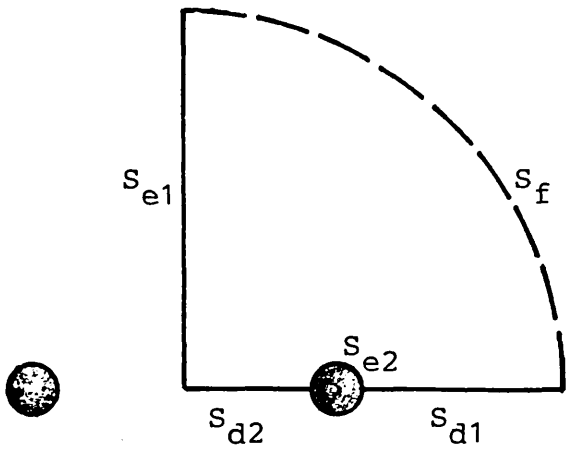

Fig. 6.21 Remote parallel cylinders : region outline.

Symmetry about the horizontal plane allows us to write

$$\text{on } S_{d1} : \quad \underline{n} \cdot \underline{D} = 0 \quad \Rightarrow \quad A^e = 0 \qquad (6.64a)$$

and

$$\text{on } S_{d2} : \quad \underline{n} \cdot \underline{D} = 0 \quad \Rightarrow \quad A^e = Q \qquad (6.64b)$$

where Q is the charge on the upper half of the conductor

$$Q = -\int_{S_{e2}} \underline{D} \cdot d\underline{S} = A^e|_{S_{d2}} \qquad (6.64c)$$

The zero potential in 6.64a is chosen arbitrarily.

The open boundary region is terminated artificially by S_f, which can be specified as an equipotential

$$\text{on } S_f : \quad \underline{n} \times \underline{E} = 0 \quad \Rightarrow \quad \phi = \phi|_{S_{e1}} = 0 \qquad (6.65a)$$

or as a flux line

$$\text{on } S_f : \quad \underline{n} \cdot \underline{D} = 0 \quad \Rightarrow \quad A^e = A^e|_{S_{d1}} = 0 \qquad (6.65b)$$

We now substitute the boundary conditions of eqns. 6.63-65 into Γ_o in eqn. 6.61; for either specification on S_f, we have

$$\Gamma_o = -[\phi , \underline{n}\cdot\underline{D}]_{S_s} = -[\phi , \underline{n}\cdot\underline{D}]_{S_{e2}} = -\phi|_{S_{e2}} \int_{S_{e2}} \underline{D}\cdot d\underline{S}$$

$$= V Q \qquad (6.66)$$

V and Q correspond to the abstract motive force and flux of eqns. 3.21 and 3.22 of sec. 3.4.2. Physical uniqueness requires one of them to be specified. Two physically

distinct possibilities arise as we substitute Γ_o back into eqn. 6.61 :

(i) Specified voltage $(V = \overline{V})$:

$$\Theta_V(E) = X(\underline{E}) \ , \qquad \Xi_V(D) = \Psi(\underline{D}) - \overline{V}\,Q \tag{6.67}$$

The term $\overline{V}\,Q$ forces the specified voltage on the D-solution, which then estimates the charge accordingly.

(ii) Specified charge $(Q = \overline{Q})$:

$$\Theta_Q(E) = X(\underline{E}) - V\,\overline{Q} \ , \qquad \Xi_Q(D) = \Psi(\underline{D}) \tag{6.68}$$

The term $V\,\overline{Q}$ forces the specified charge on the E-solution, which then estimates the voltage accordingly.

The energy bounds are obtained by applying ineq. 4.10 and eqn. 6.16 to eqns. 6.67 and 6.68 :

$$\Theta_V(E) \geq W_V \geq - \Xi_V(D) \tag{6.69a}$$

and

$$\Xi_Q(D) \geq W_Q \geq - \Theta_Q(E) \tag{6.69b}$$

where W_V and W_Q are the exact energies in the quadrant analysed for the specified voltage and specified charge problems respectively. On the electric circuit side, they are given by

$$W_V = \left(\tfrac{1}{2}\,\overline{V}^2\,C_V\right)/4 \quad \text{and} \quad W_Q = \left(\tfrac{1}{2}\,\overline{Q}^2/C_Q\right)/4 \tag{6.70}$$

where C denotes total line capacitance. Substituting into ineqs. 6.69, and rearranging, we get

$$8\Theta_V(E) \,/\, \overline{V}^2 \geq C_V \geq -8\Xi_V(D) \,/\, \overline{V}^2 \tag{6.71a}$$

and

$$8\Xi_Q(D) \,/\, \overline{Q}^2 \geq \frac{1}{C_Q} \geq -8\Theta_Q(E) \,/\, \overline{Q}^2 \tag{6.71b}$$

In both cases, the E-system is associated with the upper bound on capacitance, while the D-system is associated with the lower bound.

The dual problems of specified voltage and specified

charge are analogous to the dual problems of specified mmf and specified flux in the magnetostatic lamination example of sec. 6.5.3. The relevant discussion in that section is therefore applicable, and will not be repeated here.

Alternative specifications on the artificial boundary S_f, eqns. 6.65, give rise to another type of duality. Numerical estimates of the dual energies are shown in fig. 6.22, where $\Theta'(E)$ and $\Xi'(D)$ are the complementary energies with S_f specified as an equipotential, eqn. 6.65a, while $\Theta''(E)$ and $\Xi''(D)$ are the complementary energies with S_f specified as a flux line, eqn. 6.65b. These results correspond to a specified voltage V = 2 volts, a conductor diameter of 10 cm, and a centre-to-centre conductor separation of one metre. The figure also shows the exact quarter-space energy of the open boundary problem, W. It was obtained using eqn. 6.70 with

$$C = \pi \varepsilon_o / \ln \alpha \qquad (6.72)$$

where α is the ratio of conductor separation to radius.

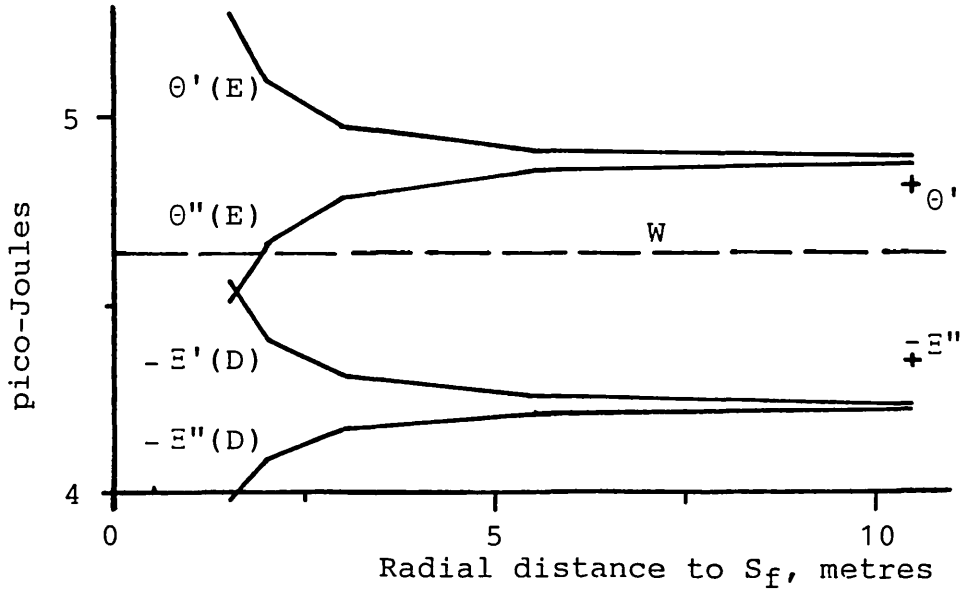

Fig. 6.22 Parallel conductors with specified voltage : effect of specification and distance at S_f on complementary energy estimates. W is the exact energy for the open boundary problem. Crosses indicate energy estimates from a refined mesh solution.

In practice, it is usual to perform only one of the four solutions of fig. 6.22; the figure shows how they relate to each other and to the exact solution. It suggests that, having opted for the present crude treatment of the open boundary region, there is little to choose from between the two specifications on S_f : with S_f too close, they are equally invalid; with S_f sufficiently far, they are practically indistinguishable. For S_f at 5.5 m, Θ' and Θ'' differ by 1.17%; the difference decreases to 0.33% at 10.5 m. The differences between Ξ' and Ξ'' are slightly smaller. The potential contours of fig. 6.23 and the D-E plots of fig. 6.24 confirm the above conclusion : at 10.5 m they are practically identical for the two specifications.

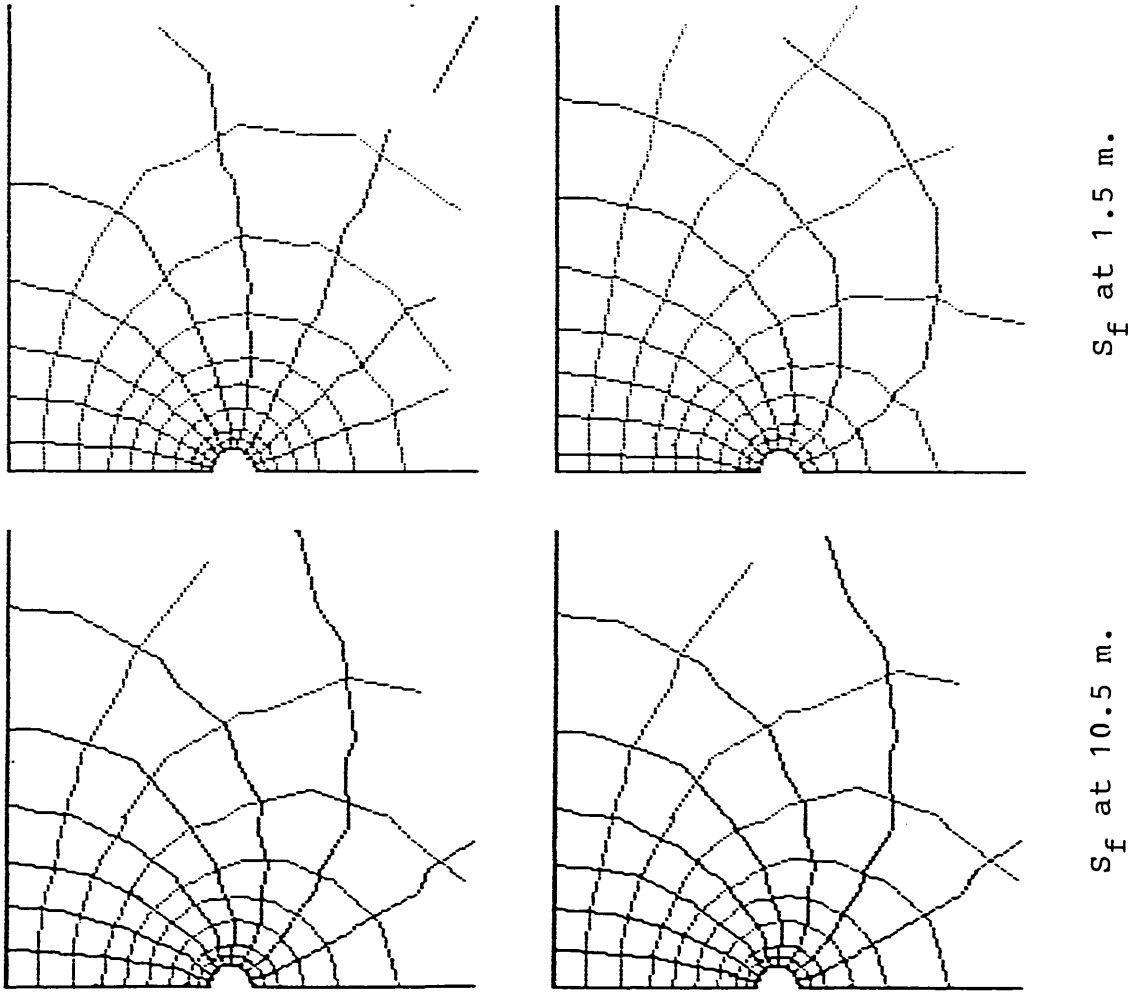

Fig. 6.23 Remote parallel conductors : potential contours.

It might appear that the E-solution has an advantage over the D-solution, the Θ's being closer to W than the Ξ's. However, this is probably problem-dependent, and certainly mesh-dependent. The curves of fig. 6.22 were obtained using rather coarse meshes (151 elements and 95 nodes at 10.5 m), with errors (Λ / $\ddot{W}$) in the region of 14%. A slight mesh refinement near the conductor (171 elements and 106 nodes) reduced the error to around 10%. The resulting energies are shown in the figure, where Ξ is seen to have improved more than Θ. Mesh dependence is highlighted in the D-E plots of fig. 6.24 : the apparent banding of points corresponds to circular layers of elements surrounding the conductor; it has, of course, no physical basis.

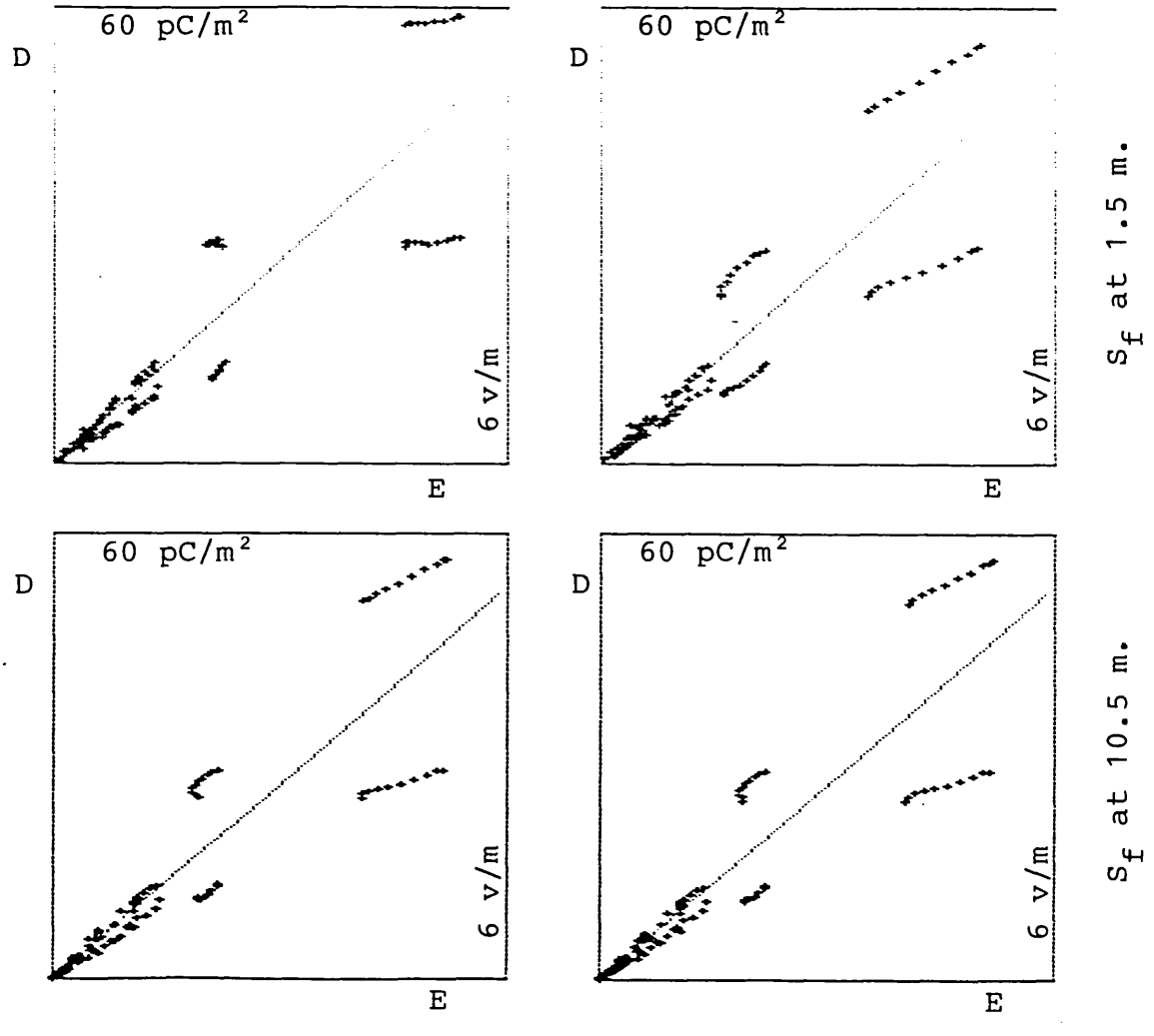

Fig. 6.24 Remote parallel conductors : D-E plots.

The boundary specifications of eqns. 6.65 describe problems that are physically different from the true, open boundary one. Eqn. 6.65a describes a problem where the conductors are surrounded by a cylinderical conducting plate at S_f, while eqn. 6.65b describes a problem where the electric permittivity is negligible beyond S_f. Strictly, the complementary energies Θ', Ξ' and Θ'', Ξ'' bound, respectively, the exact energies of the two approximate problems. When S_f is sufficiently far, however, the two problems become indistinguishable from each other, and hence from the true open boundary one; it is then possible to assume that the complementary energy estimates bound the true energy of the open boundary problem. Even then, in fact, the computed energies bound the exact energy for the polygonal conductor representing the actual circular one. This modelling approximation is necessitated by the finite element discretisation; the present solutions are for a 20-sided polygon.

We mention in passing that specified charge solutions yielded the same potential contours of fig. 6.23, and scaled versions of the D-E plots of fig. 6.24.

6.6.2 Parallel conductors near conducting plane

Fig. 6.25 shows parallel conductors situated asymmetrically near an infinite conducting plane. The cuts S_{12} and S_{1g} are introduced to convert the region with holes into a simply-connected region, as explained in sec. 3.4 and fig. 3.2. According to eqns. 6.56, and in the absence of surface charge, both fields are continuous across the cuts; thus

$$\text{on } S_{12} \text{ and } S_{1g}: \quad \underline{n} \times \Delta\underline{E} = 0, \quad \underline{n} \cdot \Delta\underline{D} = 0 \qquad (6.73a)$$

Moreover, continuity of the scalar potential ϕ in eqn. 6.58 ensures that

$$\oint \underline{E} \cdot d\underline{\ell} = 0 \qquad (6.73b)$$

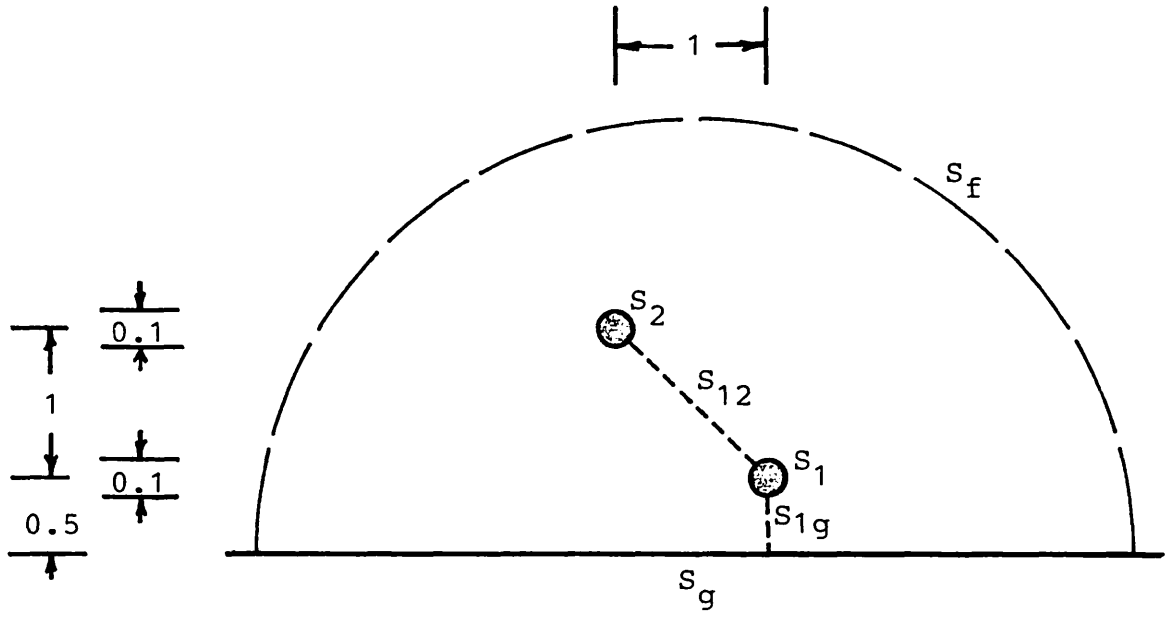

Fig. 6.25 Parallel conductors near infinite conducting plane : region outline. All dimensions in metres. S_f is at a radius of 10 m, and is not shown to scale.

for any closed path in the multiply-connected region. Enforcing eqns. 6.73 on the solution variables ensures that the cuts are correctly specified as required in sec. 3.4.2, particularly eqn. 3.39.

The same cuts are used for the constant discontinuities in A^e required by the non-zero charges on the conductors :

$$Q_1 = -\int_{S_1} \underline{D} \cdot d\underline{S} = \Delta A^e|_{S_{12}} + \Delta A^e|_{S_{1g}} \qquad (6.74a)$$

$$Q_2 = -\int_{S_2} \underline{D} \cdot d\underline{S} = -\Delta A^e|_{S_{12}} \qquad (6.74b)$$

$$Q_g = -\int_{S_g} \underline{D} \cdot d\underline{S} = -\Delta A^e|_{S_{1g}} \qquad (6.74c)$$

where $\Delta A^e = A^e_\beta - A^e_\alpha$ with A^e_β following A^e_α clockwise around S_1. Adding eqns. 6.74, we get

$$Q_1 + Q_2 + Q_g = 0 \qquad (6.74d)$$

as physically required.

The boundary conditions on the conductor surfaces are

$$\text{on } S_1 \; : \; \underline{n} \times \underline{E} = 0 \quad \Rightarrow \quad \phi = V_1 \tag{6.75a}$$

$$\text{on } S_2 \; : \; \underline{n} \times \underline{E} = 0 \quad \Rightarrow \quad \phi = V_2 \tag{6.75b}$$

and

$$\text{on } S_g \; : \; \underline{n} \times \underline{E} = 0 \quad \Rightarrow \quad \phi = V_g \tag{6.75c}$$

S_f approximates open boundary conditions by an equipotential

$$\text{on } S_f \; : \; \underline{n} \times \underline{E} = 0 \quad \Rightarrow \quad \phi = \phi|_{S_g} = V_g \tag{6.76a}$$

or by a flux line

$$\text{on } S_f \; : \; \underline{n} \cdot \underline{D} = 0 \quad \Rightarrow \quad A^e = 0 \tag{6.76b}$$

The zero potential in 6.76b is chosen arbitrarily, there being no other reference value for A^e in the region.

We now substitute the boundary conditions of eqns. 6.73-76 into Γ_o in eqn. 6.61; for either specification on S_f, we have

$$\begin{aligned} \Gamma_o &= - [\phi \, , \underline{n} \cdot \underline{D}]_{S_s} \\ &= -[\phi, \underline{n} \cdot \underline{D}]_{S_1} - [\phi, \underline{n} \cdot \underline{D}]_{S_2} - [\phi, \underline{n} \cdot \underline{D}]_{S_g} - [\phi, \underline{n} \cdot \underline{D}]_{S_f} \\ &= V_1 Q_1 + V_2 Q_2 + V_g Q_g \end{aligned} \tag{6.77a}$$

The integral on S_f vanishes if eqn. 6.76b is used, and combines with the integral on S_g if eqn. 6.76a is used; in the latter case, the surface integral on S_g in eqn. 6.74c, and hence Q_g, relate to the true infinite extent of S_g. Substituting from eqn. 6.74d into 6.77a, we can write

$$\Gamma_o = (V_1 - V_g) Q_1 + (V_2 - V_g) Q_2 \tag{6.77b}$$

It is recalled that the conductor voltages and charges correspond to the abstract motive force and flux of sec. 3.4.2, eqns. 3.21 and 3.22. As described in that section, they should be adequately specified for uniqueness. The most obvious way is to ensure that, for each conductor, either voltage or charge is specified. Voltage values can be imposed explicitly on the scalar potential ϕ in accordance with eqns. 6.75, while charge values can be imposed on the vector potential discontinuities ΔA^e in accordance with eqns. 6.74. Adequate specification for uniqueness causes

Γ_o in eqns. 6.77 to split between the E- and D-systems. In this way, the constitutive error, Λ in eqn. 6.61, generates complementary functionals for the various possible specifications of this problem.

According to eqn. 6.77b, the following are examples of physically sufficient specification : $\overline{Q_1}$ and $\overline{Q_2}$; $\overline{(V_1 - V_g)}$ and $\overline{(V_2 - V_g)}$; $\overline{Q_1}$ and $\overline{(V_2 - V_g)}$; $\overline{Q_2}$ and $\overline{(V_1 - V_g)}$. Complementary solutions were actually performed for the following specifications :

$$V_1 = \overline{V_1} = 1 \text{ volt}, \qquad V_2 = \overline{V_2} = -1 \text{ volt} \tag{6.78}$$

According to eqn. 6.77a, this leaves the term $V_g Q_g$, giving rise to the dual problems :

(i) Specified voltage on plane $(V_g = \overline{V_g})$:

$$\Theta_V(E) = X(\underline{E}) \tag{6.79a}$$

$$\Xi_V(D) = \Psi(\underline{D}) - \overline{V_1}Q_1 - \overline{V_2}Q_2 - \overline{V_g}Q_g \tag{6.79b}$$

The D-solution yields estimates of the conductor charges Q_1, Q_2, and Q_g.

(ii) Specified charge on plane $(Q_g = \overline{Q_g})$:

$$\Theta_Q(E) = X(\underline{E}) - V_g\overline{Q_g} \tag{6.80a}$$

$$\Xi_Q(D) = \Psi(\underline{D}) - \overline{V_1}Q_1 - \overline{V_2}Q_2 \tag{6.80b}$$

The E-solution yields an estimate of the plane voltage V_g, while the D-solution yields estimates of the conductor charges Q_1 and Q_2. This specification includes the special case where the plane is floating relative to the electric circuit of the conductors, i.e. $\overline{Q_g} = 0$.

Applying ineq. 4.10 and eqn. 6.16 to eqns. 6.79,

$$\Theta_V(E) \geq W_V \geq - \Xi_V(D) \tag{6.81}$$

where W_V is the exact energy in the specified voltage problem (assuming S_f is sufficiently far; see sec. 6.6.1).

Bounds on the exact stored energy W_Q are not generally available in the specified charge problem, since $\Theta_Q \neq X$ and $\Xi_Q \neq \Psi$. However, in the special case of a floating ground

$$Q_g = 0 \qquad \Rightarrow \qquad \Theta_Q(E) = X(\underline{E}) \tag{6.82a}$$

so that

$$\Theta_Q(E) \geq W_Q \geq - \Xi_Q(D) \tag{6.82b}$$

Fig. 6.26 shows equipotential contours for various specifications. Numerical solutions were performed on a mesh of 724 elements and 399 nodes; errors (Λ / $\ddot{W}$) were in the region of 10.5 - 13.5 %, being lowest for the relatively smooth $V_G = 2$ v solution.

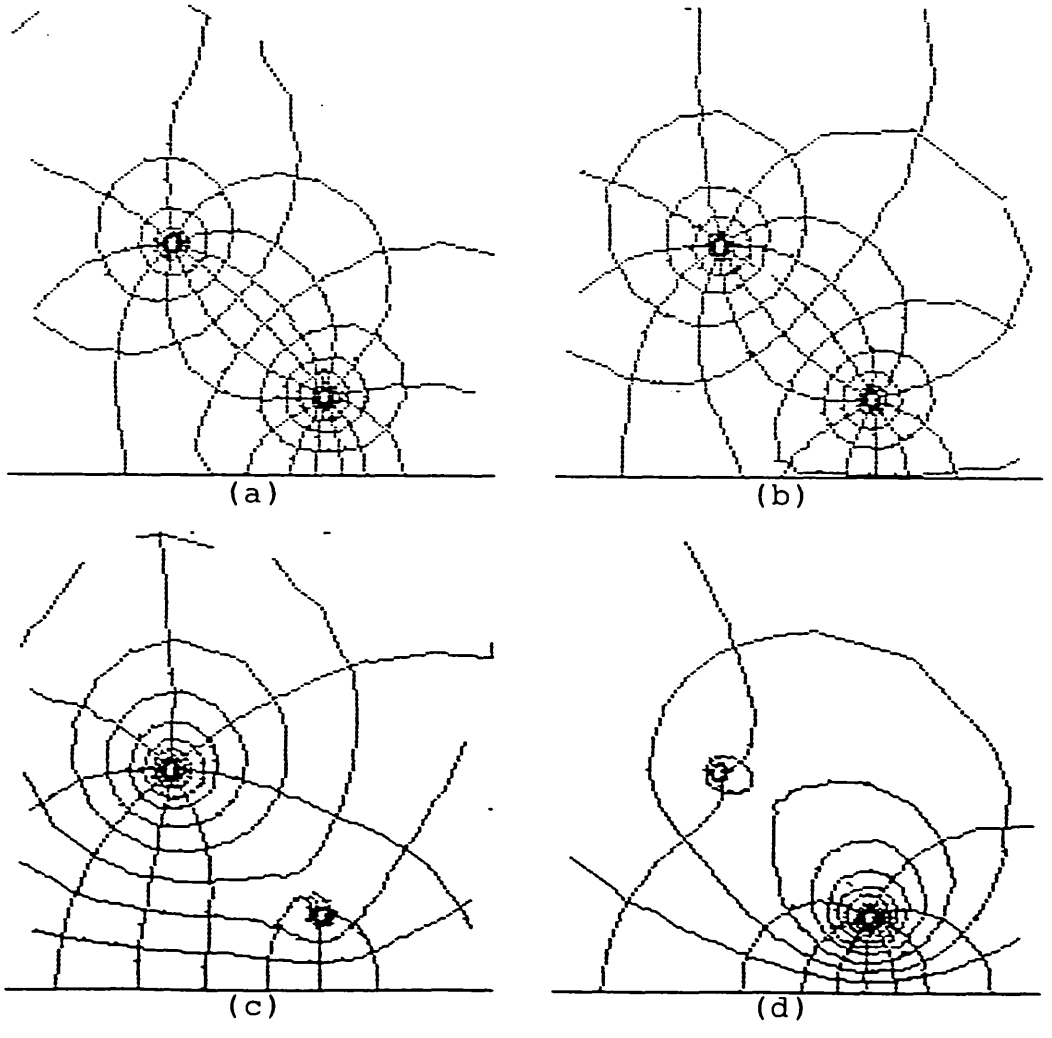

Fig. 6.26 Parallel conductors near conducting plane : potential contours.

(a) $\overline{V}_g = 0$, $Q_g = 4.59$ pC;
(b) $\overline{Q}_g = 0$, $V_g = 0.188$ v;
(c) $\overline{V}_g = 2$ v, $Q_g = -48.09$ pC;
(d) $\overline{V}_g = -2$ v, $Q_g = 57.28$ pC.

6.7 Conduction examples

The relevant equations in electric conduction are

$$0 = \text{curl } \underline{E} \quad ; \quad 0 = \text{div } \underline{J} \tag{6.83}$$

$$0 = \underline{n} \times \Delta\underline{E} \quad ; \quad 0 = \underline{n} \cdot \Delta\underline{J} \tag{6.84}$$

$$\underline{E} = -\nabla\phi \quad ; \quad \underline{J} = \nabla \times \underline{T} \tag{6.85}$$

$$0 = \Delta\phi \tag{6.86}$$

ϕ is the electric scalar potential, and $\underline{T}$ is the electric current-describing vector potential; they correspond, respectively, to the abstract potentials Ω and $\underline{A}$ of sections 3.4.3 and 3.4.4. Eqns. 6.83-86 describe the conduction problem interpretation of the abstract model of sections 3.3 and 3.4.5. The corresponding constitutive error is

$$\Lambda(\underline{E},\underline{J}) = X(\underline{E}) + \Psi(\underline{J}) - Z(\underline{E},\underline{J}) \tag{6.87}$$

Minimisation of $\Lambda(\underline{E},\underline{J})$ enforces the constitutive relationship on $\underline{E}$ and $\underline{J}$. Using the E-system scalar potential ϕ, $Z(\underline{E},\underline{J})$ splits as follows

$$Z(\underline{E},\underline{J}) = \langle \underline{E} , \underline{J} \rangle_R = -\langle \nabla\phi , \underline{J} \rangle_R = \langle \phi , \nabla\cdot\underline{J} \rangle_R - \int_R \nabla\cdot(\phi\underline{J})\, dR$$

$$= - [\phi , \underline{n}\cdot\underline{J}]_{S_s} - [\phi , \underline{n}\cdot\underline{J}]_{S_o}$$

At this stage, we can rewrite eqn. 6.87 in the form

$$\Lambda = \Theta_o(E) + \Xi_o(J) - \Gamma_o(E,J) \tag{6.88}$$

where

$$\Theta_o(E) = X(\underline{E})$$

$$\Xi_o(J) = \Psi(\underline{J})$$

$$\Gamma_o(E,J) = - [\phi , \underline{n}\cdot\underline{J}]_{S_s}$$

A common type of problem is the general two-terminal conductor, fig. 6.27. S_{e1} and S_{e2} are the terminals connected to the external circuit, while S_{j1} and S_{j2} are the insulated sides.

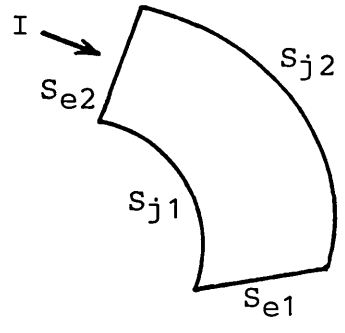

Fig. 6.27 Two-terminal conductor.

The boundary conditions are

$$\text{on } S_{e1}: \quad \underline{n} \times \underline{E} = 0 \quad \Rightarrow \quad \phi = 0 \tag{6.89a}$$

$$\text{on } S_{e2}: \quad \underline{n} \times \underline{E} = 0 \quad \Rightarrow \quad \phi = V = -\int_{\underline{r}_1}^{\underline{r}_2} \underline{E} \cdot d\underline{\ell} \tag{6.89b}$$

$$\text{on } S_{j1}: \quad \underline{n} \cdot \underline{J} = 0 \quad \Rightarrow \quad T = 0 \tag{6.90a}$$

$$\text{on } S_{j2}: \quad \underline{n} \cdot \underline{J} = 0 \quad \Rightarrow \quad T = I = \int_{S_{e1}} \underline{J} \cdot d\underline{S} \tag{6.90b}$$

where V and I are the voltage across and the current through the conductor, respectively. The specifications are entirely analogous to those of the trapezoidal lamination sub-region analysed in sec. 6.5.3, so that

$$\Gamma_o = V I \tag{6.91}$$

Once again, we get the dual problems :

(i) Specified voltage $(V = \overline{V})$:

$$\Theta_V(E) = X(\underline{E}) \ , \qquad \Xi_V(J) = \Psi(\underline{J}) - \overline{V} I \tag{6.92}$$

$$\Theta_V(E) \geq W_V \geq - \Xi_V(J) \tag{6.93}$$

(ii) Specified current $(I = \overline{I})$:

$$\Theta_I(E) = X(\underline{E}) - V \overline{I} \ , \qquad \Xi_I(J) = \Psi(\underline{J}) \tag{6.94}$$

$$\Xi_I(J) \geq W_I \geq - \Theta_I(E) \tag{6.95}$$

$2W_V$ and $2W_I$ are the exact values of the power dissipation in the two problems; on the electric circuit side, they are related to the resistance R by

$$W_V = \tfrac{1}{2} \overline{V}^2 / R_V \ , \qquad W_I = \tfrac{1}{2} \overline{I}^2 R_I \tag{6.96}$$

so that

$$2\Theta_V(E)/\overline{V}^2 \geq \frac{1}{R_V} \geq -2\Xi_V(J)/\overline{V}^2 \tag{6.97a}$$

and

$$2\Xi_I(J)/\overline{I}^2 \geq R_I \geq -2\Theta_I(E)/\overline{I}^2 \tag{6.97b}$$

In both cases, the E-system is associated with the lower bound on resistance, while the J-system is associated with the upper bound[6.18,19].

With appropriate scaling and interpretation of the various parameters, the trapezoidal lamination of sec. 6.5.3 provides an example of this common type of problem. In the following sections, we consider two less common, but possibly more interesting, types of problem.

6.7.1 Conductor with skewed terminals

Fig. 6.28 shows a cylindrical conductor with radially skewed terminals S_{e1} and S_{e2}; S_{j1} and S_{j2} are the insulated sides. S_{12} is a cut that converts the region with a hole into a simply-connected one, sec. 3.4 and fig. 3.2; it can be placed along any curve joining inner and outer cylindrical shells. Both $\underline{E}$ and $\underline{J}$ are continuous across the cut, eqn. 6.84; moreover, ϕ is continuous, eqn. 6.86, so that

$$\oint \underline{E} \cdot d\underline{\ell} = 0 \qquad (6.98)$$

for any closed path in the multiply-connected region. The

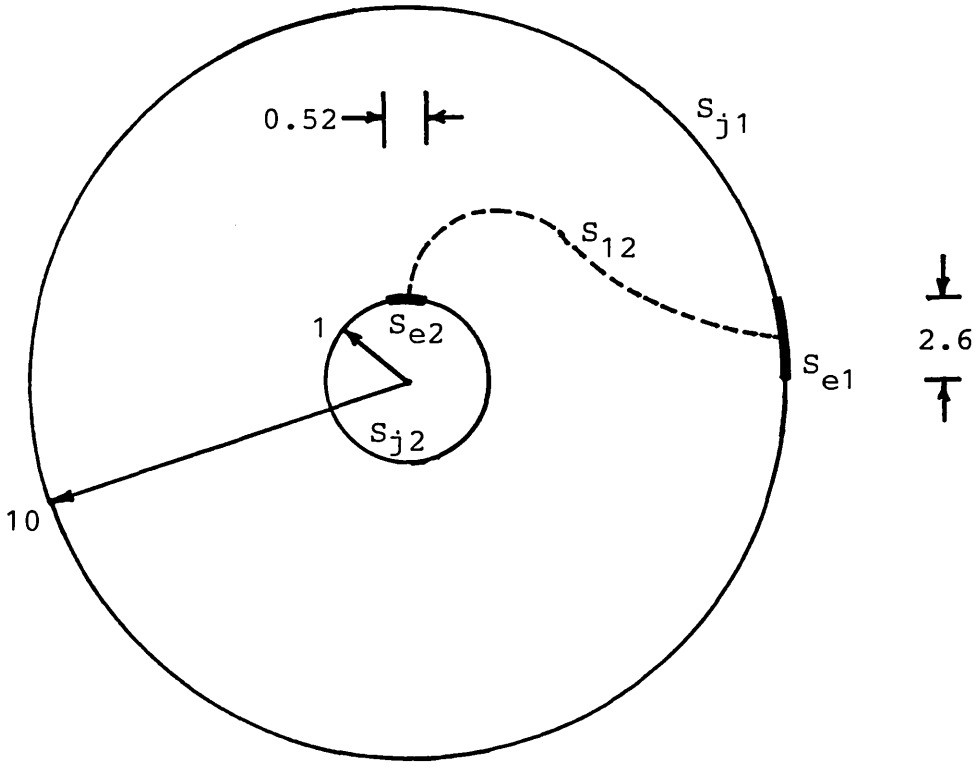

Fig. 6.28 Cylindrical conductor with radially skewed terminals : outline (not to scale). All dimensions in metres.

cut is therefore correctly specified according to sec. 3.4.2, particularly eqn. 3.39. The same cut is used for the constant discontinuity in T required by the terminal current

$$I = \int_{S_{e1}} \underline{J} \cdot d\underline{S} = - \int_{S_{e2}} \underline{J} \cdot d\underline{S} = \Delta T \qquad (6.99)$$

I is the current flowing from S_{e2} to S_{e1} inside the conductor; $\Delta T = T_\beta - T_\alpha$ with T_β following T_α in a clockwise sense. The external boundary conditions are

$$\text{on } S_{e1} : \quad \underline{n} \times \underline{E} = 0 \quad \Rightarrow \quad \phi = 0 \qquad (6.100a)$$

$$\text{on } S_{e2} : \quad \underline{n} \times \underline{E} = 0 \quad \Rightarrow \quad \phi = V = - \int_{\underline{r}_{e1}}^{\underline{r}_{e2}} \underline{E} \cdot d\underline{\ell} \qquad (6.100b)$$

$$\text{on } S_{j1} : \quad \underline{n} \cdot \underline{J} = 0 \quad \Rightarrow \quad T = 0 \qquad (6.101a)$$

$$\text{on } S_{j2} : \quad \underline{n} \cdot \underline{J} = 0 \quad \Rightarrow \quad T = I' = \int_{S'} \underline{J} \cdot d\underline{S} \qquad (6.101b)$$

V is the voltage across the conductor, and I' is the current through any section S' that extends from S_{j1} to S_{j2} without being cut by S_{12}. There are in fact two parallel paths of current flow through the conductor, fig. 6.29. The currents are related to the J-system potentials by

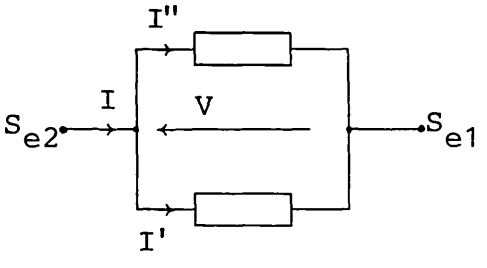

Fig. 6.29 Circuit model.

$$\begin{aligned} I &= \Delta T \\ I' &= T|_{S_{j2}} \\ I'' &= I - I' = \Delta T - T|_{S_{j2}} \end{aligned} \qquad (6.102)$$

Substituting the boundary conditions into Γ_o in eqn. 6.88, we get

$$\Gamma_o = - [\phi , \underline{n} \cdot \underline{J}]S_s = -[\phi , \underline{n} \cdot \underline{J}]S_{e2} = - V \int_{S_{e2}} \underline{J} \cdot d\underline{S}$$

$$= V I \qquad (6.103)$$

Eqn. 6.103 is identical to 6.91, so that eqns. 6.92-97 are applicable again, with specified voltage and specified current alternatives. In both cases, the J-solution yields direct estimates of the branch currents, I' and I", that correspond to the upper bound on resistance.

Complementary solutions were performed on a mesh of 695 elements and 382 nodes. For unit conductivity, the resistance was estimated at 1.89 ohms ± 5.4%. Fig. 6.30 shows potential contours and the J-E plot; the cut S_{12} is included in the former. T-contours are in fact current flow lines; separation between the parallel paths of fig. 6.29 can be discerned near the left edge of S_{e2} in fig. 6.30a, and traced to the lower edge of S_{e1}. I' circles beneath the hole, while I" flows above it; the J-solution placed their values at 0.227 I and 0.773 I respectively. The sharpest discrepancies in the J-E plot of fig. 6.30b occur near the edges of the terminals S_{e1} and S_{e2} : the transition from an insulating boundary S_j to an adjacent S_e is geometrically smooth, fig. 6.28; yet the fields, $\underline{E}$ and $\underline{J}$, are required to be tangential to the former and normal to the latter. As would be expected, this results in severe numerical errors at insulator/terminal meeting points, fig. 6.31. The detail in the vicinity of S_{e2} shown covers just over 1.2 % of the total area, yet contains more than half the global constitutive error; the black elements alone account for a third of the global error.

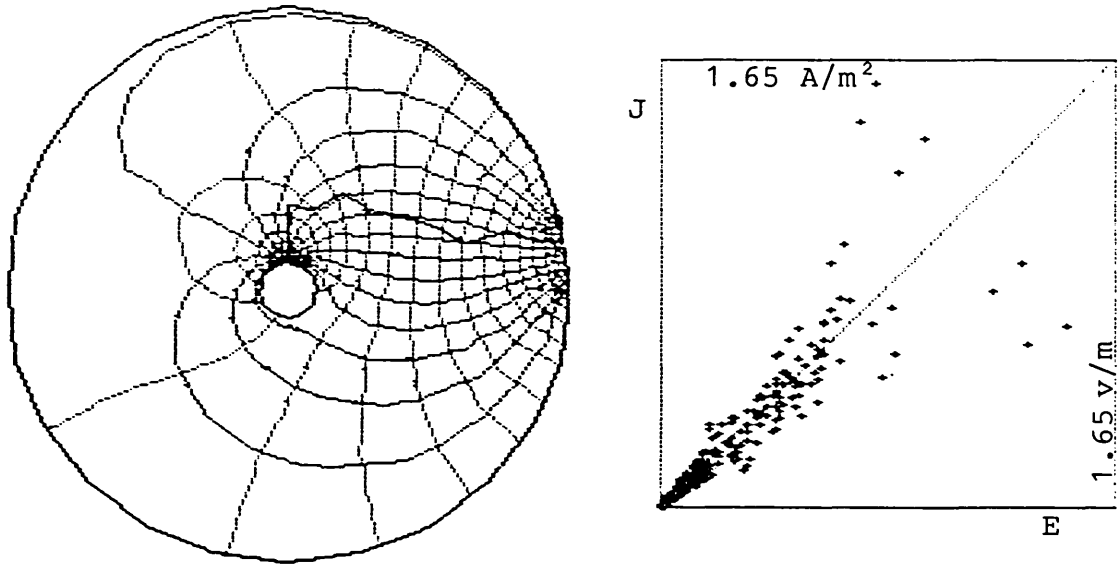

(a) potential contours (b) J-E plot

Fig. 6.30 Cylindrical conductor with radially skewed terminals.

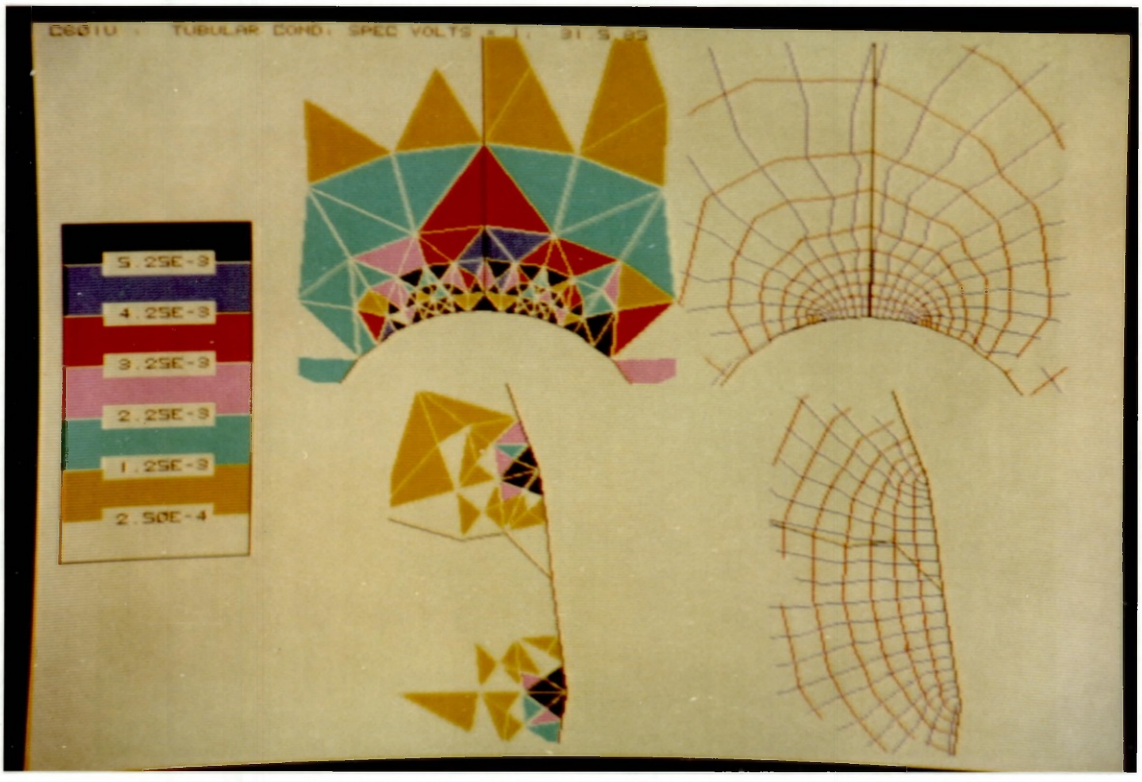

Fig. 6.31 Cylindrical conductor with radially skewed terminals : constitutive error density and equipotential contours in the vicinity of inner terminal S_{e2} (top), and outer terminal S_{e1} (bottom). Dimensional scales different in the two parts. Cut shown by black broken line.

6.7.2 Interlinked boundary specifications

Complementary functionals for the general two-terminal conductor are given in eqns. 6.92 for the specified voltage case, and in eqns. 6.94 for the specified current case. Both were derived by appropriate splitting of the constitutive error

$$\Lambda(E,J) = X(\underline{E}) + \Psi(\underline{J}) - V\,I \qquad (6.104)$$

This general expression for the constitutive error in a two-terminal conductor is obtained by substituting eqn. 6.91 for Γ_o in eqn. 6.88. There is a third way of specifying boundary conditions, namely

$$V + R_s I = V_s \qquad \text{or} \qquad I + G_s V = I_s \qquad (6.105)$$

The parameters V_s, I_s, R_s, and G_s are known; they refer to the simple circuits of fig. 6.32, where

$$G_s = 1/R_s\ , \qquad I_s = G_s V_s\ , \qquad V_s = R_s I_s \qquad (6.106)$$

Clearly, eqns. 6.105 interrelate V and I, but specify neither. In effect, they introduce an additional link, besides the constitutive relationship, between the E- and J-systems. Substitution for V or I in eqn. 6.104 from eqn. 6.105 results in only an incomplete splitting of Λ : the resulting E- and J-system functionals will have a common variable, and must therefore be extremised simultaneously to minimise Λ. Indeed, proper splitting of Λ is guaranteed only if boundary constraints are specified independently

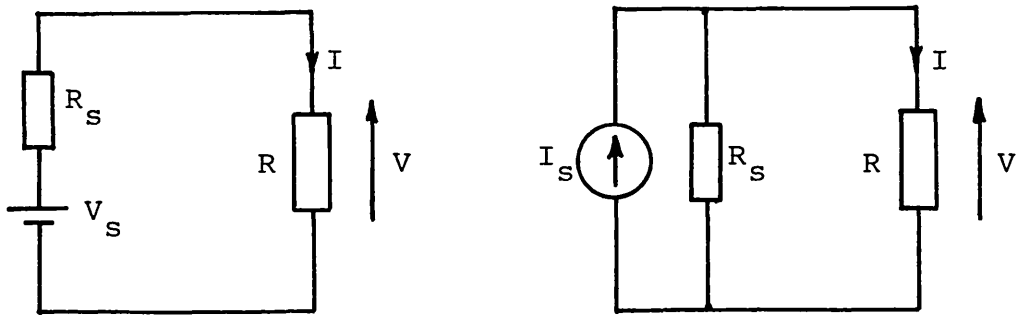

(a) voltage source (b) current source

Fig. 6.32 Conductor in circuit.

for the two systems, sec. 3.5. However, a treatment is available for the particular interlinked boundary conditions of eqns. 6.105.

It is based on constructing a lumped-parameter constitutive error for the source resistance R_s having the properties

$$\Lambda_s \geq 0 \tag{6.107a}$$

with

$$\Lambda_s = 0 \quad <=> \quad I = I_s - G_s V \quad \text{and} \quad V = V_s - R_s I \tag{6.107b}$$

We now define the total error

$$\Lambda_t = \Lambda + \Lambda_s \tag{6.108}$$

From the properties of Λ and Λ_s, we have

$$\Lambda_t \geq 0 \tag{6.109}$$

with equality occuring if, and only if, both the constitutive relationship in R and the boundary conditions 6.105 are satisfied. The solution may then be obtained by minimising Λ_t rather than Λ; this has the advantage of not requiring the boundary conditions 6.105 to be imposed explicitly : they are enforced weakly by the solution.

For the procedure to achieve its goal, Λ_s must be defined not only to satisfy eqns. 6.107, but to ensure proper splitting of Λ_t as well. As it happens, such a definition is available provided R_s is positive. It is, in fact, the lumped-parameter version of the general definition of the constitutive error in Chapter 2, eg. eqn. 2.15a. From fig. 6.32a we may write

$$\Lambda_s = \tfrac{1}{2} G_s (V_s - V)^2 + \tfrac{1}{2} R_s I^2 - (V_s - V) I \tag{6.110a}$$

Or, from fig. 6.32b

$$\Lambda_s = \tfrac{1}{2} G_s V^2 + \tfrac{1}{2} R_s (I_s - I)^2 - V (I_s - I) \tag{6.110b}$$

The two expressions are identical, as can be verified by substitution from the relationships in 6.106.

Substituting for Λ from eqn. 6.104, and for Λ_s from eqn. 6.110, eqn. 6.108 for the total error may be written in the form

$$\Lambda_t(E,J) = \Theta(E) + \Xi(J) - \Gamma \qquad (6.111)$$

where

$$\Theta(E) = X(\underline{E}) + \tfrac{1}{2} G_s V^2 - V I_s$$

$$\Xi(J) = \Psi(\underline{J}) + \tfrac{1}{2} R_s I^2 - V_s I$$

$$\Gamma = -\tfrac{1}{2} V_s I_s$$

Γ is a known constant and has no effect on the solution formulations. It may be attached to either $\Theta(E)$ or $\Xi(J)$ to yield the independent complementary functionals. The corresponding bounds are

$$\Theta(E) - \Gamma \geqq W \geqq - \Xi(J) \qquad (6.112a)$$

or

$$\Xi(J) - \Gamma \geqq W \geqq - \Theta(E) \qquad (6.112b)$$

where 2W is the exact value of the power dissipation in R and R_s together. On the electric circuit side, it is given by

$$W = \tfrac{1}{2} V_s^2 / (R + R_s) \qquad \text{or} \qquad W = \tfrac{1}{2} I_s^2 / (\frac{1}{R} + G_s) \qquad (6.113)$$

Substituting into 6.112, we get, after some manipulation,

$$- \tfrac{1}{2} V_s^2 / \Xi(J) - R_s \geqq R \geqq \tfrac{1}{2} V_s^2 / (\Theta(E) - \Gamma) - R_s \qquad (6.114a)$$

and

$$- \tfrac{1}{2} I_s^2 / \Theta(E) - G_s \geqq \frac{1}{R} \geqq \tfrac{1}{2} I_s^2 / (\Xi(J) - \Gamma) - G_s \qquad (6.114b)$$

The above derivations can be extended to non-linear resistors R and R_s provided the latter is strictly positive statically and dynamically. Uniqueness of the boundary specification 6.105 can be established in accordance with eqn. 3.28. The procedure used in the derivations of this section is instructive : complementary formulations may be derived in cases where the two systems are interlinked by additional constraints that can be cast in an appropriate error form, eqn. 6.107, so that the total error may be split.

6.8 Conclusions

The previous sections demonstrate the systematic manner with which the constitutive error approach generates complementary solution formulations for various problem specifications : the error splits, as a matter of course, into complementary functionals, provided the problem specifications are well-posed and do not interrelate the H- and B-systems on the boundary; indeed, sec. 6.7.2 shows that the second restriction is not rigid. In this way, the approach achieves a degree of generality over alternative derivations of complementary variational principles, since these are based on the primal and dual statements of sec. 4.3. The two statements are not in general equivalent. In the lamination problem of sec. 6.5.3, for example, the primal statement applies to the specified mmf case, while the dual statement applies to the specified flux case; attempting to use either statement with the wrong problem specification results in imperfect formulation[6.16]. Moreover, both statements fail to describe certain physically unique, and hence allowable, specifications of the electrostatic problem of sec. 6.6.2.

The potentials used to split the constitutive errors correspond to Fraser's primal formulations[6.16]: the vector potential in magnetostatic applications, sec. 6.5, and the scalar potential in electrostatic and electric conduction applications, sections 6.6 and 6.7. The choice is one of convenience : in each case, the potential used is continuous and free of a pre-specified field. Entirely valid dual formulations may be derived using the complementary potentials, but the derivations tend to be more cumbersome. Dual formulations are, in fact, equivalent to primal ones, since they differ only by constant terms that cannot affect the minimisation process.

Combined presentation of computational results for the two complementary systems yields a substantial amount of information on the adequacy of the numerical solution.

Acknowledging that true distributions cannot be predicted exactly, the next best thing, from a practical engineering point of view, is the ability to ascribe a realistic level of confidence to the numerically derived results. Useful indications are provided by energy distributions, equipotential contours, and B-H plots, but most comprehensively by constitutive error distributions. Use of the latter in intelligent mesh refinement[6•14,15] is demonstrated. The global constitutive error quantises confidence assessment, being a comprehensive measure of numerical error that can be meaningfully normalised with respect to the bounded energy. Moreover, computed results corroborate previous assertions that complementary solutions, in combination, can lead to substantial economy in the estimation of such global quantities as energies and lumped circuit parameters[6•12,13].

From a more theoretical, research, point of view, combined presentation of results sheds much light on the comparative numerical behaviour of complementary systems. One example of this aspect is provided by the investigation of the crude treatment of open boundaries in sec. 6.6.1; a similar study of more accurate treatments may prove beneficial.

Except for very coarse finite element meshes, the rate of convergence of complementary solutions with mesh refinement was found to be largely similar. Moreover, neither emerged as a clear favourite from the viewpoint of ICCG convergence : their comparative behaviour depended very much on the particular problem and mesh. As would be expected, the potential with the firmer reference converged faster; this was particularly obvious in problems where alternative boundary specifications are possible, for example the lamination of sec. 6.5.3.

CHAPTER SEVEN

Non-linear Applications

7.1 Introduction

The theory of Chapters 2 and 3 is applicable to non-linear and anisotropic materials, provided the constitutive relationships possess properties 1 and 2 of sec, 2.2. In this chapter, some of the magnetostatic solutions of Chapter 6 are repeated for non-linear, but still isotropic, iron. The presentation highlights deviations from the linear case. We also present, briefly in sec. 7.4, a constitutive error interpretation of the iterative process in non-linear solution.

7.2 Energy bounds

The theory of complementary variational principles, as presented in Chapter 4, is applicable to non-linear problems. In particular, the functional bounds of ineq. 4.10 still hold :

$$\Theta(H) \geq \Theta(H_o) = -\Xi(B_o) \geq -\Xi(B) \qquad (7.1a)$$

or

$$\Xi(B) \geq \Xi(B_o) = -\Theta(H_o) \geq -\Theta(H) \qquad (7.1b)$$

where $\underline{H}_o$ and $\underline{B}_o$ denote exact fields, i.e.

$$0 = \Lambda(H_o, B_o) = X(\underline{H}_o) + \Psi(\underline{B}_o) - Z(\underline{H}_o, \underline{B}_o) \qquad (7.2)$$

However, for non-linear constitutive relationships, eqns. 2.8 for $\chi(\underline{H})$ and $\psi(\underline{B})$ do not simplify to eqns. 6.14 as in the linear case, so that, in general

$$X(\underline{H}_o) \neq \Psi(\underline{B}_o) \neq \tfrac{1}{2} Z(\underline{H}_o, \underline{B}_o) \qquad (7.3)$$

The linear definition of energy, W in eqns. 6.16, is thus inapplicable. It is necessary to distinguish between energy and co-energy, whose exact values, W^e and W^c respectively, are defined as follows :

$$W^e = \Psi(\underline{B}_o) \qquad \text{and} \qquad W^c = X(\underline{H}_o) \qquad (7.4a)$$

Substituting into eqn. 7.2, and rearranging, we can write

$$W^e + W^c = Z(\underline{H}_o, \underline{B}_o) = Z^o \qquad (7.4b)$$

The bounds in ineq. 7.1 may thus relate to energy or co-energy, or possibly neither. It all depends on the manner with which Z decomposes between H- and B-systems, and the resulting composition of the complementary functionals Θ and Ξ; this, in turn, depends on problem specifications as demonstrated in the examples of Chapter 6. The examples of this chapter will show that it is not generally possible to define bounds on non-linear circuit parameters.

7.3 Magnetostatic examples

Previous complementary treatments of non-linearity are limited to problems having simple geometries, with simple representation of the B-H characteristic[7.1,2]. Here, we shall consider the geometries of sec. 6.5, with the B-H characteristic represented as in fig. 7.1. The latter has the typical form of ferromagnetic materials, where the constitutive operators are functions of field magnitudes :

$$\underline{B} = \mu(H)\,\underline{H} \qquad \text{and} \qquad \underline{H} = \nu(B)\,\underline{B} \qquad (7.5)$$

Such a constitutive relationship possesses property 1 of sec. 2.2 if the B-H curve is continuous, and has a positive slope everywhere. To verify that it possesses property 2 as well, we test by means of eqns. 2.3 :

$$\frac{\partial}{\partial H_j}\left(\mu(\underline{H})\underline{H}\right)_i = \frac{\partial}{\partial H_j}\left(\mu(H)H_i\right) = \frac{\partial \mu}{\partial H}\frac{\partial H}{\partial H_j} H_i = \frac{1}{H}\left(\frac{\partial \mu}{\partial H}\right) H_j H_i \qquad (7.6a)$$

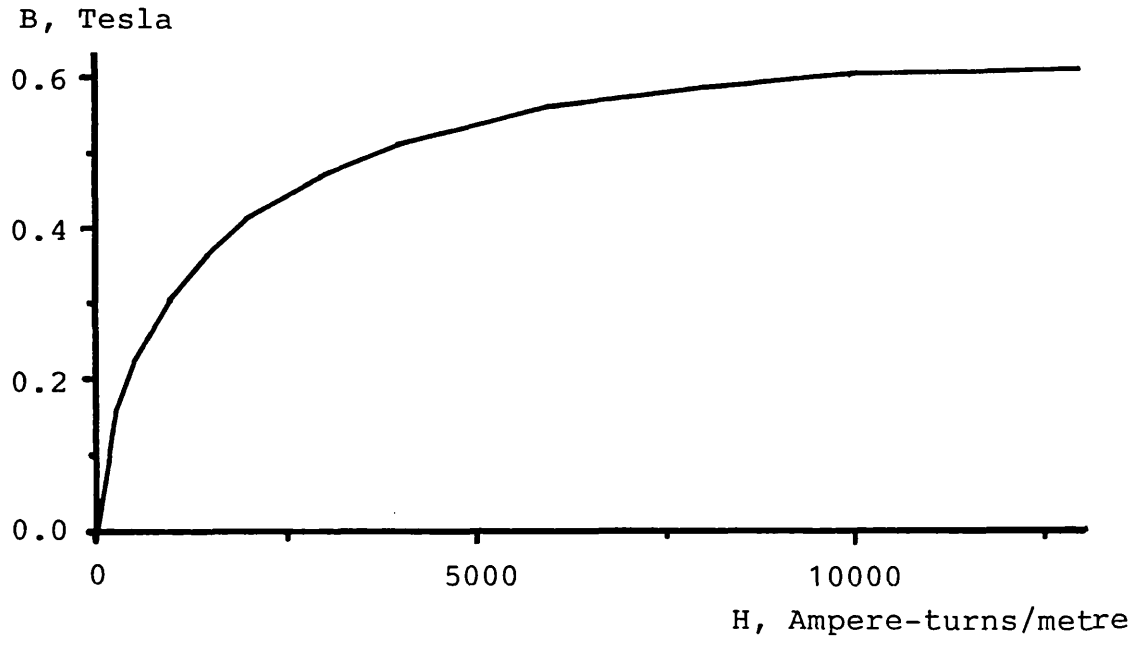

Fig. 7.1 Non-linear B-H characteristic : piecewise linear representation used in numerical solution. The slope is μ_o beyond the point 10 KA-t/m, 0.6 T.

where it is noted that

$$H = \left(\sum_k H_k^2 \right)^{\frac{1}{2}} \quad \Rightarrow \quad \partial H/\partial H_j = H_j/H \tag{7.6b}$$

Similarly

$$\frac{\partial}{\partial H_i} \left(\mu(\underline{H})\underline{H} \right)_j = \frac{1}{H} \left(\frac{\partial \mu}{\partial H} \right) H_i H_j \tag{7.6c}$$

Equality of the derivatives in 7.6a and 7.6c means that the constitutive relationship satisfies eqn. 2.3a, and hence possesses property 2.

The B-H characteristic shown in fig. 7.1 is a discrete approximation of the actual smooth one. It is the representation used in the computer solution, and may be viewed as part of the modelling approximation of physical problems. Such a piecewise linear characteristic is sufficient for well-posedness since only C^o-continuity is required, as discussed in Appendix B. The initial segment has a slope of $500\,\mu_o$, the same as the linear permeability used in the solutions of sec. 6.5. The last segment, which extends to infinity, has a slope of μ_o, the free space permeability; it corresponds to a fully saturated state.

For all three problems that will be considered, the equations of sec. 6.5 remain unchanged up to, and including, the definition of complementary functionals; examination of the derivations should reveal that they involve no assumption of linearity. Deviations emerge only when we come to define energies and their bounds, and attempt to relate them to lumped circuit parameters; at that stage, it is necessary to distinguish between energy and co-energy, sec. 7.2, since they are no longer equal as in the linear case, sec. 6.3.

7.3.1 C-magnet

The C-magnet problem is defined in sec. 6.5.1. The constitutive error and complementary functionals are given in eqns. 6.24 :

$$\Lambda = \Theta(H) + \Xi(B) \tag{7.7a}$$

with

$$\Theta(H) = X(\underline{H}) \quad \text{and} \quad \Xi(B) = \Psi(\underline{B}) - \langle \underline{J} , \underline{A} \rangle_R \tag{7.7b}$$

Comparing with eqns. 7.4 and ineq. 7.1, it is evident that bounds are defined for the co-energy W^c :

$$\Theta(H) \geqq W^c = \langle \underline{J} , \underline{A}_o \rangle_R - W^e \geqq - \Xi(B) \tag{7.8}$$

The H-solution thus yields an upper bound estimate of the co-energy, while the B-solution yields a lower bound estimate. The complementary solutions also yield estimates of the energy W^e and the product Z^o, eqns. 7.4.
From the H-solution :

$$W^e_H = \langle \mu \underline{H} , \underline{H} \rangle_R - X(\underline{H}), \qquad Z^o_H = \langle \mu \underline{H} , \underline{H} \rangle_R \tag{7.9}$$

From the B-solution :

$$W^e_B = \Psi(\underline{B}), \qquad Z^o_B = \langle \underline{J} , \underline{A} \rangle_R \tag{7.10}$$

And from the two solutions together :

$$W^e_{HB} = \langle \underline{J} , \underline{A} \rangle_R - X(\underline{H}), \qquad Z^o_{HB} = X(\underline{H}) + \Psi(\underline{B}) \tag{7.11}$$

The energy estimates in eqns. 7.9-11 do not necessarily bound the exact values W^e and Z^o. However, from the universal positivity of Λ and its definition in eqns. 7.7, we can deduce that

$$W^e_B \geq W^e_{HB} \qquad \text{and} \qquad Z^o_{HB} \geq Z^o_B \tag{7.12}$$

On the electric circuit side, the linear relationship between inductance and energy in eqn. 6.27 is now generalised to

$$W^e = \int_0^{IL(I)} i \, d(iL(i)) \tag{7.13a}$$

$$W^c = \int_0^I iL(i) \, di \quad \Rightarrow \quad \frac{dW^c}{dI} = IL(I) \tag{7.13b}$$

and

$$Z^o = I^2 L(I) \tag{7.13c}$$

Complementary solutions thus yield various estimates of inductance, using eqns. 7.13 in conjunction with eqns. 7.8-11. Bounds cannot be defined for L since its relationship to W^c, eqn. 7.13b, is not a direct algebraic one.

Complementary solutions were performed on the nine successively refined meshes described in sec. 6.5. The finest mesh placed the exact co-energy at 238.1 J ± 1.66%; The corresponding global constitutive error is 7.90 J. Convergence curves are shown in fig. 7.2. The curve for the constitutve error Λ is almost identical to that of the linear case in fig. 6.3. So are the curves for the bounds Θ and Ξ, but with a downward shift of some 6 J. The W^e- and Z^o-curves conform to the inequalities in 7.12. The figure shows clearly that W^e_B and W^e_{HB} do not bound the exact value of energy W^e which, therefore, cannot be estimated with the same confidence as the co-energy W^c. Less evident, from the figure, is the fact that Z^o_{HB} and Z^o_B do not bound the exact Z^o; however, it is clear that Z^o_{HB} does not improve monotonically with mesh refinement. It is noted that the curve for the constitutive error Λ represents the difference between each pair of corresponding curves in fig. 7.2.

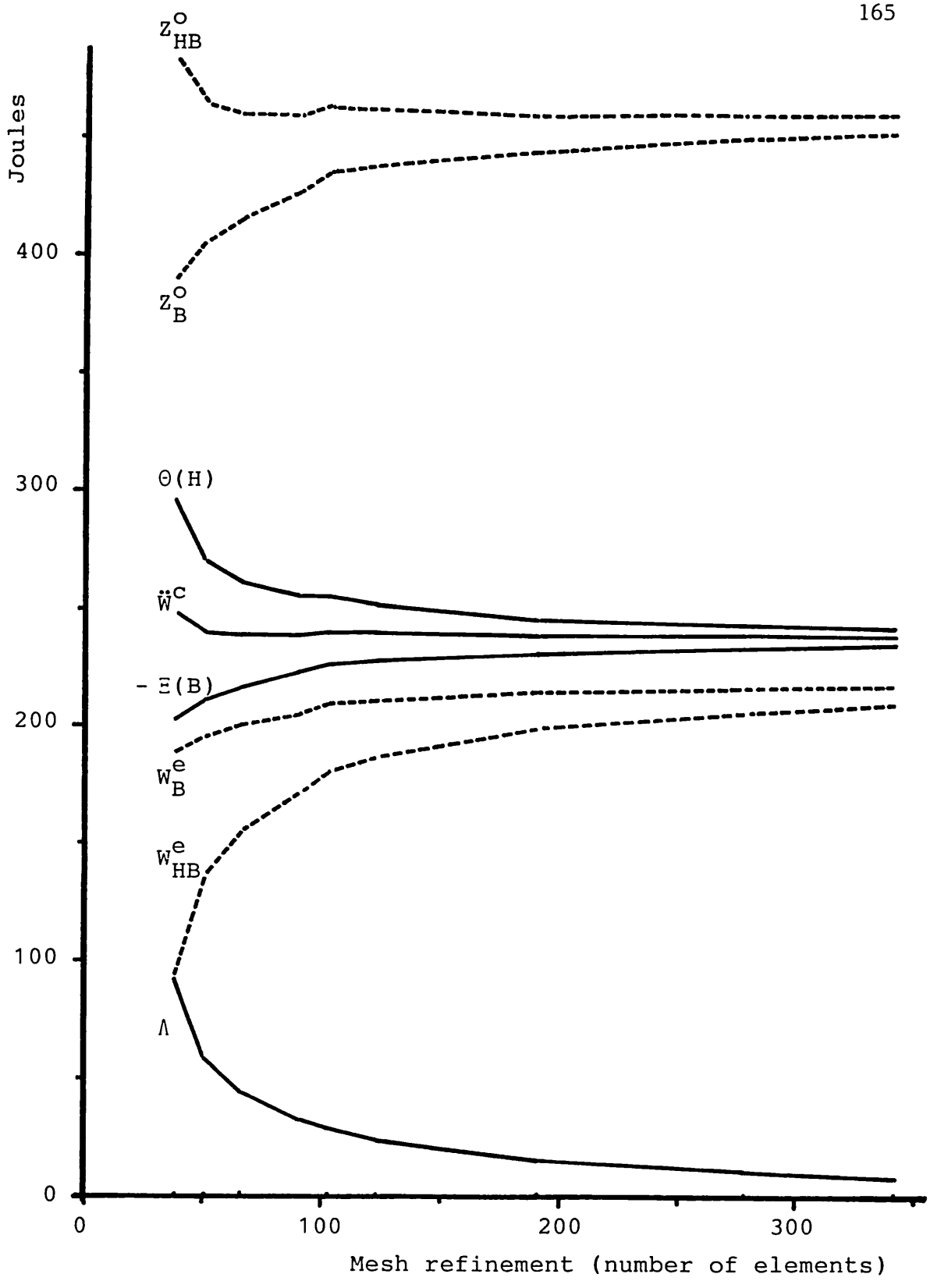

Fig. 7.2 C-magnet with non-linear iron : convergence curves.

Energy distributions in fig. 7.3 are seen to be largely unchanged from the linear case, fig. 6.4 : while there is a definite redistribution of energies, it is too small to be prominent at the discrete scale of the display. For example, at the 102-element mesh shown, X and Ψ in iron were almost equal, at 10.1 J, in the linear case; in the present, non-linear, case they go up to 33.0 J and 15.2 J respectively, still small fractions of the global estimates, 254.9 J and 209.0 J. The air-gap contributions, on the other hand, are 152.3 J and 150.9 J respectively; as in the linear case, these remained substantially unchanged through mesh refinement.

Fig. 7.3 also includes the constitutive error density distribution. It highlights discrepancies not only between complementary energy estimates, but also between linear and non-linear distributions. The iron-part contribution to the largely unchanged global error is more than doubled, from 7.8 % in the linear case to 18.3 % in the non-linear case. The most significant increases are at corners, where iron is driven more deeply into saturation. This is also evident in fig. 7.4 which shows λ-distributions for three other meshes. Note in particular the iron pole-face corners at the 277-element mesh.

The increase of iron-part contribution to substantially unchanged global errors implies, naturally, a corresponding decrease in the contributions of linear air and copper parts. This results from the reduction of permeability in non-linear iron : at air/iron and copper/iron interfaces, the permeability jump is less pronounced than in the linear case. For the same reason, error appears to spill into the air region above the magnet : as more flux leaks into that region, its artificial termination at the top becomes less justifiable. Clearly, the boundary needs to be placed further away from the iron.

Fig. 7.5 shows B-H plots and equipotential contours at three stages of mesh refinement. Comparison with the linear case, fig. 6.6, reveals that B-H plots in air are only

Fig. 7.3 C-magnet with non-linear iron : energy and error density distributions in 102-element mesh. Clockwise from top left : $\chi(\underline{H})$, $\psi(\underline{B})$, $\frac{1}{2}\zeta(\underline{H},\underline{B})$, and $\lambda(\underline{H},\underline{B})$. Upper scale corresponds to energies, lower scale to error.

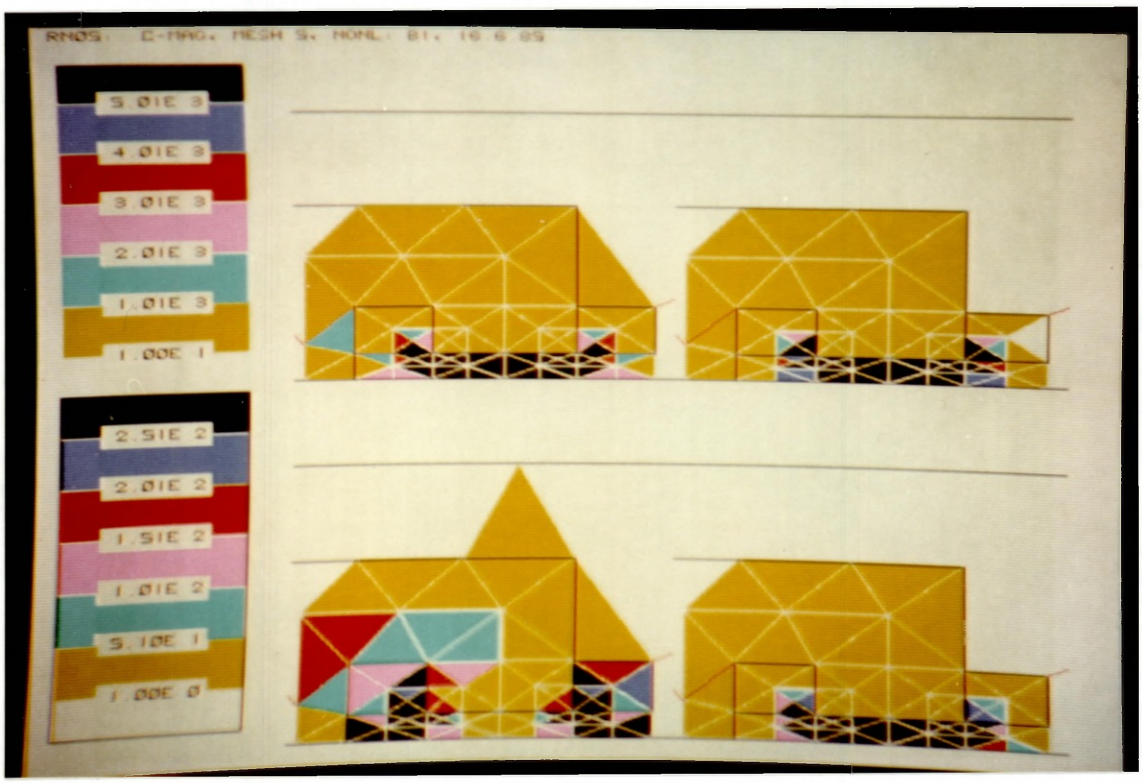

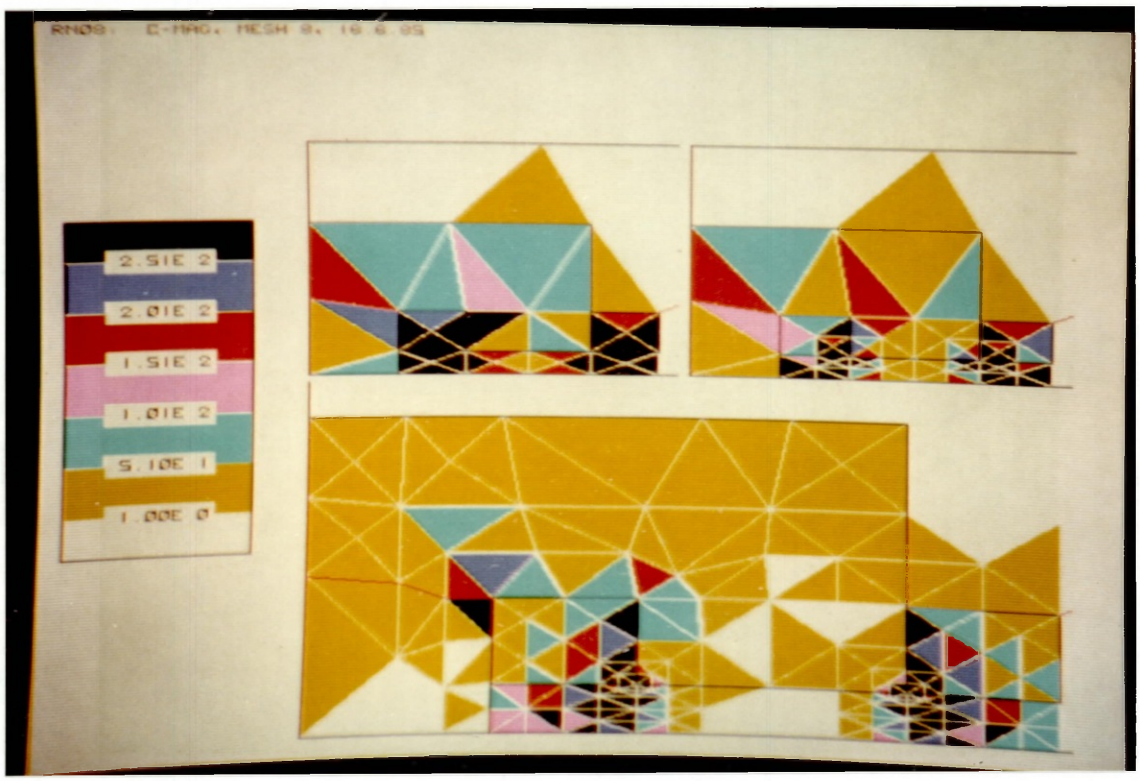

Fig. 7.4 C-magnet with non-linear iron : constitutive error density distributions at three stages of mesh refinement. Clockwise from top left : 50-, 90, and 277-element meshes.

slightly modified, the tendency being one of a general reduction in field magnitudes. B-H plots in iron, on the other hand, undergo a drastic, if expected, change, necessitating a more than four-fold expansion of the horizontal H-scale. While there is a general reduction in flux density magnitudes, B, there is a far more prominent increase in field intensity, H. Migration to the B-H characteristic with mesh refinement, as well as the climbing effect noted in sec. 6.5.1, are still in evidence. The present, non-linear results highlight, rather more emphatically, the discrepancies between complementary estimates of the fields. Partly because of the downward concavity of the B-H curve, the B-solution tends to under-

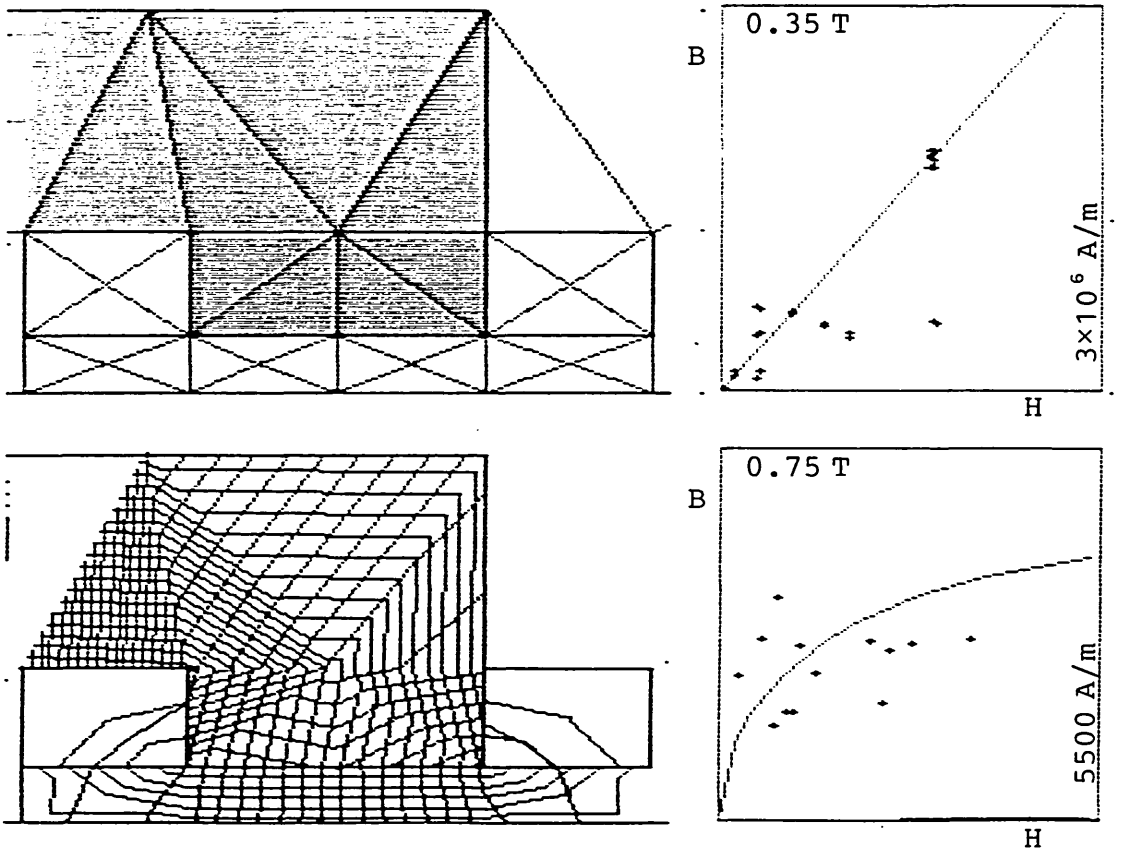

(a) 50-element, 33-node mesh; $\Lambda/\ddot{W}^{C} = 24.5\%$.

Fig. 7.5 C-magnet with non-linear iron : sub-region at three stages of mesh refinement. Clockwise from top left : finite element mesh; B-H plot in air; B-H plot in iron; and equipotential contours. NB Steps between Ω-contours in iron are 80 times smaller than in air.

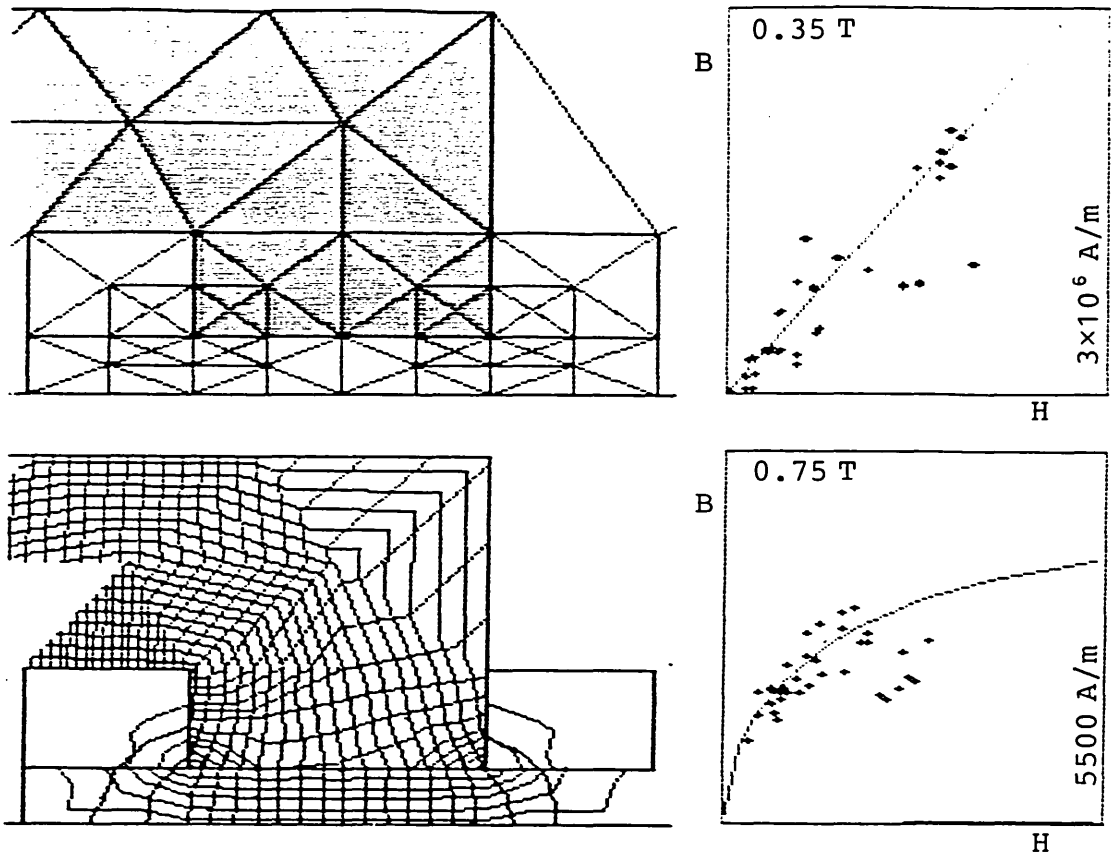

(b) 102-element, 62-node mesh; $\Lambda/\ddot{W}^C = 12.1\%$.

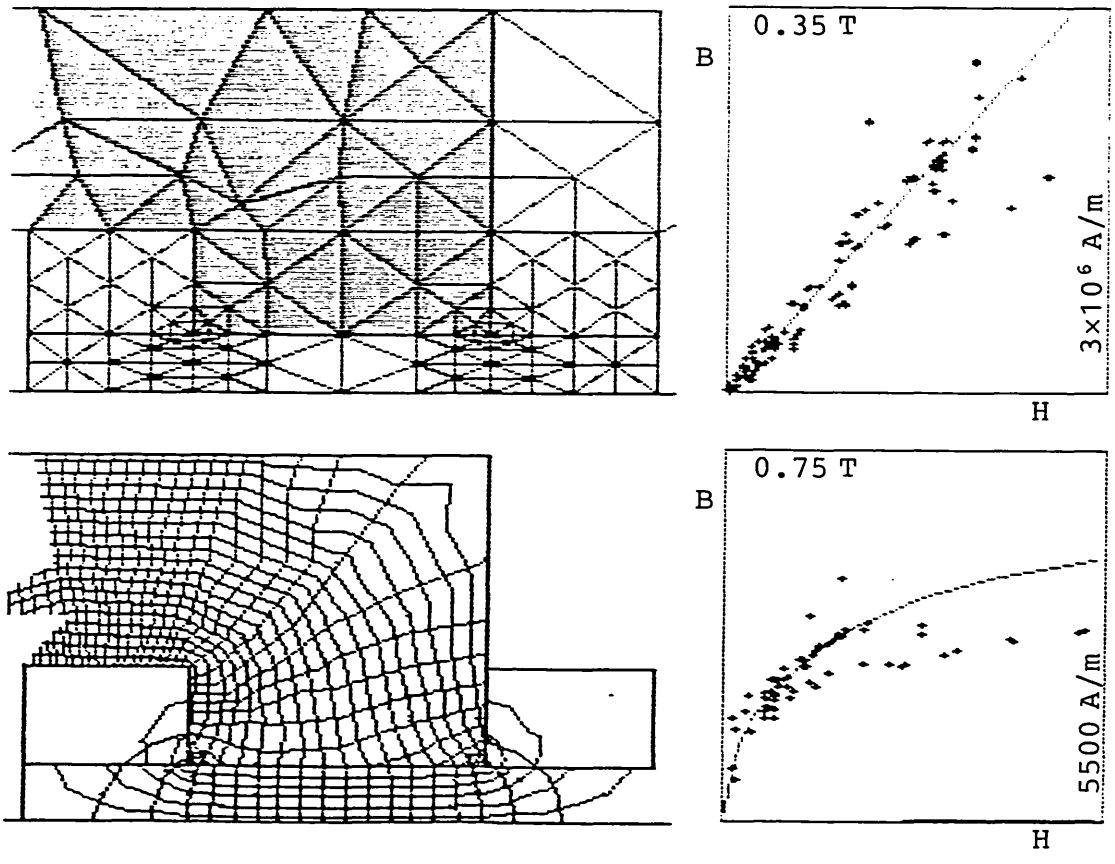

(c) 277-element, 156-node mesh; $\Lambda/\ddot{W}^C = 4.5\%$.

Fig. 7.5 (continued).

estimate field intensities, as suggested by the larger proportion of points below the curve; by the same token, the H-solution tends to over-estimate flux densities. Although B-H plots fail to predict exact values, they do indicate the degree of confidence with which to regard numerical estimates of complementary fields.

Comparison with fig. 6.6 also shows that equipotential contours in air are only slightly modified. In iron, there is a significant increase of Ω-contours, reflecting the increase of mmf required to drive flux through saturated parts. Both Ω and A are more uniformly distributed in iron, particularly near the pole-face; corner saturation effects are noted. The degree of mutual orthogonality of complementary contours does not appear to change significantly from the linear case, suggesting that the increase in iron error noted earlier is attributable, in the main, to discrepancies in field magnitudes rather than space orientations.

Comparison of B-H plots in fig. 7.5 with the B-H characteristic of fig. 7.1 indicates that the excitation used in the solution ($1\ A/mm^2 \Rightarrow 7700$ Ampere-turns) drives the magnet just beyond the knee of the curve. Fig. 7.6 shows the variation of energies with excitation, up to twice nominal; the curves are seen to lose linearity as excitation increases. The curves for $-\Xi(B)$ and W_B^e coincide in the linear, low excitation range, where energy and co-energy converge to a single W, sec. 6.3. Corresponding pairs of energy curves differ by Λ, and conform to inequalities 7.8 and 7.12. Fig. 7.7 shows the resulting inductance estimates, derived using eqns. 7.8, 10, 11, and 13. It is recalled that these estimates are not guaranteed to bound the exact values of inductance in the non-linear case. The figure shows that, at the linear limit, inductance estimates derived from the co-energy are almost symmetric about the exact value estimated in sec. 6.5.1.

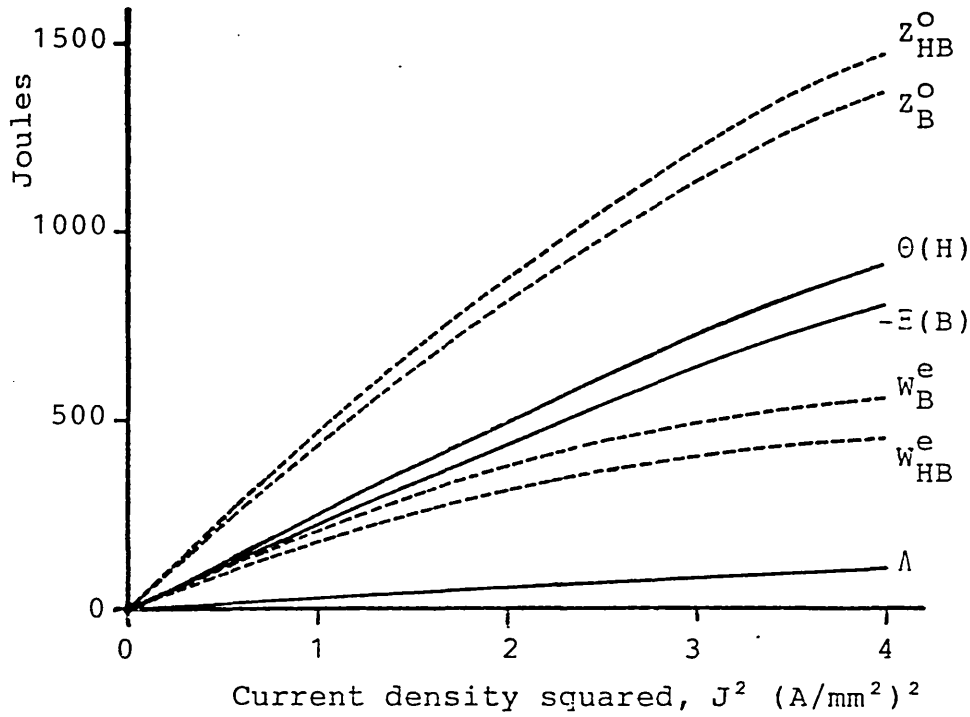

Fig. 7.6 C-magnet with non-linear iron : variation of energies with coil excitation. Solutions performed on 102-element mesh.

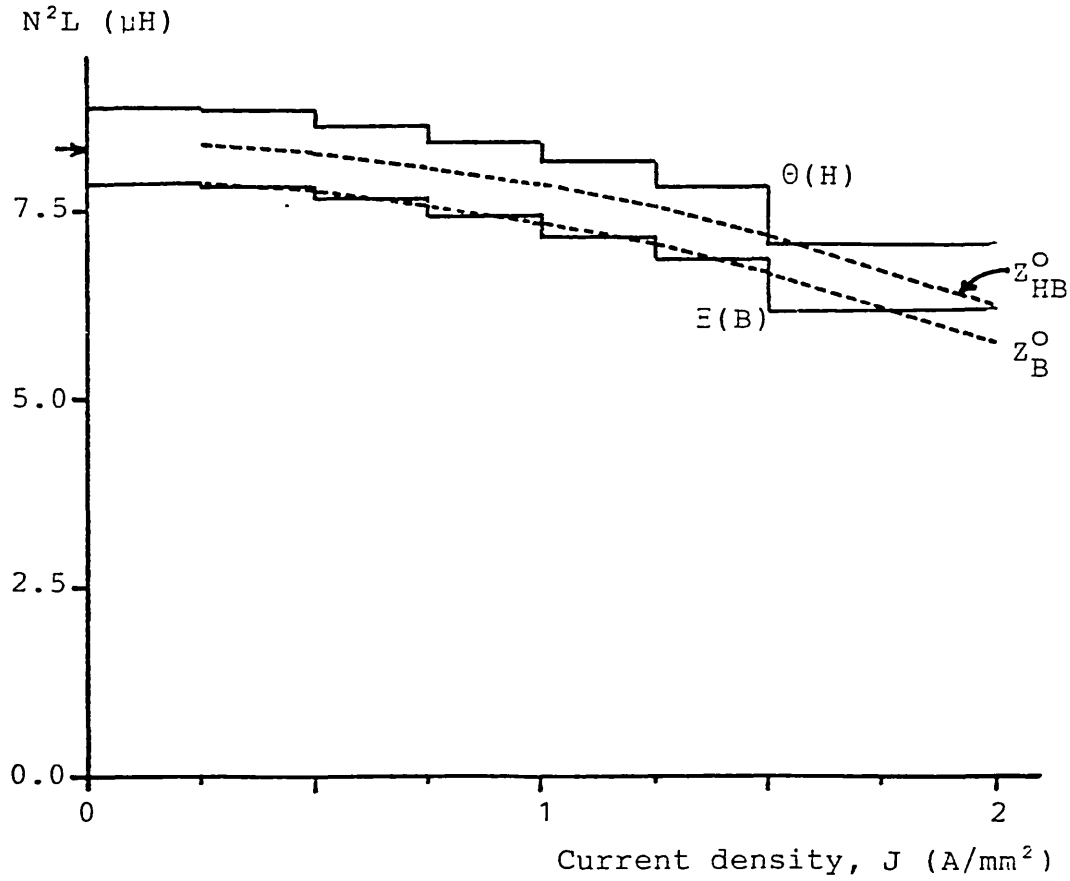

Fig. 7.7 C-magnet with non-linear iron : coil inductance computed from various energy estimates for 102-element mesh. N is the number of coil turns. LHS arrow indicates linear inductance.

7.3.2 D.C. machine

The d.c. machine problem is defined in sec. 6.5.2. Boundary specifications are similar to those of the C-magnet, so that eqns. 7.2-12 apply.

Equipotential contours and B-H plots, shown in fig. 7.8, indicate that the machine is driven well into saturation, particularly in the constricted pole base. Scalar potential contours are stacked so closely there that clarity of the display necessitated a change of scale from that of fig. 6.7; note also the altered scales of the B-H plots. The global constitutive error is 0.800 Joules, down from 1.247 J in the linear case; the co-energy is estimated at 19.05 J ± 2.1%, down by half. The energies are $W^e_B = 6.35$ J and $W^e_{HB} = 5.55$ J, down to around just a sixth.

The reduction in global error is attributable to the smoother change in permeability at material interfaces. Fig. 7.9, which shows error density distributions, supports this conclusion. For example, the air elements inside the gap and in the vicinity of the pole tip, inset to fig. 7.9, account for only 8.2% of the global error; this is to be compared with 35% of the larger linear error, sec. 6.5.2. Much of the error is now concentrated in the constricted pole base mentioned earlier; the high magnetisation points in fig. 7.8d correspond to the elements of that region. The mesh, designed to cater for errors in the linear case, is not quite suitable for the present non-linear one : it is too coarse in the pole base, and unnecessarily fine in the vicinity of the pole tip.

7.3.3 Lamination

The lamination problem is described in sec. 6.5.3, where it is shown that two definitions are possible : specified mmf, or specified flux.

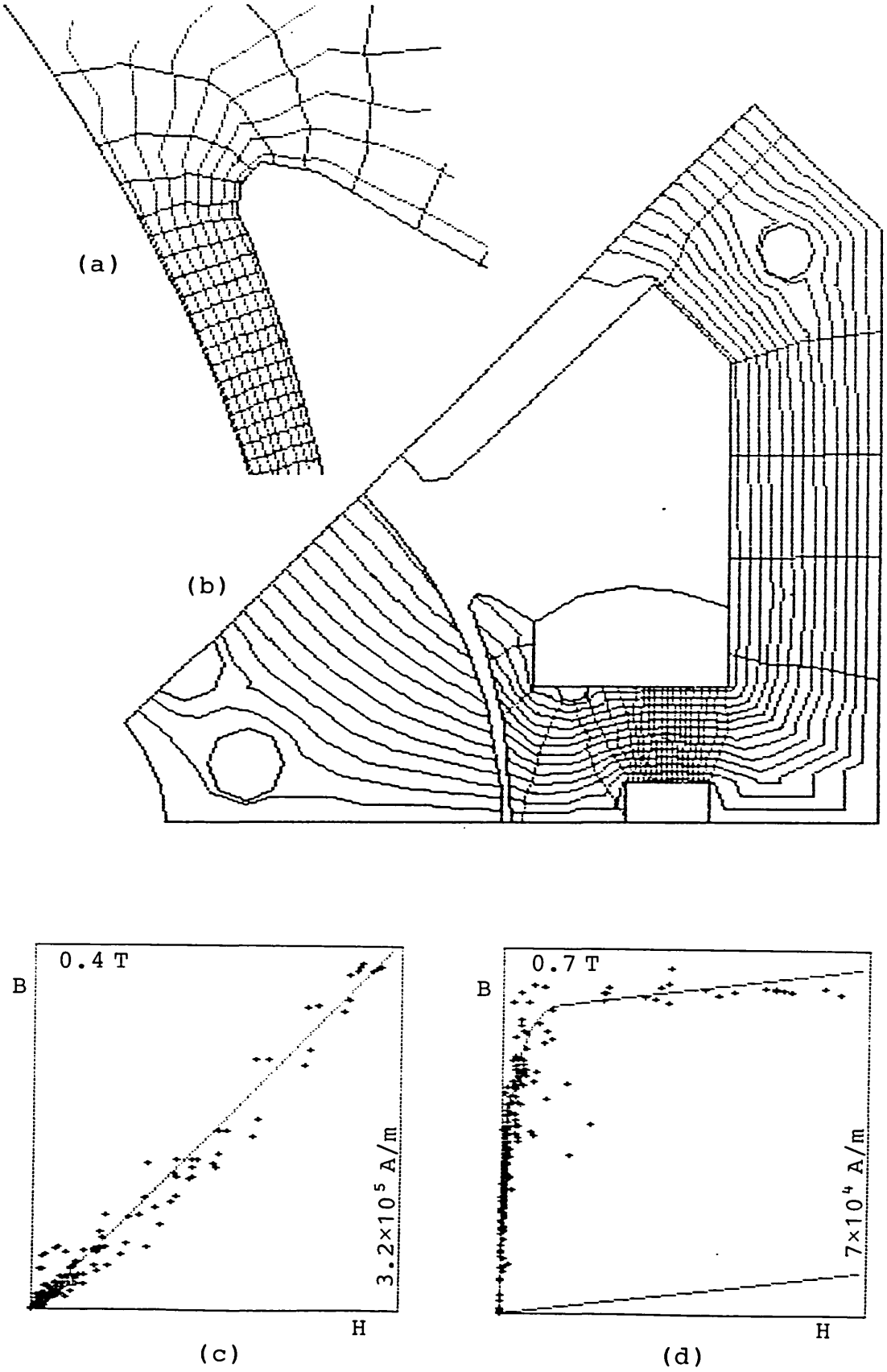

Fig. 7.8 D.C. machine with non-linear iron : (a) equi-potentials in air near pole tip; (b) equi-potentials in iron; Ω steps 6 times smaller than in air; (c) B-H plot in air; (d) B-H plot in iron.

Fig. 7.9 D.C. machine with non-linear iron : constitutive error density distribution. Inset shows enlarged air elements inside gap and near pole tip, with iron elements masked.

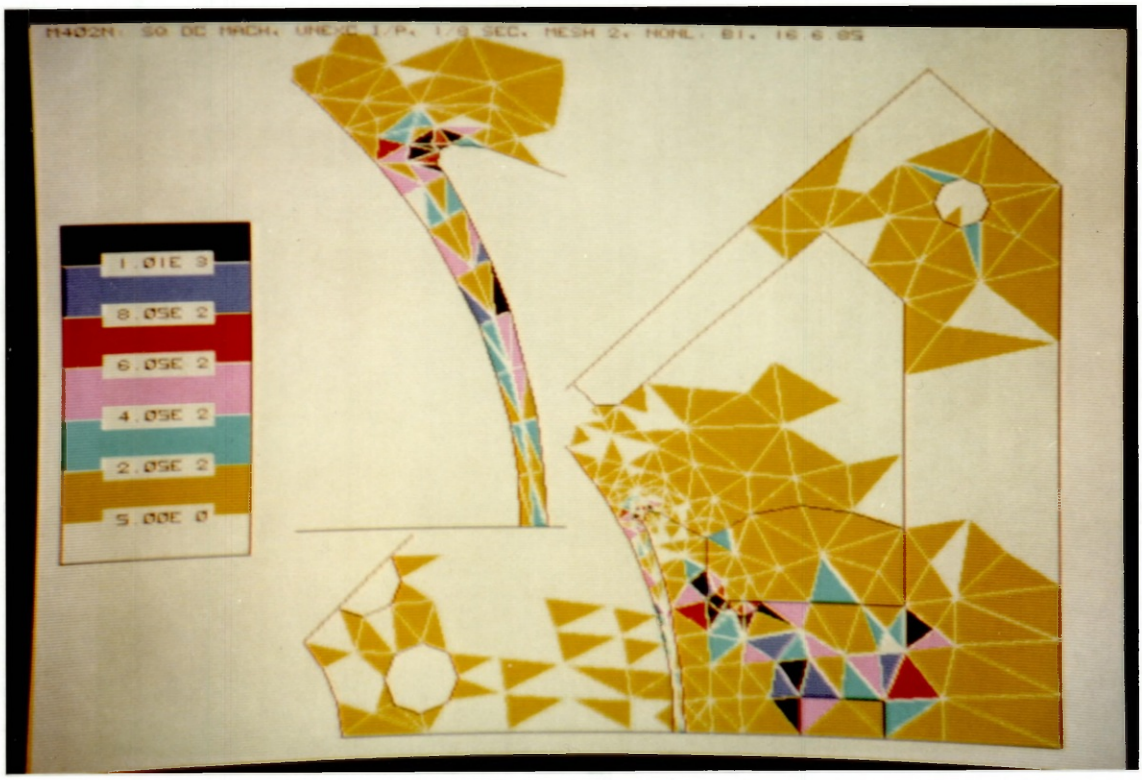

(i) Specified mmf $(M = \bar{M})$:

$$\Lambda = \Theta_M(H) + \Xi_M(B) \tag{7.14a}$$

with

$$\Theta_M(H) = X(\underline{H}) \ , \qquad \Xi_M(B) = \Psi(\underline{B}) - \bar{M}\,\phi \tag{7.14b}$$

Comparing with eqns. 7.4 and ineq. 7.1, we can write

$$\Theta_M(H) \geq W^c = \bar{M}\phi - W^e \geq -\Xi_M(B) \tag{7.15}$$

$$W^e_H = \langle \mu\underline{H}, \underline{H} \rangle_R - X(\underline{H}), \qquad Z^o_H = \langle \mu\underline{H}, \underline{H} \rangle_R \tag{7.16}$$

$$W^e_B = \Psi(\underline{B}), \qquad Z^o_B = \bar{M}\,\phi \tag{7.17}$$

$$W^e_{HB} = \bar{M}\phi - X(\underline{H}), \qquad Z^o_{HB} = X(\underline{H}) + \Psi(\underline{B}) \tag{7.18}$$

Also

$$W^e_B \geq W^e_{HB} \ , \qquad Z^o_{HB} \geq Z^o_B \tag{7.19}$$

Fig. 7.10 shows convergence curves for a series of successively refined meshes; it confirms that bounds are defined for the co-energy W^c, ineq. 7.15, but not for the energy W^e, ineq. 7.19.

(ii) Specified flux $(\phi = \bar{\phi})$:

$$\Lambda = \Theta_\phi(H) + \Xi_\phi(B) \tag{7.20a}$$

with

$$\Theta_\phi(H) = X(\underline{H}) - M\bar{\phi} \ , \qquad \Xi_\phi(B) = \Psi(\underline{B}) \tag{7.20b}$$

Comparing with eqns. 7.4 and ineq. 7.1, we can write

$$\Xi_\phi(B) \geq W^e = M\bar{\phi} - W^c \geq -\Theta_\phi(H) \tag{7.21}$$

$$W^c_H = X(\underline{H}), \qquad Z^o_H = M\,\bar{\phi} \tag{7.22}$$

$$W^c_B = \langle \nu\underline{B}, \underline{B} \rangle_R - \Psi(\underline{B}), \qquad Z^o_B = \langle \nu\underline{B}, \underline{B} \rangle_R \tag{7.23}$$

$$W^c_{HB} = M\bar{\phi} - \Psi(\underline{B}), \qquad Z^o_{HB} = X(\underline{H}) + \Psi(\underline{B}) \tag{7.24}$$

Also

$$W^c_H \geq W^c_{HB}, \qquad Z^o_{HB} \geq Z^o_{HB} \tag{7.25}$$

Fig. 7.11 shows convergence curves for the same, successively refined, meshes of fig. 7.10; it confirms that,

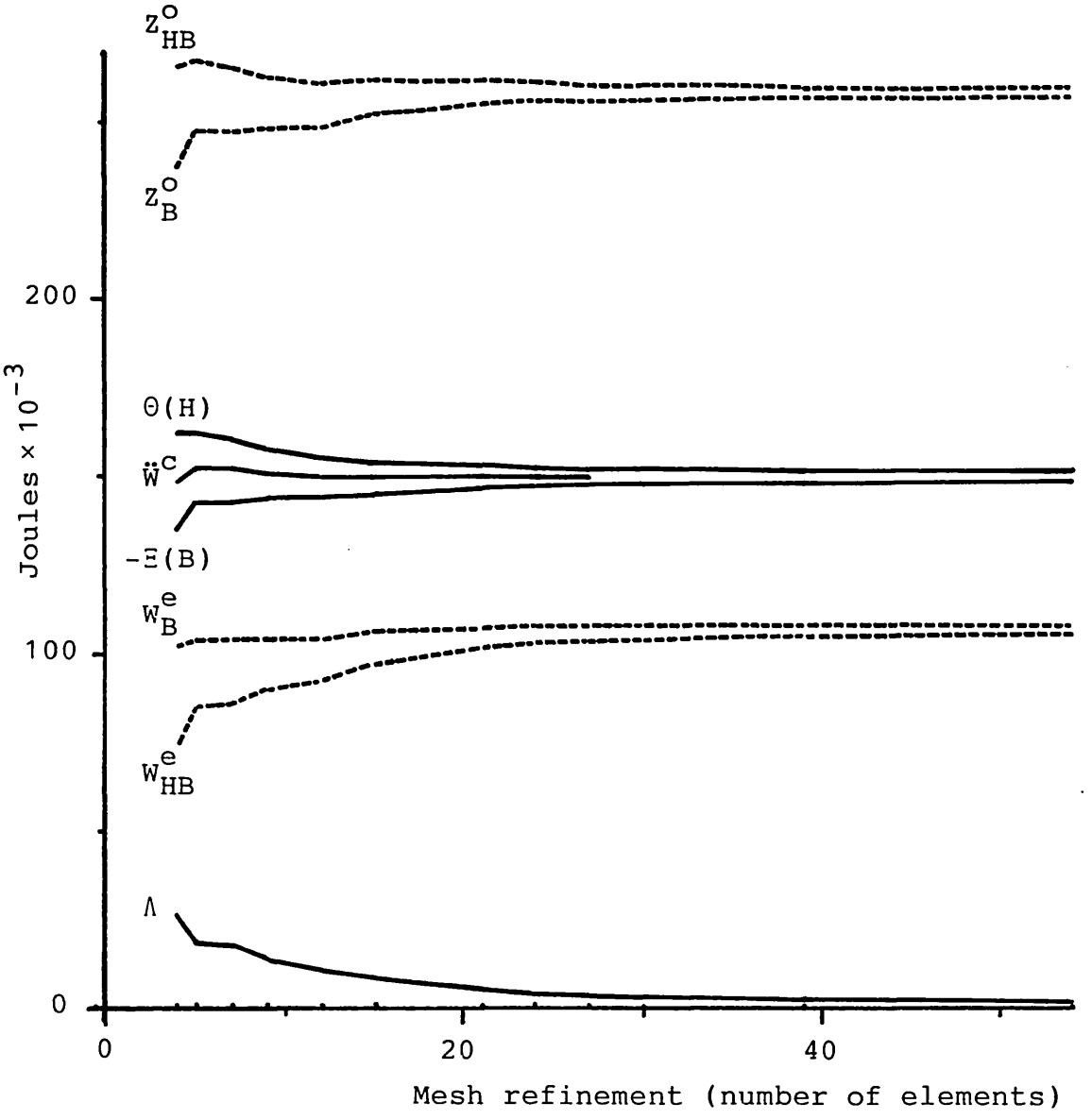

Fig. 7.10 Non-linear lamination convergence curves : specified mmf, $\overline{M} = 26$ Ampere-turns.

in the present specified flux case, bounds are defined for the energy W^e, ineq. 7.21, but not for the co-energy W^c, ineq. 7.25.

The Λ-curves in figures 7.10 and 11 are almost identical, the specified mmf error being marginally smaller (just under 2%) than the specified flux error. Both are greater than in the linear case by 11 - 36 % : error improvement at air/iron interfaces, discussed in sections 7.3.1 and 2, does not arise in the lamination problem, leaving only error increasing effects in the iron.

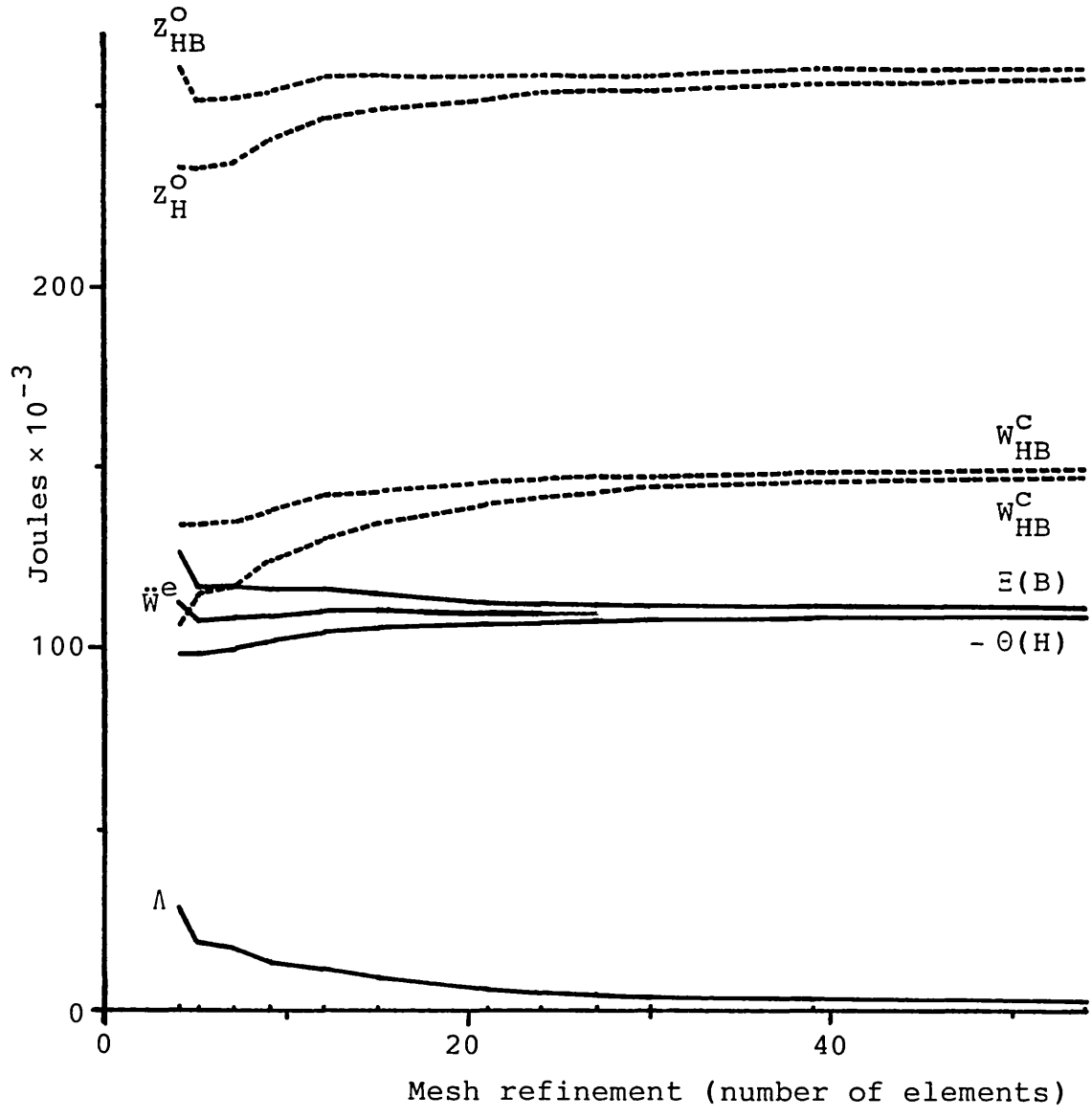

Fig. 7.11 Non-linear lamination convergence curves : specified flux, $\overline{\Phi} = 10$ milli-Webers.

The chosen values of mmf, fig. 7.10, and flux, fig. 7.11, correspond closely, but not exactly, to each other. At the finest mesh attempted (213 elements and 128 nodes), the specified mmf B-solution, $\Xi_M(B)$ in eqn. 7.14b, estimated the flux at 9.95 mWb; the specified flux H-solution, $\Theta_\phi(H)$ in eqn. 7.20b, estimated the mmf at 26.05 A-T. Recalling eqn. 7.17, the curve for Z^o_B in fig. 7.10 may be viewed as a scaled representation of ϕ; similarly, recalling eqn. 7.22, the curve for Z^o_H in fig. 7.11 may be viewed as a scaled representation of M. Both were found to increase monotonically with mesh refinement. This suggests that

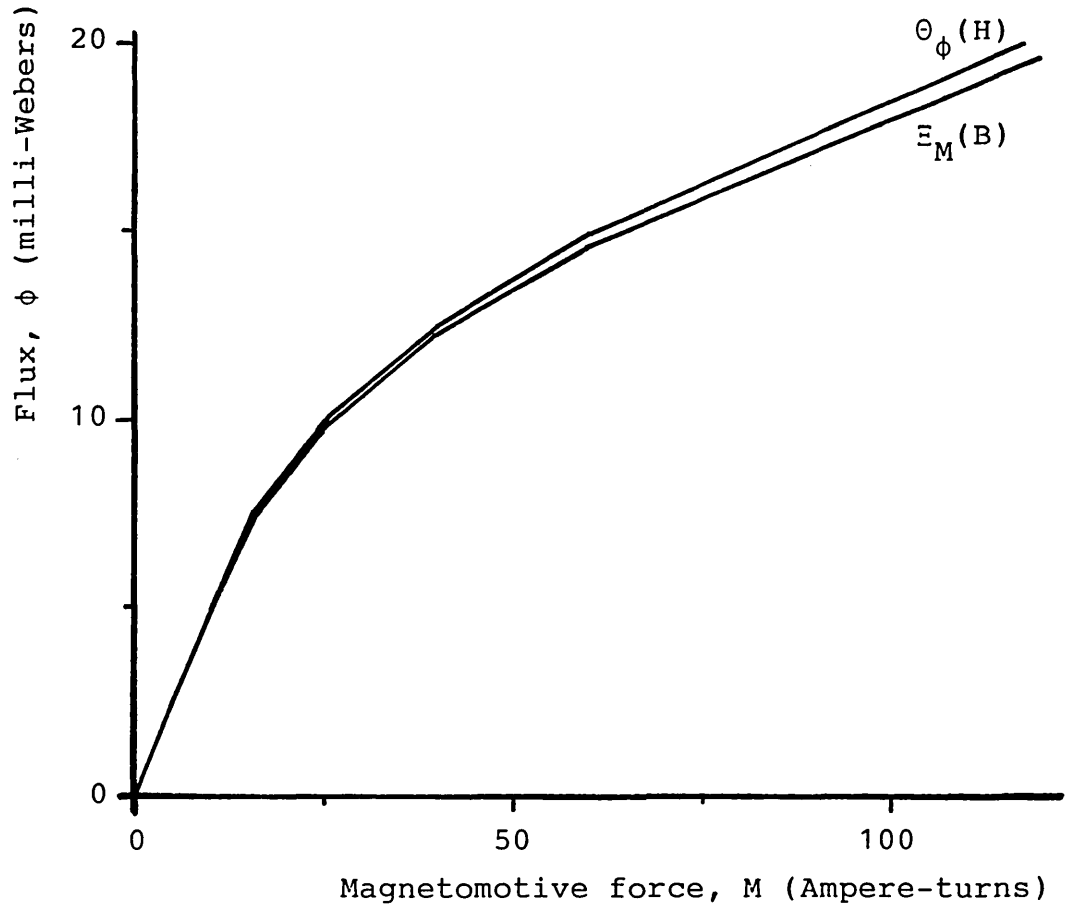

Fig. 7.12 Non-linear lamination magnetisation curves. Captions indicate solutions from which the curves were obtained. Both solutions were performed on 39-element mesh.

the exact magnetisation curve for the lamination may well lie between the two numerically derived curves of fig. 7.12, although bounds are not formally established.

The static reluctance of the trapezoidal lamination is given by

$$R = M / \phi \qquad (7.26)$$

Thus each of the magnetisation curves of fig. 7.12 yields a corresponding reluctance curve; these are shown dotted in fig. 7.13. The figure also shows alternative numerical estimates of the reluctance. These are based on the non-linear generalisation of the linear relationship between energy and reluctance in eqns. 6.41 :

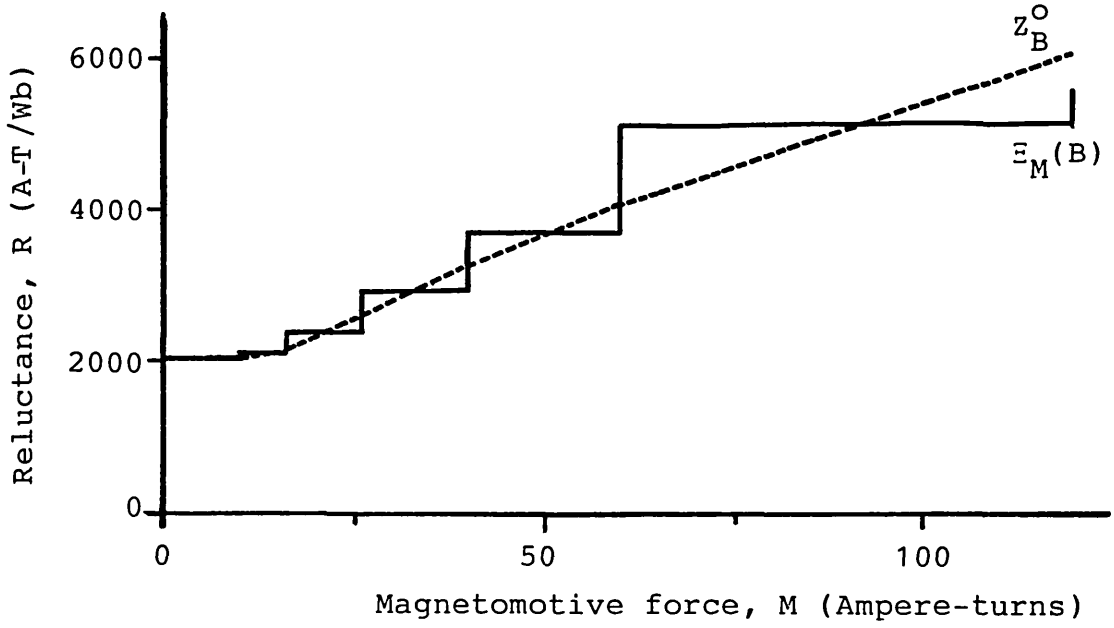

(a) Specified mmf solution.

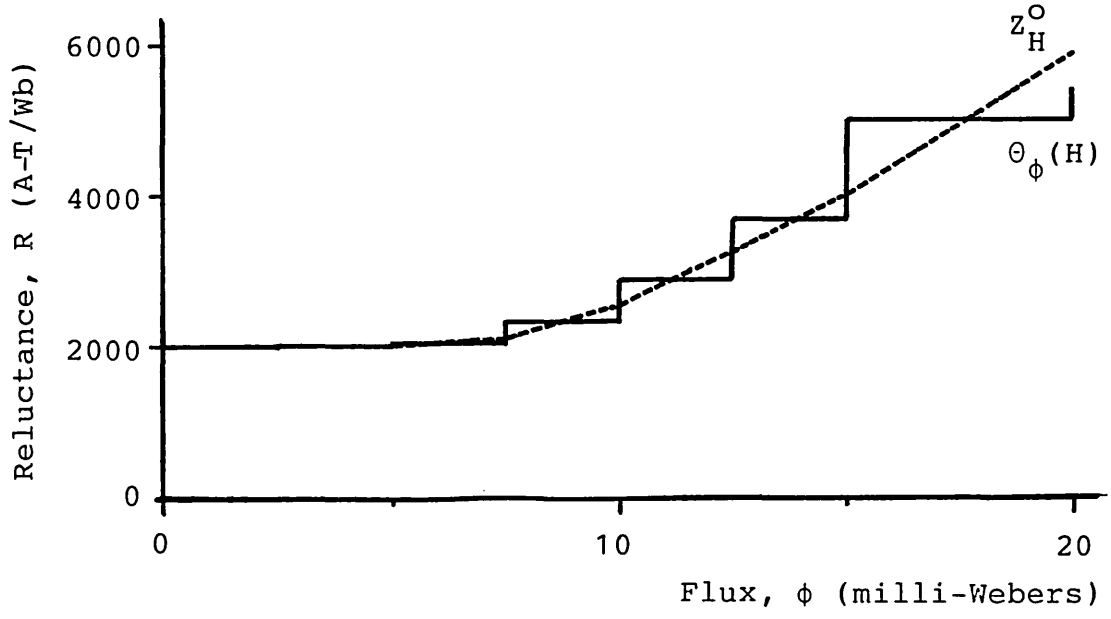

(b) Specified flux solution.

Fig. 7.13 Non-linear lamination : reluctance computed from various energy estimates for 39-element mesh.

$$W^e = \int_0^{\phi} M\, d\phi = \int_0^{\phi} \phi R(\phi)\, d\phi \quad \Rightarrow \quad \frac{dW^e}{d\phi} = \phi R(\phi) \qquad (7.27a)$$

$$W^c = \int_0^{M} \phi\, dM = \int_0^{M} \frac{M}{R(M)}\, dM \quad \Rightarrow \quad \frac{dW^c}{dM} = M/R(M) \qquad (7.27b)$$

$$Z^o = M^2/R(M) = \phi^2 R(\phi) \qquad (7.27c)$$

Bounds cannot be defined for the reluctance R since its relationships to the energy W^e and co-energy W^c are not direct algebraic ones. Reluctance calculations based on other energy estimates were found to be practically indistinguishable from those shown in fig. 7.13 at the scale used. In all cases they coincide with the linear reluctance bounds of sec. 6.5.3 at low excitation.

Figures 7.14-16 show energy distributions, error distributions, equipotential contours, and B-H plots at certain stages of mesh refinement; they are to be compared with figures 6.12-14 of the linear case. As a result of the characteristic concavity of the B-H curve, the B-scale in the B-H plots has been halved, whereas the H-scale has been more than doubled; corresponding changes are made in the sizes of steps between equipotential contours. Rather significantly, the energy and error scales remain unaltered. As might be expected, there is a more marked redistribution of $\chi(\underline{H})$ than there is of $\psi(\underline{B})$; global increases are of the order of 45% for $X(\underline{H})$, and 9% for $\Psi(\underline{B})$. It is noted that fig. 6.12 includes the distribution $\frac{1}{2}\zeta(\underline{H},\underline{B})$ which, in the linear case, is an estimate of energy density, eqn. 6.16a; as this is no longer true in the present non-linear case, fig. 7.14 includes the distribution $\zeta(\underline{H},\underline{B})$, rather than the physically insignificant $\frac{1}{2}\zeta(\underline{H},\underline{B})$.

While the tendency of error to concentrate at the inner corner is still very much in evidence, there is a clear spill of error into the rest of the lamination : in the linear case of fig. 6.13, the permeability is uniform over the entire region, whereas in the non-linear case of fig. 7.15 each element boundary is, in fact, an interface between sub-regions of differing permeabilities. As

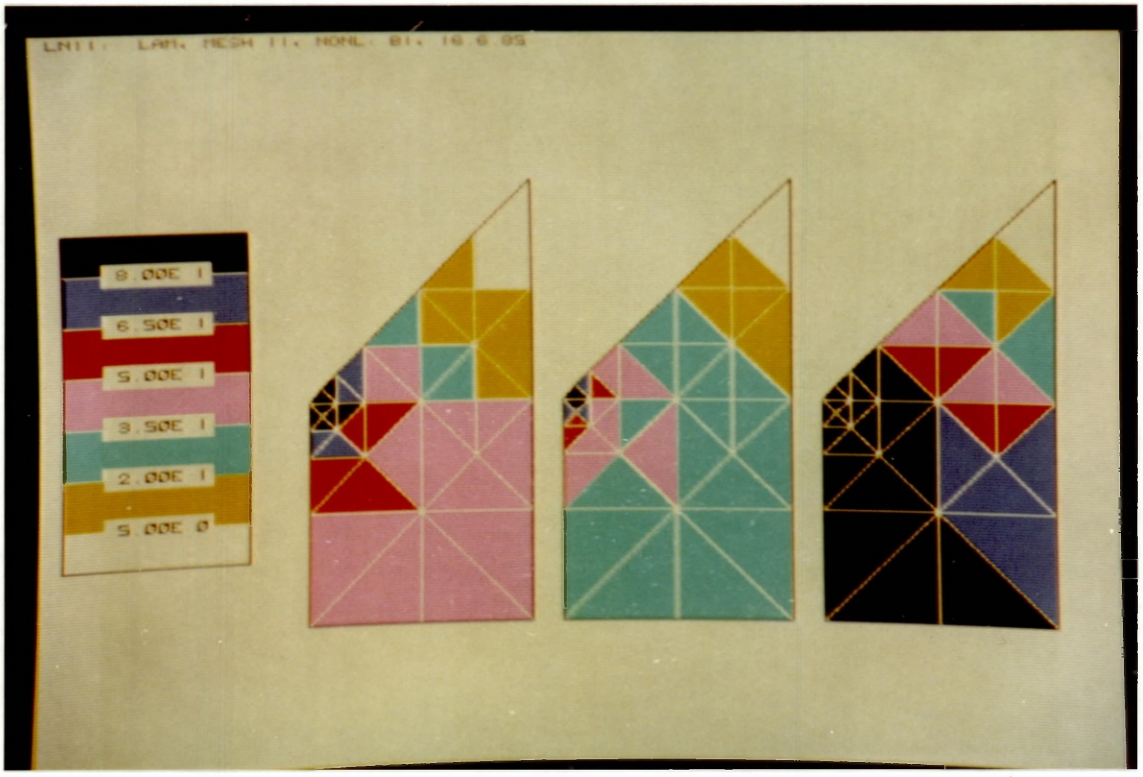

Fig. 7.14 Non-linear lamination energy density distributions in 39-element mesh. From left : $\chi(\underline{H})$, $\psi(\underline{B})$, and $\zeta(\underline{H},\underline{B})$.

Fig. 7.15 Non-linear lamination constitutive error density distributions at three stages of mesh refinement : 12, 24, and 39 elements.

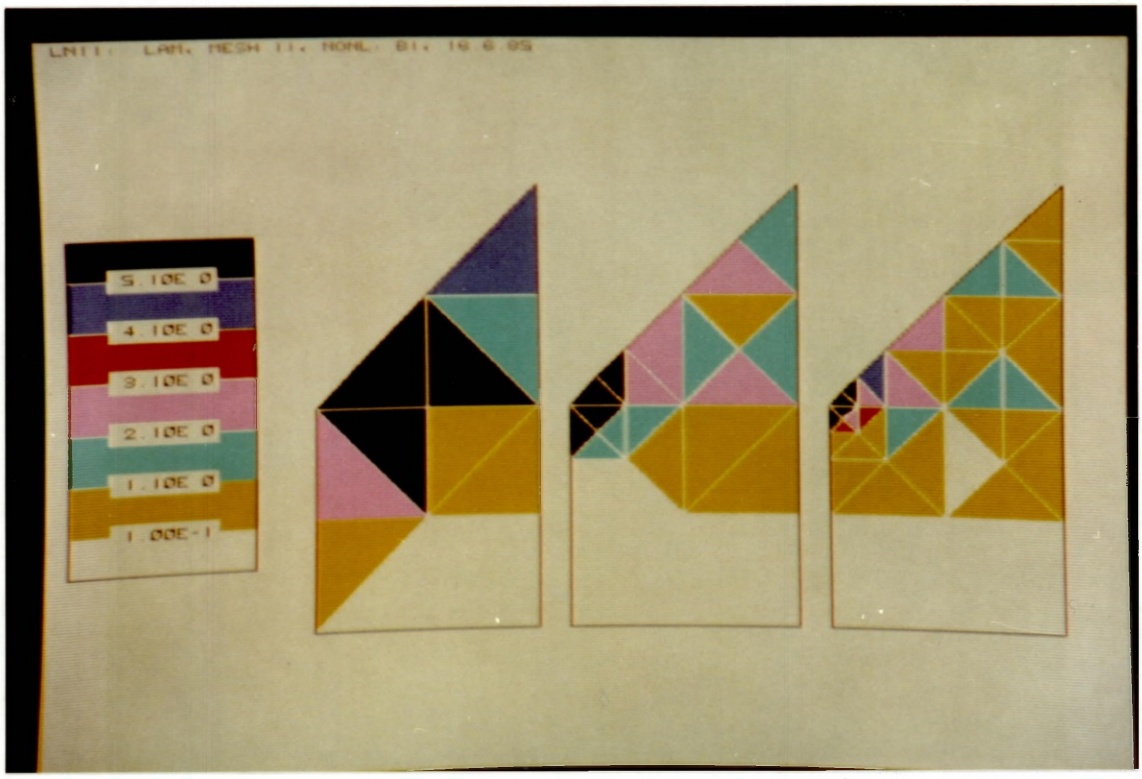

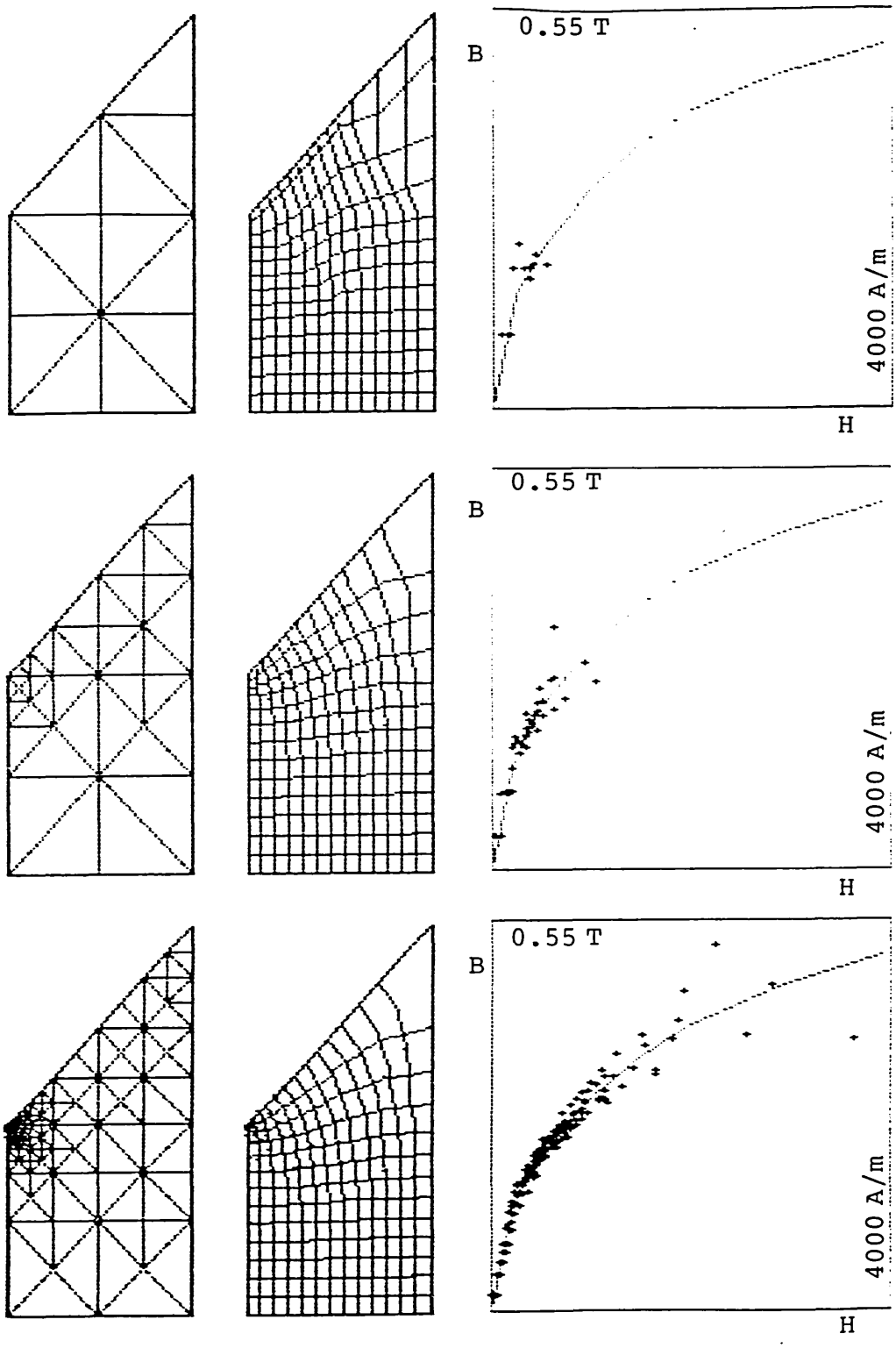

Fig. 7.16 Non-linear lamination : finite element mesh, equipotential contours, and B-H plot at three stages of mesh refinement; specified flux.

(a) 12 elements and 12 nodes; $\Lambda/\ddot{W}^e = 10.7\%$;
(b) 39 elements and 29 nodes; $\Lambda/\ddot{W}^e = 2.6\%$;
(c) 163 elements and 101 nodes; $\Lambda/\ddot{W}^e = 0.8\%$.

a result, there is an overall increase in the global constitutive error Λ, as already noted with reference to figures 7.10 and 11.

Of particular interest is the region in the vicinity of the outer corner. The distributions of fig. 7.14 and the potential contours of fig. 7.16 indicate that energies and fields are very small there. The error density, fig. 7.15, might therefore appear to be disproportionately high, especially in comparison with the base region of the lamination. A probable explanation is that, near that corner, discrepancies in direction are far more significant than discrepancies in magnitude : the fields are required to be parallel to S_{b2} and normal to S_{h2}, yet the two surfaces are angled at 45 degrees rather than 90. Nature handles the specification by setting the fields to zero at the tip of the corner; finite elements, on the other hand, concede a relatively high level of error. At the inner corner, of course, both types of discrepancy are significant. These remarks apply equally well to the linear case, although the error level, fig. 6.13, is generally lower.

7.3.4 Conclusions

The solutions of the previous sections demonstrate the application of complementary variational principles to non-linear problems. The presentation emphasises peculiarities of the non-linear case, general aspects having already been covered in Chapter 6.

The constitutive error density was found to decrease, compared to the linear case, at air/iron interfaces; this is attributed to the decrease in iron permeability, resulting from the characteristic concavity of the B-H curve. Inside iron, error tends to increase because of the previously non-existent jumps in permeability across inter-element boundaries; this effect is particularly marked in, and around, heavily saturated regions.

Non-linear B-H plots highlight the vast discrepancies possible between complementary estimates of the fields, even for what may be regarded as generally adequate meshes. A tangible level of confidence, in the numerical results, may be inferred from the degree of scatter in such plots. Of course, the constitutive error density distribution provides a more comprehensive assessment, accounting for discrepancies in both magnitude and direction. In non-linear iron, it is usually the former that are more significant.

The computed results support the theory of sec. 7.2 regarding the existence, or otherwise, of bounds : depending on problem specification, bounds may be defined either for the energy or for the co-energy, as demonstrated by the dual specifications of the lamination problem in sec. 7.3.3. In the more common magnetostatic boundary specifications of the C-magnet, sec. 7.3.1, bounds are defined for the co-energy. In practice, complementary numerical estimates of bounded quantities are roughly symmetric about the exact value, and approach it monotonically with mesh refinement. The same is not generally true of unbounded quantities, such as the product Z^{o} and circuit parameters, even when the numerical estimates appear to fall consistently above and below the exact values.

Although the presentation was restricted to magnetic non-linearity, the lamination problem can be reinterpreted as a resistance problem, as explained in sec. 6.7.1. The availability of independently solvable complementary formulations for both possible specifications of such a problem is particularly important in the present, non-linear, case, since linear scaling cannot be employed to extract one solution from the other.

7.4 Non-linear iteration

The solution of non-linear finite element matrices is essentially an iterated two-step process :

(i) Given an estimate of the field distribution, projection on the B-H characteristic yields a corresponding permeability distribution.

(ii) Given an estimate of the permeability distribution, linear equations are formed and solved to yield a corresponding field distribution.

Starting with some initial field estimate, the process is repeated until consecutive estimates agree to within a prescribed tolerance. Such a broad description of the procedure covers both simple non-linear iteration, as well as the more efficient Newton iteration[7·3]. It also leads to an interesting interpretation in terms of a modified conception of the constitutive error. The modification is this : whereas everywhere else in the thesis we associate the error with the discrepancies between complementary H- and B-solutions, in this section we shall define an H-solution error λ_H, and a B-solution error λ_B.

Consider a non-linear B-solution. Let ν_L denote the estimated reluctivity at some point in the iron, at some stage of the iterative process described above. Let $\underline{B}$ denote the resulting field estimate, step (ii). Unless the non-linear solution has converged, the situation would be as shown in fig. 7.17a or 7.17b. The non-linear B-solution constitutive error may then be defined as follows :

$$\lambda_B = \lambda_B(\nu_L\underline{B},\underline{B}) = \chi(\nu_L\underline{B}) + \psi(\underline{B}) - \zeta(\nu_L\underline{B},\underline{B}) \qquad (7.28)$$

Upon convergence, the situation will be as depicted in fig. 7.17c, where

$$\lambda_B = 0 \qquad (7.29)$$

Integrating over the iron, and recalling the properties of the constitutive error, eqns. 2.18, we can write

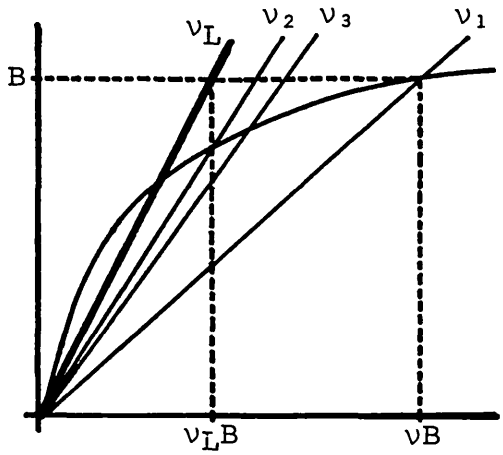

(a) $\nu B > \nu_L B$.

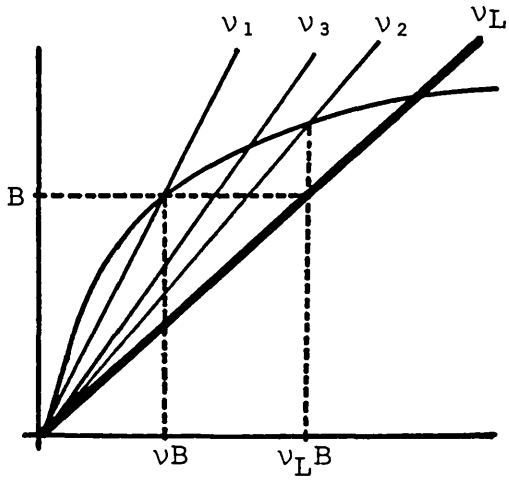

(b) $\nu B < \nu_L B$.

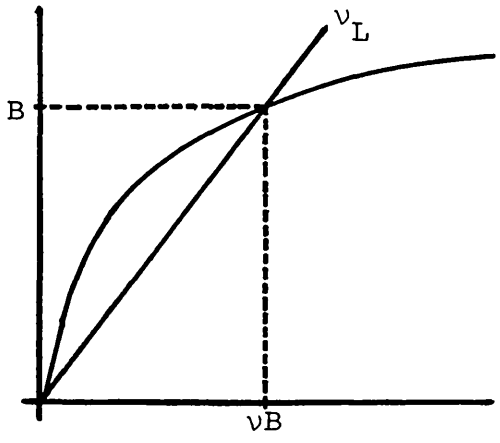

(c) $\nu B = \nu_L B$.

Fig. 7.17 Non-linear B-solution field estimates and reluctivities.

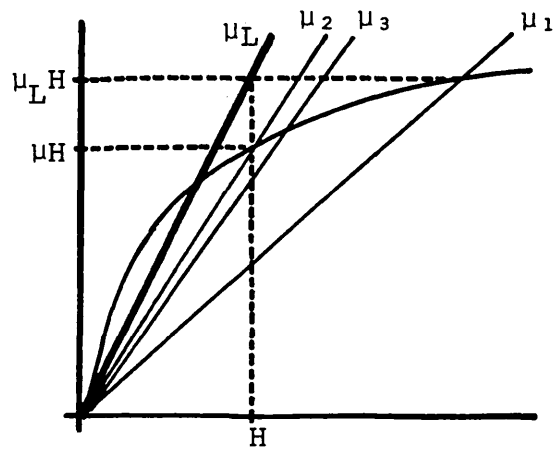

(a) $\mu H < \mu_L H$.

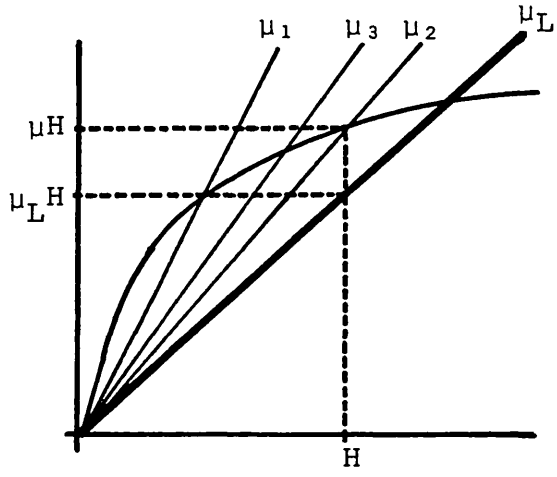

(b) $\mu H > \mu_L H$.

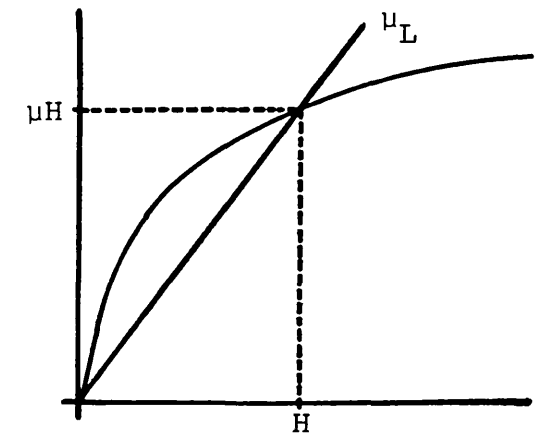

(c) $\mu H = \mu_L H$.

Fig. 7.18 Non-linear H-solution field estimates and permeabilities.

$$0 \leq \Lambda_B = X(\nu_L \underline{B}) + \Psi(\underline{B}) - Z(\nu_L \underline{B}, \underline{B}) \qquad (7.30a)$$

with

$$0 = \Lambda_B \quad <=> \quad \nu_L \underline{B} = \nu \underline{B} \quad \text{everywhere in iron} \qquad (7.30b)$$

That is to say, the global error is zero if and only if total convergence has been achieved. Moreover, as the error is strictly non-negative, non-linear iteration may be viewed as a process of minimising the modified constitutive error. The H-solution constitutive error is entirely analogous. Referring to fig. 7.18, we can write

$$0 \leq \Lambda_H = X(\underline{H}) + \Psi(\mu_L \underline{H}) - Z(\underline{H}, \mu_L \underline{H}) \qquad (7.31a)$$

with

$$0 = \Lambda_H \quad <=> \quad \mu_L \underline{H} = \mu \underline{H} \quad \text{everywhere in iron} \qquad (7.31b)$$

The error may be computed to provide a reliable indication of convergence at any stage of the iterative process. General convergence criteria can be established for the normalised error, for example with respect to $(X + \Psi)$ or Z. Fig. 7.19 presents a graphic illustration of the relationship between normalised error and non-linear convergence.

The concept of separate H- and B-solution constitutive errors may be pursued further. Returning to fig. 7.17, let us address the question : what value of reluctivity to use in forming the matrix for the following iteration ? The figure shows three possibilities, ν_1, ν_2, and ν_3. ν_1 results from direct projection of the current estimate $\underline{B}$ onto the B-H characteristic; from an energy point of view, replacing ν_L by ν_1 effectively leaves the value of $\psi(\underline{B})$ unchanged, but modifies $\chi(\nu_L \underline{B})$ and $\zeta(\nu_L \underline{B}, \underline{B})$ to set the error λ_B to zero. The second alternative, ν_2, results from direct projection of $\nu_L \underline{B}$ onto the B-H characteristic; from an energy point of view, replacing ν_L by ν_2 effectively leaves the value of $\chi(\nu_L \underline{B})$ unchanged, but modifies $\psi(\underline{B})$ and $\zeta(\nu_L \underline{B}, \underline{B})$ to set the error λ_B to zero. Finally, replacing ν_L by ν_3 effectively retains the value of $\zeta(\nu_L \underline{B}, \underline{B})$, and modifies $\chi(\nu_L \underline{B})$ and $\psi(\underline{B})$ to set λ_B to zero. All three schemes change the reluctivity in the same direction,

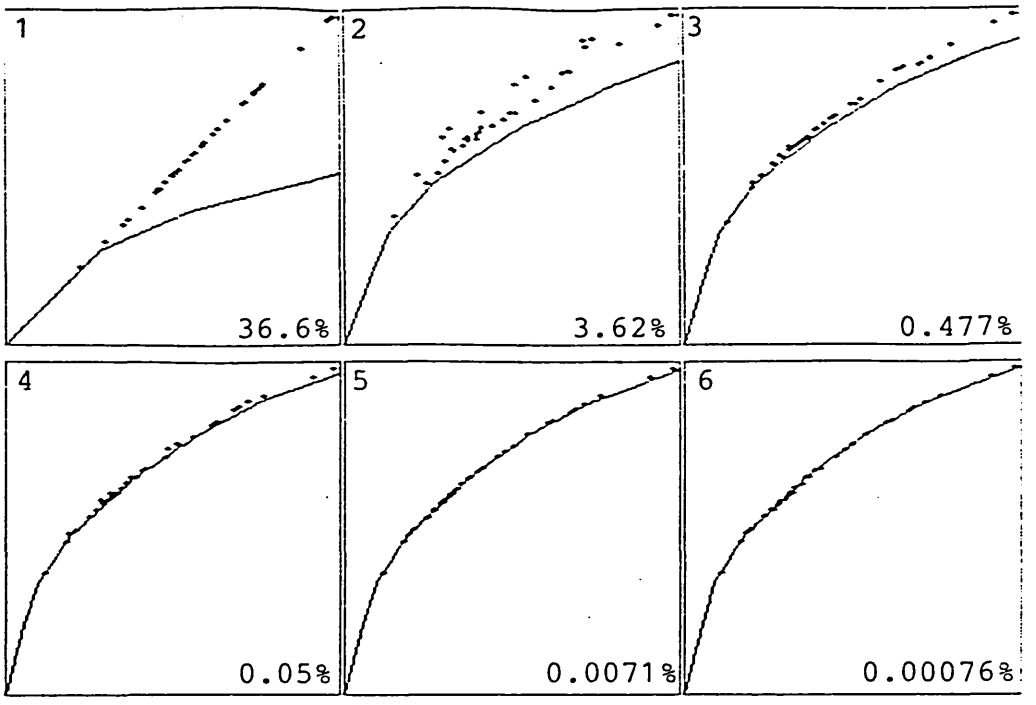

(a) B-solution.

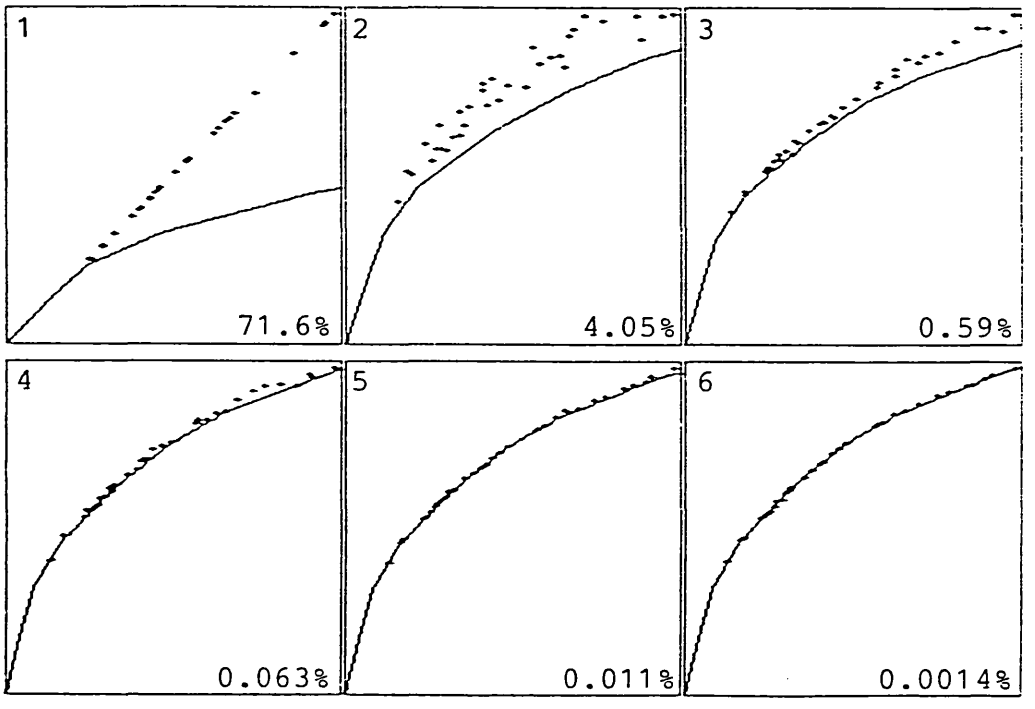

(b) H-solution.

Fig. 7.19 Field plots at consecutive non-linear iterations of C-magnet solution (7700 Ampere-turns; 102 elements), using simple iteration in conjunction with ν_3 and μ_3 (see text). Scale for each frame determined by current field maxima; percentages refer to global constitutive errors.

increasing it in fig. 7.17a, and decreasing it in fig. 7.17b. Because of the characteristic concavity of the B-H curve, ν_1 represents the greatest jump, and ν_2 the smallest; ν_3 falls in between, and may be regarded as an under-correction of the oscillation-prone ν_1, or as an over-correction of the relatively slow ν_2. Analogous choices arise in the case of the H-solution, fig. 7.18.

Non-linear solutions were performed by simple iteration using the three schemes described above, together with variants. ν_3 emerged as the clear favourite : it is more reliable than ν_1, and generally faster than ν_2. The plots of fig. 7.19 are based on ν_3 and μ_3; they are typical in that convergence is initially fast, but slows down considerably as errors become small. Oscillations do set in as the iron is driven more deeply into saturation, but the choice of under-correction factors is far less critical than is common with ν_1. Variants that merit consideration may possibly involve dynamic choice of schemes and/or relaxation factors in individual iron elements, with the choice guided by local error and/or position on the B-H curve. One treatment that was found effective proceeded as follows : start with ν_3 for fast initial convergence, shift to the slow but sure ν_2 when oscillation sets in, and return to ν_3 after a couple of iterations.

7.5 Conclusions

The theory of non-linear complementary variational principles involves no fundamental change from the linear case, with the possible exception of the problem-dependent definition of energy bounds, and the absence of bounds on circuit parameters. Tangible differences are, however, evident in the numerical behaviour of complementary solutions, especially constitutive error distributions; these are illustrated and discussed in sec. 7.3

The constitutive error approach also provides an interesting interpretation of non-linear iteration : the

process may be viewed as one of minimising separate H- and B-system constitutive errors defined in sec. 7.4. The errors provide reliable indication of non-linear convergence, and open up a variety of possibilities for what may prove to be efficient non-linear iteration algorithms.

C H A P T E R E I G H T

Pre-specified Fields in Magnetostatics

8.1 Introduction

The use of potentials to describe the physical fields necessitates the introduction of pre-specified fields to account for source distributions; from sec. 3.4.3, we have

$$\underline{H} = \underline{G} - \text{grad } \Omega \quad ; \quad \underline{B} = \underline{C} + \text{curl } \underline{A} \qquad (8.1a)$$

Ω and $\underline{A}$ are the potentials; $\underline{G}$ and $\underline{C}$ are pre-specified to satisfy

$$\text{curl } \underline{G} = \underline{J} \quad ; \quad \text{div } \underline{C} = \rho \qquad (8.1b)$$

where $\underline{J}$ and ρ are the H- and B-system source distributions, respectively.

In magnetostatics, the absence of magnetic charge ρ allows $\underline{C}$ to be set to zero. The H-system pre-specified field $\underline{G}$ is often defined by the Biot-Savart law[8.1,2]. This chapter examines the limitations of the definition in numerical applications, and proposes a simpler, and more accurate alternative; numerical results are compared.

8.2 The H-system solution formulation

A typical magnetostatic problem, in a given region R, may be specified as follows :

$$\underline{B} = \mu(\underline{H})\underline{H} + \underline{B}_r \quad ; \quad \underline{H} = \nu(\underline{B})\underline{B} + \underline{H}_c \qquad (8.2)$$

$$\underline{J} = \text{curl } \underline{H} \quad ; \quad 0 = \text{div } \underline{B} \qquad (8.3)$$

$$0 = \underline{n} \times \Delta\underline{H} \quad ; \quad 0 = \underline{n} \cdot \Delta\underline{B} \qquad (8.4)$$

The bounding surface S is composed of two simply-connected sub-sections

$$S = S_h \cup S_b \quad , \quad S_h \cap S_b = 0 \tag{8.5a}$$

with

$$0 = \underline{n} \times \underline{H} \text{ on } S_h \quad , \quad 0 = \underline{n} \cdot \underline{B} \text{ on } S_b \tag{8.5b}$$

Consider the H-formulation. The scalar potential Ω is introduced to impose H-system specifications on $\underline{H}$

$$\underline{H} = \underline{G} - \text{grad } \Omega \tag{8.6}$$

where $\underline{G}$ accounts for the current density $\underline{J}$; it is pre-specified to satisfy

$$\text{curl } \underline{G} = \underline{J} \tag{8.7}$$

so that $\underline{H}$ satisfies eqn. 8.3. From eqns. 8.4, 8.6, and 3.55, on a surface of discontinuity S_k

$$\underline{n} \times \text{grad } \Delta\Omega = \underline{n} \times \Delta\underline{G} \tag{8.8a}$$

$$\Delta\Omega(\underline{r}) = \Delta\Omega(\underline{r}_k) + \Delta\Omega\Big|_{\underline{r}_k}^{\underline{r}} + \int_{\underline{r}_k}^{\underline{r}} \Delta\underline{G} \cdot d\underline{\ell} \tag{8.8b}$$

where $\underline{r}_k$ is an arbitrary reference point on S_k. From eqns. 8.5, 8.6, and 3.54, on the boundary section S_h

$$\underline{n} \times \text{grad } \Omega = \underline{n} \times \underline{G} \tag{8.9a}$$

$$\Omega(\underline{r}) = \Omega(\underline{r}_h) + \Delta\Omega\Big|_{\underline{r}_h}^{\underline{r}} + \int_{\underline{r}_h}^{\underline{r}} \underline{G} \cdot d\underline{\ell} \tag{8.9b}$$

where $\underline{r}_h$ is an arbitrary reference point on S_h.

From sec. 6.5, or sec. 3.6.2, the H-system functional is given by

$$\Theta(H) = X(\underline{H}) \tag{8.10}$$

The solution formulation is thus given by

$$0 = \delta\Theta = \delta X = \langle \mu(\underline{H})\underline{H} + \underline{B}_r \ , \ \delta\underline{H} \rangle_R$$

Substituting for $\underline{H}$ from 8.6, and noting that $\underline{G}$ is pre-specified

$$0 = \delta\Theta = \langle \mu\nabla\Omega - \underline{B}_r \, , \, \nabla\delta\Omega \rangle_R - \langle \mu\underline{G} \, , \, \nabla\delta\Omega \rangle_R$$

Applying a vector identity and the divergence theorem to the second term :

$$0 = \delta\Theta = \langle \mu\nabla\Omega - \underline{B}_r \, , \, \delta\nabla\Omega \rangle_R + \langle \nabla\cdot(\mu\underline{G}) \, , \, \delta\Omega \rangle_R + [\underline{n} \cdot (\mu\underline{G}) \, , \, \delta\Omega]_{S_\mu} - [\underline{n} \cdot (\mu\underline{G}) \, , \, \delta\Omega]_{S_b} \qquad (8.11)$$

where S_μ denotes material interfaces; it is noted that $\delta\Omega|_{S_h}$ is zero from eqn. 8.9b.

The H-formulation solves eqn. 8.11, with $\underline{G}$ pre-specified to satisfy eqn. 8.7 in R, and Ω constrained to satisfy eqns. 8.8 and 8.9.

8.3 The Biot-Savart definition in numerical analysis

The Biot-Savart law expresses the magnetic field of current distributions in free space

$$\underline{H}_S(\underline{r}) = \int_R \frac{\underline{J}(\underline{r}') \times (\underline{r} - \underline{r}')}{4\pi \, |\underline{r} - \underline{r}'|^3} \, dR(\underline{r}') \qquad (8.12)$$

Thus

$$\text{curl } \underline{H}_S = \underline{J} \qquad (8.13)$$

Clearly, $\underline{H}_S$ provides the required definition of the pre-specified field $\underline{G}$ in eqn. 8.7. In numerical applications, however, the actual $\underline{G}$ imposed on the H-formulation can only approximate $\underline{H}_S$, so that

$$\underline{G} = \underline{H}_S + \underline{\varepsilon} \qquad (8.14)$$

The discrepancy, $\underline{\varepsilon}$, is due to the smoothness of $\underline{H}_S$, and arises in two ways :

(i) Although $\underline{H}_S$ can be computed exactly at individual points, integrating it presents a formidable task that must be handled numerically, often by means of Gaussian quadrature. Therefore there is an effective error in all integrals involving $\underline{G}$ in the formulation. Such integrals arise in : pre-processing to force H-system

continuity and boundary conditions on Ω, eqns. 8.8 and 8.9; assembly of solution matrices that will force the constitutive relationship, or B-system specifications, weakly on Ω, eqn. 8.11; and post-processing operations involving integration of $\underline{H}$, eqn. 8.6. The treatment for this source of error is to improve the accuracy of numerical integration, for example by increasing the number of integration points in Gaussian quadrature.

(ii) The numerically over-specified space variation of Ω is generally incapable of depicting smooth integrals in $\underline{G}$ in eqns. 8.8 and 8.9. The exact values can be forced on Ω and $\Delta\Omega$ at individual points, usually nodes; elsewhere on S_h and S_k, integrals in $\underline{\varepsilon}$ and $\Delta\underline{\varepsilon}$ arise, implicitly, to balance the equality. The error is due to incompatibility between the trial functions for Ω, and the smooth $\underline{G}$. The treatment is to relax the numerical over-specification, for example by refining the discretisation, or by resorting to higher order trial functions.

As a result, the current density distribution perceived by the H-formulation differs from the true one. Alternatively, the error can be interpreted in terms of physically non-existent current-sheets in eqns. 8.9 and 8.10, and magnetic charges in eqn. 8.11.

Initial experience with this definition of $\underline{G}$ indicated large errors in the computed values of $\underline{H}$ in high permeability iron [8.3]. The errors were attributed to near-cancellation effects : $\underline{H}_s$ and $\nabla\Omega$ tend to be of similar magnitude and direction in iron parts, so that estimating $\underline{H}$ by eqn. 8.6 amplifies essentially proportionate errors in Ω. However, the error analysis presented here suggests that there is a fundamental cause for the inaccuracy, namely inexact formulation. The prominence of the inaccuracy in iron parts can be explained with reference to eqn. 8.11 : $\underline{\varepsilon}$, the implicit error in $\underline{G}$, is amplified through multiplication by the high iron permeability μ.

The source of the error is substantially reduced[8•4] in linear isotropic iron parts whose contribution to the second integral in eqn. 8.11 is excluded from the formulation on the grounds that $\underline{H}_s$ is solenoidal, so that

$$\text{div } (\mu\underline{H}_s) = \mu \text{ div } \underline{H}_s = 0 \qquad (8.15)$$

A greater, and more general, improvement is achieved by setting $\underline{G}$ to zero outside conductors[8•5]. Referring to conducting and current-free sub-regions of R by R_c and R_f respectively, we write

$$\text{in } R_c : \quad \underline{G} = \underline{H}_s \quad \Rightarrow \quad \text{curl } \underline{G} = \underline{J} \neq 0 \qquad (8.16a)$$

and

$$\text{in } R_f : \quad \underline{G} = 0 \quad \Rightarrow \quad \text{curl } \underline{G} = \underline{J} = 0 \qquad (8.16b)$$

The discontinuity in $\underline{G}$ at the interface between R_c and R_f is imposed on Ω through eqn. 8.9b. Depending on the topology, it may be necessary to introduce cuts that allow Ω to be discontinuous in R_f. Eqns. 8.16 define the two-potential formulation, where Ω is called a reduced potential in R_c, and a total potential in R_f[8•5,6]. Eqns. 8.8 and 8.9 are unchanged in form, but are now restricted to the conductor surface S_c. Eqn. 8.11 simplifies to

$$0 = \delta\Theta = \langle \mu\nabla\Omega - \underline{B}_r \, , \, \delta\nabla\Omega \rangle_R - [\underline{n}\cdot(\mu_o\underline{G}) \, , \, \delta\Omega]_{S_c} \qquad (8.17)$$

where the permeability of conductors is taken to be that of free space, μ_o, so that eqn. 8.15 applies. Inexact formulation is now restricted to conductor surfaces, both in preprocessing, eqns. 8.8 and 8.9, and in matrix assembly, eqn. 8.17; the latter effect is relatively harmless due to multiplication by μ_o, the smallest possible permeability. The size, location, and discretisation of the conductor surface determines the degree of inaccuracy retained in two-potential formulation. The postprocessing error is restricted to conductors, R_c, since $\underline{G}$ is set to zero in R_f, eqns. 8.6 and 8.16. In this way, two-potential formulation limits the error inherent in the numerical application of $\underline{H}_s$.

Although the volume integral for $\underline{H}_S$ in eqn. 8.12 can usually be transformed into a somewhat simpler surface integral, the calculation of $\underline{H}_S$ at individual points is a demanding operation in terms of computer time. Therefore, error reduction by refinement of discretisation and/or numerical integration can lead to a substantial increase in run-time.

8.4 An alternative definition

The magnetostatic problem in R includes an implicit current flow problem in R_C, the conducting sub-region. In simple cases, such as two-dimensional analysis, the solution to the problem, $\underline{J}(\underline{r})$, is known exactly. However, the solution can always be performed in terms of $\underline{T}$, the current-describing vector potential of sec. 6.7 :

$$\text{curl } \underline{T} = \underline{J} \tag{8.18}$$

The two-potential formulation of eqns. 8.16 can be generalised to

$$\text{in } R_C : \quad \underline{G} = \underline{T} \quad \Rightarrow \quad \text{curl } \underline{G} = \underline{J} \neq 0 \tag{8.19a}$$

and

$$\text{in } R_f : \quad \underline{G} = 0 \quad \Rightarrow \quad \text{curl } \underline{G} = \underline{J} = 0 \tag{8.19b}$$

The definition of $\underline{G}$ is then a matter of performing the current flow solution prior to the magnetostatic solution. In principle, the solution for $\underline{T}$ can always be performed numerically using the discretisation of R_C intended for the magnetostatic solution. This may be unavoidable with irregular conductor geometry. In many practical applications, however, a general solution may be found.

Solution formulations of the current flow problem were considered in sec. 6.7. As discussed in sec. 3.4.4.2, the physical specifications alone do not force a unique vector potential $\underline{T}$; additional conditions, arbitrary but consistent with the physical specifications, are still to be introduced. $\underline{H}_S$ in eqn. 8.12 corresponds to a particular set of solvabi-

lity conditions. Alternative conditions may yield a $\underline{T}$ distribution that is better suited to numerical applications.

In the two-potential formulation of sec. 8.3, the sources of error were found to reside on the conductor surface S_c. Let us therefore examine conditions on S_k where

$$\text{on } S_k \subset S_c : \quad \underline{n} \cdot \underline{J} = 0 \tag{8.20}$$

Clearly, S_k includes the interface between R_c and R_f. Substituting for $\underline{J}$ from eqn. 8.18, introducing surface coordinates, and applying a vector identity, we find

$$0 = \underline{n} \cdot \text{curl } \underline{T} = \underline{n} \cdot \text{curl}_s \underline{T} = \text{div}_s (\underline{n} \times \underline{T})$$

It is thus possible to define $\underline{T}$ on S_k by

$$\underline{n} \times \underline{T} = - \underline{n} \times \text{grad}_s \eta \tag{8.21}$$

where η is a scalar distribution defined on S_k. Integrating along a path in S_k

$$\eta(\underline{r}) = \eta(\underline{r}_k) + \Delta\eta \Big|_{\underline{r}_k}^{\underline{r}} - \int_{\underline{r}_k}^{\underline{r}} \underline{T} \cdot d\underline{\ell} \tag{8.22}$$

where $\underline{r}_k$ is an arbitrary reference point on S_k. $\Delta\eta$ is a discontinuity given by

$$\Delta\eta = \oint_{\ell} \underline{T} \cdot d\underline{\ell} = \int_{S_\ell} \text{curl } \underline{T} \cdot d\underline{S} = \int_{S_\ell} \underline{J} \cdot d\underline{S} = I \tag{8.23}$$

where ℓ is any path, in S_k, that surrounds the conductor; S_ℓ is any surface, in R_c, that is bounded by ℓ. The discontinuity $\Delta\eta$ is thus defined across a curve, ℓ_Δ in S_k, running like a seam along the length of the conductor. $\Delta\eta$ appears in eqn. 8.22 if the integration path from $\underline{r}_k$ to $\underline{r}$ crosses ℓ_Δ. I is the current through the conductor.

Comparing eqn. 8.22 with eqn. 8.8b, and noting that $\underline{G}$ is zero in R_f, it is evident that we can set

$$\text{on } S_k : \quad \Delta\Omega = \Omega_f - \Omega_c = \eta \tag{8.24}$$

so that $\Delta\Omega|_{S_k}$ in the magnetostatic problem is represented by η in the current flow problem. Enforcing eqn. 8.24

exactly ensures compatibility between the definition of $\underline{T}$ and the trial functions for Ω on S_k. If, moreover, the definition of $\underline{T}$ is simple enough to allow exact integration, the two sources of error associated with $\underline{H}_s$ will have been avoided.

Such a definition is available in the special case of a straight conductor where the current density $\underline{J}$ is constant, being parallel to the conductor surface, eqn. 8.20. The definition is

$$\underline{T}(\underline{r}) = \tfrac{1}{2}\underline{J} \times (\underline{r} - \underline{r}_o) \tag{8.25}$$

where $\underline{r}_o$ is an arbitrary reference point in space. Taking the curl of both sides and applying a vector identity :

$$\begin{aligned}\nabla \times \underline{T} &= \tfrac{1}{2}\left(\nabla \times (\underline{J} \times \underline{r}) - \nabla \times (\underline{J} \times \underline{r}_o)\right) \\ &= \tfrac{1}{2}\left((\underline{r}\cdot\nabla)\underline{J} - \underline{r}(\nabla\cdot\underline{J}) - (\underline{J}\cdot\nabla)\underline{r} + \underline{J}(\nabla\cdot\underline{r})\right)\end{aligned}$$

The first two terms vanish because $\underline{J}$ is constant in space. The differential vector operations in the third and fourth terms yield

$$\nabla \times \underline{T} = \tfrac{1}{2}\left(-\underline{J} + 3\underline{J}\right) = \underline{J} \tag{8.26}$$

as required in eqn. 8.18. Taking the divergence of both sides in eqn. 8.25 :

$$\begin{aligned}\nabla \cdot \underline{T} &= \tfrac{1}{2}\left(\nabla \cdot (\underline{J} \times \underline{r}) - \nabla \cdot (J \times \underline{r}_o)\right) \\ &= \tfrac{1}{2}\left(\underline{r} \cdot \nabla \times \underline{J} - \underline{J} \cdot \nabla \times \underline{r}\right)\end{aligned}$$

The first term vanishes because $\underline{J}$ is constant, the second because $\underline{r}$ is irrotational. Thus

$$\nabla \cdot \underline{T} = 0 \tag{8.27}$$

which is convenient but not essential. Crossing both sides of eqn. 8.25 with the unit outward normal $\underline{n}$ on S_k, and applying a vector identity :

$$\begin{aligned}\underline{n} \times \underline{T} &= \tfrac{1}{2}\ \underline{n} \times \left(\underline{J} \times (\underline{r} - \underline{r}_o)\right) \\ &= \tfrac{1}{2}\left(\underline{n} \cdot (\underline{r} - \underline{r}_o)\right)\underline{J} - \tfrac{1}{2}(\underline{n} \cdot \underline{J})(\underline{r} - \underline{r}_o)\end{aligned}$$

The second term vanishes by eqn. 8.20. Substituting for $\underline{n} \times \underline{T}$ from eqn. 8.21, we get

$$\underline{n} \times \text{grad}_s \eta = -\tfrac{1}{2} \underline{J} \, (\underline{n} \cdot (\underline{r} - \underline{r}_o)) \qquad (8.28)$$

In numerical applications, S_k is usually discretised into planar sections. In each section, $\underline{n} \cdot \underline{r}$, and hence $\text{grad}_s \eta$, are constant. Constancy of the gradient implies linear variation of η on the section. Thus eqn. 8.24 can be enforced exactly provided $\Delta\Omega$ is at least linear over the individual sections of S_k.

In three-dimensional analysis, conductors are unlikely to be straight throughout the region of the problem. Often, however, they are discretised into straight sections. Eqn. 8.25 is applicable to the individual sections. At the junction between two consecutive sections, fig. 8.1, we have

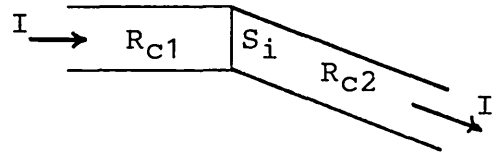

Fig. 8.1 Straight conductor sections.

$$\underline{n} \times \Delta\underline{T} = \tfrac{1}{2} \, \underline{n} \times (\underline{J}_2 \times (\underline{r} - \underline{r}_{o2}) - \underline{J}_1 \times (\underline{r} - \underline{r}_{o1})) \qquad (8.29)$$

where the subscripts 1 and 2 refer to the two sections R_{c1} and R_{c2}, and $\underline{n} = \underline{n}_1 = -\underline{n}_2$ at the interface S_i. Rearranging, and applying a vector identity :

$$\begin{aligned} \underline{n} \times \Delta\underline{T} &= \tfrac{1}{2} \, (\underline{n} \times (\Delta\underline{J} \times \underline{r}) - \underline{n} \times \Delta(\underline{J} \times \underline{r}_o)) \\ &= \tfrac{1}{2} \, (\, (\underline{n} \cdot \underline{r}) \Delta\underline{J} - (\underline{n} \cdot \Delta\underline{J}) \underline{r} - \underline{n} \times \Delta(\underline{J} \times \underline{r}_o) \,) \end{aligned}$$

The continuity of $\underline{n} \cdot \underline{J}$ at S_i causes the second term to vanish, leaving

$$\underline{n} \times \Delta\underline{T} = \tfrac{1}{2} \, (\, (\underline{n} \cdot \underline{r}) \, \Delta\underline{J} - \underline{n} \times \Delta(\underline{J} \times \underline{r}_o) \,) \qquad (8.30)$$

On the plane S_i, $\underline{n} \cdot \underline{r}$, and hence $\underline{n} \times \Delta\underline{T}$, are constant. In fact, $\underline{n} \times \underline{T}$ can be made continuous at S_i by setting $\underline{n} \times \Delta\underline{T}$ to zero in eqn. 8.30, and solving for $\underline{r}_{o2}$, given $\underline{J}_1$, $\underline{J}_2$, and $\underline{r}_{o1}$. Continuity of $\underline{n} \times \underline{T}$ allows Ω to be continuous at S_i, eqn. 8.8b. However, $\underline{n} \cdot \underline{T}$ is discontinuous, and introduces the product $[\underline{n} \cdot \mu_o \Delta\underline{T} \, , \, \delta\Omega]_{S_i}$ into eqn. 8.17.

We conclude that $\underline{T}$ in eqn. 8.25 satisfies the various requirements set for it. It is compatible with linear, and hence higher order, trial functions for Ω. It allows exact integration with practically negligible demands on computer time : the integrals of $\underline{G}$ in eqns. 8.8b, 8.9b, and 8.17 can be expanded analytically, and involve simple multiplication and addition operations at the individual nodes. Moreover, it can be shown that the definition of $\underline{T}$ in eqn. 8.25 also applies to axi-symmetric current density distributions.

8.5 Numerical performance

This section compares the numerical performance of the definitions of $\underline{G}$ in sections 8.3 and 8.4, i.e. $\underline{H}_s$ and $\underline{T}$.

In the two-dimensional magnetostatic examples of Chapters 6 and 7, all conductors have polygonal cross-sections, as in fig. 8.2, either by physical specification, or through finite element discretisation. In either case, the definition of $\underline{G}$ in terms of $\underline{T}$, eqns. 8.19 and 8.25, is applicable; the results quoted in Chapters 6 and 7 are based on $\underline{T}$.

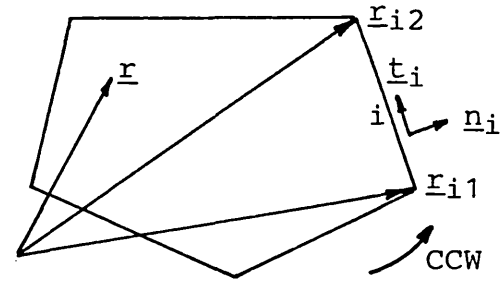

Fig. 8.2 Polygonal conductor contour. $\underline{t}_i$ and $\underline{n}_i$ are unit vectors, tangential and normal to segment i.

For such conductors, $\underline{H}_s$ in eqn. 8.12 simplifies to [8.7]

$$\underline{H}_s(\underline{r}) = \frac{J}{2\pi} \sum_i \{ \alpha_i(\underline{r} - \underline{r}_{i1}) - \alpha_i(\underline{r} - \underline{r}_{i2}) \} \underline{t}_i$$

with (8.31)

$$\alpha_i(\underline{r}') = \underline{t}_i \cdot \underline{r}' \log r' + |\underline{n}_i \cdot \underline{r}'| \tan^{-1} \frac{\underline{t}_i \cdot \underline{r}'}{|\underline{n}_i \cdot \underline{r}'|}$$

where the summation covers all segments of the contour polygon. The computational advantage of eqn. 8.25 over eqn. 8.31 is obvious; it is compounded by the need to compute $\underline{H}_s$ at all quadrature points, not only nodes, to perform the integrations of eqns. 8.8b, 8.9b, and 8.17 numerically.

The incompatibility of $\underline{H}_s$ with numerically over-specified trial functions, item (ii) of sec. 8.3, is illustrated in fig. 8.3 for some regular conductor sections. The curve of $\int \underline{H}_s \cdot d\underline{\ell}$ along one edge of a square, fig. 8.3a, is seen to differ, albeit slightly, from a straight line. The discrepancies are highlighted in fig. 8.3b, which also includes the triangle and hexagon. The curves approach zero as conductor sections approach circularity. The linear finite element shape functions used in this work to discretise Ω cannot absorb these curves exactly as required in eqns. 8.8 and 8.9. The approximation can be improved by refining the discretisation of conductor edges, or resorting to higher order shape functions. The corresponding integrals in $\underline{T}$, on the other hand, are exact straight lines; their slopes and intercepts are determined by the positions of the individual edges relative to the reference point $\underline{r}_o$, eqn. 8.25. Fig. 8.4 shows $\underline{H}_s$ and $\underline{T}$ line integrals for the half-slot of sec. 6.5.4. With $\underline{r}_o$ at corner a, the tangential component of $\underline{T}$ is zero along edges ab and fa; several solutions, of this and other examples, confirmed that the location of $\underline{r}_o$ has no perceptible effect on results. Note the enhanced curvature of the $\underline{H}_s$ integral in the vicinity of the re-entrant corner f in fig. 8.4.

The contour integral

$$\oint \underline{G} \cdot d\underline{\ell} = I \qquad (8.32)$$

provides a gross indication of one type of numerical integration error associated with $\underline{H}_s$, item (i) in sec. 8.3. I is the current enclosed by the contour. It is given at 7700 A for the C-magnet of sec. 6.5.1. Columns 4 and 5 of table 8.1 illustrate the error for two meshes and different values of M, where

$$M = \text{number of Gaussian points on element sides lying along conductor contours} \qquad (8.33)$$

The error can be reduced by increasing M, or refining edge discretisation. Table 8.1 illustrates another aspect of the error : because the two conductor sections are discretised differently in the finer mesh, the contour integrals

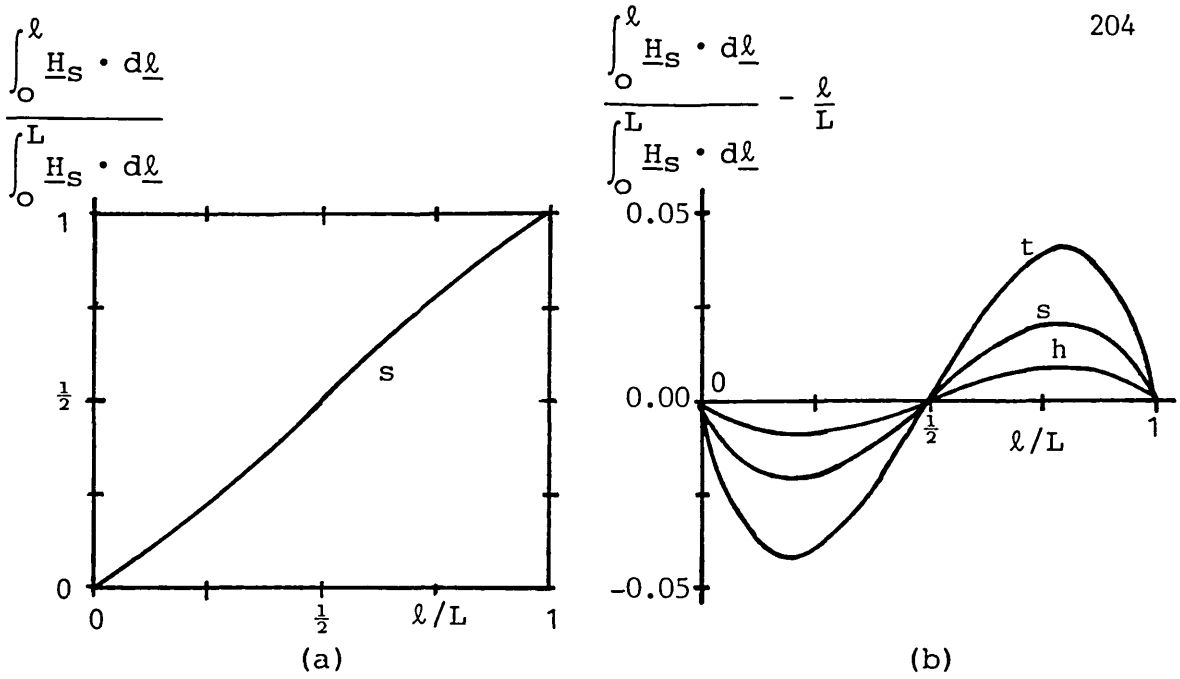

Fig. 8.3 Curvature of $\int \underline{H}_S \cdot d\underline{\ell}$ along edges of regular polygons : equilateral triangle (t), square (s), and hexagon (h). L is the edge length.

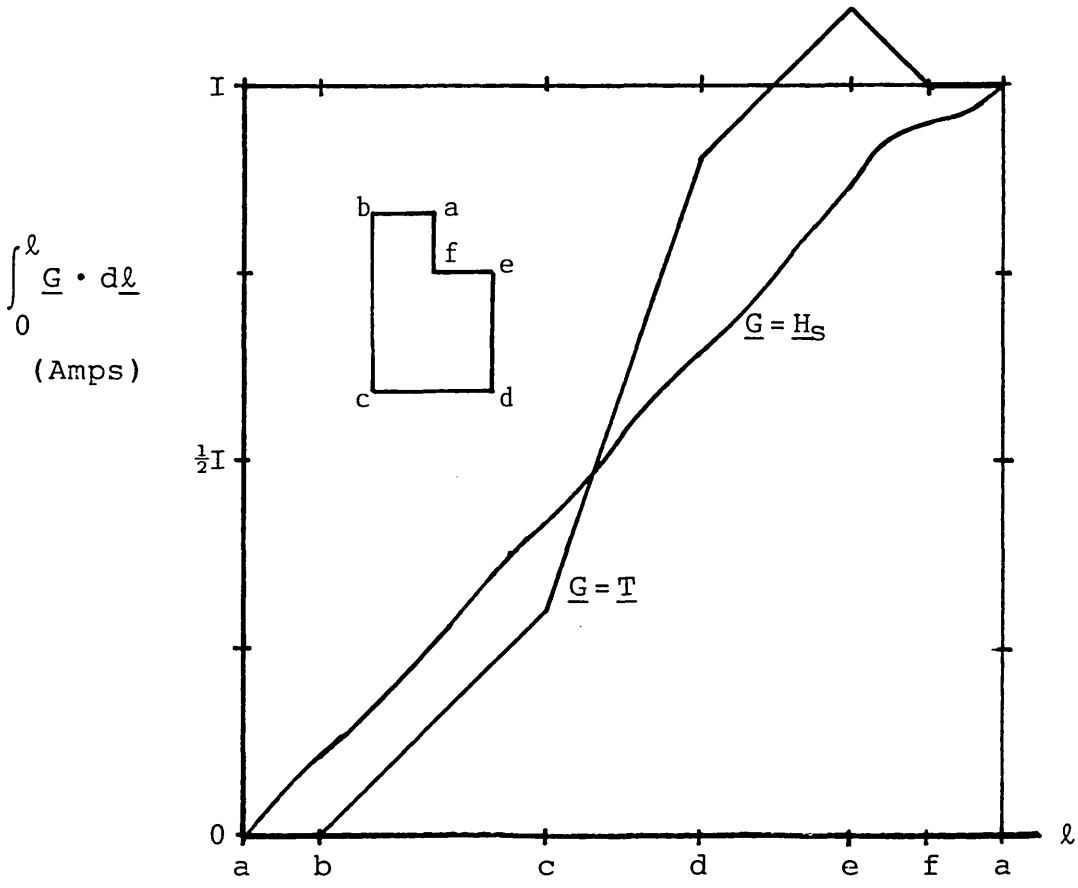

Fig. 8.4 $\int \underline{G} \cdot d\underline{\ell}$ along contour of half-slot for two definitions of $\underline{G}$. ℓ measured counter-clockwise from corner a. The reference point $\underline{r}_o$ for $\underline{T}$ is also at a. I is the current.

yield different values for what should be the same current. The $\underline{T}$ integrals yield the correct current for both meshes.

Having demonstrated quantitatively the errors associated with $\underline{H}_S$ in formulating the solution, let us now consider the errors in its outcome. This is best done in conjunction with the complementary B-solution.

Mesh	$\underline{G}$	M	$\oint \underline{G} \cdot d\underline{\ell}$ (A)		$\langle \underline{H}, \underline{B} \rangle_R$ (J)
			left section	right section	
1	2	3	4	5	6
122 elements	$\underline{H}_S$	1	8188	8188	501.5
		2	7753	7753	474.4
		3	7712	7712	471.9
		4	7704	7704	471.4
		5	7702	7702	471.2
		6	7701	7701	471.2
		7	7701	7701	471.2
		8	7700	7700	471.2
		9	7700	7700	471.1
	$\underline{T}$	-	7700	7700	471.2
341 elements	$\underline{H}_S$	1	7823	7871	492.7
		2	7708	7712	485.4
		3	7702	7703	484.9
		4	7701	7701	484.9
		5	7700	7700	484.8
	$\underline{T}$	-	7700	7700	484.9

Table 8.1 Inconsistencies in $\underline{H}_S$ solutions of C-magnet.

Column 6 of table 8.1 lists the values of the product $\langle \underline{H}, \underline{B} \rangle_R$ for the different M's used. But standard vector transformations, with the given boundary conditions, should yield

$$\langle \underline{H}, \underline{B} \rangle_R = \langle \underline{J}, \underline{A} \rangle_R \tag{8.34}$$

where the right hand side is unaffected by changes in M; its value is 471.2 J for the coarse mesh, and 484.9 J for the fine one. The $\underline{T}$ solutions yield the correct answer for both meshes. The $\underline{H}_S$ solutions approach the correct answers as M is increased. Where $\langle \underline{H}, \underline{B} \rangle_R$ differs from the expected value, we can conclude that

$$\nabla \times \underline{H} \neq \underline{J} \tag{8.35}$$

in violation of the H-system physical specifications, eqn. 8.3. According to the definitions in sec. 5.2.3, we have an inconsistent specification here.

The inconsistency is highlighted in fig. 8.5 which shows the constitutive errors of the two C-magnet meshes for different values of M and N, where

$$N = \text{number of Gaussian points within the individual conductor elements} \qquad (8.36)$$

N arises in postprocessing area integrations involving $\underline{H}_s$. The values N = 1, 3, 4, and 7 correspond to symmetric triangle integration formulae of orders 1, 2, 3, and 5 respectively[8.8]. The accuracy of the numerical integration improves as N is increased. Fig. 8.5 shows that, contrary to expectations, the constitutive error actually increases as the number of sampling points is increased from N = 1. The same trend is evident in the half-slot conductor solutions, fig. 8.6. As explained in sec. 5.2.3, the constitutive error is a comprehensive measure of the numerical errors only in consistently specified formulations; inconsistencies involve errors that are invisible to it. Highly accurate estimates of the energies are given with figures 8.5 and 8.6 for perspective. The consistent $\underline{T}$ solution error is at least comparable to, and generally marginally less than, the corresponding $\underline{H}_s$ solution error.

The $\underline{H}_s$ solutions were performed for M up to 9, and N up to 7. In general, there were no perceptible improvements beyond M = 5 and N = 4 for the problems and meshes attempted; in certain cases, lower values were found to be sufficient, as can be seen in figures 8.5 and 8.6. Clearly, the 'best' values, from a practical point of view, depend on the particular problem and mesh, as well as the requirements of the analyst.

It is interesting to observe that for a given M in table 8.1, the value of $\langle \underline{H}, \underline{B} \rangle_R$ is practically independent of N; the same was found to be true for the slot solutions. This suggests that the associated inconsistency is inherent in the over-all solution, and not local to the approximate postprocessing integration. In fact, the contribution from the C-magnet conductor sub-regions to the over-all integral is quite small, and it is only this contribution that is affected by N.

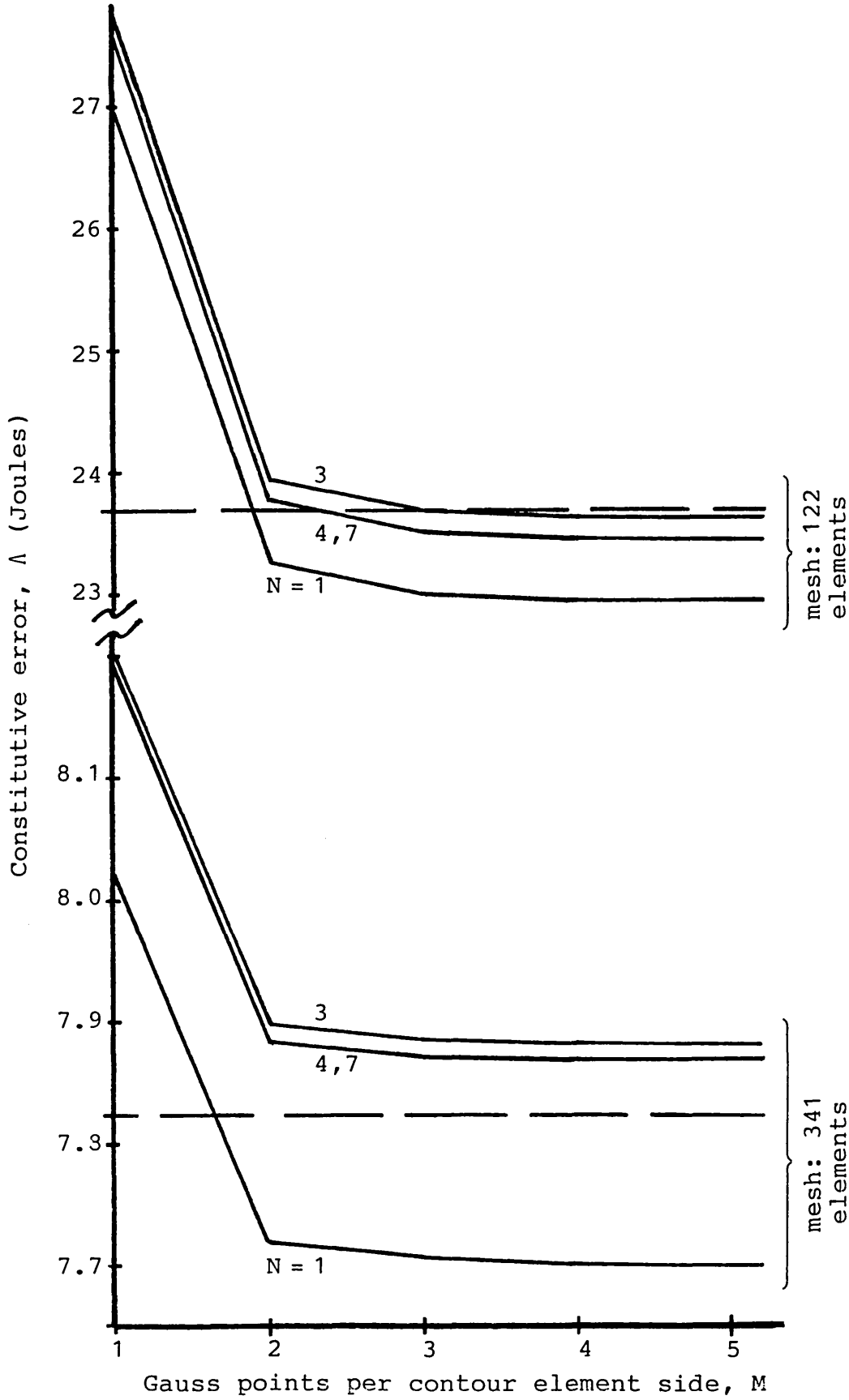

Fig. 8.5 C-magnet errors for various $\underline{H}_S$-solutions. Broken lines show errors for $\underline{T}$-solutions. N is number of internal Gauss points per element. Energy = 246.4 Joules.

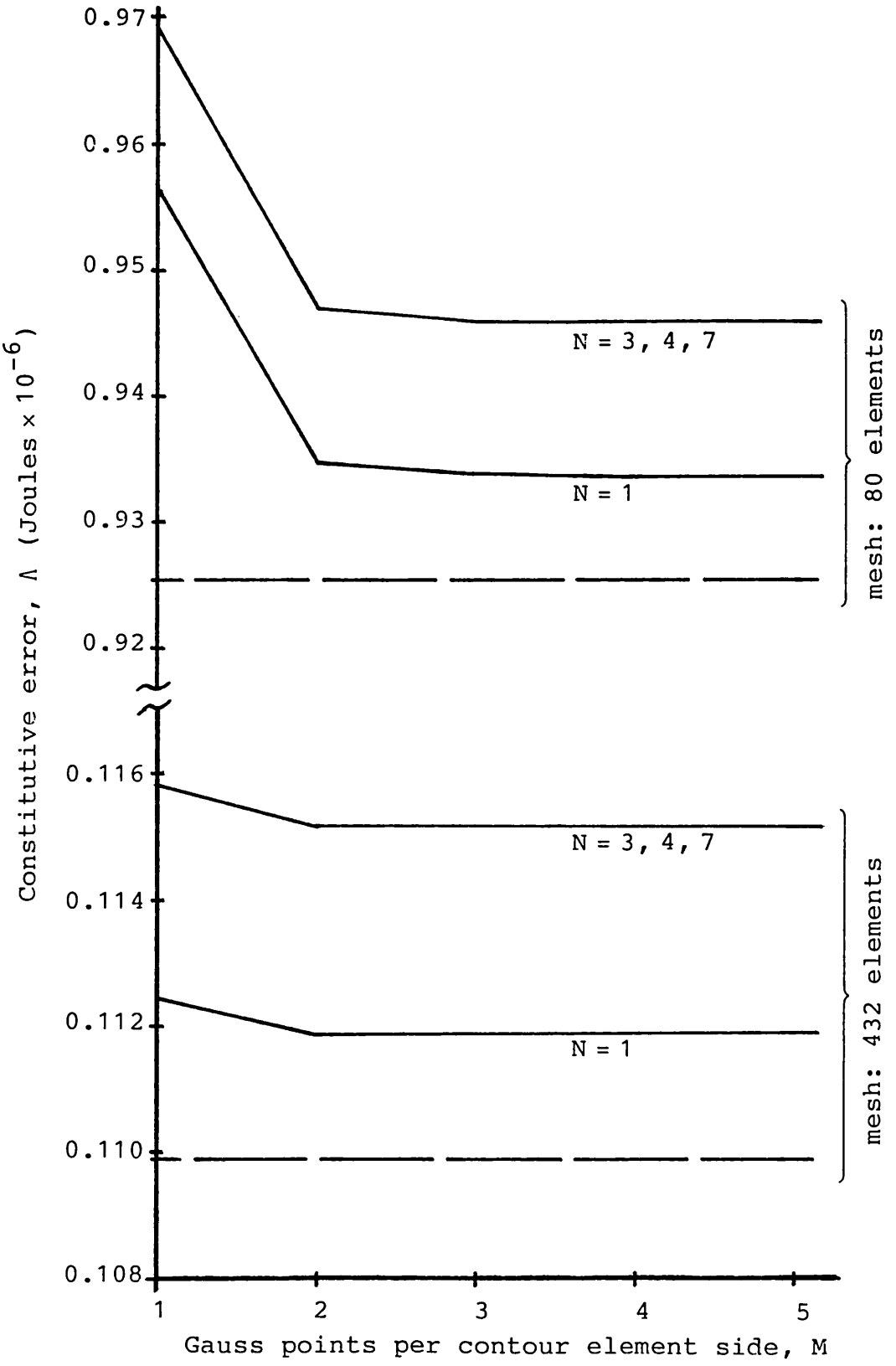

Fig. 8.6 Half-slot errors for various $\underline{\underline{H}}_S$-solutions. Broken lines show errors for $\underline{\underline{T}}$-solutions. N is number of internal Gauss points per element. Energy = 18.64 micro-Joules .

Figures 8.3-6 and table 8.1 indicate that the errors and inconsistencies associated with $\underline{H}_s$ can be made small by sufficiently refined meshing and a choice of $M > 1$. They are thus reduced to second order effects in the present two-potential formulation, but not without cost. Moreover, they affect solution accuracy in a generally indeterminate, problem- and mesh-dependent, manner. The computational effort to overcome them is rendered unnecessary in problems where $\underline{T}$ can be used since it is strictly consistent, of at least comparable accuracy to $\underline{H}_s$, and far less demanding computationally.

8.6 Conclusions

Biot-Savart pre-defined fields give rise to physically non-existent volume and sheet sources in numerical reduced scalar potential magnetostatic formulations. It is suggested that the resulting inconsistency is the true cause of errors associated with the formulation[8.3]; near-cancellation effects magnify, rather than cause, the errors. Two-potential formulations restrict the inconsistency to physically non-existent source sheets on conductor surfaces, thus reducing the error considerably; retention of a limited degree of inconsistency is demonstrated by the increase of constitutive error with improvement of the numerical volume integration.

An entirely consistent definition is proposed for conductors composed of straight longitudenal sections, and having polygonal cross-sections. The resulting constitutive error is shown to be comparable to that of the Biot-Savart based formulation. More importantly, the proposed defintion is mathematically simpler, resulting in reductions of computing time that can run into orders of magnitude.

CHAPTER NINE

Mixed Formulation

9.1 Introduction

A mixed formulation is one where the solution variable is the H-system potential in part of the region, and the B-system potential in the remainder. There has been recent interest in this type of formulation as it appears to be an economical way of tackling three-dimensional problems, particularly in eddy current applications[9.1–6]. Derivations have been based on the Galerkin method of weighted residuals. This chapter uses the constitutive error approach to derive, and examine, mixed formulation under static conditions.

9.2 Mixed complementary systems

Consider an abstract problem in a region R where the specifications on the fields $\underline{H}$ and $\underline{B}$ are

$$\underline{B} = \mu(\underline{H})\underline{H} + \underline{B}_r \quad ; \quad \underline{H} = \nu(\underline{B})\underline{B} + \underline{H}_c \qquad (9.1)$$

$$\underline{J} = \text{curl } \underline{H} \quad ; \quad \rho = \text{div } \underline{B} \qquad (9.2)$$

$$0 = \underline{n} \times \Delta\underline{H} \quad ; \quad 0 = \underline{n} \cdot \Delta\underline{B} \qquad (9.3)$$

The boundary surface S is composed of two simply-connected sub-sections S_h and S_b :

$$S = S_h \cup S_b \quad , \quad S_h \cap S_b = 0 \qquad (9.4a)$$

with

$$\underline{h} = \underline{n} \times \underline{H} \text{ on } S_h \quad ; \quad b = \underline{n} \cdot \underline{B} \text{ on } S_b \qquad (9.4b)$$

The problem specified above is that of sec. 3.6. Conventional H- and B-formulations are derived in sections 3.6.2 and 3.6.3 respectively.

To derive mixed formulations, the over-all region R is divided into two sub-regions R_1 and R_2 as in fig. 9.1 :

$$R = R_1 \cup R_2 \quad , \quad R_1 \cap R_2 = 0 \tag{9.5}$$

With the exception of the interface surface S_o, all parameters are associated with either R_1 or R_2, and will be subscripted accordingly. For ease of reference, the variables are grouped into two systems :

$$\begin{aligned} &\alpha\text{-system} : \quad \Omega_1 \, , \underline{H}_1 \; ; \; \underline{A}_2 \, , \underline{B}_2 \\ \text{and} \qquad & \qquad\qquad\qquad\qquad\qquad\qquad\qquad\qquad (9.6) \\ &\beta\text{-system} : \quad \underline{A}_1 \, , \underline{B}_1 \; ; \; \Omega_2 \, , \underline{H}_2 \end{aligned}$$

For a given problem, two mixed formulations can be defined : a primal formulation based on α-system potentials, Ω_1 and $\underline{A}_2$, and a dual formulation based on β-system potentials, $\underline{A}_1$ and Ω_2. In practice, the choice between dual formulations is critical to solution economy. Without loss of generality, we shall consider the primal formulation based on the α-system potentials, Ω_1 and $\underline{A}_2$; they are defined by

$$\underline{H}_1 = \underline{G}_1 - \nabla \Omega_1 \quad ; \quad \underline{B}_2 = \underline{C}_2 + \nabla \times \underline{A}_2 \tag{9.7}$$

with

$$\nabla \times \underline{G}_1 = \underline{J}_1 \quad ; \quad \nabla \cdot \underline{C}_2 = \rho_2 \tag{9.8a}$$

and

$$\underline{n} \times \Delta \underline{G}_1 = 0 \quad ; \quad \underline{n} \cdot \Delta \underline{C}_2 = 0 \tag{9.8b}$$

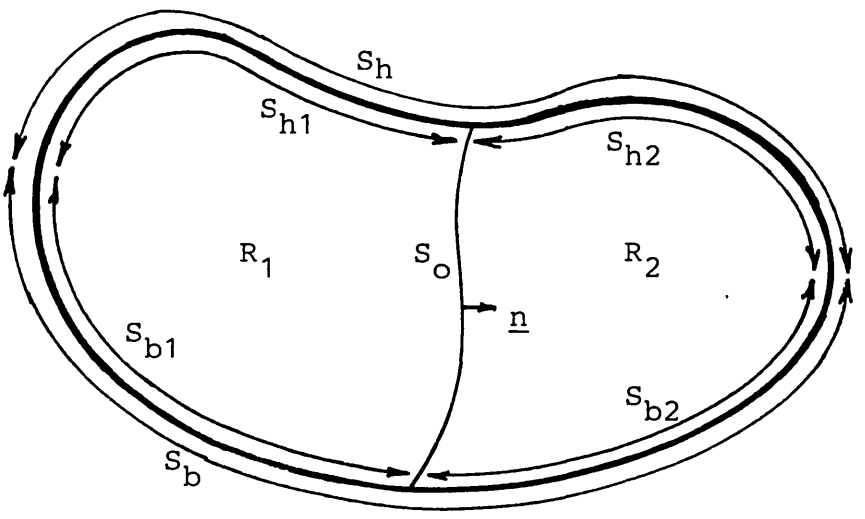

Fig. 9.1 Region subdivision.

We can choose the following continuity and boundary conditions on the potentials

$$\Delta\Omega_1 = 0 \quad ; \quad \underline{n} \times \Delta\underline{A}_2 = 0 \tag{9.9a}$$

and

$$\Omega_1 = \Omega_{h1} \text{ on } S_{h1} \quad ; \quad \underline{n} \times \underline{A}_2 = \underline{a}_{b2} \text{ on } S_{b2} \tag{9.9b}$$

as in sec. 3.6; Ω_{h1} and $\underline{a}_{b2}$ are known.

9.3 Incomplete decomposition of the constitutive error

The constitutive error is a global integral with distinct contributions from R_1 and R_2; thus

$$\Lambda(\underline{H},\underline{B}) = X(\underline{H}) + \Psi(\underline{B}) - Z(\underline{H},\underline{B}) \tag{9.10a}$$

$$= X_1(\underline{H}_1) + \Psi_1(\underline{B}_1) - Z_1(\underline{H}_1,\underline{B}_1) + X_2(\underline{H}_2) + \Psi_2(\underline{B}_2) - Z_2(\underline{H}_2,B_2) \tag{9.10b}$$

The decomposition of $Z(\underline{H},\underline{B})$ proceeds by substitution of α-system potentials, and the usual application of vector identities and the divergence theorem :

$$\begin{aligned} Z(\underline{H},\underline{B}) &= Z_1(\underline{H}_1,\underline{B}_1) + Z_2(\underline{H}_2,\underline{B}_2) = \langle \underline{H}_1 , \underline{B}_1 \rangle_{R_1} + \langle \underline{H}_2 , \underline{B}_2 \rangle_{R_2} \\ &= \langle \underline{G}_1 , \underline{B}_1 \rangle_{R_1} - \langle \nabla\Omega_1 , \underline{B}_1 \rangle_{R_1} + \langle \underline{H}_2 , \underline{C}_2 \rangle_{R_2} + \langle \underline{H}_2 , \nabla\times\underline{A}_2 \rangle_{R_2} \\ &= \langle \underline{G}_1 , \underline{B}_1 \rangle_{R_1} + \langle \Omega_1 , \rho_1 \rangle_{R_1} - [\Omega_1 , \underline{n}_1 \cdot \underline{B}_1]_{S_1 U S_o} \\ &\quad + \langle \underline{H}_2 , \underline{C}_2 \rangle_{R_2} + \langle \underline{J}_2 , \underline{A}_2 \rangle_{R_2} - [\underline{n}_2 \times \underline{H}_2 , \underline{A}_2]_{S_2 U S_o} \\ &= \langle \underline{G}_1 , \underline{B}_1 \rangle_{R_1} + \langle \Omega_1 , \rho_1 \rangle_{R_1} + \langle \underline{H}_2 , \underline{C}_2 \rangle_{R_2} + \langle \underline{J}_2 , \underline{A}_2 \rangle_{R_2} \\ &\quad - [\Omega_1 , b_1]_{S_{b1}} - [\Omega_{h1} , \underline{n}_1 \cdot \underline{B}_1]_{S_{h1}} - [\Omega_1 , \underline{n}_1 \cdot \underline{B}_1]_{S_o} \\ &\quad - [h_2 , \underline{A}_2]_{S_{h2}} + [\underline{H}_2 , \underline{a}_{b2}]_{S_{b2}} - [\underline{n}_2 \times \underline{H}_2 , \underline{A}_2]_{S_o} \end{aligned}$$

Substituting back into eqn. 9.10, we can write

$$\Lambda(\alpha,\beta) = \Theta(\alpha) + \Xi(\beta) - \Gamma(\alpha,\beta) \tag{9.11}$$

with

$$\Theta(\alpha) = \Theta(H_1,B_2) = X_1(\underline{H}_1) - \langle \Omega_1 , \rho_1 \rangle_{R_1} + [\Omega_1 , b_1]_{S_{b1}} + \Psi_2(\underline{B}_2) - \langle \underline{J}_2 , \underline{A}_2 \rangle_{R_2} + [h_2 , \underline{A}_2]_{S_{h2}}$$

$$\Xi(\beta) = \Xi(B_1,H_2) = \Psi_1(\underline{B}_1) - \langle \underline{G}_1 , \underline{B}_1 \rangle_{R_1} + [\Omega_{h1} , \underline{n}_1 \cdot \underline{B}_1]_{S_{h1}}$$
$$+ X_2(\underline{H}_2) - \langle \underline{H}_2 , \underline{C}_2 \rangle_{R_2} - [\underline{H}_2 , \underline{a}_{b2}]_{S_{b2}}$$

and

$$\Gamma(\alpha,\beta) = [\underline{n} \times \underline{H}_2 , \underline{A}_2]_{S_o} - [\Omega_1 , \underline{n} \cdot \underline{B}_1]_{S_o}$$

where $\underline{n} = \underline{n}_1 = -\underline{n}_2$ on S_o, as in fig. 9.1.

The partial decomposition of Λ between the α- and β-systems accounts for all problem specifications with the exception of field continuity across S_o and, of course, the constitutive relationship. Explicit imposition of field continuity in accordance with eqn. 9.3 yields

$$\underline{n}\times\underline{H}_1 = \underline{n}\times\underline{H}_2 = \underline{n}\times\underline{H}_o \quad \text{and} \quad \underline{n}\cdot\underline{B}_1 = \underline{n}\cdot\underline{B}_2 = \underline{n}\cdot\underline{B}_o \qquad (9.12)$$

on S_o. The fields $\underline{n} \times \underline{H}_o$ and $\underline{n} \cdot \underline{B}_o$ are then common to both α- and β-systems, so that the constitutive relationship is not the only link between the complementary systems as was the case in conventional formulations. $\underline{n} \times \underline{H}_o$ and $\underline{n} \cdot \underline{B}_o$ correspond to γ in Appendix F, and hence forbid the decomposition of Λ into complementary α- and β-system functionals that can be extremised independently of each other. This, incidentally, does not contradict the theory of sec. 3.5 which guaranteed the decomposition of Λ into complementary H- and B-system functionals.

9.4 Field continuity in error form

Mixed complementary functionals may possibly be derived from an extended error form

$$\Lambda_t = \Lambda + \Lambda_\Delta = \Theta_t(\alpha) + \Xi_t(\beta) \qquad (9.13)$$

where Λ_Δ is a positive error expression of field continuity across S_o

$$\Lambda_\Delta \geq 0 \qquad (9.14a)$$

with

$$\Lambda_\Delta = 0 \quad <=> \quad \left\{ \begin{array}{c} \underline{n} \times \Delta\underline{H} = 0 \\ \text{and} \\ \underline{n} \cdot \Delta\underline{B} = 0 \end{array} \right\} \quad \text{on } S_o \qquad (9.14b)$$

From 9.13 and 9.14, and the fundamental property of Λ in 2.18

$$\Lambda_t \geqq 0 \qquad (9.15a)$$

with

$$\Lambda_t = 0 \quad <=> \quad \Lambda = 0 \quad \text{and} \quad \Lambda_\Delta = 0 \qquad (9.15b)$$

The total error is then minimised by solving

$$\delta\Lambda_t = 0 \quad => \quad \delta\Theta_t(\alpha) = 0 \ , \ \delta\Xi_t(\beta) = 0 \qquad (9.16)$$

which imposes both outstanding physical specifications : the constitutive relationship, and field continuity across S_o.

The definition of Λ_Δ must be related to field continuity as in 9.14, and ensure the splitting of Λ_t into $\Theta_t(\alpha)$ and $\Xi_t(\beta)$ as in eqn. 9.13. Such a definition, if it exists, does not present itself readily.

9.5 Mixed complementary solution formulations

The absence of mixed complementary functionals does not invalidate the proposition that the solution to

$$0 = \delta\Lambda \qquad (9.17)$$

minimises the constitutive error Λ, and thus imposes the constitutive relationship on the fields. Substituting for Λ from eqn. 9.11, and allowing α- and β-variables free variations, eqn. 9.17 yields

$$0 = \delta\Theta_1(H_1) + [\underline{n} \cdot \underline{B}_1 \ , \ \delta\Omega_1]_{S_o} \qquad (9.18a)$$

$$0 = \delta\Theta_2(B_2) - [\underline{n} \times \underline{H}_2 \ , \ \delta\underline{A}_2]_{S_o} \qquad (9.18b)$$

and

$$0 = \delta\Xi_1(B_1) + [\Omega_1 \ , \ \delta(\underline{n} \cdot \underline{B}_1)]_{S_o} \qquad (9.19a)$$

$$0 = \delta\Xi_2(H_2) - [\underline{A}_2 \ , \ \delta(\underline{n} \times \underline{H}_2)]_{S_o} \qquad (9.19b)$$

where

$$\delta\Theta_1(H_1) = <\mu_1(\underline{H}_1)\underline{H}_1+\underline{B}_r \ , \ \delta\underline{H}_1>_{R_1} - <\rho_1 \ , \ \delta\Omega_1>_{R_1} + [b_1 \ , \ \delta\Omega_1]_{S_{b1}}$$

$$\delta\Theta_2(B_2) = <\nu_2(\underline{B}_2)\underline{B}_2+\underline{H}_c \ , \ \delta\underline{B}_2>_{R_2} - <\underline{J}_2 \ , \ \delta\underline{A}_2>_{R_2} + [\underline{h}_2 \ , \ \delta\underline{A}_2]_{S_{h2}}$$

$$\delta\Xi_1(B_1) = \langle \nu_1(\underline{B}_1)\underline{B}_1+\underline{H}_c \, , \, \delta\underline{B}_1\rangle_{R_1} - \langle \underline{G}_1 \, , \, \delta\underline{B}_1\rangle_{R_1} + [\Omega_{h1} \, , \, \delta(\underline{n}\cdot\underline{B}_1)]_{S_{h1}}$$

$$\delta\Xi_2(H_2) = \langle \mu_2(\underline{H}_2)\underline{H}_2+\underline{B}_r \, , \, \delta\underline{H}_2\rangle_{R_2} - \langle \underline{C}_2 \, , \, \delta\underline{H}_2\rangle_{R_2} - [\underline{a}_{b2} \, , \, \delta\underline{H}_2]_{S_{b2}}$$

The varied parameters in eqns. 9.18 are the α-system variables, and in eqns. 9.19 the β-system variables.

To qualify as a valid solution formulation, eqn. 9.17 must be augmented, somehow, by the imposition of field continuity across S_o ; otherwise, the conditions of physical uniqueness will be incomplete. Moreover, the resulting formulation is of practical use only if eqns. 9.18 and 9.19 are made independent of each other; otherwise, α- and β-systems must be solved simultaneously.

Both requirements relate to the interface S_o; therefore the surface integrals on S_o, in eqns. 9.18 and 9.19, are of particular significance. Their role in the solution of eqns. 9.18 is to enforce, on S_o,

$$\underline{n}\cdot\mu_1\underline{H}_1 - \underline{n}\cdot\underline{B}_1 \doteq 0 \quad , \quad \underline{n}\times\nu_2\underline{B}_2 - \underline{n}\times\underline{H}_2 \doteq 0 \qquad (9.20)$$

In the solution of 9.19 they enforce, also on S_o,

$$\underline{n}\times\nu_1\underline{B}_1 - \underline{n}\times\underline{H}_1 \doteq 0 \quad , \quad \underline{n}\cdot\mu_2\underline{H}_2 - \underline{n}\cdot\underline{B}_2 \doteq 0 \qquad (9.21)$$

The symbol $\doteq$ is used to denote weak equality through the minimisation process. For simplicity, $\underline{H}_c$ and $\underline{B}_r$ are assumed zero in eqns. 9.20 and 9.21. The equations can then be verified by standard manipulation of the volume integrals in eqns. 9.18 and 9.19.

Eqns. 9.20 and 9.21 show that the integrals on S_o enforce the constitutive relationship between α- and β-fields , which is consistent with eqn. 9.17. However, it is possible to use the integrals to enforce continuity weakly. This may be achieved by constraining the α-fields explicitly as follows

$$\underline{n}\cdot\mu_1\underline{H}_1 = \underline{n}\cdot\underline{B}_2 \quad \text{and} \quad \underline{n}\times\nu_2\underline{B}_2 = \underline{n}\times\underline{H}_1 \qquad (9.22)$$

or by constraining the β-fields explicitly as follows

$$\underline{n} \times \nu_1 \underline{B}_1 = \underline{n} \times \underline{H}_2 \qquad \text{and} \qquad \underline{n} \cdot \mu_2 \underline{H}_2 = \underline{n} \cdot \underline{B}_1 \tag{9.23}$$

Either constraint, or both, can be used. Substitution of eqns. 9.22 into 9.20, or eqns. 9.23 into 9.21, yields

$$\underline{n} \times \Delta \underline{H} \doteq 0 \qquad \text{and} \qquad \underline{n} \cdot \Delta \underline{B} \doteq 0 \tag{9.24}$$

so that field continuity across S_o is imposed weakly by the solution of eqn. 9.17, i.e. eqns. 9.18 and 9.19.

But eqns. 9.18 and 9.19 are still coupled, via the S_o integrals, and must therefore be solved simultaneously. To show how this may be avoided, we rewrite eqns. 9.18 as follows

$$0 = \delta\Theta_1(H_1) + [\underline{n} \cdot \underline{B}_2 \, , \, \delta\Omega_1]_{S_o} - [\underline{n} \cdot \Delta \underline{B} \, , \, \delta\Omega_1]_{S_o} \tag{9.25a}$$

$$0 = \delta\Theta_2(B_2) - [\underline{n} \times \underline{H}_1 \, , \, \delta \underline{A}_2]_{S_o} - [\underline{n} \times \Delta \underline{H} \, , \, \delta \underline{A}_2]_{S_o} \tag{9.25b}$$

These are α-system equations; they are coupled to the β-system variables through the terms $\underline{n} \cdot \Delta \underline{B}$ and $\underline{n} \times \Delta \underline{H}$. But in exact analysis, weak equalities are exact equalities. In particular, eqns. 9.24 can be enforced prior to the solution as a redundant over-specification, sec. 5.2.2. Eqns. 9.25 then simplify to

$$0 = \delta\Theta_1(H_1) + [\underline{n} \cdot \underline{B}_2 \, , \, \delta\Omega_1]_{S_o} \tag{9.26a}$$

$$0 = \delta\Theta_2(B_2) - [\underline{n} \times \underline{H}_1 \, , \, \delta \underline{A}_2]_{S_o} \tag{9.26b}$$

irrespective of whether the α-system constraints of eqns. 9.22, or the β-system constraints of eqns. 9.23, are used. Eqns. 9.26 are entirely in terms of α-system variables, and can therefore be solved independently of eqns. 9.19 to yield the exact fields.

Eqns. 9.26 can, of course, be formulated numerically, and solved to yield approximate estimates of the fields. In fact they are equivalent to the mixed formulation obtained by the Galerkin method of weighted residuals[9•2/3]; see Appendix H. But the present derivation verifies the validity of eqns. 9.26 in exact analysis; justification in numerical analysis is still to be examined.

According to the constitutive error approach, a proper numerical formulation would solve eqns. 9.25 simultaneously with eqns. 9.19 to minimise the error as in eqn. 9.17. The fields are constrained by eqns. 9.22 or 9.23 to enforce continuity weakly as in eqns. 9.24. But in numerical analysis, weakly enforced conditions are only approximated by the solution. Thus, replacing eqns. 9.25 by 9.26 involves an approximation that is additional to the standard numerical approximation of the proper formulation. The severity of the additional approximation can be gauged by the values the solution of eqns. 9.25 attributes to the discontinuities, $\underline{n} \times \Delta\underline{H}$ and $\underline{n} \cdot \Delta\underline{B}$, on S_o; these are given by rewriting eqns. 9.20 as follows

$$\underline{n}\cdot\Delta\underline{B} \doteq \underline{n}\cdot\underline{B}_2 - \underline{n}\cdot\mu_1\underline{H}_1 \quad , \quad \underline{n}\times\Delta\underline{H} \doteq \underline{n}\times\nu_2\underline{B}_2 - \underline{n}\times\underline{H}_1 \qquad (9.27)$$

Clearly, the smaller the discontinuities, the more justifiable eqns. 9.26 become. It would thus appear that the α-system formulation of eqns. 9.26 requires finer discretisation, especially in the vicinity of the interface S_o, than conventional H- or B-formulations of comparable overall accuracy; the mixed formulation is fully justified only with infinitely refined discretisation, i.e. exact analysis. It would also appear that constraining the α-fields by eqns. 9.22 is preferable, from the viewpoint of accuracy, to constraining the β-fields by eqns. 9.23 : substitution of eqns. 9.22 into 9.27 causes the right hand sides in the latter to vanish, so that the field discontinuities are approximated directly to zero as in eqns. 9.24. The same cannot be said of the β-system constraints of eqns. 9.23 : the desired eqns. 9.24 follow from 9.23 only after the simultaneous solution of α- and β-systems in a proper formulation; replacing the α-system solution of eqns. 9.25 by that of eqns. 9.26 effectively accepts an approximate, first iteration estimate of the discontinuities without modification by eqns. 9.19. It can thus be concluded that the α-system constraint of eqns. 9.22 has the distinct advantage of relaxing the demands on discretisation refinement. However, it also has the distinct practical disadvantage of requiring actual implementation;

in contrast, the β-system constraint of eqns. 9.23 need only be envisaged conceptually when solving the α-system by eqns. 9.26.

Eqns. 9.26 were derived from eqns. 9.25 by applying a redundant over-specification which, in numerical analysis, amounts to an approximation. An alternative derivation is possible : noting that eqns. 9.25 were extracted from $\delta\Lambda$ in eqn. 9.17, it follows that eqns. 9.26 are extracted from

$$0 = \delta\Lambda + [\underline{n} \cdot \Delta\underline{B} , \delta\Omega_1]_{S_o} + [\underline{n} \times \Delta\underline{H} , \delta\underline{A}_2]_{S_o} \qquad (9.28)$$

Formally, then, the mixed formulation of eqns. 9.26 does not minimise the constitutive error, nor impose field continuity across the interface S_o.

A complementary β-formulation is given by eqns. 9.19; its solution is dependent on the α-solution due to the presence of Ω_1 and $\underline{A}_2$. An independent, but approximate, β-formulation can also be extracted.

9.6 Conclusions

The continuity of fields across the interface S_o, which is a requirement of physical uniqueness, forbids the definition of mixed complementary functionals, or energies.

Independently solvable mixed formulations can be extracted, but involve a degree of approximation in numerical application; in effect, they are not associated with true minimum principles. Moreover, the formulations require additional constraints to be imposed explicitly on the fields; the constraints can be chosen to improve accuracy, or to simplify numerical implementation, but not both together.

The mixed formulation derived here by the constitutive error approach is equivalent to that derived by the

Galerkin method of weighted residuals[9•2,3]. The question of justification, discussed at length in sec. 9.5, can be stated in terms of the Galerkin derivation as follows : to what extent does the mixed formulation, eqns. H.8 in Appendix H, enforce the individual residual equations H.3-6 ? Eqn. H.5, it is noted, relates to field continuity across S_o, and does not arise in conventional Galerkin derivations.

Mixed dual and (pseudo-) complementary formulations are available, and can be solved simultaneously, or independently of each other. Relative accuracy of the various options can be assessed quantitatively by computing the resulting constitutive error and field discontinuities at the interface S_o.

C H A P T E R T E N

Solvability of Vector Potential Formulations

10.1 Introduction

In order that the solution of a given formulation may be performed, the variables must be uniquely specified. Section 3.4 distinguishes between the physical uniqueness of fields, and the solvability of potentials. The solvability requirements on the H-system scalar potential Ω, sec. 3.4.4.1, are simple to implement : arbitrary values are assigned to the potential, and possibly potential discontinuities, at certain reference points. The solvability requirements on the B-system vector potential $\underline{A}$, sec. 3.4.4.2, are equally simple in two-dimensional and axisymmetric applications.

In three dimensions, however, enforcing solvability on numerical vector potential formulations is not as straightforward. Over the past few years, several treatments have been proposed, often backed by satisfactory computational results. Yet there appears to be lingering confusion regarding the requirements of solvability and their implementation[10.1-3,5]. This chapter presents an overview of the subject in terms of the constitutive error approach. The various methods are examined for validity, accuracy, and possible extension and improvement.

The constitutive error approach regards potentials as mere solution tools of no fundamental physical significance. Therefore, a given treatment is considered valid if it enforces the physical specifications correctly, and results in solvable, i.e. non-singular, solution matrices, irrespective of the manner with which potential solvability is secured. Sec. 10.3 considers methods that approximate,

numerically, an analytically unique vector potential. Sec. 10.4 considers methods that enforce solvability directly on the numerically over-specified trial functions.

The presentation attempts to predict the relative accuracy of the various methods. Accuracy relates to the physical specifications, given in sec. 10.2, of which only the constitutive relationship is not satisfied exactly. Therefore, the degree to which the constitutive error is minimised by a given formulation is indicative of the accuracy to be expected from the corresponding solution. Moreover, burdening the trial functions with inessential constraints, or over-specifications, predictably restricts their ability to represent the true solution fields.

10.2 Physical uniqueness

A general magnetostatic problem, in a given region R, may be physically specified as follows :

$$\underline{B} = \mu(\underline{H})\underline{H} + \underline{B}_r \quad ; \quad \underline{H} = \nu(\underline{B})\underline{B} + \underline{H}_c \qquad (10.1)$$

$$\underline{J} = \text{curl } \underline{H} \quad ; \quad 0 = \text{div } \underline{B} \qquad (10.2)$$

$$\underline{K} = \underline{n} \times \Delta\underline{H} \quad \text{on } S_k \quad ; \quad 0 = \underline{n} \cdot \Delta\underline{B} \qquad (10.3)$$

According to sec. 3.4.2, boundary conditions that result in a physically unique solution can be specified in a variety of ways. We recall, in particular, the specifications

$$\underline{h} = \underline{n} \times \underline{H} \quad \text{on } S_h \quad ; \quad b = \underline{n} \cdot \underline{B} \quad \text{on } S_b \qquad (10.4)$$

$$V_i = \int_{\underline{r}_o}^{\underline{r}_i} \underline{H} \cdot d\underline{\ell} \quad ; \quad \Phi_i = \int_{S_{hi}} \underline{B} \cdot d\underline{S} \qquad (10.5)$$

where S_h and S_b are non-overlapping sections of the bounding surface S

$$S_h \subset S \ , \quad S_b \subset S \ , \quad S_h \cap S_b = 0 \qquad (10.6)$$

S_{hi} denotes simply-connected sub-sections of S_h; $\underline{r}_i$ is an arbitrary reference point on S_{hi}; $\underline{r}_o$ is a global reference point in R. V_i is the magnetomotive force at $\underline{r}_i$, and Φ_i is

the magnetic flux through S_{hi}. In many practical applications, the boundary specifications take the simpler form

$$\underline{h} = 0 , \qquad b = 0 , \qquad \Phi_i = 0 \tag{10.7a}$$

with

$$S = S_h \cup S_b \tag{10.7b}$$

Sec. 3.4.3 applies physical specifications to potentials in the general case. In the present problem, the B-system physical specifications in eqns. 10.2 - 5 define and constrain the vector potential $\underline{A}$ as follows

$$\underline{B} = \nabla \times \underline{A} \tag{10.8}$$

$$0 = \underline{n} \cdot (\nabla \times \Delta\underline{A}) = - \nabla_s \cdot (\underline{n} \times \Delta\underline{A}) \tag{10.9}$$

$$b = \underline{n} \cdot (\nabla \times \underline{A}) = - \nabla_s \cdot (\underline{n} \times \underline{A}) \quad \text{on } S_b \tag{10.10}$$

and

$$\Phi_i = \oint_{\ell_{hi}} \underline{A} \cdot d\underline{\ell} \tag{10.11}$$

where ℓ_{hi} is the boundary contour of S_{hi}. Eqns. 10.8, 9, 10, and 11 correspond to eqns. 3.41a, 43, 49, and 53 respectively; the pre-specified field $\underline{C}$ is set to zero due to the absence of B-system sources.

Physical uniqueness requires eqns. 10.8 - 11 to be imposed on $\underline{A}$; in numerical applications, this is usually done explicitly. In particular, the curl condition of eqn. 10.8 is enforced by substituting curl $\underline{A}$ for $\underline{B}$ in the constitutive error.

The numerical trial functions are commonly defined to make $\underline{A}$ continuous

$$\Delta\underline{A} = 0 \quad \Rightarrow \quad \underline{n} \times \Delta\underline{A} = 0 \quad \text{and} \quad \underline{n} \cdot \Delta\underline{A} = 0 \tag{10.12}$$

so that the continuity condition of eqn. 10.9 is satisfied.

Recalling eqn. 3.100b of sec. 3.6.3, the boundary condition of eqn. 10.10 can be enforced through the definition

$$\underline{n} \times \underline{A} = \underline{a}_b + \underline{n} \times \nabla_s \beta \quad \text{on } S_b \tag{10.13a}$$

where $\underline{a}_b$ is any tangential vector distribution on S_b pre-defined to satisfy

$$\nabla_s \cdot \underline{a}_b = - b \qquad (10.13b)$$

β is a scalar distribution on S_b. The topology of the various sub-sections of S, and the particular way in which eqns. 10.5 are specified, determine the form β takes : it may be pre-defined or unknown, continuous or discontinuous. The contour ℓ_{hi} in eqn 10.11 may also be a contour of S_b sub-sections. Thus a non-zero flux Φ_i may force a discontinuous β in an adjacent S_b sub-section; if, moreover, Φ_i is not known, the discontinuity cannot be pre-defined. The B-system conditions in the common boundary specification of eqns. 10.7 can be enforced by choosing

$$\underline{a}_b = 0 \ , \quad \beta = 0 \qquad (10.14a)$$

so that

$$\text{on } S_b : \ \underline{n} \times \underline{A} = 0 \qquad (10.14b)$$

The constitutive error is given by

$$\Lambda(\underline{H},\underline{B}) = X(\underline{H}) + \Psi(\underline{B}) - Z(\underline{H},\underline{B}) \qquad (10.15)$$

Decomposition of Z proceeds by substituting curl $\underline{A}$ for $\underline{B}$, eqn. 10.8, applying, as usual, vector identities and the divergence theorem, and substituting from eqns. 10.2 - 13 into the result. The theory of sec. 3.5 assures us that if the physical specifications are well-posed, Λ will split completely between the H- and B-systems :

$$\Lambda(H,B) = \Theta(H) + \Xi(B) \qquad (10.16)$$

For example, the common boundary specifications of eqns. 10.7 and 10.14 yield

$$\Theta(H) = X(\underline{H}) \qquad (10.17a)$$

and

$$\Xi(B) = \Psi(\underline{B}) - \langle \underline{J} \ , \ \underline{A} \rangle_R - [\underline{K} \ , \ \underline{A}]_{S_k} \qquad (10.17b)$$

Minimisation of the constitutive error in eqn. 10.16 produces the B-system solution formulation :

$$0 = \delta\Xi(B) \qquad (10.18)$$

This equation is not, as yet, solvable since the vector potential $\underline{A}$ has not been uniquely specified. The following sections describe methods of enforcing solvability on numerical formulations of eqn. 10.18.

10.3 Analytic solvability

An analytically unique vector potential can be defined in terms of a two-system model as in sec. 3.4.4.2 :

$$\underline{F} = \alpha\,\underline{A} \quad ; \quad \underline{A} = \alpha^{-1}\,\underline{F} \qquad (10.19)$$

$$\underline{B} = \nabla \times \underline{A} \quad ; \quad \rho' = \nabla \cdot \underline{F} \qquad (10.20)$$

$$\underline{K}' = \underline{n} \times \Delta\underline{A} \text{ on } S_\Delta \quad ; \quad \sigma' = \underline{n} \cdot \Delta\underline{F} \text{ on } S_\Delta \qquad (10.21)$$

$$\underline{a} = \underline{n} \times \underline{A} \text{ on } S_a \quad ; \quad f = \underline{n} \cdot \underline{F} \text{ on } S_f \qquad (10.22a)$$

where

$$S = S_a \cup S_f \quad \text{and} \quad S_a \cap S_f = 0 \qquad (10.22b)$$

and S_Δ denotes surfaces of discontinuity in $\underline{n}\times\underline{A}$ and $\underline{n}\cdot\underline{F}$. α, ρ', σ', and f can be chosen arbitrarily provided they do not violate the physical specifications. $\underline{K}'$ is forced by the continuity of the numerically over-specified trial functions in eqns. 10.12; thus

$$\underline{K}' = 0 \qquad (10.23)$$

Moreover, the following choices

$$\alpha = \alpha^{-1} = 1 \quad \text{and} \quad \sigma' = 0 \qquad (10.24)$$

are consistent with the continuity of $\underline{n}\cdot\underline{A}$ in eqns. 10.12. The values of ρ' and f are not constrained in any way; for simplicity, we choose

$$\rho' = 0 \quad \text{and} \quad f = 0 \qquad (10.25)$$

It is emphasised that the values in eqns. 10.24 and 25 are chosen for convenience, and can be altered if desired. As they stand, they simplify eqns. 10.19-22 to

$$\underline{F} = \underline{A} \tag{10.26}$$

$$\underline{B} = \nabla \times \underline{A} \quad ; \quad 0 = \nabla \cdot \underline{A} \tag{10.27}$$

$$0 = \underline{n} \times \Delta\underline{A} \quad ; \quad 0 = \underline{n} \cdot \Delta\underline{A} \tag{10.28}$$

$$\underline{a} = \underline{n} \times \underline{A} \text{ on } S_a \quad ; \quad 0 = \underline{n} \cdot \underline{A} \text{ on } S_f \tag{10.29}$$

It is noted that the general divergence condition of eqn. 10.20 has been reduced to the familiar Coulomb gauge in eqn. 10.27. Enforcing eqns. 10.27-29 on the solution formulation renders it solvable. The curl condition in eqn. 10.27 is enforced by substitution into Ξ. The continuity conditions of eqns. 10.28 are inherent in the numerical trial functions, eqns. 10.12. This leaves the divergence and boundary conditions, eqns. 10.27 and 29, which will be considered in the following sections.

10.3.1 Boundary conditions

Physical specifications divide the boundary S into S_h and S_b sections, eqns. 10.6, while solvability conditions divide it into S_a and S_f. Obviously, the two divisions must correspond to each other in some suitable manner.

Consider first S_h, where there are no physical specifications on $\underline{A}$ or $\underline{B}$. No constraint on $\underline{n} \times \underline{A}$ is allowed because that would effectively constrain $\underline{B}$ via

$$\nabla_s \cdot (\underline{n} \times \underline{A}) = - \underline{n} \cdot (\nabla \times \underline{A}) = - \underline{n} \cdot \underline{B} \tag{10.30}$$

and hence violate physical specifications. By elimination, then, S_h is an S_f boundary :

$$\text{on } S_h \subset S_f : \quad \underline{n} \cdot \underline{A} = 0 \tag{10.31}$$

Imposition of eqns. 10.31 on the trial functions must avoid interaction between components so as not to constrain, implicitly, $\underline{n} \times \underline{A}$, and hence $\underline{n} \cdot \underline{B}$.

Consider next S_b. Comparison of eqns. 10.13 and 10.29 indicates that S_b sections on which $\nabla_s \beta$ can be pre-defined

belong to S_a; S_b sections on which $\nabla_s\beta$ cannot be pre-defined can only belong to S_f. S_b is thus divided into two parts

$$S_b = S_{ba} \cup S_{bf} , \quad S_{ba} \cap S_{bf} = 0 \tag{10.32}$$

where

$$\text{on } S_{ba} = S_a : \quad \underline{n} \times \underline{A} = \underline{a}_b + \nabla_s\beta = \underline{a} , \quad \beta \text{ pre-defined} \tag{10.33a}$$

and

$$\text{on } S_{bf} \subset S_f : \begin{cases} \underline{n} \times \underline{A} = \underline{a}_b + \nabla_s\beta , & \beta \text{ unknown} \\ \underline{n} \cdot \underline{A} = 0 \end{cases} \tag{10.33b}$$

From eqns. 10.31-33, the divisions of S in eqns. 10.6 and 10.22 are related by

$$S_a = S_{ba} \quad \text{and} \quad S_f = S_{bf} \cup S_h \tag{10.34}$$

Eqns. 10.31-34 apply to the general case. In the common case of eqns. 10.7 they reduce to

$$\text{on } S_h = S_f : \quad \underline{n} \cdot \underline{A} = 0 \tag{10.35a}$$

and

$$\text{on } S_b = S_a : \quad \underline{n} \times \underline{A} = 0 \tag{10.35b}$$

Specification of $\underline{n} \cdot \underline{A}$ on S_a can occur implicitly due to component interaction on discretised curved boundaries, or explicitly by prescribing

$$\text{on } S_b = S_a : \quad \underline{A} = 0 \tag{10.36}$$

instead of eqn. 10.35b. This choice does not violate physical specifications as does the prescription of $\underline{n} \times \underline{A}$ on S_h boundaries; it does, however, introduce an additional, inessential constraint. In two-dimensional analysis, for example, $\underline{n} \cdot \underline{A}$ is automatically zero on the boundary.

10.3.2 The divergence condition

The definition of analytic solvability adopted here requires the divergence condition of eqns. 10.27, i.e. the

Coulomb gauge, to be enforced. This can be achieved in a weak sense by defining a 'gauge error' as follows :

$$\Lambda_g = \tfrac{1}{2} \langle \eta(\underline{r}) \nabla \cdot \underline{A} , \nabla \cdot \underline{A} \rangle_R \qquad (10.37)$$

where $\eta(\underline{r})$ is a positive scalar distribution having the units of reluctivity

$$\eta(\underline{r}) > 0 \qquad (10.38)$$

Clearly, then

$$\Lambda_g \geqq 0 \qquad (10.39a)$$

with

$$\Lambda_g = 0 \quad <=> \quad \nabla \cdot \underline{A} = 0 \qquad (10.39b)$$

The total error is now the sum of the physically-based constitutive error Λ, and the computationally required gauge error Λ_g :

$$\Lambda_t = \Lambda + \Lambda_g \qquad (10.40)$$

From the fundamental property of Λ in ineq. 2.18, and that of Λ_g in ineq. 10.39, we have

$$\Lambda_t \geqq 0 \qquad (10.41a)$$

with

$$\Lambda_t = 0 \quad <=> \quad \Lambda = 0 \quad \text{and} \quad \Lambda_g = 0 \qquad (10.41b)$$

Thus both the constitutive relationship and the gauge condition are enforced weakly by minimising the total error :

$$0 = \delta\Lambda_t = \delta\Lambda + \delta\Lambda_g \qquad (10.42)$$

The B-system functional can be extracted from eqn. 10.40 by substituting for Λ from eqn. 10.16; we can then write

$$\Lambda_t(H,B) = \Theta(H) + \Xi_t(B) \qquad (10.43)$$

where

$$\Xi_t(B) = \Xi(B) + \Lambda_g(B) \qquad (10.44)$$

Substituting from eqn. 10.43 into 10.42, we get

$$0 = \delta\Theta(H) + \delta\Xi_t(B) \qquad (10.45)$$

As the H- and B-system variables are independent of each other, $\Theta(H)$ and $\Xi_t(B)$ can be extremised independently. The B-system solution can thus be obtained by extremising $\Xi_t(B)$

$$0 = \delta\Xi_t(B) \qquad (10.46)$$

instead of $\Xi(B)$ as in eqn. 10.18. Numerical formulation of eqn. 10.46 yields a non-singular, and hence solvable, solution matrix. The outcome of the solution is a numerical approximation to the analytically unique vector potential defined in eqns. 10.27-29.

Ξ_t is essentially similar to the functionals derived by Coulomb[10.4] and by Kotiuga and Silvester[10.2]. Coulomb's definition of an analytically unique vector potential is restricted to the boundary specifications of eqns. 10.7 and 10.35 which, in fact, cover the majority of practical applications. Kotiuga and Silvester extend the definition to allow multiply-connected regions; they consider a slightly restricted version of the boundary conditions 10.34 : S_{bf} is taken to be zero, which implies that all fluxes Φ_i are pre-specified; see text following eqns. 10.13.

The present error-based derivation extends the definition and applicability of Ξ_t to all problem specifications that cause the constitutive error Λ to split into H- and B-system functionals, $\Theta(H)$ and $\Xi(B)$ in eqn. 10.16. This is guaranteed for all physically well-posed problems whose specifications do not inter-relate $\underline{H}$ and $\underline{B}$ on the boundaries. Although only S_h- and S_b-type boundaries were considered in this chapter, Ξ in Ξ_t can accommodate all boundary conditions that satisfy specification 4 of sec. 3.4.1; according to sec. 3.4.2 they include cuts to account for multiply-connected regions, as well as open boundaries, recurrence relationships, etc. In all cases, the requirements of spec. 4 must be observed not only in the physical specification of the problem, but also in the definition of a unique vector potential.

10.3.3 Implementing the weak formulation

As yet, the multiplier $\eta(\underline{r})$ in the gauge error, eqn. 10.37, has not been defined beyond the requirement that it should be positive as in ineq. 10.38. Various weak gauging schemes in the literature can, in fact, be viewed as alternative definitions of $\eta(\underline{r})$.

In principle, $\eta(\underline{r})$ can be treated as an unknown distribution to be discretised and solved for. This is the method of Lagrangian multipliers[10.5,6] ; it results in a non-linear solution with an increased number of unknowns. The solution can be linearised by replacing Λ_g in eqn. 10.44 with $(\Lambda_g)^{\frac{1}{2}}$; this, however, invalidates ineq. 10.41a, so that the extremum principle is replaced by mere stationarity.

As Λ_g has been introduced for solvability, rather than physical uniqueness, it can be argued that optimisation of $\eta(\underline{r})$ is not essential. The practical difficulties associated with Lagrangian multipliers can then be avoided by pre-assigning $\eta(\underline{r})$. Clearly, some criterion must be established to assess suitability of $\eta(\underline{r})$ distributions. The present approach views the solution as an error minimising process, ineq. 10.41 and eqn. 10.42. The solution performance and outcome are therefore expected to reflect the relative magnitudes of the two errors involved : the constitutive error Λ, and the gauge error Λ_g. In effect, the multiplier $\eta(\underline{r})$ acts as a weighting factor; to ensure both physical accuracy and solvability, $\eta(\underline{r})$ must be so chosen that neither error dominates, locally or globally, to an extent that renders the other error negligible, and hence invisible to the solution process.

Now, of the various terms in Λ, the one most directly comparable to Λ_g is $\Psi(\underline{B})$; in linear isotropic media, eqn. 2.8b for Ψ and eqn. 10.8 for $\underline{B}$ yield

$$\Psi = \tfrac{1}{2} \langle \nu \, \nabla \times \underline{A} \, , \, \nabla \times \underline{A} \rangle_R \qquad (10.47)$$

There is, of course, a fundamental difference between Ψ and

Λ_g : the former is an energy, while the latter is an error that tends to zero as the exact solution is approached. In a numerical context, however, the comparison suggests that the choice of a suitable multiplier η can be guided by the corresponding reluctivity ν :

$$\eta(\underline{r}) \propto \nu(\underline{r}) \qquad (10.48)$$

In anisotropic media, the determinant of the reluctivity tensor may be used[10.4] .

Increasing the factor of proportionality in 10.48 causes the gauge condition to dominate the solution; decreasing it causes physical accuracy to dominate, which, of course, is preferable. At both extremes, the solution equations become ill-conditioned and, ultimately, unsolvable as one requirement or the other is totally lost. This provides the error approach interpretation of the ill-conditioning associated with the method of penalty functions[10.5,6] , which assigns a constant value to η throughout the region R : according to the present argument, the same η cannot be a suitable choice for regions of widely differing reluctivities, such as iron and air. A better choice, according to 10.48, is to set

$$\eta(\underline{r}) = \nu(\underline{r}) \qquad (10.49)$$

as proposed by Coulomb[10.4] and Chari et al.[10.7] . It is noted that $\Xi_t(B)$ reduces to the vector Poisson formulation of reference 10.7 for isotropic, piecewise linear regions. Both references 10.4 and 10.7 report satisfaction with the resulting formulation, which supports the above justification of proportionality 10.48.

But the present error-based argument goes somewhat further. It suggests that accuracy can be improved by choosing a smaller value for $\eta(\underline{r})$ to increase the weight of the constitutive error Λ relative to the gauge error Λ_g. The best course is to make η the smallest fraction of ν that retains well-conditioned solvability. Test runs to establish a suitable range for the fraction can start from the

equality in 10.49. It is noted that any definition of η that differs from 10.49 introduces an integral of the form $<(\eta-\nu)\nabla\cdot\underline{A}\,,\,\nabla\cdot\underline{A}>_R$ into the functional proposed by Chari et al.[10.7], and hence modifies the corresponding vector Poisson formulation.

10.4 Numerical solvability

The weak formulation of sec. 10.3 is based on $\Xi_t(B)$ which extends the physically derived B-system functional $\Xi(B)$ to include the gauge error Λ_g; solvability of the numerical extremisation of $\Xi_t(B)$, eqn. 10.46, is guaranteed by the uniqueness of the analytic vector potential that the solution approximates. There is an alternative, explicit, approach : $\Xi(B)$ itself is extremised, eqn. 10.18, with solvability enforced through numerical over-specification of the trial functions. This section discusses three treatments that adopt this second approach.

Csendes at al.[10.1] enforce the unique vector potential defined in eqns. 10.27-29. In particular, the numerically over-specified trial functions for $\underline{A}$ are constructed to have zero divergence, eqn. 10.27, by using projection operators to filter out divergent behaviour from standard finite element shape functions. In effect, the method over-constrains the trial functions, and minimises the constitutive error; in contrast, the weak formulation of sec. 10.3.2 allows freer trial functions, but minimises the total error Λ_t rather than the physically based constitutive error Λ. Relative accuracy of the two methods may be assessed by extrapolating the argument following proportionality 10.48 : by enforcing the divergence condition exactly, the explicit method effectively gives the gauge error Λ_g infinite weight relative to the constitutive error Λ : the latter is minimised only after the former has been set to zero exactly. This viewpoint suggests that the accuracy of the explicit approach is generally inferior to that of the weak formulation.

Demerdash et al.[10.8-11] enforce a unique vector potential whose definition differs from the general analytic one of eqns. 10.27-29. The definition applies to the numerically over-specified distribution : the region is discretised into finite elements having planar facets, with $\underline{A}$ constrained to vary linearly in space within the individual elements. Moreover, $\underline{A}$ is continuous across element interfaces, so that the continuity conditions of eqns. 10.28 are retained. Lastly, the boundary S includes a section S_A composed of at least two non-coplanar sub-sections sharing an edge, on which $\underline{A}$ is pre-defined completely :

$$\text{on } S_A \subset S_{ba} : \quad \underline{A} = \underline{A}_A \tag{10.50}$$

where $\underline{A}_A$ is known, usually zero. S_A must belong to S_{ba}, eqn. 10.33a, since pre-definition of $\underline{A}$ implies pre-definition of $\underline{n} \times \underline{A}$.

The proof of uniqueness of the discrete vector potential thus defined[10.10] is valid, although not general : firstly, it requires the physically-defined boundary section S_{ba} to include a suitably angled sub-section S_A; secondly, the mechanism of the proof places rather subtle restrictions on the topology of the finite element discretisation. Provided these minor restrictions are observed, the resulting numerical formulation is solvable. The absence of a divergence condition is of no consequence; computed results indicate that div $\underline{A}$ has no fixed pattern[10.11]. It thus appears that eqns. 10.27-29 are not strictly necessary, although certainly sufficient, to define a vector distribution uniquely. Indeed, the first three specifications of vector uniqueness in sec. 3.4.1 were assumed and not derived.

Clearly, this treatment lacks the generality of the weak formulation of sec. 10.3.2, the main restriction being its limitation to first order finite elements. Within this restriction, however, the explicit method appears to be the more accurate one since it corresponds to a minimisation of the physically-based constitutive error Λ, rather than the total error Λ_t as in the weak formulation. The comparison

is not quite straightforward : although both solutions use the same trial functions and impose the same essential boundary condition on $\underline{n} \times \underline{A}|_{S_b}$, they are constrained by different inessential boundary conditions. The explicit method imposes

$$\text{on } S_A \subset S_b : \quad \underline{n} \cdot \underline{A} = 0 \tag{10.51}$$

leaving $\underline{A}$ completely unconstrained on S_h. The weak formulation, on the other hand, imposes

$$\text{on } S_{bf} \cup S_h : \quad \underline{n} \cdot \underline{A} = 0 \tag{10.52}$$

and leaves $\underline{n} \cdot \underline{A}$ unconstrained on S_{ba}, which includes S_A. The influence of the differing constraints on accuracy is not obvious, although probably small.

The third treatment circumvents the question of uniqueness altogether by addressing solvability directly : a non-singular, and hence solvable, matrix is extracted from the singular one generated by the minimisation of $\Xi(B)$ in eqn. 10.18. Davidson and Balchin[10-12] implement this method using network theory techniques, which are directly applicable to the discrete network representation they have developed. The method minimises the constitutive error Λ, rather than the total error Λ_t, without explicitly over-constraining the trial functions; its accuracy would therefore be expected to compare favourably with that of the weak formulation of sec. 10.3.2. It is noted, however, that accuracy is not necessarily the same for all possible sets of linearly independent equations that can be extracted from the original singular matrix.

10.5 Conclusions

The present error-based approach leads to a general framework which accommodates most of the methods used to implement vector potential solvability. The constitutive error Λ, and its extension into a total error Λ_t, provide a useful criterion for comparing alternative treatments.

All the treatments considered are valid, i.e. consistent with physical specifications and solvable. Analytically-based solvability, sec. 10.3, has the advantage of generality, as it does not presuppose a particular method of numerical implementation. Numerically-based solvability is, by nature, more restrictive, but tends to be more accurate.

The error-based interpretation of formulations that enforce the divergence condition weakly, sec. 10.3.3, leads to a degree of generalisation, a natural assessment of accuracy, and a suggestion for improvement.

The presentation highlights the distinctions between the essential requirements of physical uniqueness of fields, and the inessential requirements of computational uniqueness of potentials. In particular, the specification and imposition of essential and inessential boundary conditions were reviewed in some detail. Moreover, non-divergence of the vector potential was found to be neither essential nor physically significant as had been suggested[10•1,2] . Methods that do not impose a gauge condition are equally valid as , and possibly more accurate than, methods that do; section 10.4 .

CHAPTER ELEVEN

Time-varying problems

11.1 Introduction

The process of solving a given electromagnetic problem is one of imposing its various specifications on the fields. The constitutive error approach enforces Maxwell, continuity, and boundary conditions explicitly, and minimises the error to enforce constitutive relationships weakly. This basic concept, introduced in sec. 3.5 for static models, is equally applicable to time-varying problems. Its implementation involves two major extensions relative to the static case :

(i) As Maxwell's equations regain their general time-varying forms, the specifications of sec. 3.4.1 become inadequate to define physically unique fields. The extensions involved are considered briefly in sec. 11.2 in conjunction with Appendix I.

(ii) A given static problem relates to one material property, and is classified accordingly : magnetostatic, electrostatic, or d.c. conduction. A time-varying problem, on the other hand, relates to two, or possibly all three, material properties. The corresponding constitutive relationships may be enforced simultaneously by minimising a suitably weighted combination of the individual errors. Sec. 11.2 constructs a general total error, and relates it to the requirements of uniqueness.

The bulk of the present chapter, sec. 11.3, is devoted to the extraction of complementary and dual eddy-current formulations from the corresponding total constitutive error. High frequency formulations are considered briefly in sec. 11.4

11.2 The general time-varying problem

Maxwell's equations and the constitutive relationships group the electromagnetic fields into H- and E-systems :

$$\text{H-system :}\quad \underline{H},\ \underline{J},\ \underline{D} \tag{11.1a}$$

$$\text{E-system :}\quad \underline{E},\ \underline{B} \tag{11.1b}$$

Associating Maxwell's equations with their respective systems, we have for the H-system

$$\nabla \times \underline{H} = \underline{J} + p\underline{D}\ , \qquad \nabla \cdot p\underline{D} = -\nabla \cdot \underline{J} = p\rho \tag{11.2a}$$

$$\underline{n} \times \Delta\underline{H} = \underline{K}\ , \qquad \underline{n} \cdot \Delta p\underline{D} = -\underline{n} \cdot \Delta\underline{J} = p\sigma \tag{11.2b}$$

and for the E-system

$$\nabla \times \underline{E} = -\, p\underline{B}\ , \qquad \nabla \cdot \underline{B} = 0 \tag{11.3a}$$

$$\underline{n} \times \Delta\underline{E} = 0\ , \qquad \underline{n} \cdot \Delta\underline{B} = 0 \tag{11.3b}$$

The general structure is shown in fig. 11.1. The fields are related in pairs by the constitutive relationships, eqns. 3.2, 3.7, and 3.12 of sec. 3.2.

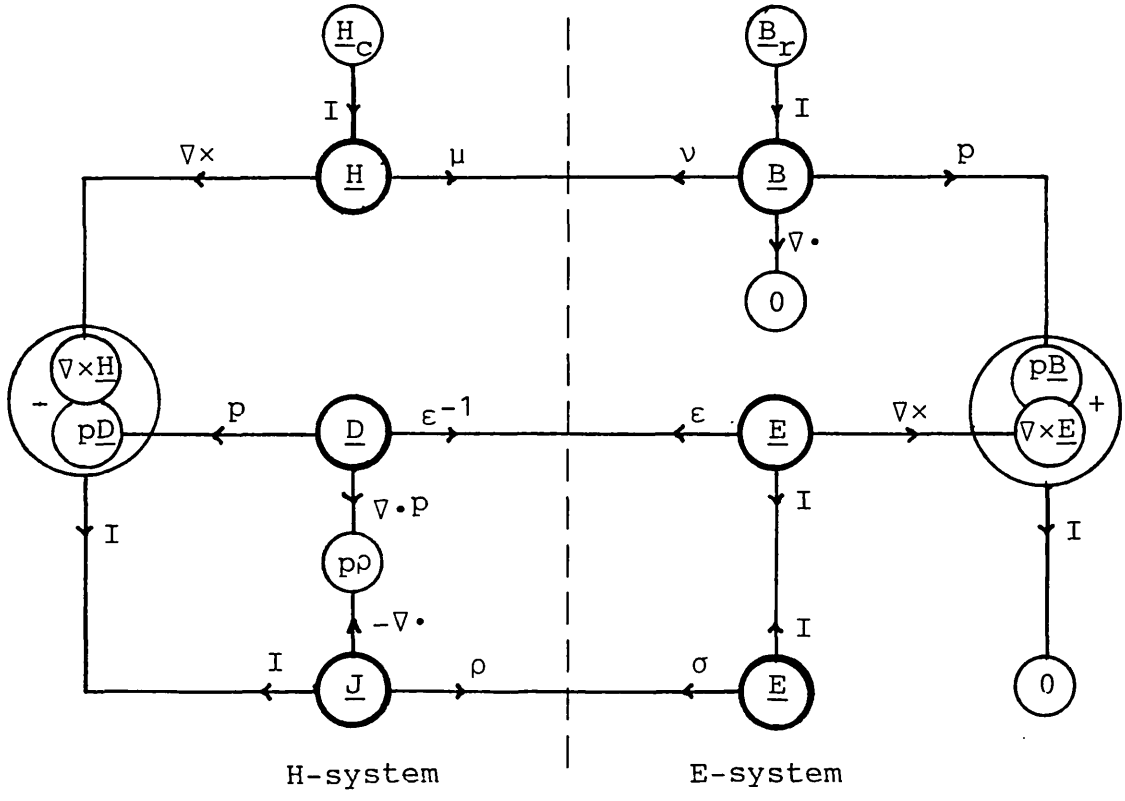

Fig. 11.1 General structure of time-varying systems.

The conditions of physical uniqueness may be derived by postulating two sets of fields as in sec. 3.4.1. Provided that the constitutive relationships retain property 1 of sec. 2.2, we can write

$$0 \leq W^m = \langle \delta\underline{H} , \delta\underline{B} \rangle_R$$

with

$$0 = W^m \quad <=> \quad \delta\underline{H} = 0 \quad \text{and} \quad \delta\underline{B} = 0 \tag{11.4a}$$

$$0 \leq W^e = \langle \delta\underline{D} , \delta\underline{E} \rangle_R$$

with

$$0 = W^e \quad <=> \quad \delta\underline{D} = 0 \quad \text{and} \quad \delta\underline{E} = 0 \tag{11.4b}$$

and

$$0 \leq W^f = \langle \delta\underline{J} , \delta\underline{E} \rangle_R$$

with

$$0 = W^f \quad <=> \quad \delta\underline{J} = 0 \quad \text{and} \quad \delta\underline{E} = 0 \tag{11.4c}$$

The required conditions are those which ensure that all three W's vanish. As each of the W's is positive, we can work with their weighted sum W :

$$0 \leq W = \beta^m W^m + \beta^e W^e + \beta^f p^{-1} W^f \tag{11.5a}$$

with

$$0 = W \quad <=> \quad W^m = 0 \ , \ W^e = 0 \ , \text{ and } \ W^f = 0 \tag{11.5b}$$

where β^m, β^e, and β^f are suitable positive coefficients. The time integration of W^f is necessitated by the physical units; if W^m and W^e are differentiated instead, positivity of the resulting sum cannot be guaranteed. Appendix I sketches a general derivation of uniqueness conditions.

If the constitutive relationships retain property 2 of sec. 2.2 as well, instantaneous constitutive error densities can be defined as follows :

$$0 \leq \lambda^m = \chi^m(\underline{H}) + \psi^m(\underline{B}) - \zeta^m(\underline{H},\underline{B}) \tag{11.6a}$$

with

$$0 = \lambda^m \quad <=> \quad \underline{B} = \mu\underline{H} + \underline{B}_r \quad \text{and} \quad \underline{H} = \nu\underline{B} + \underline{H}_c \tag{11.6b}$$

$$0 \leq \lambda^e = \chi^e(\underline{E}) + \psi^e(\underline{D}) - \zeta^e(\underline{D},\underline{E}) \tag{11.7a}$$

with

$$0 = \lambda^e \quad <=> \quad \underline{E} = \varepsilon^{-1}\underline{D} \quad \text{and} \quad \underline{D} = \varepsilon\underline{E} \tag{11.7b}$$

and

$$0 \leq \lambda^f = \chi^f(\underline{E}) + \psi^f(\underline{J}) - \zeta^f(\underline{J},\underline{E}) \qquad (11.8a)$$

with

$$0 = \lambda^f \quad <=> \quad \underline{E} = \rho\underline{J} \text{ and } \underline{J} = \sigma\underline{E} \qquad (11.8b)$$

λ^m, λ^e, and λ^f are the magnetic, electric, and current flow error densities, respectively. Their volume integrals over R yield the global errors Λ^m, Λ^e, and Λ^f. The constitutive relationships can be imposed on the fields by minimising the errors

$$0 = \delta\Lambda^m(\underline{H},\underline{B}), \quad 0 = \delta\Lambda^e(\underline{D},\underline{E}), \text{ and } \quad 0 = \delta\Lambda^f(\underline{J},\underline{E}) \qquad (11.9)$$

Under static conditions, the individual equations can be solved independently of each other as in previous chapters. Under general time-varying conditions, on the other hand, Maxwell's equations interrelate the fields so that the three equations must, in principle, be solved simultaneously. As each of the errors is positive, we can work with their weighted sum Λ :

$$0 \leq \Lambda = \alpha^m\Lambda^m + \alpha^e\Lambda^e + \alpha^f p^{-1}\Lambda^f \qquad (11.10a)$$

with

$$0 = \Lambda \quad <=> \quad \Lambda^m = 0 \ , \ \Lambda^e = 0 \ , \text{ and } \ \Lambda^f = 0 \qquad (11.10b)$$

where α^m, α^e, and α^f are arbitrary positive coefficients. Simultaneous solution of the three equations in 11.9 can thus be effected by minimising the total error :

$$0 = \delta\,\Lambda \qquad (11.11)$$

Substitution of eqns. 11.6-8 into 11.10a yields the initial composition of Λ :

$$\Lambda(H,E) = \Theta(H) + \Xi(E) - \Gamma(H,E) \qquad (11.12)$$

where

$$\Theta(H) = \alpha^m X^m(\underline{H}) + \alpha^e\psi^e(\underline{D}) + \alpha^f p^{-1}\psi^f(\underline{J})$$

$$\Xi(E) = \alpha^m\psi^m(\underline{B}) + \alpha^e X^e(\underline{E}) + \alpha^f p^{-1}X^f(\underline{E})$$

$$\Gamma(H,E) = \alpha^m Z^m(\underline{H},\underline{B}) + \alpha^e Z^e(\underline{D},\underline{E}) + \alpha^f p^{-1}Z^f(\underline{J},\underline{E})$$

$$= \alpha^m\langle\underline{H}\,,\,\underline{B}\rangle_R + \alpha^e\langle\underline{D}\,,\,\underline{E}\rangle_R + \alpha^f p^{-1}\langle\underline{J}\,,\,\underline{E}\rangle_R$$

We note the kinship between W in eqn. 11.5a and Γ. The

former must be zero for uniqueness, while the latter must be split between the H- and E-systems for separate , and independent, solution formulations. In general, complete decomposition of Γ, and hence Λ, is not guaranteed even for well-posed problems with independent H- and E-system boundary and continuity conditions. Such guarantees apply only to the static case, sec. 3.5. Their absence from the general time-varying case can be traced to the volume terms of the time integral of eqn. I.7 in Appendix I : there can be no step in the decomposition of Γ that corresponds to their elimination from W as in eqn. I.8.

The total constitutive error in its general form of eqn. 11.12 is of limited practical use. In most applications physical conditions and/or justifiable assumptions simplify Maxwell's equations and the corresponding composition of Λ. In particular, Λ^f does not arise in non-conductors, and Λ^e can be negligible at sufficiently slow time variation.

11.3 The eddy current problem

Under quasi-static conditions, the displacement current $p\underline{D}$ can be neglected, which reduces the H-system equations 11.2 to

$$\nabla \times \underline{H} = \underline{J} \quad , \quad \nabla \cdot \underline{J} = 0 \qquad (11.13a)$$

$$\underline{n} \times \Delta\underline{H} = \underline{K} \quad , \quad \underline{n} \cdot \Delta\underline{J} = 0 \qquad (11.13b)$$

The H-system potentials are defined by

$$\underline{H} = \underline{T} - \nabla\Omega \quad , \quad \underline{J} = \nabla \times \underline{T} \qquad (11.14)$$

Discontinuities in $\underline{T}$ and Ω are related as in sections 3.4.3 and 3.4.4.1 (with $\underline{G}$ replaced by $\underline{T}$). The E-system equations 11.3 are unchanged

$$\nabla \times \underline{E} = -p\underline{B} \quad , \quad \nabla \cdot \underline{B} = 0 \qquad (11.15a)$$

$$\underline{n} \times \Delta\underline{E} = 0 \quad , \quad \underline{n} \cdot \Delta\underline{B} = 0 \qquad (11.15b)$$

The E-system potentials are defined by

$$\underline{E} = - p\underline{A} - \nabla\phi \quad , \qquad \underline{B} = \nabla \times \underline{A} \tag{11.16a}$$

$$0 = \Delta\phi \quad , \qquad 0 = \underline{n} \times \Delta\underline{A} \tag{11.16b}$$

The two systems are related by the magnetic and conduction constitutive relationships

$$\underline{B} = \mu\underline{H} + \underline{B}_r \quad , \qquad \underline{H} = \nu\underline{B} + \underline{H}_c \tag{11.17}$$

$$\underline{E} = \rho\underline{J} \quad , \qquad \underline{J} = \sigma\underline{E} \tag{11.18}$$

Fig. 11.2 shows the structure of the eddy current problem. Fig. 11.3 shows the general division of the over-all region R into an eddy-current sub-region R_1 and a specified-current sub-region R_2

$$R = R_1 \cup R_2 \quad , \qquad R_1 \cap R_2 = 0 \tag{11.19}$$

Denoting the bounding surfaces of R, R_1, and R_2 by S, S_1, and S_2 respectively, we can write

$$S_{11} = S \cap S_1 \quad , \qquad S_{22} = S \cap S_2 \tag{11.20a}$$

$$S_1 = S_{11} \cup S_{12} \quad , \qquad S_2 = S_{22} \cup S_{12} \tag{11.20b}$$

and

$$S = S_{11} \cup S_{22} \quad , \qquad S_{12} = S_1 \cap S_2 \tag{11.20c}$$

R_1 refers to conductors where currents can be induced. R_2 includes source conductors where currents are specified, $\underline{J} = \underline{J}_s$ and $\underline{K} = \underline{K}_s$, as well as current-free parts, $\underline{J} = 0$. The current-describing vector potential $\underline{T}$ is pre-defined in R_2.

The presentation will be restricted to the following set of common boundary specifications, although the analysis can be extended to accommodate a wider range :

$$\text{on } S_{12} : \quad \underline{n} \cdot \underline{J} = 0 \tag{11.21a}$$

$$\text{on } S_{h1} : \quad \underline{n} \times \underline{H} = \underline{h} = 0 \quad \Rightarrow \quad \underline{n} \cdot \underline{J} = 0 \tag{11.21b}$$

$$\text{on } S_{e1} : \quad \underline{n} \times \underline{E} = \underline{e} \quad \Rightarrow \quad \underline{n} \times \underline{A} = \underline{a}, \quad \phi = \text{constant} \tag{11.21c}$$

$$\text{on } S_{h2} : \quad \underline{n} \times \underline{H} = \underline{h} \tag{11.21d}$$

$$\text{on } S_{b2} : \quad \underline{n} \cdot \underline{B} = b \quad \Rightarrow \quad n \times \underline{A} = \underline{a} \tag{11.21e}$$

$\underline{h}$, $\underline{e}$, b, and $\underline{a}$ are pre-defined, usually zero. Moreover

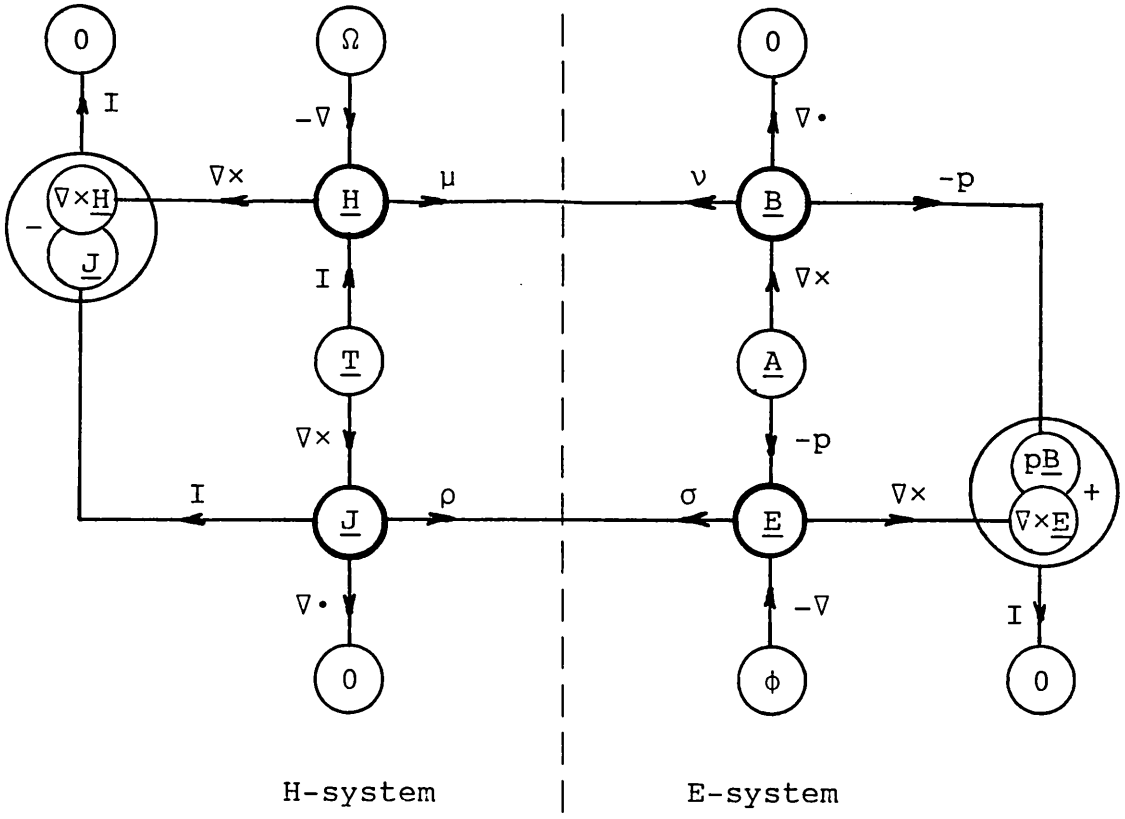

Fig. 11.2 Structure of the eddy-current problem, including potentials. $\underline{H}_c$ and $\underline{B}_r$ omitted for clarity.

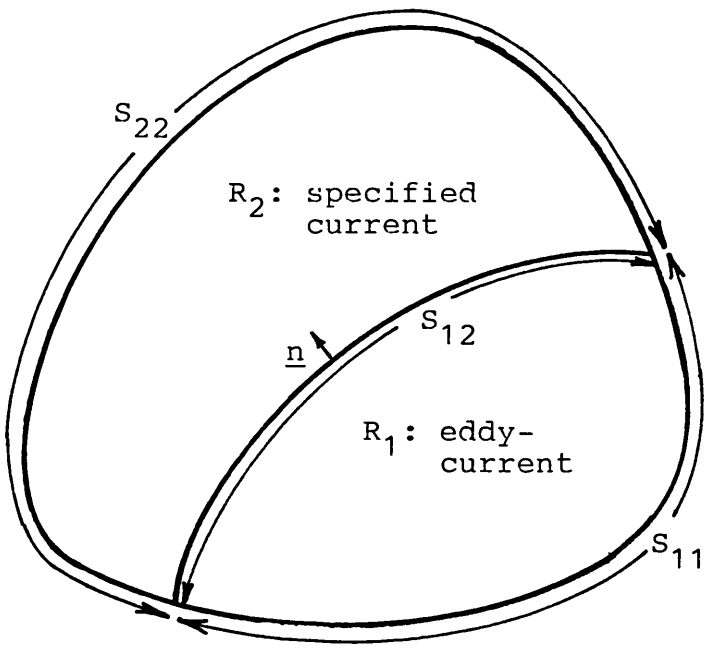

$$\underline{n}|_{S_{12}} = \underline{n}_1 = -\underline{n}_2$$

Fig. 11.3 Region partitioning in the eddy-current problem.

$$S_{11} = S_{h1} \cup S_{e1} \,, \qquad S_{h1} \cap S_{e1} = 0 \qquad (11.22a)$$

and

$$S_{22} = S_{h2} \cup S_{b2} \,, \qquad S_{h2} \cap S_{b2} = 0 \qquad (11.22b)$$

The boundary condition on S_{12}, eqn. 11.21a, arises from the continuity of $\underline{n} \cdot \underline{J}$ in eqns. 11.13b. If the eddy current region R_1 is wholly enclosed by R_2, we have

$$S_1 = S_{12} \,, \qquad S_{11} = 0 \qquad (11.23)$$

and the conditions on S_{h1} and S_{e1}, eqns. 11.21b and c, are irrelevant. Otherwise, S_{e1} usually denotes conductor terminals connected to the external circuit, with either voltage or current pre-defined, and S_{h1} denotes a plane of symmetry parallel to current flow. The boundary conditions on S_{h2} and S_{b2}, eqns. 11.21d and e, arise from symmetry, or approximate far boundaries, as in the magnetostatic case.

The total constitutive error Λ includes a magnetic error in R, Λ^m_R, and a current flow error in R_1, Λ^f_{R1}. Thus, eqns. 11.10 simplify to

$$0 \leq \Lambda = \Lambda^m_R + \alpha p^{-1} \Lambda^f_{R1} \qquad (11.24a)$$

with

$$0 = \Lambda \quad <=> \quad \Lambda^m_R = 0 \quad \text{and} \quad \Lambda^f_{R1} = 0 \qquad (11.24b)$$

No loss of generality is incurred by having set $\alpha^m = 1$. Exclusion of the electric error Λ^e may be based on the assumption that the electric constitutive relationship between $\underline{D}$ and $\underline{E}$ is satisfied exactly, or that, in an approximate solution, Λ^e is negligible compared to the retained errors, Λ^m and Λ^f. The current flow error in R_2, Λ^f_{R2}, is identically zero. Physically, the electric field $\underline{E}$ is indeterminate in non-conducting sub-regions of R_2; computationally, $\underline{E}$ in R_2 is irrelevant to the solution.

The initial composition of Λ can be obtained by substituting the volume integrals of eqns. 11.6a and 11.8a into 11.24a; we can then write

$$\Lambda(H,E) = \Theta_o(H) + \Xi_o(E) - \Gamma_o(H,E) \qquad (11.25)$$

where

$$\Theta_o(H) = X_R^m(\underline{H}) + \alpha p^{-1} \Psi_{R1}^f(\underline{J})$$

$$\Xi_o(E) = \Psi_R^m(\underline{B}) + \alpha p^{-1} X_{R1}^f(\underline{E})$$

$$\Gamma_o(H,E) = Z_R^m(\underline{H},\underline{B}) + \alpha p^{-1} Z_{R1}^f(\underline{J},\underline{E})$$

We now seek to split Λ between the H- and E-systems by decomposing the coupling term Γ_o. Recalling the general definition of Z in eqn. 2.11, we can write

$$\Gamma_o(H,E) = \langle \underline{H} , \underline{B} \rangle_R + \alpha p^{-1} \langle \underline{J} , \underline{E} \rangle_{R_1} \qquad (11.26)$$

Substituting for $\underline{B}$ and $\underline{E}$ by the E-system potentials $\underline{A}$ and ϕ according to eqns. 11.16, and applying vector identities and the divergence theorem :

$$\Gamma_o = \langle \underline{H} , \nabla \times \underline{A} \rangle_R - \alpha p^{-1} \langle \underline{J} , p\underline{A} + \nabla\phi \rangle_{R_1}$$

$$= \langle \nabla \times \underline{H} , \underline{A} \rangle_R + [\underline{n} \times \Delta\underline{H} , \underline{A}]_{S_k} - [\underline{n} \times \underline{H} , \underline{A}]_S$$

$$- \alpha p^{-1} \left(\langle \underline{J} , p\underline{A} \rangle_{R_1} - \langle \nabla \cdot \underline{J} , \phi \rangle_{R_1} + [\underline{n} \cdot \underline{J} , \phi]_{S_1} \right)$$

Substituting from the H-system equations 11.13 for $\nabla \times \underline{H}$, $\nabla \cdot \underline{J}$, and $\underline{n} \times \Delta\underline{H}$, and from the boundary conditions 11.21 into the boundary integrals :

$$\Gamma_o = \langle \underline{J}_s , \underline{A} \rangle_{R_2} + \langle \underline{J} , \underline{A} \rangle_{R_1} + [\underline{K}_s , \underline{A}]_{S_k} - [\underline{h} , \underline{A}]_{S_h}$$

$$+ [\underline{H} , \underline{a}]_{S_b} - \alpha p^{-1} \langle \underline{J} , p\underline{A} \rangle_{R_1} + \alpha p^{-1} \sum_{S_{el}} \phi I \qquad (11.27)$$

where

$$S_h = S_{h1} \cup S_{h2} , \qquad S_b = S_{e1} \cup S_{b2}$$

and the summation is over the terminals of the conductor R_1; ϕ and I denote the voltage and current inflow at the individual terminals. The ϕI products account for external circuit connections; they decompose readily if either voltage or current is specified. External connections through impedance may possibly be treated by defining an extended error as in sec. 6.7.2.

Substituting eqn. 11.27 back into 11.25, and rearranging, we can write

$$\Lambda(H,E) = \Theta(H) + \Xi(E) - \Gamma(H,E) \qquad (11.28)$$

where

$$\Theta(H) = X_R^m(\underline{H}) + \alpha p^{-1} \Psi_{R1}^f(\underline{J}) - [\underline{H},\underline{a}]_{S_b} - \alpha p^{-1} \sum \bar{I}\bar{\phi}$$

$$\Xi(E) = \Psi_R^m(\underline{B}) - \langle \underline{J}_s, \underline{A} \rangle_{R_2} + \alpha p^{-1} X_{R1}^f(\underline{E}) - [\underline{K}_s,\underline{A}]_{S_k} + [\underline{h},\underline{A}]_{S_h} - \alpha p^{-1} \sum \bar{I}\phi$$

$$\Gamma(H,E) = \langle \underline{J}, \underline{A} \rangle_{R_1} - \alpha p^{-1} \langle \underline{J}, p\underline{A} \rangle_{R_1}$$

$\bar{\phi}$ and $\bar{I}$ denote specified voltages and currents, respectively, on the terminals of R_1. Eqn. 11.28 represents the final stage of general decomposition of Λ; strictly, no further decomposition is possible as explained following eqn. 11.12. However, solution formulations can be extracted, although they do not correspond to a strict minimisation of the constitutive error Λ. Harmonic and transient formulations will be derived in sections 11.3.1 and 11.3.2 respectively. The multiplying factor α and the limits of the time integral will be shown to have prominent roles.

Having verified the separation of the boundary and current-sheet integrals in 11.28, we shall ignore them for simplicity. Further derivations will therefore be restricted to the following versions of Θ, Ξ, and Γ :

$$\Theta(H) = X_R^m(\underline{H}) + \alpha p^{-1} \Psi_{R1}^f(\underline{J}) \qquad (11.29a)$$

$$\Xi(E) = \Psi_R^m(\underline{B}) - \langle \underline{J}_s, \underline{A} \rangle_{R_2} + \alpha p^{-1} X_{R1}^f(\underline{E}) \qquad (11.29b)$$

$$\Gamma(H,E) = \langle \underline{J}, \underline{A} \rangle_{R_1} - \alpha p^{-1} \langle \underline{J}, p\underline{A} \rangle_{R_1} \qquad (11.29c)$$

The coupling term Γ, which will be the focus of our attention in the following sections, is unchanged from 11.28. The boundary integrals can always be reintroduced into the resultant formulations.

Eqns. 11.28 and 11.29 express Λ in what may be referred to as a primal form. An equally valid dual form can be derived by using the H-system potentials Ω and $\underline{T}$ to decompose Γ_o in eqn. 11.26. Potential discontinuities at conductor surfaces and cuts make the dual form rather awkward to work with in a treatment that aims at generality. We shall therefore consider the primal form only.

11.3.1 Steady a.c. conditions

Steady a.c. conditions, where all fields vary sinusoidally at the supply frequency, can arise only if all material properties are linear. Therefore, the present treatment assumes linear magnetic and conductive constitutive relationships. According to property 2 of sec. 2.2, linear constitutive operators are symmetric. Thus, for example

$$\chi(\underline{H}) = \tfrac{1}{2}\langle \mu\underline{H} , \underline{H}\rangle \quad \text{and} \quad \langle \mu\underline{H}_1 , \underline{H}_2\rangle = \langle \mu\underline{H}_2 , \underline{H}_1\rangle \tag{11.30}$$

Components of harmonic fields and potentials are represented by

$$u(\underline{r},t) = \hat{u}(\underline{r}) \cos(\omega t + \theta(\underline{r})) \tag{11.31}$$

where $\hat{u}(\underline{r})$ is the amplitude, $\theta(\underline{r})$ the phase angle, and ω the angular frequency. $u(\underline{r},t)$ may also be expressed in the form

$$u(\underline{r},t) = \frac{1}{\sqrt{2}}\left(u^c(\underline{r})e^{j\omega t} + u^*(\underline{r})e^{-j\omega t}\right) \tag{11.32a}$$

$$= \sqrt{2}\ \mathrm{Re}\{\, u^c(\underline{r})\ e^{j\omega t}\,\} \tag{11.32b}$$

where

$$u^c = \hat{u}e^{j\theta}/\sqrt{2} \quad \text{and} \quad u^* = \hat{u}e^{-j\theta}/\sqrt{2} \tag{11.32c}$$

u^c is the complex phasor associated with the instantaneous u; u^* is the complex conjugate of u^c. The instantaneous value of the product of two sinusoidal variables u and v is given by

$$\eta(\underline{r},t) = \langle u(\underline{r},t) , v(\underline{r},t)\rangle$$

$$= \eta^s(\underline{r}) + \tfrac{1}{2}\eta^c(\underline{r})e^{2j\omega t} + \tfrac{1}{2}\eta^*(\underline{r})e^{-2j\omega t}$$

$$= \eta^s(\underline{r}) + \mathrm{Re}\{\, \eta^c(\underline{r})\, e^{2j\omega t}\,\} \tag{11.33}$$

where

$$\eta^s = \tfrac{1}{2}\left(\langle u^c , v^*\rangle + \langle u^* , v^c\rangle\right)$$

$$= \mathrm{Re}\ \langle u^c , v^*\rangle = \mathrm{Re}\ \langle u^* , v^c\rangle$$

$$\eta^c = \langle u^c , v^c\rangle \quad \text{and} \quad \eta^* = \langle u^* , v^*\rangle = (\eta^c)^*$$

The product η has a time-invariant component η^s, and a double-frequency component whose associated phasor is η^c.

Ineq. 11.24a and eqn. 11.24b apply to the instantaneous constitutive error $\Lambda(t)$. As Λ and its components Θ, Ξ, and Γ in eqns. 11.28 and 11.29 are sums of products essentially similar to η in eqns. 11.33, they will each have time-invariant and double-frequency parts. In particular

$$\Gamma(t) = \Gamma^s + \tfrac{1}{2}\Gamma^c e^{2j\omega t} + \tfrac{1}{2}\Gamma^* e^{-2j\omega t} \qquad (11.34)$$

Using eqns. 11.32 to represent $\underline{J}(\underline{r},t)$ and $\underline{A}(\underline{r},t)$ in eqn. 11.29c for $\Gamma(t)$, performing the algebra, and collecting terms, we find

$$\Gamma^s = \mathrm{Re}\{ (1 + j\alpha\omega\tau)\langle \underline{J}^c , \underline{A}^* \rangle_{R_1} \}$$

$$\Gamma^c = \left(1 - \alpha \sin\omega\tau \,(\sin\omega\tau - j\cos\omega\tau)\right)\langle \underline{J}^c , \underline{A}^c \rangle_{R_1} \qquad (11.35)$$

where $\tau = t - t_o$ is the interval of the time integral of Λ^f in eqn. 11.24a. No values have, as yet, been assigned to α and τ; the choices are restricted by

$$\alpha > 0 \quad \text{and} \quad \tau > 0 \qquad (11.36)$$

to ensure positivity of the instantaneous error $\Lambda(t)$ as in ineq. 11.24a. Clearly, Γ^s cannot be eliminated, or split between the H- and E-systems, for any combination of values for α and τ. Γ^c on the other hand can be eliminated by choosing

$$\alpha = 1 \quad \text{and} \quad \omega\tau = \pi/2 \qquad (11.37)$$

Subject to ineq. 11.36, this is the only combination of α and τ that sets the coefficient in the expression for Γ^c in 11.35 to zero.

As already noted, the total constitutive error Λ can be expressed in the form

$$\Lambda(t) = \Lambda^s + \tfrac{1}{2}\Lambda^c e^{2j\omega t} + \tfrac{1}{2}\Lambda^* e^{-2j\omega t} \qquad (11.38a)$$

$$= \Lambda^s + \mathrm{Re}\{ \Lambda^c e^{2j\omega t} \} \qquad (11.38b)$$

Using eqns. 11.32 to represent the fields and potentials in eqns. 11.29, performing the algebra, and collecting terms, we can express the real, time-invariant component Λ^s as

$$\Lambda^s = \Theta^s(H) + \Xi^s(E) - \Gamma^s(H,E) \qquad (11.39)$$

where

$$\Theta^s = \frac{1}{2}\langle \mu \underline{H}^c , \underline{H}^* \rangle_R + \frac{\xi}{2}\langle \rho \underline{J}^c , \underline{J}^* \rangle_{R_1}$$

$$\Xi^s = \frac{1}{2}\langle \nu \underline{B}^c , \underline{B}^* \rangle_R + \frac{\xi}{2}\langle \sigma \underline{E}^c , \underline{E}^* \rangle_{R_1} - \mathrm{Re}\langle \underline{J}_s^c , \underline{A}^* \rangle_{R_2}$$

$$\Gamma^s = \mathrm{Re}\{ (1 + j\omega\xi) \langle \underline{J}^c , \underline{A}^* \rangle_{R_1} \}$$

and

$$\xi = \alpha\tau \quad (= \pi / 2\omega)$$

With α and τ as in eqns. 11.37, the complex phasor Λ^c, corresponding to the double-frequency component of Λ, can be expressed in the form

$$\Lambda^c = \Theta^c(H) + \Xi^c(E) \qquad (11.40)$$

where

$$\Theta^c = \frac{1}{2}\langle \mu \underline{H}^c , \underline{H}^c \rangle_R + \frac{1}{2j\omega}\langle \rho \underline{J}^c , \underline{J}^c \rangle_{R_1}$$

and

$$\Xi^c = \frac{1}{2}\langle \nu \underline{B}^c , \underline{B}^c \rangle_R + \frac{1}{2j\omega}\langle \sigma \underline{E}^c , \underline{E}^c \rangle_{R_1} - \langle \underline{J}_s^c , \underline{A}^c \rangle_{R_2}$$

The above results can be expressed in two-part notation where the general harmonic variable of eqn. 11.31 is represented in the form

$$u(\underline{r},t) = \sqrt{2}\,(u^r(\underline{r}) \cos\omega t - u^i(\underline{r}) \sin\omega t) \qquad (11.41a)$$

where

$$u^r = \hat{u} \cos\theta / \sqrt{2} \quad \text{and} \quad u^i = \hat{u} \sin\theta / \sqrt{2} \qquad (11.41b)$$

u^r and u^i are real variables. The product in eqn. 11.33 can also be expressed in two-part notation :

$$\eta(\underline{r},t) = \eta^s(\underline{r}) + \eta^r(\underline{r}) \cos 2\omega t - \eta^i(\underline{r}) \sin 2\omega t \qquad (11.42)$$

where

$$\eta^s = \langle u^r , v^r \rangle + \langle u^i , v^i \rangle$$

$$\eta^r = \langle u^r , v^r \rangle - \langle u^i , v^i \rangle$$

and

$$\eta^i = \langle u^r , v^i \rangle + \langle u^i , v^r \rangle$$

Respective comparison of eqns. 11.41 and 11.42 with eqns. 11.32 and 11.33 leads to

$$u^c = u^r + j u^i \quad \text{and} \quad \eta^c = \eta^r + j\eta^i \qquad (11.43)$$

u^c, u^r, and u^i correspond to the root mean square value of the instantaneous variable u, while η^c, η^r, and η^i correspond to the peak value of the instantaneous product η. The complex functionals in eqns. 11.38 and 11.40 can be expressed in two-part notation

$$\Lambda^c = \Lambda^r + j\,\Lambda^i \tag{11.44a}$$

$$\Theta^c = \Theta^r + j\,\Theta^i \tag{11.44b}$$

$$\Xi^c = \Xi^r + j\,\Xi^i \tag{11.44c}$$

Substituting for the variables and products in eqns. 11.38-40 by their two-part forms of eqns. 11.43, and collecting terms according to eqns. 11.44, we can write

$$\Lambda(t) = \Lambda^s + \Lambda^r \cos 2\omega t - \Lambda^i \sin 2\omega t \tag{11.45}$$

$$\Lambda^s(H,E) = \Theta^s(H) + \Xi^s(E) - \Gamma^s(H,E) \tag{11.46}$$

where

$$\Theta^s = \frac{1}{2}\langle \mu \underline{H}^r, \underline{H}^r \rangle_R + \frac{1}{2}\langle \mu \underline{H}^i, \underline{H}^i \rangle_R + \frac{\xi}{2}\langle \rho \underline{J}^r, \underline{J}^r \rangle_{R_1} + \frac{\xi}{2}\langle \rho \underline{J}^i, \underline{J}^i \rangle_{R_1}$$

$$\Xi^s = \frac{1}{2}\langle \nu \underline{B}^r, \underline{B}^r \rangle_R + \frac{1}{2}\langle \nu \underline{B}^i, \underline{B}^i \rangle_R + \frac{\xi}{2}\langle \sigma \underline{E}^r, \underline{E}^r \rangle_{R_1} + \frac{\xi}{2}\langle \sigma \underline{E}^i, \underline{E}^i \rangle_{R_1}$$
$$- \langle \underline{J}_s^r, \underline{A}^r \rangle_{R_2} - \langle \underline{J}_s^i, \underline{A}^i \rangle_{R_2}$$

$$\Gamma^s = \langle \underline{J}^r, \underline{A}^r \rangle_{R_1} + \langle \underline{J}^i, \underline{A}^i \rangle_{R_1} + \omega\xi \langle \underline{J}^r, \underline{A}^i \rangle_{R_1} - \omega\xi \langle \underline{J}^i, \underline{A}^r \rangle_{R_1}$$

$$\Lambda^r(H,E) = \Theta^r(H) + \Xi^r(E) \tag{11.47}$$

where

$$\Theta^r = \frac{1}{2}\langle \mu \underline{H}^r, \underline{H}^r \rangle_R - \frac{1}{2}\langle \mu \underline{H}^i, \underline{H}^i \rangle_R + \frac{1}{\omega}\langle \rho \underline{J}^r, \underline{J}^i \rangle_{R_1}$$

$$\Xi^r = \frac{1}{2}\langle \nu \underline{B}^r, \underline{B}^r \rangle_R - \frac{1}{2}\langle \nu \underline{B}^i, \underline{B}^i \rangle_R + \frac{1}{\omega}\langle \sigma \underline{E}^r, \underline{E}^i \rangle_{R_1}$$
$$- \langle \underline{J}_s^r, \underline{A}^r \rangle_{R_2} + \langle \underline{J}_s^i, \underline{A}^i \rangle_{R_2}$$

$$\Lambda^i(H,E) = \Theta^i(H) + \Xi^i(E) \tag{11.48}$$

where

$$\Theta^i = \langle \mu \underline{H}^r, \underline{H}^i \rangle_R - \frac{1}{2\omega}\langle \rho \underline{J}^r, \underline{J}^r \rangle_{R_1} + \frac{1}{2\omega}\langle \rho \underline{J}^i, \underline{J}^i \rangle_{R_1}$$

$$\Xi^i = \langle \nu \underline{B}^r, \underline{B}^i \rangle_R - \frac{1}{2\omega}\langle \sigma \underline{E}^r, \underline{E}^r \rangle_{R_1} + \frac{1}{2\omega}\langle \sigma \underline{E}^i, \underline{E}^i \rangle_{R_1}$$
$$- \langle \underline{J}_s^r, \underline{A}^i \rangle_{R_2} - \langle \underline{J}_s^i, \underline{A}^r \rangle_{R_2}$$

Having derived the expressions for the constitutive error $\Lambda(t)$ and its various components, we are now ready to consider solution formulations. It is emphasised that although the derivations employed the theory of complex numbers, $\Lambda(t)$ itself is real, instantaneous, and, indeed, non-negative. From eqns. 11.38, 44a, and 45, we can write

$$\Lambda(t) = \Lambda^s + |\Lambda^c| \cos\left(2\omega t + \tan^{-1}\frac{\Lambda^i}{\Lambda^r}\right) \qquad (11.49)$$

where

$$|\Lambda^c| = \left((\Lambda^r)^2 + (\Lambda^i)^2\right)^{\frac{1}{2}}$$

According to ineq. 11.24a then

$$\Lambda(t) \geqq 0 \quad \Rightarrow \quad \Lambda^s \geqq |\Lambda^c| \geqq 0 \qquad (11.50)$$

The above relationships are illustrated in fig. 11.4. From

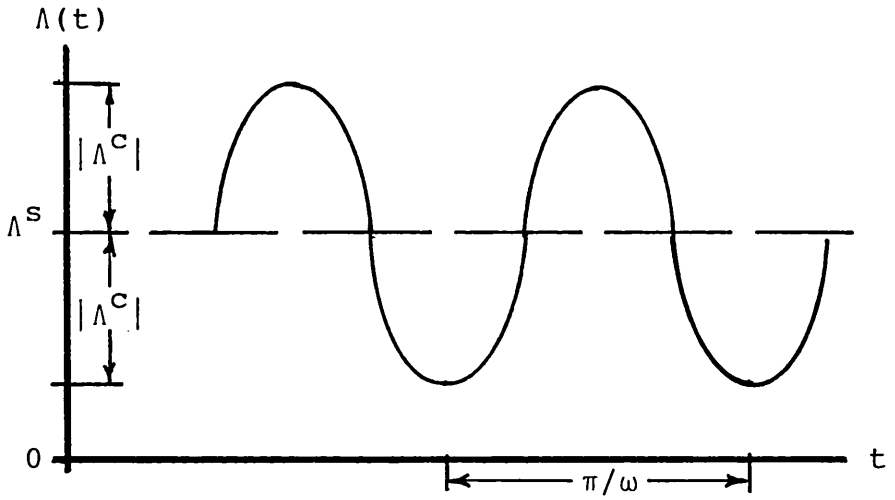

Fig. 11.4 The constitutive error as a function of time.

eqns. 11.24b and 11.38, we have at the exact solution

$$\Lambda(t) = 0 \quad \Rightarrow \quad \Lambda^s = 0 \quad \text{and} \quad \Lambda^c = 0 \qquad (11.51)$$

According to eqns. 11.11 and 11.45, the constitutive error is minimised by solving

$$0 = \delta\Lambda(t) = \delta\Lambda^s + (\delta\Lambda^r)\cos 2\omega t - (\delta\Lambda^i)\sin 2\omega t \qquad (11.52)$$

or

$$0 = \delta\Lambda^s \qquad (11.53)$$

$$0 = \delta\Lambda^r \quad \text{and} \quad 0 = \delta\Lambda^i \qquad (11.54)$$

Eqns. 11.54 can be combined using eqn. 11.44a :

$$0 = \delta\Lambda^r + j\,\delta\Lambda^i$$
$$= \delta\Lambda^c \qquad (11.55)$$

The constitutive error approach thus identifies two distinct variational principles, one based on the time-invariant component, eqn. 11.53, and the other on the double-frequency component, eqns. 11.54 and 11.55. We shall now examine the two principles and the solution formulations they generate.

As the time-invariant component Λ^s is non-negative, ineq. 11.50, its stationary point in eqn. 11.53 is a strict minimum. As it stands, however, eqn. 11.53 does not yield independent H- and E-system solution formulations because Λ^s does not split between the two systems, eqns. 11.39 and 11.46. Such formulations can only be derived from an approximate minimisation of Λ^s. Appendix J outlines the procedure involved, and, by way of example, extracts the following E-system formulation :

$$0 = \tfrac{1}{2}\delta\langle\nu\underline{B}^c,\underline{B}^*\rangle_R - \frac{1}{\omega}\mathrm{Im}\langle\sigma\underline{E}^c,\delta\underline{E}^*\rangle_{R_1} - \mathrm{Re}\langle\underline{J}_s^c,\delta\underline{A}^*\rangle_{R_2} \qquad (11.56)$$

The right hand side, specifically the second term, cannot be integrated to produce a functional. Eqn. 11.56 corresponds to solving

$$0 = \delta\Lambda^s - \xi\mathrm{Re}\langle\sigma\underline{E}^c-\underline{J}^c,\delta\underline{E}^*\rangle_{R_1} - \frac{1}{\omega}\mathrm{Im}\langle\sigma\underline{E}^c-\underline{J}^c,\delta E^*\rangle_{R_1} \qquad (11.57)$$

as an approximation to eqn. 11.53. In exact analysis, the additional term with Λ^s in 11.57 is set to zero as a redundant over-specification, sec. 5.2.2, since the solution is expected to impose the conductive constitutive relationship, eqns. 11.18, exactly. In numerical analysis, on the other hand, eqn. 11.56 describes an approximate formulation that lacks a minimum principle. Other formulations can be derived from alternative approximations of eqn. 11.53.

Alternatively, independent H- and E-system solution formulations can be obtained from the variational principle corresponding to the double-frequency component, eqns. 11.54 and 11.55. No assumptions or approximations are

needed because Λ^c, Λ^r, and Λ^i separate completely into H- and E-system functionals, eqns. 11.40, 47, and 48, resulting in the following complementary solution formulations :

$$0 = \delta\Theta^r(H) \quad , \quad 0 = \delta\Xi^r(E) \tag{11.58}$$

$$0 = \delta\Theta^i(H) \quad , \quad 0 = \delta\Xi^i(E) \tag{11.59}$$

$$0 = \delta\Theta^c(H) \quad , \quad 0 = \delta\Xi^c(E) \tag{11.60}$$

Unlike Λ^s, and indeed $\Lambda(t)$, Λ^r and Λ^i can be either positive or negative. It follows that variational principles based on the double-frequency component of the constitutive error, eqns. 11.54, 55, and 58-60, represent mere stationarity and are not extremal. The Θ and Ξ functionals correspond to the double-frequency component of system energy. Each is a convex-concave (or concave-convex) saddle functional[11.1] ; $\Theta^r(H)$, for example, is convex with respect to $\underline{H}^r$ and concave with respect to $\underline{H}^i$, eqn. 11.47. At the exact solution we have, from eqn. 11.51,

$$0 = \Lambda^r = \Theta^r + \Xi^r \quad \Rightarrow \quad \Theta^r = -\Xi^r \tag{11.61a}$$

$$0 = \Lambda^i = \Theta^i + \Xi^i \quad \Rightarrow \quad \Theta^i = -\Xi^i \tag{11.61b}$$

$$0 = \Lambda^c = \Theta^c + \Xi^c \quad \Rightarrow \quad \Theta^c = -\Xi^c \tag{11.61c}$$

In the numerical formulation of static problems, it was possible to state that the solution picks out the field distributions corresponding to the minimum constitutive error for the given numerical over-specifications or constraints. In the harmonic eddy-current problem, such a statement would apply to the true minimisation of the time-invariant error Λ^s in eqn. 11.53, which requires simultaneous solution of H- and E-systems. The statement does not hold for formulations based on approximate minimisation of Λ^s, eg. eqn. 11.56, or on the non-extremal double-frequency component, eqns. 11.58-60. Moreover, energy bounds are not defined : Λ^s does not split between the H- and E-systems, while Λ^i and Λ^r are not guaranteed to be non-negative. The constitutive error, on the other hand, is always defined and computable.

The analysis and derivations presented in this section indicate that the constitutive error approach is an effective tool for constructing complementary and dual formulations of the harmonic eddy-current problem. Perhaps more importantly, the approach provides an interpretive framework, in terms of steady and double-frequency error components, that can accommodate various formulations. Appendix K, which outlines alternative derivations of complementary formulations, shows that Hammond's approach[11.2] corresponds to the steady error, while Fraser's[11.3] corresponds to the double-frequency error. The Appendix further shows that the present error-based approach is in agreement with their respective solution formulations, but not with the complex power and energy functionals they propose.

11.3.2 Transient conditions

The transient problem starts from known initial field distributions; subsequent time-dependence of the fields is not known. Eqn. 11.28 expresses the instantaneous constitutive error $\Lambda(t)$ which does not split into independent H- and E-system functionals : the coupling term, Γ in eqn. 11.29c, cannot be split or eliminated. The solution can still be obtained by minimising $\Lambda(t)$:

$$0 = \delta\Lambda = \delta\Theta(H) + \delta\Xi(E) - \delta\Gamma(H,E) \qquad (11.62a)$$

$$= \delta_H + \delta_E \qquad (11.62b)$$

where, using eqns. 11.29,

$$\delta_H = \langle \mu\underline{H}+\underline{B}_r, \delta\underline{H}\rangle_R + \alpha\int_{t_o}^{t}\langle \rho\underline{J}, \delta\underline{J}\rangle_{R_1}dt$$
$$- \langle \underline{A}, \delta\underline{J}\rangle_{R_1} + \alpha\int_{t_o}^{t}\langle p\underline{A}, \delta\underline{J}\rangle_{R_1}dt \qquad (11.63a)$$

$$\delta_E = \langle \nu\underline{B}+\underline{H}_c, \delta\underline{B}\rangle_R - \alpha\int_{t_o}^{t}\langle \sigma\underline{E}, \nabla\delta\phi\rangle_{R_1}dt - \alpha\int_{t_o}^{t}\langle \sigma\underline{E}, \delta p\underline{A}\rangle_{R_1}$$
$$- \langle \underline{J}_s, \delta\underline{A}\rangle_{R_2} - \langle \underline{J}, \delta\underline{A}\rangle_{R_1} + \alpha\int_{t_o}^{t}\langle \underline{J}, \delta p\underline{A}\rangle_{R_1}dt \qquad (11.63b)$$

All variables and products are at time t unless otherwise

indicated. α and t_o may be chosen arbitrarily provided

$$\alpha > 0 \qquad \text{and} \qquad t_o < t \tag{11.64}$$

to maintain the positivity of $\Lambda(t)$, ineq. 11.24a. The notation δ_H and δ_E reflects the absence of corresponding functionals. Only H-system parameters are varied in δ_H, and only E-system parameters are varied in δ_E. As these parameters are independent of each other, eqn. 11.62b generates the complementary formulations

$$0 = \delta_H \tag{11.65a}$$

and

$$0 = \delta_E \tag{11.65b}$$

In principle, the two equations must be solved simultaneously due to the presence of the E-system variable $\underline{A}$ in δ_H, and the H-system variable $\underline{J}$ in δ_E.

In exact analysis, the solutions can be uncoupled by introducing redundant over-specifications, sec. 5.2.2, in conjunction with suitable values of α and t_o. For example, we may set

$$\alpha = 1 \qquad \text{and} \qquad t_o = 0 \tag{11.66}$$

where $t = 0$ is the initial instant at which the fields are known. Substituting into 11.63b, and performing standard calculus operations, δ_E can be rewritten in the form

$$\delta_E = \delta_{EE} + \delta_{EH} \tag{11.67}$$

where

$$\delta_{EE} = \langle \nu\underline{B}+\underline{H}_c, \delta\underline{B}\rangle_R - \langle \underline{J}_s, \delta\underline{A}\rangle_{R_2} - \langle \sigma\underline{E}, \delta\underline{A}\rangle_{R_1}$$
$$- \int_0^t \langle \sigma\underline{E}, \nabla\delta\phi\rangle_{R_1} dt + \langle \sigma\underline{E} - \underline{J}\ ,\ \delta\underline{A}\rangle_{R_1}\Big|_{t=0}$$

and

$$\delta_{EH} = \int_0^t \langle p(\sigma\underline{E} - \underline{J})\ ,\ \delta\underline{A}\rangle_{R_1} dt$$

It is noted that δ_{EE} is free of H-system variables, $\underline{J}\big|_{t=0}$ being known. Replacing eqns. 11.62 by

$$0 = \delta\Lambda - \delta_{EH} = \delta_H + \delta_{EE} \tag{11.68}$$

we obtain the modified complementary formulations

$$0 = \delta_H \tag{11.69a}$$

and

$$0 = \delta_{EE} \tag{11.69b}$$

Eqn. 11.69b describes an E-formulation that can be solved independently. The solution is not associated with a minimum principle because it corresponds to the approximate minimisation of Λ in 11.68 rather than its true minimisation in 11.62. The approximation is justified by the fact that exact solution enforces the conductive constitutive relationship exactly, so that

$$\delta_{EH} = 0 \tag{11.70}$$

can be viewed as a redundant over-specification. Other formulations can be derived from alternative approximations of eqn. 11.62. The treatment is similar to that described in Appendix J for the harmonic case, with eqns. 11.56 and 57 as a particular example.

Non-extremal formulations similar to eqn. 11.69b can, of course, be formulated numerically. However, it is more practical to introduce the approximate minimisation after $\Lambda(t)$ has been discretised in time : the discrete time-dependence of the variables may suggest α and t_o values that differ from those of the corresponding exact formulation, eg. eqns. 11.66, as we shall now illustrate.

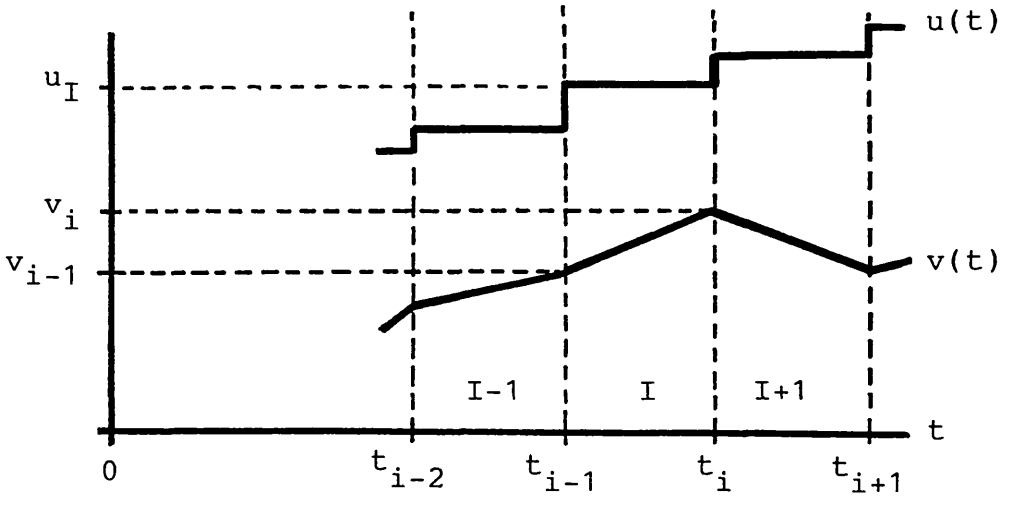

Fig. 11.5 Time discretisation.

With time divided into discrete intervals as in fig. 11.5, the solution starts at the first interval, with known initial fields at $t = 0$, and proceeds forward in steps. During interval I, where

$$t_{i-1} \leqq t \leqq t_i \tag{11.71}$$

we choose

$$t_o = t_{i-1} \tag{11.72}$$

so that the constitutive error of eqn. 11.24a is now defined by

$$\Lambda(t) = \Lambda_R^m(t) + \alpha \int_{t_{i-1}}^{t} \Lambda_{R1}^f(t)\, dt \tag{11.73}$$

The solution may then be obtained by minimising the error

$$0 = \delta\Lambda(t) \tag{11.74}$$

at one or more instants, depending on the number of degrees of freedom associated with the discrete representation of the variables during interval I. Fig. 11.5 illustrates zero and first order time functions :

$$u(t) = u_I \tag{11.75}$$

and

$$v(t) = \frac{1}{\Delta t}\left((t_i - t)v_{i-1} + (t - t_{i-1})v_i\right) \tag{11.76}$$

where

$$\Delta t = t_i - t_{i-1} \tag{11.77}$$

Each of the two functions has one degree of freedom within interval I : u_I in eqn. 11.75, and v_i in eqn. 11.76. v_{i-1} in eqn. 11.76 is known from the solution of the preceding interval I-1; thus, during interval I,

$$\delta v_{i-1} = 0 \tag{11.78}$$

With the variables represented by either function, Λ can be minimised at only one instant. Any instant other than $t_{i-1} = t_o$ may be selected. We shall choose t_i, but note that the choice is not, in general, trivial as it leads to differing numerical formulations and hence computational results.

Let us now use eqn. 11.75 to discretise the eddy-current distribution $\underline{J}$ and its vector potential $\underline{T}$, and use eqn. 11.76 to discretise all other fields and potentials. This choice is entirely consistent within the H- and E-systems individually. The apparent inconsistency between a constant $\underline{J}$ and a linear $\underline{E}$ is legitimate because the constitutive relationship linking them is not enforced rigidly, but weakly through error minimisation, eqn. 11.74. It is noted that the magnetic vector potential discretisation must be at least continuous in time due to the presence of $p\underline{A}$ in the integrals of eqns. 11.63; thus $\underline{A}$, and hence $\underline{B}$, may not be represented by eqn. 11.75. With the variables discretised in time as just described, eqns. 11.63 and 11.65 yield the following interdependent complementary formulations at t_i :

$$0 = \langle \mu \underline{H}_i + \underline{B}_r, \delta \underline{H}_i \rangle_R + \alpha \Delta t \langle \rho \underline{J}_I, \delta \underline{J}_I \rangle_{R_1} - \langle \alpha \underline{A}_{i-1} + (1-\alpha) \underline{A}_i, \delta \underline{J}_I \rangle_{R_1} \quad (11.79a)$$

and

$$0 = \langle \nu \underline{B}_i + \underline{H}_c, \delta \underline{B}_i \rangle_R - \frac{\alpha}{2} \langle \sigma \underline{E}_{i-1} + \sigma \underline{E}_i, \delta \underline{A}_i \rangle_{R_1} + \frac{\alpha \Delta t}{6} \langle \sigma \underline{E}_{i-1} + 2\sigma \underline{E}_i, \delta \nabla \phi_i \rangle_{R_1} - \langle \underline{J}_s(t_i), \delta \underline{A}_i \rangle_{R_2} + (\alpha - 1) \langle \underline{J}_I, \delta \underline{A}_i \rangle_{R_1} \quad (11.79b)$$

The two equations are coupled through their respective last terms. The natural choice for α appears to be

$$\alpha = 1 \quad (11.80)$$

which simplifies eqns. 11.79 to

$$0 = \langle \mu \underline{H}_i + \underline{B}_r, \delta \underline{H}_i \rangle_R + \Delta t \langle \rho \underline{J}_I, \delta \underline{J}_I \rangle_{R_1} - \langle \underline{A}_{i-1}, \delta \underline{J}_I \rangle_{R_1} \quad (11.81a)$$

and

$$0 = \langle \nu \underline{B}_i + \underline{H}_c, \delta \underline{B}_i \rangle_R - \frac{1}{2} \langle \sigma \underline{E}_{i-1} + \sigma \underline{E}_i, \delta \underline{A}_i \rangle_{R_1} + \frac{\Delta t}{6} \langle \sigma \underline{E}_{i-1} + 2\sigma \underline{E}_i, \delta \nabla \phi_i \rangle_{R_1} - \langle \underline{J}_s(t_i), \delta \underline{A}_i \rangle_{R_2} \quad (11.81b)$$

Clearly, the choice of α in eqn. 11.80 has eliminated the coupling term from the E-formulation of eqn. 11.81b, which can now be solved independently of eqn. 11.81a. The same cannot be said of the H-formulation of eqn. 11.81a which has retained the E-system potential $\underline{A}_{i-1}$; true minimisation of the constitutive error requires the E-solution of the

preceding interval I-1 to be available as input to the H-solution of 11.81a. Approximate minimisation can be achieved as follows. Integrating eqn. 11.16a, and rearranging, $\underline{A}_{i-1}$ may be expressed by

$$\underline{A}_{i-1} = \underline{A}(0) - \int_0^{t_{i-1}} \nabla\phi \, dt - \int_0^{t_{i-1}} \underline{E} \, dt \qquad (11.82)$$

This is to be substituted for $\underline{A}_{i-1}$ in the last term of eqn. 11.81a. Now $\underline{A}(0)$ is known from initial conditions. The product involving the ϕ integral can be transformed into surface integrals over S_1 where either ϕ or $\underline{n} \cdot \underline{J}_I$ is known. Assuming $\underline{A}(0)$ and ϕ are zero for simplicity, eqn. 11.81a can be written in the form

$$0 = \langle \mu\underline{H}_i + \underline{B}_r, \delta\underline{H}_i \rangle_R + \Delta t \langle \rho\underline{J}_I, \delta\underline{J}_I \rangle_{R_1} + \langle \int_0^{t_{i-1}} \rho\underline{J} \, dt \, , \delta\underline{J}_I \rangle_{R_1}$$
$$+ \langle \int_0^{t_{i-1}} (\underline{E} - \rho\underline{J}) dt \, , \delta\underline{J}_I \rangle_{R_1} \qquad (11.83)$$

Dropping the last term yields an independent H-formulation which corresponds to the approximate minimisation

$$0 = \delta\Lambda(t_i) - \langle \int_0^{t_{i-1}} (\underline{E} - \rho\underline{J}) dt \, , \delta\underline{J}_I \rangle_{R_1} \qquad (11.84)$$

rather than the true one of eqn. 11.74.

Let us next derive the formulations with all variables, including $\underline{J}$ and $\underline{T}$, discretised linearly in time as in eqn. 11.76. Eqns. 11.63 and 11.65 then yield the following complementary formulations at t_i :

$$0 = \langle \mu\underline{H}_i + \underline{B}_r, \delta\underline{H}_i \rangle_R + \frac{\alpha\Delta t}{6} \langle \rho\underline{J}_{i-1} + 2\rho\underline{J}_i, \delta\underline{J}_i \rangle_{R_1}$$
$$+ \frac{1}{2} \langle \alpha\underline{A}_{i-1} + (2 - \alpha)\underline{A}_i \, , \delta\underline{J}_i \rangle_{R_1} \qquad (11.85a)$$

and

$$0 = \langle \nu\underline{B}_i + \underline{H}_c, \delta\underline{B}_i \rangle_R - \frac{\alpha}{2} \langle \sigma\underline{E}_{i-1} + \sigma\underline{E}_i, \delta\underline{A}_i \rangle_{R_1}$$
$$+ \frac{\alpha\Delta t}{6} \langle \sigma\underline{E}_{i-1} + 2\sigma\underline{E}_i, \delta\nabla\phi_i \rangle_{R_1} - \langle \underline{J}_s(t_i), \delta\underline{A}_i \rangle_{R_2}$$
$$+ \frac{1}{2} \langle \alpha\underline{J}_{i-1} + (\alpha - 2)\underline{J}_i \, , \delta\underline{A}_i \rangle_{R_1} \qquad (11.85b)$$

Once again, the two equations are coupled through their respective last terms. In this case, however, no value of α can make either formulation independent. Let us choose

$$\alpha = 2 \qquad (11.86)$$

This choice assigns more weight to the conductive constitutive error, eqn. 11.73, causing a true minimum solution to cater for the conductive constitutive relationship. Substitution into eqns. 11.85 simplifies them to

$$0 = \langle \mu \underline{H}_i + \underline{B}_r, \delta \underline{H}_i \rangle_R + \frac{\Delta t}{3} \langle \rho \underline{J}_{i-1} + 2\rho \underline{J}_i, \delta \underline{J}_i \rangle_{R_1} - \langle \underline{A}_{i-1}, \delta \underline{J}_i \rangle_{R_1} \qquad (11.87a)$$

and

$$0 = \langle \nu \underline{B}_i + \underline{H}_c, \delta \underline{B}_i \rangle_R - \langle \sigma \underline{E}_i, \delta \underline{A}_i \rangle_{R_1} + \frac{\Delta t}{3} \langle \sigma \underline{E}_{i-1} + 2\sigma \underline{E}_i, \delta \nabla \phi_i \rangle_{R_1} - \langle \underline{J}_s(t_i), \delta \underline{A}_i \rangle_{R_2} + \langle \underline{J}_{i-1} - \sigma \underline{E}_{i-1}, \delta \underline{A}_i \rangle_{R_1} \qquad (11.87b)$$

As expected, the coupling terms have not been eliminated completely. Rather interestingly, the two equations can be solved independently of each other during the current interval I, but each requires the complementary solution of the previous interval I-1 : the H-formulation of eqn. 11.87a requires the E-system potential $\underline{A}_{i-1}$, while the E-formulation of eqn. 11.87b requires the H-system current density $\underline{J}_{i-1}$. For true minimisation of $\Lambda(t_i)$, the two solutions must proceed together through time; they can be interleaved since the equations need not be solved simultaneously at the individual intervals. As on previous occasions, independent formulations can be extracted from approximate minimisation. The coupling term retained in eqn. 11.87a is similar to that of eqn. 11.81a, and can be treated in the same way; the corresponding approximation is that of eqn. 11.84 with $\underline{J}_I$ replaced by $\underline{J}_i$. Similarly, dropping the last term in eqn. 11.87b yields an independent E-formulation corresponding to the approximate minimisation

$$0 = \delta \Lambda(t_i) - \langle \underline{J}_{i-1} - \sigma \underline{E}_{i-1}, \delta \underline{A}_i \rangle_{R_1} \qquad (11.88)$$

The independent E-formulation extracted from eqn. 11.87b is not identical to that of eqn. 11.81b despite the fact that the time discretisation of the E-system variables is the same in both cases. This is due to the differing values of α, eqns. 11.80 and 86, in conjunction with differing time discretisations of the complementary, H-system variables. Indeed, the presentation is intended to illustrate the range of options available; clearly, these

have not been exhausted, so that other formulations are possible. One factor that was mentioned, but not explored, is the choice of particular instant(s), within the interval, at which the constitutive error is minimised.

The E-formulation of eqn. 11.81b is of particular interest as it corresponds to a true minimisation of the constitutive error, yet employs the simplest allowable time functions : piecewise constant in $\underline{J}$, and linear in $\underline{B}$. Higher order polynomials are generally associated with better accuracy; however, they lead to approximate, rather than true, minimisation. The degree of divergence from a true minimum principle is indicated by the variational statement of the approximate minimisation, eg. eqns. 11.68, 84, and 88.

The constitutive error cannot be split completely between the H- and E-systems. This has led to the general absence of minimum principles. It also implies that energy bounds cannot be defined. The error itself is, as usual, defined and computable, locally and globally.

The complementary formulations of this section may be regarded as belonging to a primal set originating in eqn. 11.28, which was derived from the general expression for the constitutive error using E-system potentials. Use of H-system potentials for the purpose yields a dual set of complementary formulations.

11.3.3 Conclusions

The physical specifications of the eddy-current problem do not allow the constitutive error to split into independent H- and E-system functionals. This results in the absence of bounds on energy estimates. Moreover, with the exception of eqn. 11.81b, the solution formulations are not associated with minimum principles. Minimisation of the universally positive constitutive error can be regarded as a reference point from which the formulations diverge by

varying, and generally identifiable, degrees, eg. eqns. 11.57, 68, 84, and 88. These equations describe the approximate minimisations effected by their corresponding formulations. Alternatively, the formulations may be considered to effect a true minimisation of the constitutive error, but with certain complementary fields approximated by own system estimates, say $\sigma\underline{E}$ for $\underline{J}$, or $\rho\underline{J}$ for $\underline{E}$. This simpler viewpoint has the disadvantage of masking the processes involved in the solution.

The adverse effects on solution accuracy and economy arising from the absence of a minimum principle may be countered by refining time and space discretisations to approach exact conditions where the formulations are totally justified, eqn. 11.70. However, this diminishes the acknowledged advantage of independent complementary solutions over simultaneous H- and E-system solutions : although the latter solve for variables of both systems, they can do with coarser discretisations because they truly minimise the constitutive error. This is particularly significant in cases where the simultaneous solutions are only loosely interdependent; for example, eqns. 11.87 are solved independently in the individual intervals, as already explained.

11.4 A high frequency problem

In the absence of conduction currents, Maxwell's H-system equations 11.2 reduce to

$$\nabla \times \underline{H} = p\,\underline{D} \quad , \quad \nabla \cdot \underline{D} = 0 \qquad (11.89a)$$

$$\underline{n} \times \Delta\underline{H} = 0 \quad , \quad n \cdot \Delta\underline{D} = 0 \qquad (11.89b)$$

The E-system equations 11.3 are unchanged

$$\nabla \times \underline{E} = -p\,\underline{B} \quad , \quad \nabla \cdot \underline{B} = 0 \qquad (11.90a)$$

$$\underline{n} \times \Delta\underline{E} = 0 \quad , \quad \underline{n} \cdot \Delta\underline{B} = 0 \qquad (11.90b)$$

The two systems are related by linear magnetic and electric

constitutive relationships :

$$\underline{B} = \mu \underline{H} \quad , \quad \underline{H} = \nu \underline{B} \tag{11.91a}$$

and

$$\underline{E} = \varepsilon^{-1} \underline{D} \quad , \quad \underline{D} = \varepsilon \underline{E} \tag{11.91b}$$

The following conditions will be assumed on the bounding surface S

$$\underline{n} \times \underline{H} = \underline{h} \text{ on } S_h \quad , \quad \underline{n} \times \underline{E} = \underline{e} \text{ on } S_e \tag{11.92a}$$

where

$$S = S_h \cup S_b \quad , \quad 0 = S_h \cap S_b \tag{11.92b}$$

Fig. 11.6 shows the structure of the high frequency problem specified by the above equations.

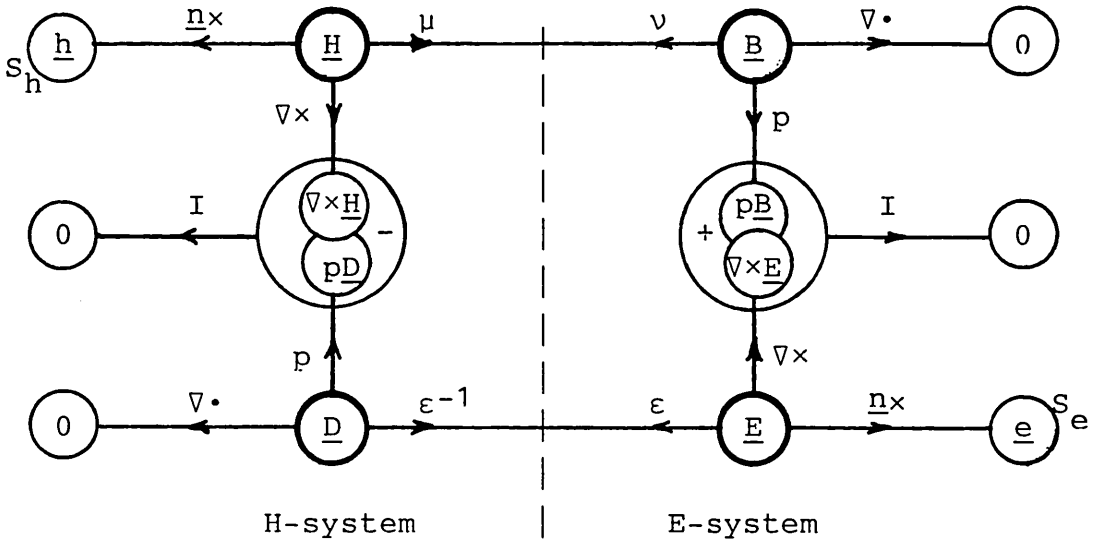

Fig. 11.6 Structure of the high frequency problem.

The total constitutive error $\Lambda(t)$ is composed of the magnetic and electric errors Λ_R^m and Λ_R^e. Thus eqns. 11.10 simplify to

$$0 \leq \Lambda = \Lambda_R^m + \alpha \Lambda_R^e \tag{11.93a}$$

with

$$0 = \Lambda \quad <=> \quad \Lambda_R^m = 0 \quad \text{and} \quad \Lambda_R^e = 0 \tag{11.93b}$$

The errors are instantaneous, and the weighting factor α is positive

$$\alpha > 0 \tag{11.94}$$

The two constitutive relationships can be imposed on the

fields by minimising the total constitutive error

$$0 = \delta\Lambda(t) \tag{11.95}$$

The initial composition of Λ can be obtained by substituting the volume integrals of eqns. 11.6a and 11.7a into 11.93a; noting that the material properties are linear, we can write

$$\Lambda(H,E) = \Theta_o(H) + \Xi_o(E) - \Gamma_o(H,E) \tag{11.96}$$

where

$$\Theta_o(H) = \frac{1}{2}\langle \mu\underline{H} , \underline{H}\rangle_R + \frac{\alpha}{2}\langle \varepsilon^{-1}\underline{D} , \underline{D}\rangle_R$$

$$\Xi_o(E) = \frac{1}{2}\langle \nu\underline{B} , \underline{B}\rangle_R + \frac{\alpha}{2}\langle \varepsilon\underline{E} , \underline{E}\rangle_R$$

$$\Gamma_o(H,E) = \langle \underline{H} , \underline{B}\rangle_R + \alpha \langle \underline{D} , \underline{E}\rangle_R$$

All fields are instantaneous; as they are sinusoidal functions of time, they will be represented as in eqns. 11.32 of sec. 11.3.1. All products may then be represented as in eqns. 11.33, being composed of time-invariant and double-frequency terms.

We now seek to decompose Γ_o between the H- and E-systems. From eqn. 11.96, we can write

$$\Gamma_o = \Gamma_1 + \alpha\Gamma_2 \tag{11.97}$$

where

$$\Gamma_1 = \langle \underline{H} , \underline{B}\rangle_R \quad , \quad \Gamma_2 = \langle \underline{D} , \underline{E}\rangle_R$$

Consider Γ_1 first. According to eqns. 11.33 :

$$\Gamma_1^s = \mathrm{Re}\langle \underline{H}^c , \underline{B}^*\rangle_R$$

$$\Gamma_1^c = \langle \underline{H}^c , \underline{B}^c\rangle_R$$

Substituting for $\underline{B}$ from Maxwell's E-system eqns. 11.90a :

$$\Gamma_1^s = \mathrm{Re}\left\{ \frac{1}{j\omega}\langle \underline{H}^c , \nabla \times \underline{E}^*\rangle_R \right\}$$

$$\Gamma_1^c = -\frac{1}{j\omega}\langle \underline{H}^c , \nabla \times \underline{E}^c\rangle_R$$

Applying vector identities and the divergence theorem :

$$\Gamma_1^s = \mathrm{Re}\left\{ \frac{1}{j\omega}\langle \nabla \times \underline{H}^c , \underline{E}^*\rangle_R - \frac{1}{j\omega}[\underline{n} \times \underline{H}^c , \underline{E}^*]_S \right\}$$

$$\Gamma_1^c = -\frac{1}{j\omega}\langle \nabla \times \underline{H}^c , \underline{E}^c\rangle_R + \frac{1}{j\omega}[\underline{n} \times \underline{H}^c , \underline{E}^c]_S$$

Substituting for $\nabla \times \underline{H}$ from Maxwell's H-system equations 11.89a :

$$\Gamma_1^s = \mathrm{Re}\langle \underline{D}^c , \underline{E}^* \rangle_R - \mathrm{Re}\{\frac{1}{j\omega}[\underline{n} \times \underline{H}^c , \underline{E}^*]_S\} \qquad (11.98a)$$

$$\Gamma_1^c = - \langle \underline{D}^c , \underline{E}^c \rangle_R + \frac{1}{j\omega}[\underline{n} \times \underline{H}^c , \underline{E}^c]_S \qquad (11.98b)$$

Consider Γ_2 next. According to eqns. 11.33 :

$$\Gamma_2^s = \mathrm{Re}\langle \underline{D}^c , \underline{E}^* \rangle_R \qquad (11.99b)$$

$$\Gamma_2^c = \langle \underline{D}^c , \underline{E}^c \rangle_R \qquad (11.99b)$$

Comparing eqns. 11.98 and 11.99, we find

$$\Gamma_1^s = \Gamma_2^s - \mathrm{Re}\{\frac{1}{j\omega}[\underline{n} \times \underline{H}^c , \underline{E}^*]_S\} \qquad (11.100a)$$

$$\Gamma_1^c = - \Gamma_2^c + \frac{1}{j\omega}[\underline{n} \times \underline{H}^c , \underline{E}^c]_S \qquad (11.100b)$$

Substituting eqns. 11.98 and 11.99 for Γ_1 and Γ_2 in 11.97, we can write

$$\Gamma_o^s = \mathrm{Re}\{ (\alpha + 1)\langle \underline{D}^c , \underline{E}^* \rangle_R - \frac{1}{j\omega}[\underline{n} \times \underline{H}^c , \underline{E}^*]_S \} \qquad (11.101a)$$

$$\Gamma_o^c = (\alpha - 1)\langle \underline{D}^c , \underline{E}^c \rangle_R + \frac{1}{j\omega}[\underline{n} \times \underline{H}^c , \underline{E}^c]_S \qquad (11.101b)$$

Substituting from eqns. 11.101 for Γ_o in 11.96, and enforcing the boundary conditions of eqns. 11.92, the instantaneous constitutive error may be expressed as follows

$$\begin{aligned} \Lambda(t) &= \Lambda^s + \tfrac{1}{2}\Lambda^c e^{2j\omega t} + \tfrac{1}{2}\Lambda^* e^{-2j\omega t} \\ &= \Lambda^s + \mathrm{Re}\{ \Lambda^c e^{2j\omega t} \} \end{aligned} \qquad (11.102)$$

where

$$\Lambda^s = \Theta^s(H) + \Xi^s(E) - \Gamma^s(H,E) \qquad (11.103)$$

with

$$\Theta^s = \frac{1}{2}\langle \mu \underline{H}^c , \underline{H}^* \rangle_R + \frac{\alpha}{2}\langle \varepsilon^{-1} \underline{D}^c , \underline{D}^* \rangle_R - \mathrm{Re}\{\frac{1}{j\omega}[\underline{H}^c , \underline{e}^*]_{S_e}\}$$

$$\Xi^s = \frac{1}{2}\langle \nu \underline{B}^c , \underline{B}^* \rangle_R + \frac{\alpha}{2}\langle \varepsilon \underline{E}^c , \underline{E}^* \rangle_R + \mathrm{Re}\{\frac{1}{j\omega}[\underline{h}^c , \underline{E}^*]_{S_h}\}$$

$$\Gamma^s = (\alpha + 1)\,\mathrm{Re}\,\langle \underline{D}^c , \underline{E}^* \rangle_R$$

and

$$\Lambda^C = \Theta^C(H) + \Xi^C(E) - \Gamma^C(H,E) \qquad (11.104)$$

with

$$\Theta^C = \frac{1}{2}\langle \mu \underline{H}^C , \underline{H}^C \rangle_R + \frac{\alpha}{2}\langle \varepsilon^{-1} \underline{D}^C , \underline{D}^C \rangle_R + \frac{1}{j\omega}[\underline{H}^C , \underline{e}^C]_{S_e}$$

$$\Xi^C = \frac{1}{2}\langle \nu \underline{B}^C , \underline{B}^C \rangle_R + \frac{\alpha}{2}\langle \varepsilon \underline{E}^C , \underline{E}^C \rangle_R - \frac{1}{j\omega}[\underline{h}^C , \underline{E}^C]_{S_e}$$

$$\Gamma^C = (\alpha - 1)\langle \underline{D}^C , \underline{E}^C \rangle_R$$

Clearly, Γ^S cannot be split or eliminated for any positive value of α, which means that the steady error Λ^S cannot be decomposed into independent H- and E-system functionals, or energies. Γ^C, on the other hand, is readily eliminated by choosing

$$\alpha = 1 \qquad (11.105)$$

which splits Λ^C, the complex phasor corresponding to the double-frequency error. This value of α assigns equal weight to the magnetic and electric errors in eqn. 11.93a. Using it in eqn. 11.104, and substituting for $\underline{D}$ and $\underline{B}$ from Maxwell's equations 11.89a and 11.90a respectively, we can write

$$\Lambda^C = \Theta^C(H) + \Xi^C(E) \qquad (11.106)$$

with

$$\Theta^C = \frac{1}{2}\langle \mu \underline{H}^C, \underline{H}^C \rangle_R - \frac{1}{2\omega^2}\langle \varepsilon^{-1} \nabla \times \underline{H}^C, \nabla \times \underline{H}^C \rangle_R + \frac{1}{j\omega}[\underline{H}^C, \underline{e}^C]_{S_e}$$

$$\Xi^C = \frac{1}{2}\langle \varepsilon \underline{E}^C, \underline{E}^C \rangle_R - \frac{1}{2\omega^2}\langle \nu \nabla \times \underline{E}^C, \nabla \times \underline{E}^C \rangle_R - \frac{1}{j\omega}[\underline{h}^C, \underline{E}^C]_{S_h}$$

The real and imaginary parts of these complementary functionals are stationary, but not extremal, at the required solution, eqn. 11.95. Solution formulations can also be extracted from eqn. 11.103, but these correspond to only approximate minimisation of Λ^S. The derivations will not be given here because they are virtually identical to eqns. 11.49-61 of sec. 11.3.1 on the harmonic eddy-current problem.

The complementary functionals of eqn. 11.106 introduce boundary integrals into those proposed by Ferrari[11.4]. He avoids boundary terms by associating the functionals with dual problems having different inhomogeneous Dirichlet

conditions. Inclusion of the boundary terms in eqn. 11.106 allows such boundary conditions to be enforced naturally, so that either functional can be used with either problem.

The only value of α that splits the steady error Λ^s is

$$\alpha = -1 \tag{11.107}$$

Using it in eqn. 11.103, and substituting for $\underline{D}$ and $\underline{B}$ from eqns. 11.89a and 11.90a respectively, we can write

$$\Lambda_1^s = \Theta_1^s(H) + \Xi_1^s(E) \tag{11.108}$$

with

$$\Theta_1^s = \frac{1}{2}\langle\mu\underline{H}^c,\underline{H}^*\rangle_R - \frac{1}{2\omega^2}\langle\varepsilon^{-1}\nabla\times\underline{H}^c,\nabla\times\underline{H}^*\rangle_R - \mathrm{Re}\{\frac{1}{j\omega}[\underline{H}^c,\underline{e}^*]_{S_e}\}$$

$$\Xi_1^s = \frac{1}{2}\langle\varepsilon\underline{E}^c,\underline{E}^*\rangle_R - \frac{1}{2\omega^2}\langle\nu\nabla\times\underline{E}^c,\nabla\times\underline{E}^*\rangle_R + \mathrm{Re}\{\frac{1}{j\omega}[\underline{h}^c,\underline{E}^*]_{S_h}\}$$

Θ_1^s and Ξ_1^s are real complementary functionals, similar to those derived by Hammond[11.2]. Now α in eqn. 11.107 violates the requirement of positivity in ineq. 11.94, causing eqns. 11.93 to degenerate to

$$0 \gtrless \Lambda_1 = \Lambda_R^m - \Lambda_R^e \tag{11.109a}$$

with

$$0 = \Lambda_1 \quad <=> \quad \Lambda_R^m = \Lambda_R^e \tag{11.109b}$$

Clearly, in this case we cannot conclude that Λ_1 is stationary at the unique correct solution where

$$\Lambda_R^m = \Lambda_R^e = 0 \tag{11.110}$$

Therefore, the constitutive error approach cannot verify that Θ_1^s and Ξ_1^s are stationary at the required solution.

11.5 Conclusions

Extension of the constitutive error approach to the time-varying case is based on summing the relevant errors. Splitting of the total error depends, to a large extent, on the relative weights assigned to the component errors, and on the interval of the time integral of the current flow error, if included. In general, solution formulations are not associated with minimum principles, and energy bounds cannot be established.

Steady harmonic derivations are based on the instantaneous error to avoid the difficulty of interpreting complex energies and their stationary points. Appendix K compares formulations derived here with previously proposed ones : there is agreement on the fundamental derivations of solution formulations, but not on the associated energies.
A degree of generalisation may be claimed for the present approach as it leads to two possible treatments, one based on the steady component of error, the other on the double-frequency harmonic component.

C H A P T E R T W E L V E

Conclusions

12.1 Preview

In this thesis, the solution of electromagnetic field problems is regarded as a process of minimising the constitutive error, with the fields constrained to satisfy Maxwell's equations, continuity conditions, and boundary conditions. The previous chapters show that the proposed view provides a unifying framework which leads to systematic derivation of complementary and dual solution formulations, and sheds useful light on various aspects of computational electromagnetics. The present chapter summarises main findings arrived at in the various topics considered, and suggests further areas that may benefit from the approach.

12.2 Complementary functionals and solution formulations

Under static conditions, the constitutive error splits into complementary functionals for well-posed and consistently specified problems. Chapter 6 derives the functionals for a variety of problem specifications, including certain boundary conditions that had previously been thought to hinder truly complementary formulations. The only restriction here is the requirement that boundary conditions be specified independently for the complementary systems, although sec. 6.7.2 extends the approach to handle a particular set of interlinked boundary conditions.

Having split the error completely between the H- and B-systems, its minimisation is achieved by extremising the complementary functionals independently of each other,

which thus provides the complementary solution formulations sought.

In mixed-potential solutions, and in time-varying problems, the error does not, in general, split completely into complementary functionals. In such cases, error minimisation provides a reference formulation which, upon the introduction of additional assumptions, generates complementary solution formulations. The assumptions constitute redundant over-specification in exact analysis, and approximate error minimisation in numerical analysis. In effect, the solution formulations have no corresponding functionals, and are not associated with minimum principles. The derivations of Chapters 9 and 11 reveal the alternative assumptions available and their implications.

It is emphasised that decomposition of the constitutive error is achieved by imposing the physical specifications of the problem on the fields in the universal expression for the error. If, upon exhaustion of the specifications, the error still has not split completely between the complementary systems, it may be concluded that independent complementary functionals cannot be defined for the given problem.

12.3 Upper and lower bounds

In cases where the error does split into complementary functionals, their numerical values constitute bounding approximations to the same global quantity. The latter may thus be estimated, to a high degree of accuracy, by averaging the bounds. This can be done in conventional static formulations where, depending on problem specifications, the bounded quantity may correspond to energy or co-energy, or possibly neither. Bounds on lumped circuit parameters are derived from energy bounds. Although complementary estimates of circuit parameters are always available, they do not necessarily bound the exact values

in non-linear solutions, since their relationships to energies are not direct algebraic ones.

In cases where the error does not split completely into complementary functionals, such as mixed formulations and time-varying problems, upper and lower bounds are not defined for any quantity.

12.4 Numerical techniques

The proposed approach is particularly suited to numerical analysis because it acknowledges, at the outset, an error that has a standard positive form, and is totally attributable to the numerical constraints on the variables. Chapter 5 shows that finite difference, finite element, and boundary integral scalar and vector potential formulations can be derived as alternative implementations of constitutive error minimisation. As the error is always defined and computable, it can serve as a basis for comparison.

12.5 Error computation

The constitutive error cannot be apportioned between the complementary systems. It reflects, quantitatively, the local and global adequacy of the numerical discretisation. The error tends to be dense in regions of sharp field changes, be they material interfaces or severely stepped boundary conditions. At air/iron interfaces, error in non-linear solutions is less than in linear solutions because of the reduction in iron permeability; within the iron, error increases because of the discrete steps in permeability.

Adaptive mesh refinement schemes may be based on the constitutive error density distribution; the global error, which must also be monitored, can be meaningfully normalised with respect to energy.

12.6 Complementary field estimates

The computations of Chapters 6 and 7 indicate that discrepancies between complementary estimates of the field distributions can be considerable, especially in non-linear media; this was evident even with generally acceptable discretisations. Unlike global energies, local distributions cannot be predicted, to a higher degree of accuracy, from complementary estimates. However, the B-H plots do serve to ascribe a realistic level of confidence to numerically derived field estimates.

12.7 Magnetostatic scalar potential formulations

Chapter 8 suggests that errors associated with reduced scalar potential formulations may be attributed to the inconsistency of Biot-Savart pre-defined fields with numerical discretisation; near-cancellation effects magnify, rather than cause, the errors. Two-potential formulations retain a limited degree of inconsistency on conductor surfaces. An alternative, entirely consistent, definition is proposed for conductors composed of straight sections; it is computationally simpler than the Biot-Savart definition, and results in comparable constitutive errors for two-potential formulations.

12.8 Mixed formulations

Chapter 9 shows that existing mixed formulations are based on approximate treatment of field continuity across the interface separating scalar potential and vector potential sub-regions. Dual and pseudo-complementary formulations, based on alternative treatments of continuity, are developed, paving the way for quantitative assessment and comparison.

12.9 Vector potential solvability

Section 3.4.4.2 and Chapter 10 investigate vector potential solvability, emphasising the distinctions between the essential requirements of physically unique fields, and the inessential requirements of computationally unique potentials. It is concluded that the imposition of a divergence condition on the vector potential is not strictly necessary in numerical analysis, alternative treatments being equally valid, and possibly more accurate.

Chapter 10 also interprets the weak imposition of a divergence condition in terms of a gauge error to be added to the constitutive error; minimisation of the weighted sum provides the solution formulation. Experimentation is needed to determine the most suitable relative weights, which are shown to constitute a compromise between accuracy and well-behaved solvability.

12.10 Time-varying problems

Chapter 11 extends the proposed approach to time-varying problems by constructing suitably weighted sums of the constitutive errors corresponding to the relevant material properties; the weighting factors are shown to play a prominent role in extracting workable solution formulations. Complementary formulations are derived for the eddy-current and high frequency problems. In general, time-varying solution formulations are not associated with minimum principles, and energy bounds cannot be established.

Under steady harmonic conditions, formulations can be derived in two ways. (i) Minimisation of the time-invariant component of the constitutive error; however, complementary time-invariant functionals cannot be defined, so that solution formulations correspond to approximate minimisation of the constitutive error. (ii) Solving for the stationary point of the double-frequency alternating component of the

constitutive error; complementary functionals are defined, but they are merely stationary, not extremal, at the required solution. In both approaches, derivations are based on the instantaneous error to avoid the difficulty of interpreting complex energies and their stationary points. Appendix K compares complementary eddy-current formulations derived here with previously proposed ones.

Chapter 11 also derives complementary formulations for the transient eddy-current problem with alternative time discretisations.

12.11 Two solutions better than one ?

The argument for performing both complementary solutions, rather than settling for only one, forces itself on a number of occasions in the thesis. These are reviewed briefly here.

Averaging bounds obtained from relatively coarse discretisations can yield highly accurate estimates of the bounded quantity, say energy. Such a procedure is more economical than single-sided estimates, since these would require highly refined discretisations to achieve comparable accuracy.

The constitutive error is a comprehensive measure of numerical inaccuracy, and thus provides a natural basis for adaptive mesh refinement. Error computation requires both solutions to be performed.

Combined presentation of complementary computational results, such as equipotential contours, B-H plots, and constitutive error density distributions, provides the designer with a tangible and realistic appreciation of the confidence level with which to regard distributions of interest.

For the purposes of research, where solution economy is somewhat less critical than in industry, combined presentation of results leads to deeper insight into the numerical behaviour of complementary solutions, and aids in assessing alternatives.

The absence of minimum principles from single-sided time-varying solutions erodes their acknowledged economic advantage over simultaneous complementary solutions which actually minimise the constitutive error; this is particularly significant in cases where the complementary solutions are only loosely interlinked.

12.12 Further applications

The constitutive error approach is a powerful tool that can provide insight into various topics of interest in computational electromagnetics : solution formulations can be derived systematically, and alternatives assessed theoretically and practically. A number of topics that have been considered theoretically in this thesis may be further investigated by actually performing complementary solutions and computing the corresponding errors. These include anisotropic media, three-dimensional problems, allernative numerical techniques, mixed formulations, vector potential solvability, harmonic and transient eddy-current problems, and high frequency applications. Other topics that may benefit from the approach would include open boundary problems, force computations, moving media, permanent magnets, etc. It may also prove fruitful to develop the non-linear iteration algorithms suggested in sec. 7.4; convergence, it has been shown, may be reliably monitored through the modified, separate system constitutive errors.

12.13 The Ligurian

It seems inappropriate to close this treatise without mentioning that, within the electromagnetics CAD group at Imperial College, the constitutive error is better known as the 'Ligurian'. The name derives from the beautiful coast on the Gulf of Genoa where, some two years ago, the author began to appreciate the potential of the constitutive error concept. The term 'Ligurian' has the advantage of compactness over the more descriptive 'constitutive error'. This may be quite relevant if the concept becomes accepted and commonly used.

A P P E N D I C E S

A. Potential operators and potentials

This Appendix seeks to establish a fundamental implication of prop. 2 of sec. 2.2, namely that $\mu\underline{H}+\underline{B}_r$ and $\nu\underline{B}+\underline{H}_c$ are potential operators; it also derives their corresponding potentials, $\chi(\underline{H})$ and $\psi(\underline{B})$.

The derivations will be made by analogy with some familiar concepts from vector calculus. Consider a vector field $\underline{F}(\underline{r})$, where $\underline{r}$ is the position vector in a Cartesian coordinate system (x, y, z)

$$\underline{r} = x\,\underline{a}_x + y\,\underline{a}_y + z\,\underline{a}_z \qquad (A.1)$$

$\underline{a}_x$, $\underline{a}_y$, and $\underline{a}_z$ are unit vectors in the three coordinate directions. The line integral

$$I = \int_{\underline{r}_1}^{\underline{r}_2} \underline{F}(\underline{r})\cdot d\underline{r} \qquad (A.2)$$

is, in general, a function of the path between the two end-points $\underline{r}_1$ and $\underline{r}_2$. However, if $\underline{F}(\underline{r})$ is the gradient of some scalar $\phi(\underline{r})$, i.e.

$$\underline{F} = \text{grad } \phi \qquad (A.3)$$

then

$$I = \int_{\underline{r}_1}^{\underline{r}_2} \text{grad } \phi(\underline{r}) \cdot d\underline{r} = \phi(\underline{r}_2) - \phi(\underline{r}_1)$$

$$= I(\underline{r}_1, \underline{r}_2) \qquad (A.4)$$

and I depends on the end-points only. It is sufficient that $\underline{F}(\underline{r})$ be irrotational for it to be a gradient; i.e.

$$\text{curl } \underline{F}(\underline{r}) = 0 \iff \underline{F}(\underline{r}) = \text{grad } \phi \qquad (A.5)$$

The above results will now be used as a basis for analogy. At any point in the given region R, it is possible to postulate an orthogonal coordinate system (H_α, H_β, H_γ), so that the field $\underline{H}$, given by

$$\underline{H} = H_\alpha \, \underline{a}_\alpha + H_\beta \, \underline{a}_\beta + H_\gamma \, \underline{a}_\gamma \qquad (A.6)$$

is analogous to the position vector $\underline{r}$ in eqn. A.1 ; $\underline{a}_\alpha$, $\underline{a}_\beta$, and $\underline{a}_\gamma$ are unit vectors in the respective directions of the components H_α, H_β, and H_γ. The field $\mu(\underline{H})\underline{H}+\underline{B}_r$ is a function of $\underline{H}$, and hence is analogous to $\underline{F}(\underline{r})$. The integral

$$J = \int_{\underline{H}_1}^{\underline{H}_2} \langle \mu(\underline{h})\underline{h} + \underline{B}_r \, , \, d\underline{h} \rangle \qquad (A.7)$$

is a function of the path between $\underline{H}_1$ and $\underline{H}_2$ unless $\mu(\underline{H})\underline{H}+\underline{B}_r$ is a gradient of some scalar $\chi(\underline{H})$, in which case we have

$$J = \int_{\underline{H}_1}^{\underline{H}_2} \langle \mathrm{grad}_h \, \chi \, , \, d\underline{h} \rangle = \chi(\underline{H}_2) - \chi(\underline{H}_1)$$

$$= J(\underline{H}_1, \underline{H}_2) \qquad (A.8)$$

and the integral J depends only on the end-points $\underline{H}_1$ and $\underline{H}_2$. The condition for $\mu(\underline{H})\underline{H}+\underline{B}_r$ to be a gradient is given by

$$\mathrm{curl}_H(\mu(\underline{H})\underline{H}+\underline{B}_r) = 0 \iff \mu(\underline{H})\underline{H}+\underline{B}_r = \mathrm{grad}_H \, \chi \qquad (A.9)$$

as in A.5 . To see the implications of A.9 , the curl operation is performed as in Cartesian coordinates, and the result set to zero; this yields

$$\frac{\partial}{\partial H_j} (\mu(\underline{H})\underline{H})_i = \frac{\partial}{\partial H_i} (\mu(\underline{H})\underline{H})_j \quad \text{for } i,j = \alpha,\beta,\gamma; \; i \neq j \qquad (A.10a)$$

Noting that $\mu(\underline{H})$ is a tensor (or dyad), A.10a expands to

$$\mu_{ij} + \sum_k H_k \frac{\partial}{\partial H_j} \mu_{ik} = \mu_{ji} + \sum_k H_k \frac{\partial}{\partial H_i} \mu_{jk} \qquad (k = \alpha,\beta,\gamma) \qquad (A.10b)$$

Eqns. A.10 simply state that $\partial(\mu(\underline{H})\underline{H})/\partial\underline{H}$ is symmetric, which is prop. 2 of sec. 2.2.

We thus conclude that for a constitutive relationship that possesses prop. 2 of sec. 2.2, we can write

$$\mu(\underline{H})\underline{H} + \underline{B}_r = \text{grad}_H \chi \qquad \text{(A.11a)}$$

with

$$\chi(\underline{H}_2) = \chi(\underline{H}_1) + \int_{\underline{H}_1}^{\underline{H}_2} \langle \mu(\underline{h})\underline{h} + \underline{B}_r \, , \, d\underline{h} \rangle \qquad \text{(A.11b)}$$

in accordance with eqns. A.7 - 9 Similarly

$$\nu(\underline{B})\underline{B} + \underline{H}_c = \text{grad}_B \psi \qquad \text{(A.12a)}$$

with

$$\psi(\underline{B}_2) = \psi(\underline{B}_1) + \int_{\underline{B}_1}^{\underline{B}_2} \langle \nu(\underline{b})\underline{b} + \underline{H}_c \, , \, d\underline{b} \rangle \qquad \text{(A.12b)}$$

B. Convexity

This Appendix seeks to show that the scalars $\chi(\underline{H})$ and $\psi(\underline{B})$, derived in Appendix A , are strictly convex for a constitutive relationship that is strictly monotone, i.e. possesses prop. 1 of sec. 2.2.

Consider ineq. 2.2a. Substituting for $\underline{B}_1$ and $\underline{B}_2$ from eqn. 2.1a

$$\langle \underline{H}_2 - \underline{H}_1 \, , \, \mu(\underline{H}_2)\underline{H}_2 - \mu(\underline{H}_1)\underline{H}_1 \rangle \geq 0 \qquad \text{(B.1)}$$

with strict inequality for distinct $\underline{H}_1$ and $\underline{H}_2$. Substituting from 2.4a, and rearranging

$$\langle \underline{H}_2 - \underline{H}_1 \, , \, \text{grad}_{H_2} \chi \rangle \geq \langle \underline{H}_2 - \underline{H}_1 \, , \, \text{grad}_{H_1} \chi \rangle \qquad \text{(B.2)}$$

where the subscripts H_1 and H_2 indicate the points, in the H-coordinate system, at which the gradients are evaluated. Prop. 1, or, equally well, eqn. B.1 , implies single-valuedness, so that $\mu\underline{H}+\underline{B}_r = \text{grad}_H \chi$ is a continuous function of $\underline{H}$; this, in turn, implies that $\chi(\underline{H})$ is smooth to at least its first derivative (C^1-continuous w.r.t. $\underline{H}$). The mean

value theorem may therefore be applied to yield

$$\chi(\underline{H}_2) - \chi(\underline{H}_1) = \langle \underline{H}_2 - \underline{H}_1 \, , \, \mathrm{grad}_{H_m} \chi \rangle \qquad (B.3)$$

where

$$\underline{H}_m = \eta \, \underline{H}_2 + (1-\eta) \, \underline{H}_1 \qquad \text{with} \quad 0 < \eta < 1 \qquad (B.4a)$$

so that

$$\underline{H}_2 - \underline{H}_m = (1-\eta) \, (\underline{H}_2 - \underline{H}_1) \qquad (B.4b)$$

Ineq. B.2 can, of course, be applied to $\underline{H}_2$ and $\underline{H}_m$:

$$\langle \underline{H}_2 - \underline{H}_m \, , \, \mathrm{grad}_{H_2} \chi \rangle \geq \langle \underline{H}_2 - \underline{H}_m \, , \, \mathrm{grad}_{H_m} \chi \rangle$$

Substituting for $(\underline{H}_2 - \underline{H}_m)$ from B.4b :

$$(1-\eta) \langle \underline{H}_2 - \underline{H}_1 \, , \, \mathrm{grad}_{H_2} \chi \rangle \geq (1-\eta) \langle \underline{H}_2 - \underline{H}_1 \, , \, \mathrm{grad}_{H_m} \chi \rangle$$

As $(1-\eta)$ is positive by definition, eqn. B.4a , it is cancelled out without altering the inequality. Substituting, moreover, for the right hand side from eqn. B.3 , we finally get

$$\langle \underline{H}_2 - \underline{H}_1 \, , \, \mathrm{grad}_{H_2} \chi \rangle \geq \chi(\underline{H}_2) - \chi(\underline{H}_1) \qquad (B.5a)$$

which formally defines $\chi(\underline{H})$ to be convex[2-1]; it is, in fact, strictly convex since we have strict inequality for distinct field values $\underline{H}_1$ and $\underline{H}_2$ [2-1]. Similarly, $\psi(\underline{B})$ is strictly convex with

$$\langle \underline{B}_2 - \underline{B}_1 \, , \, \mathrm{grad}_{B_2} \psi \rangle \geq \psi(\underline{B}_2) - \psi(\underline{B}_1) \qquad (B.5b)$$

Prop. 1 of sec. 2.2 requires $\mu(\underline{H})\underline{H}+\underline{B}_r$ to be a (C^0-) continuous function of $\underline{H}$; accordingly, the scalar $\chi(\underline{H})$ is smooth (C^1-continuous). If, however, $\mu(\underline{H})\underline{H}+\underline{B}_r$ is itself smooth, the mean value theorem can be applied to ineq. B.1 to yield

$$\langle \underline{H}_2 - \underline{H}_1 \, , \, \frac{\partial}{\partial \underline{H}} (\mu(\underline{H})\underline{H}) \Big|_{\underline{H}_m} (\underline{H}_2 - \underline{H}_1) \rangle \geq 0 \qquad (B.6)$$

with strict inequality for distinct field values $\underline{H}_1$ and $\underline{H}_2$. As B.6 holds for all $\underline{H}_1$ and $\underline{H}_2$, and hence for any $\underline{H}_m$, it

formally defines the derivative $\partial(\mu(\underline{H})\underline{H})/\partial\underline{H}$ to be positive-definite. It is recalled that prop. 2 of sec. 2.2 requires the same derivative to be symmetric.

Similarly, the derivative $\partial(\nu(\underline{B})\underline{B})/\partial\underline{B}$ is positive-definite if $\nu(\underline{B})\underline{B}+\underline{H}_c$ is a smooth function of $\underline{B}$.

C. The fundamental property of λ

This Appendix derives eqns. 2.12 which constitute a statement of the fundamental property of λ.

λ is defined in eqn. 2.10 as

$$\lambda(\underline{H},\underline{B}) = \chi(\underline{H}) + \psi(\underline{B}) - \zeta(\underline{H},\underline{B}) \qquad (C.1)$$

where $\underline{H}$ and $\underline{B}$ are estimates that are not necessarily related by the constitutive relationship, eqns. 2.1. Substituting eqns. 2.8, 2.9, and 2.11 into C.1, and combining integrals :

$$\lambda(\underline{H},\underline{B}) = \int_{\underline{H}_c}^{\underline{H}} <\mu\underline{h}+\underline{B}_r, d\underline{h}> + \int_0^{\underline{B}} <\nu\underline{b}+\underline{H}_c, d\underline{b}> - <\underline{H},\underline{B}> \qquad (C.2)$$

Let us first evaluate the density $\lambda(\underline{H}_1,\underline{B}_1)$ where $\underline{H}_1$ and $\underline{B}_1$ do satisfy the constitutive relationship, i.e. they are related by eqns. 2.1. In this case

$$\lambda(\underline{H}_1,\underline{B}_1) = \int_{\underline{H}_c}^{\underline{H}_1} <\mu\underline{h}+\underline{B}_r, d\underline{h}> + \int_0^{\underline{B}_1} <\nu\underline{b}+\underline{H}_c, d\underline{b}> - <\underline{H}_1,\underline{B}_1>$$

Substituting into the integrands from eqns. 2.1 :

$$\lambda(\underline{H}_1,\underline{B}_1) = \int_{\underline{H}_c}^{\underline{H}_1} <\underline{b}(\underline{h}), d\underline{h}> + \int_0^{\underline{B}_1} <\underline{h}(\underline{b}), d\underline{b}> - <\underline{H}_1,\underline{B}_1>$$

According to Appendix A the integrals are independent of the integration paths. Since, moreover, both the upper and lower limits of the two integrals are related by eqns. 2.1, it is possible to choose paths throughout which $\underline{h}$ and $\underline{b}$ are

related by eqns. 2.1. This allows the two integrals to be combined :

$$\lambda(\underline{H}_1,\underline{B}_1) = \int_{\underline{H}_c,0}^{\underline{H}_1,\underline{B}_1} (\langle \underline{b} , d\underline{h}\rangle + \langle \underline{h} , d\underline{b}\rangle) - \langle \underline{H}_1 , \underline{B}_1\rangle$$

$$= \int_{\langle \underline{H}_c,0\rangle}^{\langle \underline{H}_1,\underline{B}_1\rangle} d\langle \underline{h} , \underline{b}\rangle - \langle \underline{H}_1 , \underline{B}_1\rangle$$

Performing the integration, we find

$$\lambda(\underline{H}_1,\underline{B}_1) = \langle \underline{H}_1 , \underline{B}_1\rangle - \langle \underline{H}_c , 0\rangle - \langle \underline{H}_1 , \underline{B}_1\rangle$$

$$= 0 \qquad \text{(C.3)}$$

Clearly, then, λ is zero for any pair of H- and B-field estimates that satisfies the constitutive relationship.

Let us next postulate another pair of field estimates, $\underline{H}_2$ and $\underline{B}_2$, that are also related to each other by eqns. 2.1, but with

$$\underline{H}_2 \neq \underline{H}_1 \qquad \text{(C.4a)}$$

and hence, according to prop. 1 of sec. 2.2,

$$\underline{B}_2 \neq \underline{B}_1 \qquad \text{(C.4b)}$$

To evaluate $\lambda(\underline{H}_2,\underline{B}_1)$ we apply eqn. C.1

$$\lambda(\underline{H}_2,\underline{B}_1) = \chi(\underline{H}_2) + \psi(\underline{B}_1) - \zeta(\underline{H}_2, \underline{B}_1) \qquad \text{(C.5)}$$

But from eqns. C.1 and C.3 we have

$$\lambda(\underline{H}_1,\underline{B}_1) = \chi(\underline{H}_1) + \psi(\underline{B}_1) - \zeta(\underline{H}_1,\underline{B}_1) = 0$$

so that substitution for $\psi(\underline{B}_1)$ in C.5 yields

$$\lambda(\underline{H}_2,\underline{B}_1) = \chi(\underline{H}_2) - \zeta(\underline{H}_2,\underline{B}_1) - \chi(\underline{H}_1) + \zeta(\underline{H}_1,\underline{B}_1)$$

Substituting for the two ζ's from eqn. 2.11, and combining terms

$$\lambda(\underline{H}_2,\underline{B}_1) = \chi(\underline{H}_2) - \chi(\underline{H}_1) + \langle \underline{H}_1 - \underline{H}_2 , \underline{B}_1 \rangle$$

Substituting, finally, for $\underline{B}_1$ from eqn. 2.1a and rearranging

$$\lambda(\underline{H}_2,\underline{B}_1) = \langle \underline{H}_1 - \underline{H}_2 , \mu(\underline{H}_1)\underline{H}_1+\underline{B}_r \rangle - (\chi(\underline{H}_1)-\chi(\underline{H}_2)) \qquad (C.6)$$

Consider now ineq. 2.6a; making a trivial change in subscripts, and substituting for the gradient from eqn. 2.4a, it becomes

$$\langle \underline{H}_1 - \underline{H}_2 , \mu(\underline{H}_1)\underline{H}_1+\underline{B}_r \rangle \geq \chi(\underline{H}_1) - \chi(\underline{H}_2) \qquad (C.7)$$

Comparing eqn. C.6 with ineq. C.7 , recalling that $\chi(\underline{H})$ is strictly convex, and noting inequalities C.4 , we can conclude that

$$\lambda(\underline{H}_2,\underline{B}_1) > 0 \qquad (C.8)$$

for any pair of field estimates, $\underline{H}_2$ and $\underline{B}_1$, that does not satisfy the constitutive relationship, eqns. 2.1.

Combining ineq. C.8 with eqn. C.3 , we can state that

$$\lambda(\underline{H},\underline{B}) \geq 0 \qquad (C.9)$$

for any pair of estimates, $\underline{H}$ and $\underline{B}$, with strict inequality unless

$$\underline{B} = \mu(\underline{H})\underline{H} + \underline{B}_r \qquad (C.10a)$$

and

$$\underline{H} = \nu(\underline{B})\underline{B} + \underline{H}_c \qquad (C.10b)$$

i.e. $\underline{H}$ and $\underline{B}$ satisfy the constitutive relationship.

D. Unique boundary specification

In this Appendix we seek to impose specs. 2 and 3 of sec. 3.4.1 on W in eqn. 3.25 to derive eqns. 3.27.

Noting that both $\underline{H}_1$ and $\underline{H}_2$ satisfy eqn. 3.18, spec. 2, application of the curl operation to both sides of 3.24a yields

$$\text{curl } \delta\underline{H} = 0 \qquad \text{(D.1a)}$$

everywhere in R. Requiring, moreover, $\underline{H}_1$ and $\underline{H}_2$ to satisfy eqn. 3.20, spec. 3, we can write

$$\underline{n} \times \Delta(\delta\underline{H}) = 0 \qquad \text{(D.1b)}$$

across any surface in R. As R is simply-connected, eqns. D.1 imply that there exists a continuous scalar distribution $\phi(\underline{r})$ such that

$$\delta\underline{H} = \text{grad } \phi \qquad \text{(D.2a)}$$

and

$$\phi(\underline{r}) = \phi(\underline{r}_o) + \int_{\underline{r}_o}^{\underline{r}} \delta\underline{H} \cdot d\underline{\ell} \qquad \text{(D.2b)}$$

where $\underline{r}_o$ defines an arbitrary global reference point in R.

Noting that both $\underline{B}_1$ and $\underline{B}_2$ satisfy eqn. 3.19, spec. 2, application of the divergence operation to both sides of 3.24b yields

$$\text{div } \delta\underline{B} = 0 \qquad \text{(D.3a)}$$

everywhere in R. Requiring, moreover, $\underline{B}_1$ and $\underline{B}_2$ to satisfy eqn. 3.21, spec. 3, we can write

$$\underline{n} \cdot \Delta(\delta\underline{B}) = 0 \qquad \text{(D.3b)}$$

across any surface in R.

Substituting from eqn. D.2a for $\delta\underline{H}$ in 3.25 :

$$W = \langle \text{grad } \phi \, , \, \delta\underline{B} \rangle_R$$

Applying a vector identity :

$$W = - \langle \phi \ , \ \mathrm{div}\ \delta\underline{B} \rangle_R + \int_R \mathrm{div}(\phi\ \delta\underline{B})\ dR$$

The first term on the RHS is zero by eqn. D.3a . Applying the divergence theorem to the second term, and noting that by eqns. D.1 and D.3b $\phi(\underline{r})$ and $\underline{n}\cdot\delta\underline{B}$ are, respectively, continuous, we find

$$W = [\phi \ , \ \underline{n} \cdot \delta\underline{B}]_S$$

Substituting for ϕ from D.2b :

$$W = \phi(\underline{r}_o) \times \oint_S \delta\underline{B}\cdot d\underline{S} + [\int_{\underline{r}_o}^{\underline{r}} \delta\underline{H}\cdot d\underline{\ell} \ , \ \underline{n}\cdot\delta\underline{B}]_S$$

The first term on the RHS is zero by a reverse application of the divergence theorem and eqn. D.3a . Thus

$$W = [\int_{\underline{r}_o}^{\underline{r}} \delta\underline{H} \cdot d\underline{\ell} \ , \ \underline{n} \cdot \delta\underline{B}]_S \qquad (D.4)$$

which represents the final reduction of W. We can, however, express it in a more convenient form by using the sub-division of S in 3.22 ; thus

$$W = \sum_{n=1}^{N} w_n \qquad (D.5a)$$

with

$$w_n = [\int_{\underline{r}_o}^{\underline{r}} \delta\underline{H} \cdot d\underline{\ell} \ , \ \underline{n} \cdot \delta\underline{B}]_{S_n} \qquad (D.5b)$$

where S_n is the nth simply-connected sub-section of S. If, moreover, we use $\underline{r}_n$ to define a local reference point on each S_n, we can break the line integration of D.5b into two stages

$$w_n = [\int_{\underline{r}_o}^{\underline{r}_n} \delta\underline{H}\cdot d\underline{\ell} \ , \ \underline{n}\cdot\delta\underline{B}]_{S_n} + [\int_{\underline{r}_n}^{\underline{r}} \delta\underline{H}\cdot d\underline{\ell} \ , \ \underline{n}\cdot\delta\underline{B}]_{S_n}$$

But the line integral in the first term is independent of $\underline{r}$, and hence can be taken out of the surface integration, so that

$$w_n = (\delta\int_{\underline{r}_o}^{\underline{r}_n} \underline{H}\cdot d\underline{\ell})\,(\delta\int_{S_n} \underline{B}\cdot d\underline{S}) + [\delta\int_{\underline{r}_n}^{\underline{r}} \underline{H}\cdot d\underline{\ell} \ , \ \delta(\underline{n}\cdot\underline{B})]_{S_n} \qquad (D.6)$$

where the following relationships, obtainable directly from 3.24, were used :

$$\int \delta \underline{H} \cdot d\underline{\ell} = \delta \int \underline{H} \cdot d\underline{\ell}, \quad \int \delta \underline{B} \cdot d\underline{S} = \delta \int \underline{B} \cdot d\underline{S}, \text{ and } \underline{n} \cdot \delta \underline{B} = \delta (\underline{n} \cdot \underline{B}) \tag{D.7}$$

Eqns. D.5a and D.6 express W in the final form that we shall use. They clearly relate to boundary conditions. In conjunction with ineq. 3.26, they constitute a general statement on allowable boundary specifications for well-posedness.

E. Partial decomposition of the constitutive error

In this Appendix we impose specs. 2 and 3 of sec. 3.4.1 on Λ in eqn. 3.71 to decompose it partially.

From eqn. 2.11, we have

$$Z(\underline{H},\underline{B}) = \langle \underline{H} \ , \ \underline{B} \rangle_R$$

Substituting for $\underline{H}$ from 3.40a :

$$Z = \langle \underline{G} \ , \ \underline{B} \rangle_R - \langle \text{grad } \Omega \ , \ \underline{B} \rangle_R$$

Applying a vector identity to the second term on the RHS :

$$Z = \langle \underline{G} \ , \ \underline{B} \rangle_R + \langle \Omega \ , \ \text{div } \underline{B} \rangle_R - \int_R \text{div}(\Omega \ \underline{B}) \ dR$$

Substituting eqn. 3.19 for div $\underline{B}$ in the second term, and applying the divergence theorem to the third term :

$$Z = \langle G \ , \ \underline{B} \rangle_R + \langle \Omega \ , \ \rho \rangle_R - [\Omega \ , \ \underline{n} \cdot \underline{B}]_S$$
$$- \sum_{m=1}^{M} \{ [\Omega_1 \ , \ \underline{n}_1 \cdot \underline{B}_1]_{S_m^\Delta} + [\Omega_2 \ , \ \underline{n}_2 \cdot \underline{B}_2]_{S_m^\Delta} \}$$

where the summation is over surfaces of discontinuity; the subscripts 1 and 2 refer to the two sides of S_m^Δ. Substituting for Ω in the third term from 3.54b, and manipulating the variables in the summation term :

$$Z = \langle \underline{G},\underline{B} \rangle_R + \langle \Omega,\rho \rangle_R - \Omega(\underline{r}_o) \oint_S \underline{B} \cdot d\underline{S} - [\sum \Delta\Omega \int_{\underline{r}_o}^{\underline{r}} + \int_{\underline{r}_o}^{\underline{r}} \underline{G} \cdot d\underline{\ell}, \underline{n} \cdot \underline{B}]_S$$
$$+ [\int_{\underline{r}_o}^{\underline{r}} \underline{H} \cdot d\underline{\ell}, \underline{n} \cdot \underline{B}]_S + \sum_{m=1}^{M} \{ [\Omega_1, \underline{n} \cdot \Delta\underline{B}]_{S_m^\Delta} + [\Delta\Omega, \underline{n} \cdot \underline{B}_2]_{S_m^\Delta} \}$$

where $\underline{r}_o$ is an arbitrary global reference point, and the

sum in the fourth term covers discontinuities in Ω encountered by the path from $\underline{r}_o$ to $\underline{r}$. Applying the divergence theorem to the third term, and substituting from eqns. 3.19 and 3.21 into the result, we finally get

$$Z = \langle \underline{G} , \underline{B} \rangle_R + \langle \Omega , \rho \rangle_R - \Omega(\underline{r}_o) \left(\int_R \rho \, dR + \sum_{m=1}^{M} \int_{S_m^\Delta} \sigma \, dS \right)$$
$$- \left[\sum \Delta\Omega \int_{\underline{r}_o}^{\underline{r}} + \int_{\underline{r}_o}^{\underline{r}} \underline{G} \cdot d\underline{\ell} \, , \, \underline{n} \cdot \underline{B} \right]_S + \left[\int_{\underline{r}_o}^{\underline{r}} \underline{H} \cdot d\underline{\ell} \, , \, \underline{n} \cdot \underline{B} \right]_S$$
$$+ \sum_{m=1}^{M} \{ [\Omega_1 , \sigma]_{S_m^\Delta} + [\Delta\Omega , \underline{n} \cdot \underline{B}_2]_{S_m^\Delta} \} \qquad \text{(E.1)}$$

Substituting the above for Z in 3.71, Λ decomposes partially as in 3.72.

F. Minimisation of a decomposed functional

Consider a functional T which has decomposed into two functionals, U and V, as follows

$$T(\alpha,\beta,\gamma) = U(\alpha,\gamma) + V(\beta,\gamma) \qquad \text{(F.1)}$$

where α, β, and γ are independent variables, all functions of position. T has decomposed in α and β, but not in γ, which appears in both component functionals so that they are not quite independent of each other. From F.1 a free variation in T can be written

$$\delta T(\alpha,\beta,\gamma) = \delta U(\alpha,\gamma) + \delta V(\beta,\gamma) \qquad \text{(F.2)}$$

Consider the case where T constitutes a valid variational principle for a well-posed problem which has a unique solution at $(\alpha_o, \beta_o, \gamma_o)$; then

$$0 = \delta T(\alpha,\beta,\gamma) \qquad \text{at } \alpha,\beta,\gamma = \alpha_o,\beta_o,\gamma_o \qquad \text{(F.3)}$$

and from F.2

$$0 = \delta U(\alpha,\gamma) + \delta V(\beta,\gamma) \quad \text{at } \alpha,\beta,\gamma = \alpha_o,\beta_o,\gamma_o \qquad \text{(F.4)}$$

Now suppose we assign arbitrary values to β and γ, say

$$\beta = \beta_1 \quad \text{and} \quad \gamma = \gamma_1 \tag{F.5a}$$

then

$$\delta V(\beta_1, \gamma_1) = 0 \tag{F.5b}$$

and F.2 reduces to

$$\delta T(\alpha, \beta_1, \gamma_1) = \delta U(\alpha, \gamma_1) \tag{F.5c}$$

If, in particular, we choose

$$\beta_1 = \beta_o \quad \text{and} \quad \gamma_1 = \gamma_o \tag{F.6a}$$

then

$$0 = \delta T(\alpha, \beta_o, \gamma_o) = \delta U(\alpha, \gamma_o) \quad \text{at } \alpha = \alpha_o \tag{F.6b}$$

which results from substituting F.5c and F.6a into F.3 . Similarly, if α and γ are assigned their unique solution values, α_o and γ_o, then

$$0 = \delta T(\alpha_o, \beta, \gamma_o) = \delta V(\beta, \gamma_o) \quad \text{at } \beta = \beta_o \tag{F.6c}$$

We can extract the following results from F.6b and F.6c :

$$0 = \delta U(\alpha, \gamma_o) \quad \text{at} \quad \alpha = \alpha_o \tag{F.7a}$$

and

$$0 = \delta V(\beta, \gamma_o) \quad \text{at} \quad \beta = \beta_o \tag{F.7b}$$

Clearly, $U(\alpha, \gamma_o)$ and $V(\beta, \gamma_o)$ are themselves stationary at, respectively, the true solutions α_o and β_o. Provided that the true solution for γ, namely γ_o, is known and inserted into U and V, the functionals can be extremised independently of each other, as in eqns. F.7 , to obtain the solutions for α and β. In the absence of such knowledge, the extremisation is performed as in F.3 or, equivalently, F.4 which involves both functionals simultaneously.

Of particular interest is the special case where the components U and V are functionals of completely independent variables, i.e. γ is absent from eqn. F.1 , which becomes

$$T(\alpha, \beta) = U(\alpha) + V(\beta) \tag{F.8}$$

with α and β independent variables, as before. Applying

eqns. F.7 to this special case, we find

$$0 = \delta U(\alpha) \quad \text{at} \quad \alpha = \alpha_o \tag{F.9a}$$

and

$$0 = \delta V(\beta) \quad \text{at} \quad \beta = \beta_o \tag{F.9b}$$

$U(\alpha)$ and $V(\beta)$ are themselves stationary at, respectively, the true solutions α_o and β_o which can thus be determined from the independent extremisation of the two functionals.

These conclusions can be applied to the constitutive error and its component functionals in eqn. 3.75. If the problem specifications leave the H-system variables and the B-system variables completely independent of each other, we can extremise Θ and Ξ as in 3.78 and 3.79, which correspond to F.9. Otherwise, we resort to 3.77, which correspond to F.3 and F.4.

G. The constitutive error in alternative derivations of complementary variational principles

This Appendix determines the relationship between the constitutive error Λ and the Lagrangians of analytical mechanics, sec. 4.4, and between Λ and the Hu-Washizu functionals of elasticity, sec. 4.5.

Consider the Lagrangians first. Substituting from eqns. 4.28 and 4.32 into 4.54, and noting 4.12, we find

$$\Lambda = \int_R \left(L_{sp}(\Omega,\underline{H}) - L_{cp}(\underline{B})\right) dR + [\Omega\,,\, \underline{n}\cdot\underline{B}]_S$$

for the primal Lagrangians of sec. 4.4.1. Similarly, substituting from eqns. 4.36 and 4.40 into 4.54, and noting 4.12, we find

$$\Lambda = \int_R \left(L_{sd}(\underline{A},\underline{B}) - L_{cd}(\underline{H})\right) dR + [\underline{n}\times\underline{H}\,,\, \underline{A}]_S$$

for the dual Lagrangians of sec. 4.4.2.

Consider the Hu-Washizu functionals next. Substituting the primal equations 4.13, 14, 16, and 17 into eqn. 4.41, and multiplying by 2 for convenience :

$$2\Pi_p = \langle \underline{G},\underline{B}\rangle_R - \langle \rho,\Omega\rangle_R + \langle \mu\underline{H}-\underline{B},\underline{H}\rangle_R + [\underline{n}\cdot\underline{B},\Omega]_{S_b} - [\underline{n}\cdot\underline{B},\Omega]_{S_h}$$

Substituting the dual equations 4.19, 20, 22, and 23 into eqn. 4.47, and multiplying by 2 :

$$2\Pi_d = \langle \underline{C},\underline{H}\rangle_R - \langle \underline{J},\underline{A}\rangle_R + \langle \nu\underline{B}-\underline{H},\underline{B}\rangle_R + [\underline{n}\times\underline{H},\underline{A}]_{S_h} - [\underline{n}\times\underline{H},\underline{A}]_{S_b}$$

Adding :

$$\begin{aligned} 2(\Pi_p + \Pi_d) = {} & \left(\langle \mu\underline{H} - \underline{B} , \underline{H}\rangle_R + \langle \nu\underline{B} - \underline{H} , \underline{B}\rangle_R\right) \\ & + \left(\langle \underline{G},\underline{B}\rangle_R - \langle \rho,\Omega\rangle_R + \langle \underline{C},\underline{H}\rangle_R - \langle \underline{J},\underline{A}\rangle_R\right) \\ & + [\underline{n}\cdot\underline{B},\Omega]_{S_b} - [\underline{n}\cdot\underline{B},\Omega]_{S_h} + [\underline{n}\times\underline{H},\underline{A}]_{S_h} - [\underline{n}\times\underline{H},\underline{A}]_{S_b} \end{aligned}$$

The term inside the first pair of brackets is twice the constitutive error for the linear case, eqn. 2.15b. The term inside the second pair of brackets can be simplified by substituting for $\underline{H}$ and $\underline{B}$ from eqns. 4.13 and 4.22 respectively, and applying vector identities and the divergence theorem to the result; dividing by 2, we get

$$\begin{aligned} \Pi_p + \Pi_d = \Lambda + \langle \underline{C} , \underline{G}\rangle_R + \tfrac{1}{2}\Big(& [\underline{n}\cdot\underline{B},\Omega]_{S_b} - [\underline{n}\cdot\underline{B},\Omega]_{S_h} - [\underline{n}\cdot\underline{C},\Omega]_S \\ & + [\underline{n}\times\underline{H},\underline{A}]_{S_h} - [\underline{n}\times\underline{H},\underline{A}]_{S_b} - [\underline{n}\times\underline{G},\underline{A}]_S\Big) \end{aligned}$$

Substituting for $\underline{H}$ and $\underline{B}$ on the boundary S from eqns. 4.13 and 4.22, applying 4.12, and collecting terms :

$$\begin{aligned} \Pi_p + \Pi_d = {} & \Lambda + \langle \underline{C} , \underline{G}\rangle_R - [\underline{n}\cdot\underline{C} , \Omega]_{S_h} - [\underline{n}\times\underline{G} , \underline{A}]_{S_b} \\ & + \tfrac{1}{2}\int_{S_b} (\nabla\Omega\times\underline{A} + \Omega\nabla\times\underline{A})\cdot d\underline{S} - \tfrac{1}{2}\int_{S_h} (\nabla\Omega\times\underline{A} + \Omega\nabla\times\underline{A})\cdot d\underline{S} \end{aligned}$$

We now substitute for Ω in the third term from 4.14, and for $\underline{n}\times\underline{A}$ in the fourth term from eqn. 4.20; we also apply a vector identity and Stokes' theorem to the integrands in the last two terms; upon rearranging, we get

$$\begin{aligned} \Lambda = {} & \Pi_p + \Pi_d - \langle \underline{C},\underline{G}\rangle_R + [\underline{n}\cdot\underline{C},\Omega_h]_{S_h} - [\underline{G},\underline{a}_b]_{S_b} \\ & - \tfrac{1}{2}\oint_{\ell_b} \Omega\,\underline{A}\cdot d\underline{\ell} + \tfrac{1}{2}\oint_{\ell_h} \Omega\,\underline{A}\cdot d\underline{\ell} \end{aligned}$$

where ℓ_b and ℓ_h are the contours of S_b and S_h respectively. But according to 4.12, ℓ_h is simply ℓ_b traversed in reverse, so that the two line integrals can be combined :

$$\Lambda = \Pi_p + \Pi_d - \left(\langle \underline{C} , \underline{G} \rangle_R - [\underline{n} \cdot \underline{C} , \Omega_h]_{S_h} + [\underline{G} , \underline{a}_b]_{S_b} + \oint_{\ell_b} \Omega \underline{A} \cdot d\underline{\ell} \right)$$

This relationship between Λ and the functionals Π_p and Π_d has been derived by enforcing the primal and dual specifications of sec. 4.3, with the exception of the constitutive relationship, eqns. 4.15 and 4.21. It is shown in sec. 4.6 that the primal and dual statements of the problem in sec. 4.3 are not, in general, equivalent. For cases where they are, with both Ω_h and $\underline{a}_b$ pre-specified, the entire bracketed term is pre-specified; in such cases, the variation is given by

$$\delta\Lambda = \delta\Pi_p + \delta\Pi_d$$

since the variation of the known term in brackets is zero.

H. Galerkin derivation of mixed formulation

The following derivation of mixed formulation is essentially that of references 9.2 and 9.3, limited to static problems. It focuses on physical specifications, and assumes that vector potential solvability can be imposed by suitable extension. As in the constitutive error-based derivation, the mixed formulation sought here is in terms of the α-system variables, defined in 9.6.

In contrast to the constitutive error approach, the method of weighted residuals imposes the constitutive relationship explicitly :

$$\underline{B}_1 = \mu_1(\underline{H}_1)\underline{H}_1 + \underline{B}_r \quad , \qquad \underline{H}_2 = \nu_2(\underline{B}_2)\underline{B}_2 + \underline{H}_c \qquad \text{(H.1)}$$

The α-system specifications are imposed on the fields $\underline{H}_1$ and $\underline{B}_2$ by defining the potentials Ω_1 and $\underline{A}_2$ as in eqns. 9.7 - 9. Scalar weighting functions, u_1, are defined in R_1, and vector weighting functions, $\underline{v}_2$, are defined in R_2. In the Galerkin approach, the weighting functions u_1 and $\underline{v}_2$ are the basis functions for Ω_1 and $\underline{A}_2$ respectively. As

the α-system boundary conditions are enforced explicitly on S_{h1} and S_{b2}, we set

$$u_1|_{S_{h1}} = 0 \quad , \quad \underline{v}_2|_{S_{b2}} = 0 \qquad \text{(H.2)}$$

The β-system specifications are enforced weakly by constructing weighted residual errors, and requiring them to vanish :

$$0 = \langle \nabla\cdot\underline{B}_1 - \rho_1 \, , \, u_1 \rangle_{R_1} \quad , \quad 0 = \langle \nabla\times\underline{H}_2 - \underline{J}_2 \, , \, \underline{v}_2 \rangle_{R_2} \qquad \text{(H.3)}$$

$$0 = [\underline{n}\cdot\Delta\underline{B}_1 \, , \, u_1]_{S_{\Delta 1}} \quad , \quad 0 = [\underline{n}\times\Delta\underline{H}_2 \, , \, \underline{v}_2]_{S_{\Delta 2}} \qquad \text{(H.4)}$$

$$0 = [\underline{n}\cdot\underline{B}_2 - \underline{n}\cdot\underline{B}_1 \, , \, u_1]_{S_o} \quad , \quad 0 = [\underline{n}\times\underline{H}_2 - \underline{n}\times\underline{H}_1 \, , \, \underline{v}_2]_{S_o} \qquad \text{(H.5)}$$

$$0 = [\underline{n}\cdot\underline{B}_1 - b_1 \, , \, u_1]_{S_{b1}} \quad , \quad 0 = [\underline{n}\times\underline{H}_2 - \underline{h}_2 \, , \, \underline{v}_2]_{S_{h2}} \qquad \text{(H.6)}$$

The residuals in eqns. H.3 , 4 , 5 , and 6 correspond to the physical specifications of eqns. 9.2, 3, 3, and 4 respectively. Applying vector identities and the divergence theorem to eqns. H.3, they become

$$0 = -\langle \underline{B}_1 \, , \, \nabla u_1 \rangle_{R_1} - \langle \rho_1 \, , \, u_1 \rangle_{R_1} - [\underline{n}\cdot\Delta\underline{B}_1 \, , \, u_1]_{S_{\Delta 1}} + [\underline{n}_1\cdot\underline{B}_1 \, , \, u_1]_{S_o} + [\underline{n}\cdot\underline{B}_1 \, , \, u_1]_{S_{b1}} + [\underline{n}\cdot\underline{B}_1 \, , \, u_1]_{S_{h1}} \qquad \text{(H.7a)}$$

and

$$0 = \langle \underline{H}_2 \, , \, \nabla\times\underline{v}_2 \rangle_{R_2} - \langle \underline{J}_2 \, , \, \underline{v}_2 \rangle_{R_2} - [\underline{n}\times\Delta\underline{H}_2 \, , \, \underline{v}_2]_{S_{\Delta 2}} + [\underline{n}_2\times\underline{H}_2 \, , \, \underline{v}_2]_{S_o} + [\underline{n}\times\underline{H}_2 \, , \, \underline{v}_2]_{S_{h2}} + [\underline{n}\times\underline{H}_2 \, , \, \underline{v}_2]_{S_{b2}} \qquad \text{(H.7b)}$$

Adding eqns. H.4, H.5, and H.6 to H.7, and substituting from eqns. H.1 and H.2 into the result, we get

$$0 = -\langle \mu_1(\underline{H}_1)\underline{H}_1 + \underline{B}_r \, , \, \nabla u_1 \rangle_{R_1} - \langle \rho_1 \, , \, u_1 \rangle_{R_1} + [b_1 \, , \, u_1]_{S_{b1}} + [\underline{n}\cdot\underline{B}_2 \, , \, u_1]_{S_o} \qquad \text{(H.8a)}$$

and

$$0 = \langle \nu_2(\underline{B}_2)\underline{B}_2 + \underline{H}_c \, , \, \nabla\times\underline{v}_2 \rangle_{R_2} - \langle \underline{J}_2 \, , \, \underline{v}_2 \rangle_{R_2} + [\underline{h}_2 \, , \, \underline{v}_2]_{S_{h2}} - [\underline{n}\times\underline{H}_1 \, , \, \underline{v}_2]_{S_o} \qquad \text{(H.8b)}$$

where $\underline{n} = \underline{n}_1 = -\underline{n}_2$ on S_o as in fig. 9.1. Eqns. H.8 represent the α-system mixed formulation.

I. Uniqueness of time-varying fields

Maxwell's equations interrelate time-varying electromagnetic fields, but do not define them uniquely. Further specifications of physical uniqueness may be derived by seeking the conditions which cause the weighted product sum W of eqns. 11.5 to vanish. Choosing

$$\beta^m = \beta^e = 1 , \qquad \beta^f = 2 \tag{I.1}$$

eqn. 11.5a for W becomes

$$W = W^m + W^e + 2\int_{t_o}^{t} W^f \, dt \tag{I.2}$$

where, according to eqns. 11.4, the constituent products are given by

$$W^m = \langle \delta\underline{H} , \delta\underline{B} \rangle_R \tag{I.3a}$$

$$W^e = \langle \delta\underline{D} , \delta\underline{E} \rangle_R \tag{I.3b}$$

$$W^f = \langle \delta\underline{J} , \delta\underline{E} \rangle_R \tag{I.3c}$$

All terms are at time t unless otherwise indicated. W^m can be expressed in terms of its value at the initial time t_o :

$$W^m = \langle \delta\underline{H}, \delta\underline{B} \rangle_R \Big|_{t_o} + \int_{t_o}^{t} p\langle \delta\underline{H}, \delta\underline{B} \rangle_R \, dt$$

$$= \langle \delta\underline{H}, \delta\underline{B} \rangle_R \Big|_{t_o} + \int_{t_o}^{t} (\langle p\delta\underline{H}, \delta\underline{B} \rangle_R + \langle \delta\underline{H}, p\delta\underline{B} \rangle_R) dt \tag{I.4}$$

Similarly for W^e :

$$W^e = \langle \delta\underline{D}, \delta\underline{E} \rangle_R \Big|_{t_o} + \int_{t_o}^{t} (\langle p\delta\underline{D}, \delta\underline{E} \rangle_R + \langle \delta\underline{D}, p\delta\underline{E} \rangle_R) dt \tag{I.5}$$

Substituting for $\underline{J}$ in W^f from Maxwell's H-system equation 11.2a, applying a vector identity and the divergence theorem, enforcing the continuity conditions of eqns. 11.2b and 11.3b, and substituting for curl $\underline{E}$ from Maxwell's E-system equation 11.3a, we have

$$W^f = \langle \nabla\times\delta\underline{H}, \delta\underline{E} \rangle_R - \langle p\delta\underline{D}, \delta\underline{E} \rangle_R$$

$$= \langle \delta\underline{H}, \nabla\times\delta\underline{E} \rangle_R - [\delta\underline{K}, \delta\underline{E}]_{S_k} + [\delta(\underline{n}\times\underline{H}), \delta\underline{E}]_S - \langle p\delta\underline{D}, \delta\underline{E} \rangle_R$$

$$= -\langle \delta\underline{H}, p\delta\underline{B} \rangle_R - \langle p\delta\underline{D}, \delta\underline{E} \rangle_R - [\delta\underline{K}, \delta\underline{E}]_{S_k} + [\delta(\underline{n}\times\underline{H}), \delta\underline{E}]_S \tag{I.6}$$

where S_k denotes surfaces across which $\underline{n} \times \underline{H}$ is discontinuous. Substituting eqns. I.4-6 back into I.2, cancelling terms where appropriate, and rearranging, we obtain

$$\begin{aligned} W = & \quad \langle \delta\underline{H} , \delta\underline{B} \rangle_R \Big|_{t_o} + \langle \delta\underline{D} , \delta\underline{E} \rangle_R \Big|_{t_o} \\ & + \int_{t_o}^{t} \Big(2[\delta(\underline{n} \times \underline{H}) , \delta\underline{E}]_S - 2[\delta\underline{K} , \delta\underline{E}]_{S_k} \\ & \quad + (\langle p\delta\underline{H} , \delta\underline{B} \rangle_R - \langle \delta\underline{H} , p\delta\underline{B} \rangle_R) \\ & \quad + (\langle \delta\underline{D} , p\delta\underline{E} \rangle_R - \langle p\delta\underline{D} , \delta\underline{E} \rangle_R) \Big) \, dt \end{aligned} \qquad (I.7)$$

Uniqueness is ensured by any set of specifications that causes W to vanish as in eqn. 11.5b. The individual terms in eqn. I.7 can be made to vanish in a variety of ways; typical sufficient specifications are given below. It is noted that eqn. I.7 already accounts for Maxwell's equations and constitutive relationships possessing property 1 of sec. 2.2.

The two terms at t_o in eqn. I.7 relate to initial conditions; the first one vanishes if either $\underline{H}(\underline{r},t_o)$ or $\underline{B}(\underline{r},t_o)$ is given, the second if either $\underline{D}(\underline{r},t_o)$ or $\underline{E}(\underline{r},t_o)$. The surface integral over S, in the time integrand, relates to boundary conditions; it vanishes if, on each section of S, either $\underline{n} \times \underline{H}$ or $\underline{n} \times \underline{E}$ is specified. The surface integral over S_k relates to continuity conditions; it can be eliminated by specification of either $\underline{K}$ or $\underline{n} \times E$ on S_k. The volume integrals in the time integrand, bracketed in pairs, relate to the magnetic and electric constitutive relationships; they vanish for linear symmetric constitutive operators :

$$\begin{aligned} \langle p\delta\underline{H} , \delta\underline{B} \rangle - \langle \delta\underline{H} , p\delta\underline{B} \rangle &= \langle p\delta\underline{H} , \mu\delta\underline{H} \rangle - \langle \delta\underline{H} , \mu p\delta\underline{H} \rangle \\ &= \langle p\delta\underline{H} , \mu\delta\underline{H} \rangle - \langle \mu\delta\underline{H} , p\delta\underline{H} \rangle \\ &= 0 \end{aligned} \qquad (I.8)$$

Similarly for the second bracket. It is recalled that linear operators that are symmetric possess prop. 2 of sec. 2.2. The requirement of linearity can be relaxed by using infinitesimal time intervals and induction, provided the constitutive operator is smooth and possesses property 2.

J. Approximate minimisation of the eddy-current error under steady a.c. conditions

Under steady a.c, conditions, the instantaneous constitutive error is composed of a time-invariant component and a harmonic, double-frequency component. According to ineq. 11.50 and eqns. 11.51, the time-invariant component has the property

$$\Lambda^s \geq 0 \tag{J.1a}$$

with

$$\Lambda^s = 0 \quad <=> \quad \Lambda(t) = 0 \tag{J.1b}$$

Minimisation of Λ^s

$$0 = \delta\Lambda^s \tag{J.2}$$

minimises $\Lambda(t)$, and hence completes the imposition of the problem specifications on the fields. As it stands, eqn. J.2 does not generate independent H- and E-system solution formulations since Λ^s does not split between the two systems, eqns. 11.39 and 11.46. The coupling term is given by

$$\begin{aligned}\Gamma^s = & <\underline{J}^r , \underline{A}^r>_{R_1} + <\underline{J}^i , \underline{A}^i>_{R_1} \\ & + \omega\xi<\underline{J}^r , \underline{A}^i>_{R_1} - \omega\xi<\underline{J}^i , \underline{A}^r>_{R_1}\end{aligned} \tag{J.3}$$

This Appendix demonstrates a procedure for extracting independent H- and E-system formulations from an approximate minimisation of Λ^s.

The electric field $\underline{E}$ is related to the E-system potentials $\underline{A}$ and ϕ as in eqns. 11.16a; for harmonic variables in two-part notation, we get

$$\underline{E}^r = \omega\underline{A}^i - \nabla\phi^r \qquad \underline{E}^i = -\omega\underline{A}^r - \nabla\phi^i \tag{J.4}$$

Substituting for $\underline{A}^r$ and $\underline{A}^i$ from J.4 into J.3, we get

$$\begin{aligned}\Gamma^s = & -\frac{1}{\omega}<\underline{J}^r , \underline{E}^i>_{R_1} + \frac{1}{\omega}<\underline{J}^i , \underline{E}^r>_{R_1} \\ & + \xi<\underline{J}^r , \underline{E}^r>_{R_1} + \xi<\underline{J}^i , \underline{E}^i>_{R_1}\end{aligned} \tag{J.5}$$

where the $<\underline{J} , \nabla\phi>_{R_1}$ products have been dropped by applying a vector identity and the divergence theorem, using $\nabla\cdot\underline{J} = 0$

and $\underline{n}\cdot\underline{J}|_{S_{12}} = 0$, and neglecting boundary terms, if any, since they match terms already dropped from eqns. 11.29. Performing the variation of Λ^s in eqn. 11.46 with Γ^s as expressed in eqn. J.5, we get

$$\delta\Lambda^s = \delta_{HH} + \delta_{HE} + \delta_{EE} + \delta_{EH} \tag{J.6}$$

where

$$\delta_{HH} = \langle\mu\underline{H}^r, \delta\underline{H}^r\rangle_R + \langle\mu\underline{H}^i, \delta\underline{H}^i\rangle_R + \frac{1}{\omega}\langle\rho\underline{J}^i, \delta\underline{J}^r\rangle_{R_1} - \frac{1}{\omega}\langle\rho\underline{J}^r, \delta\underline{J}^i\rangle_{R_1}$$

$$\delta_{HE} = \langle\xi(\rho\underline{J}^r - \underline{E}^r) - \frac{1}{\omega}(\rho\underline{J}^i - \underline{E}^i)\ ,\ \delta\underline{J}^r\rangle_{R_1} + \langle\frac{1}{\omega}(\rho\underline{J}^r - \underline{E}^r) + \xi(\rho\underline{J}^i - \underline{E}^i)\ ,\ \delta\underline{J}^i\rangle_{R_1}$$

$$\delta_{EE} = \langle\nu\underline{B}^r, \delta\underline{B}^r\rangle_R + \langle\nu\underline{B}^i, \delta\underline{B}^i\rangle_R - \frac{1}{\omega}\langle\sigma\underline{E}^i, \delta\underline{E}^r\rangle_{R_1} + \frac{1}{\omega}\langle\sigma\underline{E}^r, \delta\underline{E}^i\rangle_{R_1} - \langle\underline{J}_s^r, \delta\underline{A}^r\rangle_{R_2} - \langle\underline{J}_s^i, \delta\underline{A}^i\rangle_{R_2}$$

$$\delta_{EH} = \langle\xi(\sigma\underline{E}^r - \underline{J}^r) + \frac{1}{\omega}(\sigma\underline{E}^i - \underline{J}^i)\ ,\ \delta\underline{E}^r\rangle_{R_1} + \langle-\frac{1}{\omega}(\sigma\underline{E}^r - \underline{J}^r) + \xi(\sigma\underline{E}^i - \underline{J}^i)\ ,\ \delta\underline{E}^i\rangle_{R_1}$$

Or, in the more compact complex notation,

$$\delta_{HH} = \tfrac{1}{2}\delta\langle\mu\underline{H}^c\ ,\ \underline{H}^*\rangle_R + \frac{1}{\omega}\,\mathrm{Im}\,\langle\rho\underline{J}^c\ ,\ \delta\underline{J}^*\rangle_{R_1}$$

$$\delta_{HE} = \xi\,\mathrm{Re}\,\langle\rho\underline{J}^c - \underline{E}^c\ ,\ \delta\underline{J}^*\rangle_{R_1} - \frac{1}{\omega}\,\mathrm{Im}\,\langle\rho\underline{J}^c - \underline{E}^c\ ,\ \delta\underline{J}^*\rangle_{R_1}$$

$$\delta_{EE} = \tfrac{1}{2}\delta\langle\nu\underline{B}^c\ ,\ \underline{B}^*\rangle_R - \frac{1}{\omega}\,\mathrm{Im}\,\langle\sigma\underline{E}^c\ ,\ \delta\underline{E}^*\rangle_{R_1} - \mathrm{Re}\langle\underline{J}_s^c\ ,\ \delta\underline{A}^*\rangle_{R_2}$$

$$\delta_{EH} = \xi\,\mathrm{Re}\,\langle\sigma\underline{E}^c - \underline{J}^c\ ,\ \delta\underline{E}^*\rangle_{R_1} + \frac{1}{\omega}\,\mathrm{Im}\,\langle\sigma\underline{E}^c - \underline{J}^c\ ,\ \delta\underline{E}^*\rangle_{R_1}$$

The notation δ_{HH} etc. reflects the absence of corresponding functionals. Close scrutiny reveals that only H-system variables appear in δ_{HH}, and only E-system variables appear in δ_{EE}. δ_{HE} and δ_{EH}, on the other hand, depend on both system variables.

Approximating eqn. J.2 by

$$0 = \delta\Lambda^s - \delta_{HE} = \delta_{HH} + (\delta_{EE} + \delta_{EH}) \tag{J.7}$$

generates an independent H-system solution formulation

$$0 = \delta_{HH} \tag{J.8a}$$

as well as a dependent E-system formulation

$$0 = \delta_{EE} + \delta_{EH} \qquad \text{(J.8b)}$$

Alternatively, eqn. J.2 is approximated by

$$0 = \delta\Lambda^{s} - \delta_{EH} = (\delta_{HH} + \delta_{HE}) + \delta_{EE} \qquad \text{(J.9)}$$

to yield

$$0 = \delta_{EE} \qquad \text{(J.10a)}$$

and

$$0 = \delta_{HH} + \delta_{HE} \qquad \text{(J.10b)}$$

It is noted that only E-system parameters are varied in eqn. J.8b, and only H-system parameters are varied in eqn. J.10b. Eqns. J.8a and J.10a are the required H- and E-system solution formulations; they can be solved independently of each other. The approximations which generated them are justified by the fact that in exact analysis, the conductive constitutive relationship, eqns. 11.18, is satisfied exactly, so that

$$\delta_{HE} = 0 \qquad \text{and} \qquad \delta_{EH} = 0 \qquad \text{(J.11)}$$

Other formulations can be derived by basing the approximate minimisation on exact satisfaction of the magnetic constitutive relationship, eqns. 11.17.

K. Alternative derivations of complementary variational formulations of the harmonic eddy-current problem

This Appendix outlines the approaches developed by Hammond[11.2] and Fraser[11.3], and compares their formulations with those derived by the constitutive error approach in section 11.3.1.

Hammond devises a conceptual adjoint system, having negative conductivity or time sequence, to generate the power dissipated by the actual system. He then derives various dual principles of virtual power to maintain equilibrium instantaneously. One such principle is

$$0 = \delta^{c}_{ee} = \omega^2 \langle \nu \underline{B}^{*} , \delta \underline{B}^{c} \rangle_R - j\omega \langle \sigma \underline{E}^{*} , \delta \underline{E}^{c} \rangle_R \qquad (K.1)$$

where the surface term has been omitted, and

$$R = R_1 \quad , \quad R_2 = 0 \qquad (K.2)$$

Introducing two-part notation, eqn. 11.43, we can rewrite eqn. K.1 in the form

$$0 = \delta^{c}_{ee} = \delta^{r}_{ee} + j\,\delta^{i}_{ee} \qquad (K.3)$$

where

$$\delta^{r}_{ee} = \omega^2 \langle \nu \underline{B}^{r}, \delta \underline{B}^{r} \rangle_R + \omega^2 \langle \nu \underline{B}^{i}, \delta \underline{B}^{i} \rangle_R - \omega \langle \sigma \underline{E}^{i}, \delta \underline{E}^{r} \rangle_R + \omega \langle \sigma \underline{E}^{r}, \delta \underline{E}^{i} \rangle_R$$

$$\delta^{i}_{ee} = -\omega^2 \langle \nu \underline{B}^{i}, \delta \underline{B}^{r} \rangle_R + \omega^2 \langle \nu \underline{B}^{r}, \delta \underline{B}^{i} \rangle_R - \omega \langle \sigma \underline{E}^{r}, \delta \underline{E}^{r} \rangle_R - \omega \langle \sigma \underline{E}^{i}, \delta \underline{E}^{i} \rangle_R$$

According to basic complex number theory, eqn. K.3 generates the simultaneous equations

$$0 = \delta^{r}_{ee} \qquad (K.4a)$$

$$0 = \delta^{i}_{ee} \qquad (K.4b)$$

Comparing the expression for δ^{r}_{ee} in eqn. K.3 with the expression for δ_{EE} in eqn. J.6 of Appendix J, it is clear that, subject to eqns. K.2, the two are related by

$$\delta^{r}_{ee} = \omega^2 \delta_{EE} \qquad (K.5)$$

It immediately follows that eqn. K.4a is entirely equivalent to eqn. J.10a, and hence to eqn. 11.56, ω being constant.

Thus Hammond's approach corresponds to, and is in basic agreement with, the approximate minimisation of the time-invariant error Λ^S described in Appendix J and discussed in sec. 11.3.1. This conclusion is quite general, although established here for a particular case. For example, eqn. K.4b can also be derived by the basic procedure of Appendix J, but with the redundant over-specification imposed on the magnetic constitutive relationship instead of the conductive one. Moreover, Hammond's H-system formulations can be derived in a similar way. However, the two approaches diverge as Hammond goes on to integrate eqn. K.1 to obtain the variational principle

$$0 = \delta \left(-\tfrac{1}{2} j\omega \langle \nu \underline{B}^C , \underline{B}^* \rangle_R - \tfrac{1}{2} \langle \sigma \underline{E}^C , \underline{E}^* \rangle_R \right) \qquad \text{(K.6)}$$

Justification of the varied functional, which does not arise in the constitutive error derivation, is not obvious. For example

$$\delta \tfrac{1}{2} \langle \sigma \underline{E}^C , \underline{E}^* \rangle_R = \tfrac{1}{2} \langle \sigma \underline{E}^C , \delta \underline{E}^* \rangle_R + \tfrac{1}{2} \langle \sigma \underline{E}^* , \delta \underline{E}^C \rangle_R$$
$$\neq \langle \sigma \underline{E}^* , \delta \underline{E}^C \rangle_R \qquad \text{(K.7)}$$

Fraser[11.3] also questions the validity of the functional in eqn. K.6, and concludes that the complex function approach is unacceptable for deriving complementary energy functionals. Indeed, it is the difficulty of interpreting complex energies and their stationary points that prompted the instantaneous approach adopted in the harmonic derivations of sec. 11.3.1.

Fraser's own treatment represents the variables as ordered pairs of real functions corresponding to the real and imaginary parts. He then extends his formal approach of direct integration to construct the complementary functionals $\Theta_F(H)$ and $\Xi_F(E)$. These turn out to be identical to the real components associated with the double-frequency error, $\Theta^r(H)$ and $\Xi^r(E)$ in eqn. 11.47; i.e.

$$\Theta_F(H) = \Theta^r(H) \qquad \text{and} \qquad \Xi_F(E) = \Xi^r(E) \qquad \text{(K.8)}$$

Thus Fraser's approach corresponds to, and is in basic agreement with, the variational principles of eqns. 11.54

which relate to the double-frequency component of the constitutive error. However, the two approaches diverge as Fraser goes on to map the real functionals Θ_F and Ξ_F into complex ones Θ_F^c and Ξ_F^c. His expression for the latter, with $\underline{J}_s^i$ taken to be zero, is

$$\Xi_F^c = \tfrac{1}{2}\langle \nu \underline{B}^r, \underline{B}^r \rangle_R + \tfrac{1}{2}\langle \nu \underline{B}^i, \underline{B}^i \rangle_R - \langle \underline{J}_s^r, \underline{A}^r \rangle_{R_2} - \frac{1}{j\omega}\langle \sigma \underline{E}^r, \underline{E}^i \rangle_{R_1} \qquad \text{(K.9)}$$

It is not clear how this functional, which does not arise in the constitutive error derivation, is implied by Ξ^r as given in eqn. 11.47.

It can thus be concluded that the constitutive error approach may be used to generate the solution formulations derived by both Hammond[11.2] and Fraser[11.3], but not the complex power and energy functionals they propose.

Hammond uses his complex power functionals to define upper and lower bounds on circuit inductance and resistance. Fraser uses his complex energy functionals to define bounds on the inductance, and to conclude that there are no bounds on resistance. The constitutive error approach cannot verify any of the bounds.

R E F E R E N C E S

1.1 C.J. CARPENTER: 'Comparison of alternative formulations of 3-dimensional magnetic-field and eddy-current problems at power frequencies'. Proc IEE, 124, (11), Nov 1977, pp 1026-1034.

1.2 J. SIMKIN and C.W. TROWBRIDGE: 'Which potential ? A comparison of the various scalar and vector potentials for the numerical solution of the non-linear Poisson problem'. RL-78-009/B, Rutherford Lab, Jan 1978.

1.3 P. HAMMOND: 'Energy methods in electromagnetism'. Clarendon Press, Oxford, 1981.

1.4 J. PENMAN and J.R. FRASER: 'Unified approach to problems in electromagnetism'. Proc IEE, 131, Pt A, (1), Jan 1984, pp. 55-61.

1.5 R.D. PILLSBURY: 'A three-dimensional eddy current formulation using two potentials: the magnetic vector potential and total magnetic scalar potential'. IEEE Trans, MAG-19, (6), Nov 1983, pp. 2284-2287.

1.6 C.J. CARPENTER: 'Finite-element network models and their application to eddy-current problems'. Proc IEE, 122, (4), April 1975, pp. 455-462.

1.7 J.A.M. DAVIDSON and M.J. BALCHIN: 'Three-dimensional eddy-current calculation using loop variables to represent magnetic vector potential in conducting regions'. Proc IEE, 131, Pt A, (8), Nov 1984, pp. 577-583.

1.8 A.M. WINSLOW: 'Numerical solution of the quasilinear Poisson equation in a nonuniform triangle mesh'. J Comp Phys, 2, 1967, pp. 149-172.

1.9 O.C. ZIENKIEWICZ, P.L. ARLETT, and A.K. BAHRANI: 'Solution of three-dimensional field problems by the finite element method'. The Engineer, 27 Oct 1967.

1.10 C.W. TROWBRIDGE: 'Applications of integral equation methods to the numerical solution of magnetostatic and eddy-current problems'. In M.V.K. CHARI and P.P. SILVESTER (editors): 'Finite elements in electrical and magnetic field problems'. Wiley, Chichester, 1980.

1.11 J.H. MCWHIRTER, J.J. ORAVEL, and R.W. HAACH: 'Computation of magnetostatic fields in three dimensions based on Fredholm integral equations'. IEEE Trans, MAG-18, (2), March 1982, pp. 373-378.

1.12 B.H. MCDONALD and A. WEXLER: 'Mutually constrained partial differential and integral equation field formulations'. In M.V.K. CHARI and P.P. SILVESTER (editors): 'Finite elements in electrical and magnetic field problems'. Wiley, Chichester, 1980.

1.13 C.F. BRYANT: 'A mixed integral differential method for low frequency electromagnetic fields'. Ph. D. thesis, University of London, 1981.

1.14 J.R. FRASER: 'Complementary and dual finite element principles'. Ph. D. thesis, University of Aberdeen, 1982.

1.15 O.C. ZIENKIEWICZ: 'Finite elements - the basic concepts and an application to 3-d magnetostatic problems'. In M.V.K. CHARI and P.P. SILVESTER (editors): 'Finite elements in electrical and magnetic field problems'. Wiley, Chichester, 1980.

1.16 P. SILVESTER and M.V.K. CHARI: 'Finite element solution of saturable magnetic field problems'. IEEE Trans, PAS-89, (7), Sep/Oct 1970, pp. 1642-1651.

1.17 M.V.K. CHARI and P. SILVESTER: 'Analysis of turbo-alternator magnetic fields by finite elements'. IEEE Trans, PAS-90, (2), March/April 1971, pp. 454-464.

1.18 N.A. DEMERDASH and T.W. NEHL: 'An evaluation of the methods of finite elements and finite differences in the solution of nonlinear electromagnetic fields in electric machines'. IEEE Trans, PAS-98, (1), Jan/Feb 1979, pp. 74-87.

1.19 E.F. FUCHS and G.A. MCNAUGHTON: 'Comparison of first-order finite difference and finite element algorithms for the analysis of magnetic fields. Part I: theoretical analysis'. IEEE Trans, PAS-101, (5), May 1982, pp. 1170-1180.

1.20 G.A. MCNAUGHTON and E.F. FUCHS: 'Comparison of first-order finite difference and finite element algorithms for the analysis of magnetic fields. Part II: numerical results'. IEEE Trans, PAS-101, (5), May 1982, pp. 1181-1201.

1.21 A.M. ARTHURS: 'Complementary variational principles', second edition. Clarendon Press, Oxford, 1980.

1.22 G.K. CAMBRELL: 'Linear operators and variational principles in electromagnetic theory'. Ph. D. thesis, Monash University, 1972.

1.23 J. PENMAN and J.R. FRASER: 'Dual and complementary methods in electromagnetism'. IEEE Trans, MAG-19, (6), Nov 1983, pp. 2311-2316.

1.24 K. WASHIZU: 'Variational methods in elesticity and plasticity', second edition. Pergamon Press, Oxford, 1975.

1.25 J. PENMAN and J.R. FRASER: 'Complementary and dual finite element principles in magnetostatics'. IEEE Trans, MAG-18, (2), March 1982, pp. 319-324.

1.26 J.L. SYNGE: 'The hypercircle in mathematical physics'. Cambridge University Press, 1957.

1.27 P. HAMMOND and J. PENMAN: 'Calculation of inductance and capacitance by means of dual energy principles'. Proc IEE, 123, (6), June 1976, pp. 554-559.

1.28 P. HAMMOND: 'Physical basis of the variational method for the computation of magnetic field problems'. COMPUMAG Proceedings, Oxford, 1976.

1.29 P. HAMMOND, M.C. ROMERO-FUSTER, and S.A. ROBERTSON: 'Fast numerical method for calculation of electric and magnetic fields based on potential-flux duality'. Proc IEE, 132, Pt A, (2), March 1985, pp. 84-94.

1.30 P. HAMMOND and T.D. TSIBOUKIS: 'Dual finite element calculations for static electric and magnetic fields'. Proc IEE, 130, Pt A, (3), May 1983, pp. 105-111.

1.31 P. HAMMOND and J. PENMAN: 'Calculation of eddy currents by dual energy methods'. Proc IEE, 125, (7), July 1978, pp. 701-708.

1.32 R.W. THATCHER: 'Assessing the error in a finite element solution'. IEEE Trans, MTT-30, (6), June 1982, pp. 911-915.

1.33 Z.J. CENDES, D. SHENTON, and H. SHAHNASSER: 'Magnetic field computation using Delaunay triangulation and complementary finite element methods'. IEEE Trans, MAG-19, (6), Nov 1983, pp. 2551-2554.

2.1 A.M. ARTHURS: 'Complementary variational principles', second edition. Clarendon Press, Oxford, 1980.

3.1 C.J. CARPENTER: 'Comparison of alternative formulations of 3-dimensional magnetic-field and eddy-current problems at power frequencies'. Proc IEE, 124, (11), Nov 1977, pp. 1026-1034.

4.1 A.M. ARTHURS: 'Complementary variational principles', second edition. Clarendon Press, Oxford, 1980.

4.2 G.K. CAMBRELL: 'Linear operators and variational principles in electromagnetic theory'. Ph.D. thesis, Monash University, 1972.

4.3 P. HAMMOND and J. PENMAN: 'Calculation of inductance and capacitance by means of dual energy principles'. Proc IEE, 123, (6), June 1976, pp. 554-559.

4.4 P. HAMMOND: 'Energy methods in electromagnetism'. Clarendon Press, Oxford, 1981.

4.5 J.R. FRASER: 'Complementary and dual finite element principles'. Ph.D. thesis, University of Aberdeen, 1982.

4.6 J. PENMAN and J.R. FRASER: 'Dual and complementary methods in electromagnetism'. IEEE Trans, MAG-19, (6), Nov 1983, pp. 2311-2316.

4.7 K. WASHIZU: 'Variational methods in elasticity and plasticity', second edition. Pergamon Press, Oxford, 1975.

4.8 P. HAMMOND: 'Energy methods in electromagnetism'. Clarendon Press, Oxford, 1981; pp. 54, 60, and 133.

5.1 O.C. ZIENKIEWICZ: 'Finite elements - the basic concepts and an application to 3-d magnetostatic problems'. In M.V.K. CHARI and P.P. SILVESTER (editors): 'Finite elements in electrical and magnetic field problems'. Wiley, Chichester, 1980.

5.2 G.E. FORSYTHE and W.R. WASOW: 'Finite difference methods for partial differential equations'. Wiley, New York, 1960; section 20.8.

5.3 E.F. FUCHS and G.A. MCNAUGHTON: 'Comparison of first-order finite difference and finite element algorithms for the analysis of magnetic fields. Part I: theoretical analysis'. IEEE Trans, PAS-101, (5), May 1982, pp. 1170-1180.

5.4 O.C. ZIENKIEWICZ: 'The finite element method', third edition. McGraw-Hill, London, 1977.

5.5 M.V.K. CHARI and P.P. SILVESTER (editors): 'Finite elements in electrical and magnetic field problems'. Wiley, Chichester, 1980.

5.6 R.W. THATCHER: 'Assessing the error in a finite element solution'. IEEE Trans, MTT-30, (6), June 1982, pp. 911-915.

5.7 Z.J. CENDES, D. SHENTON, and H. SHAHNASSER: 'Magnetic field computation using Delaunay triangulation and complementary finite element methods'. IEEE Trans, MAG-19, (6), Nov 1983, pp. 2551-2554.

6.1 O.C. ZIENKIEWICZ: 'The finite element method', third edition. McGraw-Hill, London, 1977.

6.2 P.P. SILVESTER and R.L. FERRARI: 'Finite elements for electrical engineers'. Cambridge University Press, Cambridge, 1983.

6.3 E.M. FREEMAN: 'CAE of electrical machines'. Electronics and Power, Jan 1983, pp. 31-35.

6.4 D.A. LOWTHER and P.P. SILVESTER: 'Computer aided design in magnetics'. Springer-Verlag, 1985 (to be published).

6.5 Z.J. CSENDES, E.M. FREEMAN, D.A. LOWTHER, and P.P. SILVESTER: 'Interactive computer graphics in magnetic field analysis and electric machine design'. IEEE Trans, PAS-100, (6), June 1981, pp. 2862-2869.

6.6 MAGMESH User's Manual, Release 2, Feb 1982; Infolytica Corp.

6.7 J.A. MEIJERINK and H.A. VAN DER VORST: 'An iterative solution method for linear systems of which the coefficient matrix is a symmetric M-matrix'. Maths Comp, 31, 1977.

6.8 D.S. KERSHAW: 'The incomplete Cholesky-conjugate gradient method for the iterative solution of systems of linear equations'. Journal of Computational Physics, 26, (1), Jan 1978, pp. 43-65.

6.9 QUARTO Graphics Package, User's Manual, Version 2.1, March 1983; Infolytica Corp.

6.10 J. SIMKIN and C.W. TROWBRIDGE: 'Three-dimensional non-linear electromagnetic field computations, using scalar potentials'. Proc IEE, 127, Pt B, (6), 1980, pp. 368-374.

6.11 C.W. TROWBRIDGE: 'Applications of integral equation methods to the numerical solution of magnetostatic and eddy-current problems'. In M.V.K. CHARI and P.P. SILVESTER (editors): 'Finite elements in electrical and magnetic field problems'. Wiley, Chichester, 1980.

6.12 J. PENMAN and J.R. FRASER: 'Complementary and dual finite element principles in magnetostatics'. IEEE Trans, MAG-18, (2), March 1982, pp. 319-324.

6.13 P. HAMMOND and T.D. TSIBOUKIS: 'Dual finite element calculations for static electric and magnetic fields'. Proc IEE, 130, Pt A, (3), May 1983, pp. 105-111.

6.14 R.W. THATCHER: 'Assessing the error in a finite element solution'. IEEE Trans, MTT-30, (6), June 1982, pp. 911-915.

6.15 Z.J. CENDES, D. SHENTON, and H. SHAHNASSER: 'Magnetic field computation using Delaunay triangulation and complementary finite element methods'. IEEE Trans, MAG-19, (6), Nov 1983, pp. 2551-2554.

6.16 J.R. FRASER: 'Complementary and dual finite element principles'. Ph.D. thesis, University of Aberdeen, 1982.

6.17 P. HAMMOND and J. PENMAN: 'Calculation of inductance and capacitance by means of dual energy principles'. Proc IEE, 123, (6), June 1976, pp. 554-559.

6.18 P. HAMMOND: 'Energy methods in electromagnetism'. Clarendon Press, Oxford, 1981.

6.19 P. HAMMOND, M.C. ROMERO-FUSTER, and S.A. ROBERTSON: 'Fast numerical method for calculation of electric and magnetic fields based on potential-flux duality'. Proc IEE, 132, Pt A, (2), March 1985, pp. 84-94.

6.20 D.E. JONES, N. MULLINEUX, J.R. REED, and R.L. STOLL: 'Solid rectangular and T-shaped conductors in semi-closed slots'. Journal of Engineering Mathematics, 3, (2), April 1969, pp. 123-135.

7.1 P. HAMMOND and J. PENMAN: 'Calculation of inductance and capacitance by means of dual energy principles'. Proc IEE, 123, (6), June 1976, pp. 554-559.

7.2 P. HAMMOND: 'Energy methods in electromagnetism'. Clarendon Press, Oxford, 1981.

7.3 P.P. SILVESTER and R.L. FERRARI: 'Finite elements for electrical engineers'. Cambridge University Press, Cambridge, 1983.

8.1 C.W. TROWBRIDGE: 'Applications of integral equation methods to the numerical solution of magnetostatic and eddy-current problems'. In M.V.K. CHARI and P.P. SILVESTER (editors): 'Finite elements in electrical and magnetic field problems'. Wiley, Chichester, 1980.

8.2 P.P. SILVESTER and R.L. FERRARI: 'Finite elements for electrical engineers'. Cambridge University Press, Cambridge, 1983.

8.3 J. SIMKIN and C.W. TROWBRIDGE: 'On the use of total scalar potential in the numerical solution of field problems in electromagnetics'. Int J Num Meth Eng, 14, 1979, pp. 423-440.

8.4 T.W. MCDANIEL, R.B. FERNANDEZ, R.R. ROOT, and R.B. ANDERSON: 'An accurate scalar potential finite element method for linear two-dimensional magnetostatics problems'. Int J Num Meth Eng, 19, 1983, pp. 725-737.

8.5 J. SIMKIN and C.W. TROWBRIDGE: 'Three-dimensional non-linear electromagnetic field computations, using scalar potentials'. Proc IEE, 127, Pt B, (6), 1980, pp. 368-374.

8.6 C.W. TROWBRIDGE: 'Numerical solution of electromagnetic field problems in two and three dimensions'. RL-81-075, Rutherford Lab, 1981.

8.7 J.R. FRASER: 'Complementary and dual finite element principles'. Ph.D. thesis, University of Aberdeen, 1982.

8.8 O.C. ZIENKIEWICZ: 'The finite element method', third edition. McGraw-Hill, London, 1977.

9.1 R.D. PILLSBURY: 'A three-dimensional eddy current formulation using two potentials: the magnetic vector potential and total magnetic scalar potential'. RL-83-019, Rutherford Lab: Eddy Current Seminar, April 1982.

9.2 R.D. PILLSBURY: 'A three-dimensional eddy current formulation using two potentials: the magnetic vector potential and total magnetic scalar potential'. IEEE Trans, MAG-19, (6), Nov 1983, pp. 2284-2287.

9.3 C.R.I. EMSON and J. SIMKIN: 'An optimal method for 3-d eddy currents'. IEEE Trans, MAG-19, (6), Nov 1983, pp. 2450-2452.

9.4 D. RODGER and J.F. EASTHAM: 'Finite element solution of 3-d eddy current flow in magnetically linear conductors at power frequencies'. IEEE Trans, MAG-18, (2), March 1982, pp. 481-485.

9.5 D. RODGER: 'A finite element method for calculating power frequency 3-dimensional electromagnetic field distributions'. Proc IEE, 130, Pt A, (5), July 1983, pp. 233-238.

9.6 S.J. POLAK, A.J.H. WACHTERS, and J.S. VAN WELIJ: 'A new 3-d eddy current model'. IEEE Trans, MAG-19, (6), Nov 1983, pp. 2447-2449.

10.1 Z.J. CSENDES, J. WEISS, and S.R.H. HOOLE: 'Alternative vector potential formulations of 3-d magnetostatic field problems'. IEEE Trans, MAG-18, (2), March 1982, pp. 367-372.

10.2 P.R. KOTIUGA and P.P. SILVESTER: 'Vector potential formulation for three-dimensional magnetostatics'. J Appl Phys, 53, (11), Nov 1983, pp. 8399-8401.

10.3 J. WEISS and Z.J. CENDES: 'On the uniqueness of vector potential formulation for three-dimensional magneto-static field problems'. IEEE Trans, MAG-19, (6), Nov 1983, pp. 2288-2291.

10.4 J.L. COULOMB: 'Finite element three dimensional field computation'. IEEE Trans, MAG-17, (6), Nov 1981, pp. 3241-3246.

10.5 M.V.K. CHARI, P.P. SILVESTER, A. KONRAD, Z.J. CSENDES, and M.A. PALMO: 'Three-dimensional magnetostatic field analysis of electric machinery by the finite element method'. IEEE Trans, PAS-100, (8), Aug 1981, pp. 4007-4015.

10.6 O.C. ZIENKIEWICZ: 'The finite element method', third edition. McGraw-Hill, London, 1977.

10.7 O.C. ZIENKIEWICZ: 'Finite elements - the basic concepts and an application to 3-d magnetostatic problems'. In M.V.K. CHARI and P.P. SILVESTER (editors): 'Finite elements in electrical and magnetic field problems'. Wiley, Chichester, 1980.

10.8 N.A. DEMERDASH, T.W. NEHL, F.A. FOUAD, and O.A. MOHAMMED: 'Three dimensional finite element vector potential formulation of magnetic fields in electrical apparatus'. IEEE Trans, PAS-100, (8), Aug 1981, pp. 4104-4111.

10.9 N.A. DEMERDASH, T.W. NEHL, O.A. MOHAMMED, and F.A. FOUAD: 'Experimental verification and application of three dimensional finite element magnetic vector potential method in electrical apparatus'. IEEE Trans, PAS-100, (8), Aug 1981, pp. 4112-4119.

10.10 O.A. MOHAMMED, W.A. DAVIS, B.D. POPOVIC, T.W. NEHL, and N.A. DEMERDASH: 'On the uniqueness of solution of magnetostatic vector-potential problems by three-dimensional finite-element methods'. J Appl Phys, 53, (11), Nov 1982, pp. 8402-8404.

10.11 O.A. MOHAMMED, N.A. DEMERDASH, and T.W. NEHL: 'Validity of finite element formulation and solution of three dimensional magnetostatic problems in electrical devices with applications to transformers and reactors'. IEEE Trans, PAS-103, (7), July 1984, pp. 1846-1853.

10.12 J.A.M. DAVIDSON and M.J. BALCHIN: 'Three-dimensional eddy-current calculation using loop variables to represent magnetic vector potential in conducting regions'. Proc IEE, 131, Pt A, (8), Nov 1984, pp. 577-583.

11.1 A.M. ARTHURS: 'Complementary variational principles', second edition. Clarendon Press, Oxford, 1980.

11.2 P. HAMMOND: 'Energy methods in electromagnetism'. Clarendon Press, Oxford, 1981.

11.3 J.R. FRASER: 'Complementary and dual finite element principles'. Ph.D. thesis, University of Aberdeen, 1982.

11.4 R.L. FERRARI: 'Finite element analysis of three-dimensional high frequency structures containing lossy materials'. RL-84-80, Rutherford Lab: Eddy Current Seminar, April 1984.